CONTRIBUTIONS TO MODELING AND OPTIMIZATION OF FUZZY CONTROL SYSTEMS

Teză destinată obținerii
titlului științific de doctor inginer
la
Universitatea Politehnica Timişoara
în domeniul INGINERIA SISTEMELOR
de către

Ing. Radu-Codruţ David

Conducător științific: Prof.Dr.Eng. Radu-Emil Precup
Referenţi stiinţifici: Prof.Dr.Eng. Vladimir-Ioan Creţu
Prof.Dr.Eng. Dumitru Popescu
Prof.Dr.Eng. Vladimir Răsvan
Prof.Dr.Eng. Stefan Preitl

Ziua susținerii tezei: 24.04.2015

Seriile Teze de doctorat ale UPT sunt:

1. Automatică
2. Chimie
3. Energetică
4. Ingineria Chimică
5. Inginerie Civilă
6. Inginerie Electrică
7. Inginerie Electronică şi Telecomunicaţii
8. Inginerie Industrială
9. Inginerie Mecanică
10. Ştiinţa Calculatoarelor
11. Ştiinţa şi Ingineria Materialelor
12. Ingineria sistemelor
13. Inginerie energetică
14. Calculatoare şi tehnologia informaţiei
15. Ingineria materialelor
16. Inginerie şi Management

Universitatea Politehnica Timişoara a iniţiat seriile de mai sus în scopul diseminării expertizei, cunoştinţelor şi rezultatelor cercetărilor întreprinse în cadrul şcolii doctorale a universităţii. Seriile conţin, potrivit H.B.Ex.S Nr. 14 / 14.07.2006, tezele de doctorat susţinute în universitate începând cu 1 octombrie 2006.

România, 300159 Timişoara, Bd. Republicii 9,
tel. 0256 403823, fax. 0256 403221
e-mail: editura@edipol.upt.ro

PREFACE

This thesis represents a synthesis of my research during PhD studies within the Department of Automation and Applied Informatics at the Politehnica University of Timişoara, Romania.

First and foremost I would like to express my sincere gratitude to my advisor Prof. Dr. Eng. Radu-Emil Precup for his continuous support and dedication. It has been an honor to be his Ph.D. student. The joy and enthusiasm he has for research was contagious and motivational for me.

I would like to give a special thank you to Prof. Dr. Eng. Stefan Preitl, Assoc. Prof. Dr. Eng. Florin Drăgan, Lect. Dr. Eng. Mircea-Bogdan Rădac, Lect. Dr. Eng. Claudia-Adina Bojan-Dragoş, Lect. Dr. Eng. Daniel Iercan, Assist. Lect. Dr. Eng. Alexandra-Iulia Stînean, PhD student Eng. Lucian-Ovidiu Fedorovici, PhD student Eng. Constantin Purcaru from the Politehnica University of Timişoara, as well as the other coauthors from the University of Ottawa, Canada, and the Óbuda University, Budapest, Hungary, with special focus on Prof. Emil M. Petriu and Prof. János Fodor. The cooperation with them has been inspiring and successful. I do hope that our fruitful cooperation will continue.

I acknowledge the efforts of the members of my PhD committee and their constructive remarks on my research. I would like to express my gratitude to Prof. Dr. Eng. Dumitru Popescu from the Politehnica University of Bucharest, Prof. Dr. Eng. Vladimir Răsvan from the University of Craiova and Prof. Dr. Eng. Vladimir-Ioan Crețu from the Politehnica University of Timişoara, for accepting to be members of the committee and for the advices given in the final phase of the preparation of this thesis.

Last but not least, I am grateful to my parents, for their love and support throughout the years.

David Radu-Codruţ,
Contributions to Modeling and Optimization of Fuzzy Control Systems

Teze de doctorat ale UPT, Seria 12, Nr. 14, Editura Politehnica, 2015, 187 pagini, 71 figuri, 87 tabele.

ISSN:2068-7990

ISBN:978-606-554-932-6

Cuvinte cheie: sisteme de conducere fuzzy, optimizare, regulatoare fuzzy de tip Takagi-Sugeno, sensibilitate parametrică, modele de sensibilitate, algoritmi inspiraţi din natură, Particle Swarm Optimization, Simulated Annealing, Gravitational Search Algorithm, Charged System Search, algoritmi hibrizi.

Rezumat,

În cadrul tezei sunt propuse diverse soluţii pentru modelarea şi optimizarea sistemelor de conducere fuzzy. Contribuţiile cercetării sunt reprezentate de: definirea problemelor de optimizare a regulatoarelor fuzzy de tip Takagi-Sugeno cu sensibilitate parametrică redusă, a problemelor de optimizare parametrică a modelelor fuzzy de tip Takagi-Sugeno cu dinamică, noi algoritmi inspiraţi din natură aplicaţi în rezolvarea acestor probleme de optimizare prin minimizarea a diverse funcţii obiectiv şi rezultatele îmbunătăţite obţinute în urma aplicării algoritmilor. Calitatea rezultatelor obţinute este evaluată prin prisma unor indicatori de performanţă originali. Soluţiile propuse sunt validate experimental pentru trei echipamente de laborator: un servosistem neliniar, un sistem anti-blocaj al roţilor şi un sistem cu levitaţie magnetică.

CONTENTS

LIST OF TABLES

LIST OF FIGURES

1. INTRODUCTION

1.1 MOTIVATION BEHIND THE RESEARCH

A consistent way to achieve the performance specifications of fuzzy control systems involves tuning the parameters of fuzzy controllers or fuzzy models with the aid of defined optimization problems with variables matching those parameters. The performance specifications are met by solving these optimization problems that ensure the optimal tuning of fuzzy controllers and fuzzy models. This process may lead to multi-objective optimization problems due to the complexity of the process and controller's structures and nonlinearities as the objective functions associated to the optimization problems could be non-convex and non-differentiable.

For control systems, the performance indices are usually expressed as empirical control system performance indices (e.g., overshoot, settling time, phase margin, etc.). A common practice of achieving the desired performance specifications of fuzzy control systems is to define them through optimization problems based on objective functions, which use as variables the tuning parameters of the controller, with the appropriate constraints imposed. Optimal tuning parameters are reached by solving these optimization problems, which, in most cases, implies the minimization of the objective functions. The optimal tuning of fuzzy controllers is applied in this thesis in the context of the above mentioned systematic way to design and tune these nonlinear controllers.

For the design and tuning of optimal control systems, idealized linear or linearized models of the controlled processes are generally used. Nevertheless, industrial processes are subjected to parametric variations of the controlled processes, which can put the systems in undesired states or even unstable ones. In order to avoid these situations, a sensitivity analysis with respect to the parametric variations of controlled processes is required and state sensitivity models with respect to the variable parameters of the controlled process are derived. The parameters are considered variable if the initial process models are nonlinear and next linearized around several operating points in order to ensure the convenient and easily understandable controller design and tuning. The objective functions considered in this thesis will include the output sensitivity functions in appropriate sensitivity models, so optimal controllers with a reduced parametric sensitivity are offered because the optimization problems are defined such that to minimize the objective functions.

Solving the optimization problems specific to the optimal tuning of fuzzy controllers is a complex task due to the complicated expressions of the objective functions and the risk of getting trapped in local minima situations. This depends on the processes and on the fuzzy controller structures, with suggestive examples discussed in [Prei97], [Pre99], [Pre04], [Prei02], [Fen06], [Prei06], [Lin11], [Oh11],

[Pre11a], [Teo12], [Ang13], [Bla13], [Joe13], [Moh14]. In order to reduce the computational cost for minimizing these objective functions nature-inspired algorithms can be used due to their derivative-free characteristic. Additionally, the use of these nature-inspired algorithms to optimally tune the parameters of fuzzy controllers can offer the following advantages: reduced running costs, transparency in the design, low-cost design and implementation, and gradient information replaced by actual objective function value.

The first objective of the research carried out in this thesis is the optimal tuning of fuzzy controllers using nature-inspired optimization algorithms. The optimization problems are defined such that to include objective functions that ensure the sensitivity reduction with respect to the parametric variations of the controlled processes.

The problem of fuzzy modeling by means of Takagi-Sugeno (T-S) fuzzy models has been approached in the recent literature. The models can be considered in the general framework of fuzzy models for several processes [Joh10], [Vas10], [Hab10]. Some representative applications will be discussed as follows. By analyzing the braking process and the dynamic model of vehicle and wheel behavior, a T-S fuzzy model of deceleration in proposed in [Zhe11]. Using the computation of minimum and maximum values of input variables and the local linearization at several operating points, two discrete time dynamic T-S fuzzy models of Anti-lock Braking System (ABS) processes are proposed in [Pre12c], based on the modal equivalence principle [Gal95] and on the sector nonlinearity approach [Oht01].

A fuzzy neural network that contains sensor intelligence in order to estimate the true gap in a range of temperature after training is suggested in [Yon11]. A linear T-S fuzzy model obtained using a linear self-constructing neural fuzzy inference network applied to an optimal fuzzy controller is introduced in [Yu03] to model a nonlinear magnetic bearing system. A design method of T-S fuzzy models for magnetic bearing of high-speed motors is described in [Wan10] in the context of parallel distributed compensation controllers. An analysis concerning the stability of T-S fuzzy control systems controlling Single Input-Single Output nonlinear time-varying system is presented in [Pre11f].

The very good quality of T-S fuzzy models is necessary for both fuzzy modeling and describing the dynamics and nonlinearities of nonlinear dynamic processes, and for getting simple models that are useful in the model-based design of fuzzy controllers. Once the fuzzy models are obtained, several approaches are given in the literature to improve their quality (i.e., performance) by optimally tuning the parameters of these models, on the bases of the appropriate definition of optimization problems that target the minimization of objective functions in order to reduce as much as possible the modeling errors.

Taking into account the structure of fuzzy models, several parameters of each of the modules of these models can be optimally tuned: parameters from the fuzzification module, parameters from the inference engine (including the rule base and the rule antecedents of T-S fuzzy models), and parameters from the defuzzification module. Applications on optimal tuning of fuzzy models concern the tuning of the parameters of input membership functions in fuzzy control systems for general nonlinear systems [Liu00], the optimization of the parameters in the rule antecedents and consequents of Takagi-Sugeno fuzzy models [Alm10], the optimal tuning of the rule base and of the parameters in the inference engine [Bod05], the optimization of the fuzzy rule base [Cab06], and the reduction of the rule base and inference engine of fuzzy controllers [Pir13].

The second objective of the research carried out in this thesis is the optimal tuning of the parameters of the input membership functions of the dynamic fuzzy models of processes using nature-inspired optimization algorithms. The optimization problems are defined such that to include objective functions that ensure the reduction of the modeling errors towards the minimization of the objective functions. The thesis will be focused on the optimal tuning of some parameters of the input membership functions of T-S fuzzy models.

The latest solutions for solving optimization problems comprising parameter tuning of fuzzy controllers and fuzzy models are built upon nature-inspired optimization algorithms that include Simulated Annealing (SA) [Pre11c], [Pre12b], Particle Swarm Optimization (PSO) [Oh11], [Pre13a], Gravitational Search Algorithms (GSAs) [Dav13], [Pre13b], Charged System Search (CSS) algorithms [Pre14c], genetic algorithms [Oni12], Ant Colony Optimization [Cha12]. These solutions comprise both objectives of the thesis.

1.2 THESIS OVERVIEW

This thesis is organized in five chapters. A brief description of these chapters is presented in the following section:

Chapter 1 contains the introduction in which the motivation for the presented research is described.

Chapter 2 introduces in the first part an original design and tuning method for Takagi-Sugeno proportional-integral fuzzy controllers for nonlinear servo systems with a reduced parametric sensitivity. The class of nonlinear servo systems is structured as a series connection of second-order dynamics with an integral component, and saturation and dead zone static nonlinearity placed on the process input.

The design method ensures the parameter tuning of the fuzzy controllers by solving four types of optimization problems, which constitute the goal of this thesis, using nature-inspired optimization algorithms. The optimization problems are defined along with their corresponding objective functions and the required constraint. The rationale for employing nature-inspired algorithms for solving the optimization problems contained by the proposed design method is supported by a bibliographic research in the second part of the chapter.

In **Chapter 3** nature-inspired algorithm based solutions are proposed for solving the optimizations problems defined in the previous chapter. The seven algorithms used here contain four standard algorithm versions of: Simulated Annealing, Particle Swarm Optimization, Gravitational Search Algorithms and Charged System Search; one hybrid algorithm based on Particle Swarm Optimization and Gravitational Search Algorithm and two adaptive versions of Gravitational Search Algorithms and Charged System Search algorithms which use parameter variations based on a learning model. The implementation of these nature-inspired algorithms is carried out according to the fourth step of the novel design method dedicated to the Takagi-Sugeno PI-fuzzy controllers described in Chapter 2.

The results corresponding to each of the optimization problems obtained as a result of several simulation runs are synthetized with complete values of the optimal controller tuning parameters and the minimum values of the objective functions. Along with these simulation results, experimental results are presented, for each proposed nature-inspired algorithm-based solution, in order to validate the

proposed method. The search process is portrayed for each solution by a number of illustrations presenting the evolution of exploration agents. The quality of the obtained results is evaluated using three original performance indices which assess the convergence of the solution by monitoring the mean value of the objective function during a number of algorithm runs, the average number of required algorithm steps for convergence speed and an accuracy index to evaluate the precision of the solution.

Chapter 4 is dedicated to solving two optimization problems concerning the input membership functions of Takagi-Sugeno models initially obtained by the modal equivalence principle. The Takagi-Sugeno models are applied to two laboratory equipment setups: an anti-lock braking system and a magnetic levitation system. The modeling approach used in this chapter employs Simulated Annealing algorithm to optimize the parameters of Takagi-Sugeno fuzzy models.

The proposed modelling approach is different to other approaches because it starts with the first-principle mathematical model of the process and it offers a strong advantage by the verification of the performance of the optimal Takagi-Sugeno fuzzy models in terms of real-time experiments on two types of laboratory equipment. Another important aspect of the proposed modeling approach is its applicability to a wide category of industrial applications with suitable generalizations of reduced complexity degree. Although this modelling approach cannot guarantee that the global minimum of objective functions is reached, a considerable decrease of objective functions values was observed during the real-time experiments, clearly indicating the performance improvement offered by the optimally tuned Takagi-Sugeno fuzzy models.

Chapter 5 addresses three categories of problems by restating and synthesizes the conclusions drawn in the previous chapters of this thesis and adding new information. First, the new contributions proposed in this thesis are presented. Second, the future research directions are pointed out. Third, the dissemination of results is offered, by giving the list of papers, their impact factors and indexing in several international databases and by highlighting the independent citations of these papers and the impact factors.

2. PROBLEM SETTING CONCERNING THE OPTIMAL TUNING OF FUZZY CONTROLLERS WITH A REDUCED PROCESS PARAMETRIC SENSITIVITY

2.1. CONTROL SYSTEM MODELS, SENSITIVITY MODELS AND DEFINITIONS OF OPTIMIZATION PROBLEMS

The fuzzy control system structure is presented in Fig. 2.1 as a set-point filter fuzzy control system structure derived from [Pre09a], where FC is the fuzzy controller, P is the process, F is the set-point filter, r is the reference input (the set-point), r_1 is the filtered reference input, d is the disturbance input, y is the controlled output, u is the control signal, e is the control error:

$$e = r_1 - y \,, \tag{2.1}$$

$\boldsymbol{\alpha} = [\alpha_1 \quad \alpha_2 \quad \dots \quad \alpha_{m_P}]^T \in \mathbf{R}^{m_P}$ is the process parameter vector with the elements $\alpha_\tau,\ \tau = 1 \dots m_P$, which are the parameters of the process, $\boldsymbol{\rho} = [\rho_1 \quad \rho_2 \quad \dots \quad \rho_q]^T \in \mathbf{R}^q$ is the controller parameter vector with the elements $\rho_\gamma,\ \gamma = 1 \dots q$, which are the tuning parameters of the controller and the filter parameters can be included in this vector as indicated in Fig. 2.1, and the superscript T indicates the matrix transposition. The fuzzy control system structure presented in Fig. 2.1 belongs to the two-degree-of-freedom (2-DOF) control system structures.

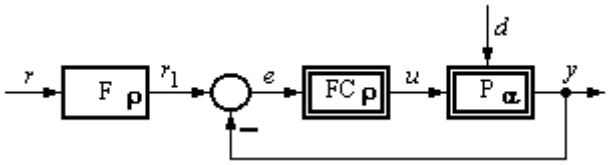

Fig. 2.1. Structure of set-point filter fuzzy control system.

As shown in [Ara03], [Vis04], [Vra11], [Ala12], [Gha12], [Hu12], [Iwa12], [Kan12], [Pel12], [Sza12], [Vil12], [Kum13], the 2-DOF control system structures (with PI and PID controllers) have an advantage over the one-degree-of-freedom (1-DOF) control system structures by high performance in reference input tracking and regulation in the presence of disturbance inputs. The main drawback of 2-DOF linear controllers is that the overshoot reduction is paid by a slower response with respect to the reference input. Several ways to introduce this additional block in

fuzzy control systems are presented in [Pre09a] and [Pre11a]. The introduction of fuzzy logic in 2-DOF control system structures leads to improved control system performance indices in both tracking and regulation; very good results in different applications are reported in [Prei10], [Dra11a], [Liu12], [Sil12], [Sti12a], [Sti12b], [Pre13a].

This thesis will consider a crisp set-point filter F. The set-point filter can be considered as a fuzzy logic block as well and accordingly designed and tuned, but this will represent a direction of future research. Fig. 2.1 highlights the linear set-point filter F, the fuzzy controller FC as a nonlinear system and the nonlinear process P.

The process is represented by the Single Input-Single Output (SISO) discrete-time state-space model [Pre13a]:

$$\begin{aligned} \mathbf{x}_P(t_d+1) &= \mathbf{f}_{Pd}(\mathbf{x}_P(t_d),\boldsymbol{\alpha},u(t_d),d(t_d)),\\ y(t_d) &= g_{Pd}(\mathbf{x}_P(t_d),\boldsymbol{\alpha},d(t_d)),\\ \mathbf{x}_P(t_{d0}) &= \mathbf{x}_{P0}, \end{aligned} \tag{2.2}$$

where $t_{d0}\in\mathbf{N}$ is the initial time moment, $t_d,\ t_d\in\mathbf{N}$, $t_d\geq t_{d0}$, is the discrete time argument, $\mathbf{x}_P=[x_{P,1}\quad x_{P,2}\quad \dots\quad x_{P,n}]^T\in\mathbf{R}^n$ is the state vector of the process, $\mathbf{x}_{P0}\in\mathbf{R}^n$ is the initial state vector of the process, and the functions $\mathbf{f}_{Pd}:\mathbf{R}^{n+m_P+2}\to\mathbf{R}^n$ and $g_{Pd}:\mathbf{R}^{n+m_P+1}\to\mathbf{R}$ are differentiable with respect to the parameter $\alpha_\tau,\ \tau=1\dots m_P$. The state-space models presented in (2.2) is a nonlinear model without direct feedthrough, and it can be obtained from a SISO continuous-time state-space model accepting that the inputs *u* and *d* are changing at the discrete sampling intervals, i.e., accepting the presence of the zero-order hold (ZOH).

The set-point filter is modeled by the following nonlinear SISO discrete-time state-space model that can be also derived from a SISO continuous-time state-space model:

$$\begin{aligned} \mathbf{x}_F(t_d+1) &= \mathbf{f}_{Fd}(\mathbf{x}_F(t_d),\boldsymbol{\rho},r(t_d)),\\ r_1(t_d) &= g_{Fd}(\mathbf{x}_F(t_d),\boldsymbol{\rho},r(t_d)),\\ \mathbf{x}_F(t_{d0}) &= \mathbf{x}_{F0}, \end{aligned} \tag{2.3}$$

where $\mathbf{x}_F=[x_{F,1}\quad x_{F,2}\quad \dots\quad x_{F,n_F}]^T\in\mathbf{R}^{n_F}$ is the state vector of the set-point filter and $\mathbf{x}_{F0}\in\mathbf{R}^{n_F}$ is the initial state vector of the set-point filter. The functions $\mathbf{f}_{Fd}:\mathbf{R}^{n_F+q+1}\to\mathbf{R}^{n_F}$ and $g_{Fd}:\mathbf{R}^{n_F+q+1}\to\mathbf{R}$ should contribute to the assurance of the differentiability of state-space model of the fuzzy control system with respect to the parameter $\alpha_\tau,\ \tau=1\dots m_P$.

The fuzzy controller is characterized by the general nonlinear SISO discrete-time state-space model:

$$\begin{aligned} \mathbf{x}_C(t_d+1) &= \mathbf{f}_{Cd}(\mathbf{x}_C(t_d),\boldsymbol{\rho},e(t)),\\ u(t_d) &= g_{Cd}(\mathbf{x}_C(t_d),\boldsymbol{\rho},e(t_d)),\\ \mathbf{x}_C(t_{d0}) &= \mathbf{x}_{C0}, \end{aligned} \tag{2.4}$$

where $\mathbf{x}_C=[x_{C,1}\quad x_{C,2}\quad \dots\quad x_{C,n_C}]^T\in\mathbf{R}^{n_C}$ is the state vector of the controller, $\mathbf{x}_{C0}\in\mathbf{R}^{n_C}$ is the initial state vector of the controller. The functions $\mathbf{f}_{Cd}:\mathbf{R}^{n_C+q+1}\to\mathbf{R}^{n_C}$ and $g_{Cd}:\mathbf{R}^{n_C+q+1}\to\mathbf{R}$ in the model (2.4) should also contribute to the assurance of

the differentiability of state-space model of the fuzzy control system with respect to the parameter $\alpha_\tau,\ \tau = 1...m_P$. Moreover, the convergence of the objective functions requires that the controller should have an integral component in order to ensure the zero steady-state value of the control error *e* for several types of disturbance inputs.

The state vector of the process $\mathbf{x}_P$, the state vector of the controller $\mathbf{x}_C$ and the state vector of the set-point filter $\mathbf{x}_F$ are grouped in the state vector of the control system **x**:

$$\mathbf{x} = \begin{bmatrix} \mathbf{x}_P \\ \mathbf{x}_C \\ \mathbf{x}_F \end{bmatrix} = [x_1 \quad x_2 \quad \dots \quad x_{n+n_C+n_F}]^T \in \mathbf{R}^{n+n_C+n_F},$$
$$x_\upsilon = \begin{cases} x_{P,\upsilon}, & \text{if } \upsilon = 1...n, \\ x_{C,\upsilon-n}, & \text{if } \upsilon = n+1...n+n_C, \\ x_{F,\upsilon-n-n_C}, & \text{if } \upsilon = n+n_C+1...n+n_C+n_F, \end{cases} \quad \upsilon = 1...n+n_C+n_F. \tag{2.5}$$

The state-space models (2.2) – (2.4) are merged using equations (2.1) and (2.5). This leads to the following discrete-time state-space model of the fuzzy control system:

$$\begin{aligned} &\mathbf{x}(t_d+1) \\ &= \begin{bmatrix} \mathbf{f}_{Pd}(\mathbf{x}_P(t_d),\boldsymbol{\alpha},g_{Cd}\{\mathbf{x}_C(t_d),\boldsymbol{\rho},g_{Fd}[\mathbf{x}_F(t_d),\boldsymbol{\rho},r(t_d)]-g_{Pd}[\mathbf{x}_P(t_d),\boldsymbol{\alpha},d(t_d)]\},d(t_d)) \\ \mathbf{f}_{Cd}\{\mathbf{x}_C(t_d),\boldsymbol{\rho},g_{Fd}[\mathbf{x}_F(t_d),\boldsymbol{\rho},r(t_d)]-g_{Pd}[\mathbf{x}_P(t_d),\boldsymbol{\alpha},d(t_d)]\} \\ \mathbf{f}_{Fd}(\mathbf{x}_F(t_d),\boldsymbol{\rho},r(t_d)) \end{bmatrix} \\ &= \mathbf{f}_d(\mathbf{x}(t_d),\boldsymbol{\alpha},\boldsymbol{\rho},r(t_d),d(t_d)) = [f_1(t_d) \quad f_2(t_d) \quad \dots \quad f_{n+n_C+n_F}(t_d)]^T, \\ &y(t_d) = g_{Pd}(\mathbf{x}_P(t_d),\boldsymbol{\alpha},d(t_d)) = h_{Pd}(\mathbf{x}(t_d),\boldsymbol{\alpha},d(t_d)), \\ &\mathbf{x}(t_{d0}) = \begin{bmatrix} \mathbf{x}_{P0} \\ \mathbf{x}_{C0} \\ \mathbf{x}_{F0} \end{bmatrix}, \end{aligned} \tag{2.6}$$

where the functions $\mathbf{f}_d : \mathbf{R}^{n+n_C+n_F+m_P+q+2} \to \mathbf{R}^{n+n_C+n_F}$ and $h_{Pd} : \mathbf{R}^{n+n_C+n_F+m_P+1} \to \mathbf{R}$ are differentiable with respect to the process parameter $\alpha_\tau,\ \tau = 1...m_P$.

The state sensitivity functions $\lambda_{\alpha_\tau,\upsilon},\ \upsilon = 1...n+n_C+n_F$, and the output sensitivity function σ_{α_τ} are defined as follows [Ros00]:

$$\lambda_{\alpha_\tau,\upsilon} = \left[\frac{\partial x_\upsilon}{\partial \alpha_\tau}\right]_{\alpha_\tau 0},\ \sigma_{\alpha_\tau} = \left[\frac{\partial y}{\partial \alpha_\tau}\right]_{\alpha_\tau 0},\ \upsilon = 1...n+n_C+n_F,\ \tau = 1...m_P, \tag{2.7}$$

where the subscript 0 indicates the nominal value of the process parameter $\alpha_\tau,\ \tau = 1...m_P$, which is subjected to variations. These variations justify the sensitivity reduction and the design and tuning of fuzzy controllers with a reduced parametric sensitivity.

Using equations (2.7) to calculate the partial derivatives in the model (2.6), the state sensitivity models of the fuzzy control system with respect to the process parameter $\alpha_\tau,\ \tau = 1...m_P$, are:

$$\lambda_{\alpha_\tau,\upsilon}(t_d+1)=\sum_{\nu=1}^{n+n_C+n_F}\{\left[\frac{\partial f_\upsilon(t_d)}{\partial x_\nu}\right]_{\alpha_\tau 0}\lambda_{\alpha_\tau,\nu}(t_d)\}+\left[\frac{\partial f_\upsilon(t_d)}{\partial \alpha_\tau}\right]_{\alpha_\tau 0},$$

$$\sigma_{\alpha_\tau}(t_d)=\sum_{\nu=1}^{n}\{\left[\frac{\partial h_{Pd}(t_d)}{\partial x_\nu}\right]_{\alpha_\tau 0}\lambda_{\alpha_\tau,\nu}(t_d)\}+\left[\frac{\partial h_{Pd}(t_d)}{\partial \alpha_\tau}\right]_{\alpha_\tau 0}, \tag{2.8}$$

$$\lambda_{\alpha_\tau,\upsilon}(t_{d0})=0,\ \upsilon=1\ldots n+n_C+n_F,\ \tau=1\ldots m_P.$$

The initial state variables are important in the analysis of the state sensitivity models (2.8).

The following discrete-time objective functions are defined to ensure the sensitivity reduction with respect to the modifications of $\alpha_\tau,\ \tau=1\ldots m_P$:

$$J_{1,\alpha_\tau}(\boldsymbol{\rho})=\sum_{t_d=0}^{\infty}\{e^2(t_d,\boldsymbol{\rho})+(\gamma_{\alpha_\tau})^2[\sigma_{\alpha_\tau}(t_d,\boldsymbol{\rho})]^2\},\ \tau=1\ldots m_P, \tag{2.9}$$

$$J_{2,\alpha_\tau}(\boldsymbol{\rho})=\sum_{t_d=0}^{\infty}\{|e(t_d,\boldsymbol{\rho})|+(\gamma_{\alpha_\tau})^2[\sigma_{\alpha_\tau}(t_d,\boldsymbol{\rho})]^2\},\ \tau=1\ldots m_P, \tag{2.10}$$

$$J_{3,\alpha_\tau}(\boldsymbol{\rho})=\sum_{t_d=0}^{\infty}\{t_d e^2(t_d,\boldsymbol{\rho})+(\gamma_{\alpha_\tau})^2[\sigma_{\alpha_\tau}(t_d,\boldsymbol{\rho})]^2\},\ \tau=1\ldots m_P, \tag{2.11}$$

$$J_{4,\alpha_\tau}(\boldsymbol{\rho})=\sum_{t_d=0}^{\infty}\{t_d\,|e(t_d,\boldsymbol{\rho})|+(\gamma_{\alpha_\tau})^2[\sigma_{\alpha_\tau}(t_d,\boldsymbol{\rho})]^2\},\ \tau=1\ldots m_P, \tag{2.12}$$

where $\gamma_{\alpha_\tau},\ \tau=1\ldots m_P$, are the weighting parameters. The objective function $J_{1,\alpha_\tau}(\boldsymbol{\rho})$ is referred to as the sum of squared control errors plus squared output sensitivity function, the objective function $J_{2,\alpha_\tau}(\boldsymbol{\rho})$ is referred to as the sum of absolute control errors plus squared output sensitivity function, the objective function $J_{3,\alpha_\tau}(\boldsymbol{\rho})$ is referred to as the sum of squared control errors multiplied by time plus squared output sensitivity function, and the objective function $J_{4,\alpha_\tau}(\boldsymbol{\rho})$ is referred to as the sum of absoluter control errors multiplied by time plus squared output sensitivity function. The vector variable of the objective functions $\boldsymbol{\rho}$ will be omitted in the sequel in certain situations for the sake of simplicity.

The convergence of the objective functions defined in (2.9) – (2.12) requires that the steady-state values of the functions in the right-hand terms should be zero. Since the zero steady-state value of the control error *e* for several types of disturbance inputs is guaranteed by controllers with an integral component, the zero steady-state value of the output sensitivity function σ_{α_τ} is also necessary.

In practical control problem solutions the sums in (2.9) – (2.12) should be truncated such that to capture all transients of the fuzzy control systems during the time horizon. The time horizon should include the moments when the objective functions reach their steady-state values. The upper limit of the sum depends on the dynamics of the particular process under consideration.

The minimization of the objective functions defined in (2.9) – (2.12) aims the sensitivity reduction, and it is expressed in terms of the optimization problems:

$$\boldsymbol{\rho}^* = \arg\min_{\boldsymbol{\rho}\in D_{\boldsymbol{\rho}}} J_{1,\alpha_\tau}(\boldsymbol{\rho}),\ \tau = 1...m_P\,, \tag{2.13}$$

$$\boldsymbol{\rho}^* = \arg\min_{\boldsymbol{\rho}\in D_{\boldsymbol{\rho}}} J_{2,\alpha_\tau}(\boldsymbol{\rho}),\ \tau = 1...m_P\,, \tag{2.14}$$

$$\boldsymbol{\rho}^* = \arg\min_{\boldsymbol{\rho}\in D_{\boldsymbol{\rho}}} J_{3,\alpha_\tau}(\boldsymbol{\rho}),\ \tau = 1...m_P\,, \tag{2.15}$$

$$\boldsymbol{\rho}^* = \arg\min_{\boldsymbol{\rho}\in D_{\boldsymbol{\rho}}} J_{4,\alpha_\tau}(\boldsymbol{\rho}),\ \tau = 1...m_P\,, \tag{2.16}$$

where $\boldsymbol{\rho}^*$ is the optimal controller parameter vector, i.e., the optimal value of the vector $\boldsymbol{\rho}$, and $D_{\boldsymbol{\rho}}$ is the feasible domain of $\boldsymbol{\rho}$. Several constraints including the stability of the fuzzy control system can be imposed and expressed by means of $D_{\boldsymbol{\rho}}$. Such constraints can be expressed as several stability conditions that are derived generally for nonlinear systems [Pas04], [Dan05], [Pre06a], [Pre07], [Bla10], [Hot10], [Li10], [Bla11], [Vil13], or specifically for fuzzy control systems with Mamdani fuzzy controllers [Pre97], [Sug99], [Pre06b], [Liu10b], or with Takagi-Sugeno fuzzy controllers [Skr05], [Fen06], [Pre09c], [Pre11a], [Pre13e], [Cha14], or they can account for various regimes of the control systems [Car05], [Fil08], [Fil09], [Dan11], [Wan12b], [Fer13], [Hus13], [Cor14], [Wu14].

This thesis will consider only the output sensitivity functions in the objective functions (2.9) – (2.12). The state sensitivity functions can be considered as well, and this represents a direction of future research.

Let the process as part of servo systems be characterized by the following nonlinear continuous-time time-invariant Single Input-Single Output (SISO) state-space model which defines a rather general class of servo systems:

$$m(t) = \begin{cases} -1, & \text{if } u(t) \le -u_b, \\ \dfrac{u(t)+u_c}{u_b-u_c}, & \text{if } -u_b < u(t) < -u_c, \\ 0, & \text{if } -u_c \le |u(t)| \le u_a, \\ \dfrac{u(t)-u_a}{u_b-u_a}, & \text{if } u_a < u(t) < u_b, \\ 1, & \text{if } u(t) \ge u_b, \end{cases}$$

$$\dot{\mathbf{x}}_P(t) = \begin{bmatrix} 0 & 1 \\ 0 & -1/T_\Sigma \end{bmatrix} \mathbf{x}_P(t) + \begin{bmatrix} 0 \\ k_P/T_\Sigma \end{bmatrix} m(t) + \begin{bmatrix} 1 \\ 0 \end{bmatrix} d(t), \tag{2.17}$$

$$y(t) = [1 \quad 0]\,\mathbf{x}_P(t),$$

where t is the continuous time argument, $t \in \mathbf{R},\ t \ge 0$, k_P is the process gain, T_Σ is the small time constant, the control signal u is a pulse width modulated duty cycle, and m is the output of the saturation and dead zone static nonlinearity specific to the actuator. The nonlinearity is modeled by the first equation in (2.17) with the parameters u_a, u_b and u_c, with $0 < u_a < u_b$, $0 < u_c < u_b$. The state-space model (2.17) includes the actuator and measuring element dynamics. The state vector $\mathbf{x}_P(t)$ is expressed as follows in (angular) position applications for $n = 2$:

$$\mathbf{x}_P(t) = [x_{P,1}(t) \quad x_{P,2}(t)]^T = [\alpha(t) \quad \omega(t)]^T\,, \tag{2.18}$$

where $\alpha(t)$ is the angular position and $\omega(t)$ is the angular speed. The process structure is illustrated in Fig. 2.2.

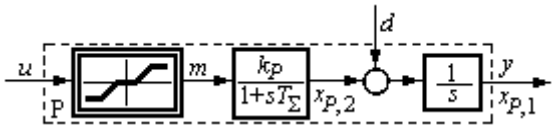

Fig. 2.2. Structure of process with saturation and dead zone static nonlinearity.

The nonlinearity in (2.17) is neglected in the following simplified model of the process expressed as the transfer function $P(s)$:

$$P(s) = k_{EP} /[s(1 + T_\Sigma s)] . \tag{2.19}$$

This transfer function is considered for *u* as input and *y* as output. The equivalent process gain is k_{EP}:

$$k_{EP} = \begin{cases} \dfrac{k_P}{u_b - u_c}, & \text{if } -u_b < u(t) < -u_c, \\ \dfrac{k_P}{u_b - u_a}, & \text{if } u_a < u(t) < u_b. \end{cases} \tag{2.20}$$

Therefore, $P(s)$ can be used in the controller design and tuning in two cases out of the five cases concerning the nonlinearity in (2.17).

The process models (2.17) and (2.19) can be employed in the control designs of servo systems in various applications accepting that the parameters k_P and T_Σ depend on the operating point. Therefore, the design of control systems with a reduced parametric sensitivity with respect to k_P and T_Σ is justified. In this context, $m_P = 2$, and the process parameter vector obtains the following particular expression in the design of control systems with a reduced process parametric sensitivity for this class of servo systems:

$$\boldsymbol{\alpha} = [\alpha_1 \quad \alpha_2]^T, \ \alpha_1 = k_P, \ \alpha_2 = T_\Sigma . \tag{2.21}$$

As shown in [Ast95], [Prei99], [Pre09a], the PI controllers can cope with the process modeled in (2.19) if they are inserted in 2-DOF linear control system structures as that shown in Fig. 2.1 with a PI controller instead of FC. The transfer function of the PI controller is:

$$C(s) = k_c(\frac{1 + sT_i}{s}) = k_C(1 + \frac{1}{sT_i}), \ k_C = k_c T_i , \tag{2.22}$$

where k_c is the controller gain and T_i is the integral time constant. The PI controllers can be tuned by the Extended Symmetrical Optimum (ESO) method [Prei99] to guarantee a desired compromise to the performance specifications (i.e., maximum values of control system performance indices) imposed to the control system using a single design parameter referred to as β, with the recommended values within $1 < \beta \le 20$. The diagrams presented in Fig. 2.3 can be used in setting the value of the design parameter β and, therefore, the compromise to the control system performance indices expressed as percent overshoot $\sigma_1[\%]$, settling time t_s and rise time t_r.

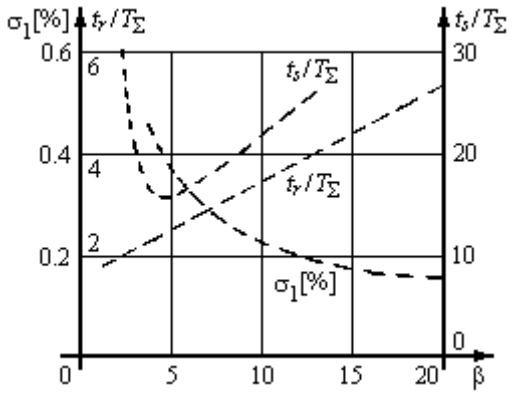

Fig. 2.3. Control system performance indices with respect to reference input versus design parameter β in the ESO method.

The PI tuning conditions specific to the ESO method are:

$$k_c = 1/(\beta\sqrt{\beta}\,k_{EP}\,T_\Sigma^2),\ T_i = \beta T_\Sigma,\ k_C = 1/(\sqrt{\beta}\,k_{EP}\,T_\Sigma)\ . \tag{2.23}$$

Fig. 2.3 is important because both possible values of k_{EP} according to (2.20) should be used in setting certain values of β which ensure the fulfillment of the performance specifications imposed to the control system. A simple version of set-point filter which ensures the performance improvement of the linear control system by the cancellation of a zero in the closed-loop transfer function with respect to the reference input is:

$$F(s) = 1/(1+\beta T_\Sigma s)\ . \tag{2.24}$$

The Takagi-Sugeno PI-fuzzy controllers (T-S PI-FCs) are designed starting with the linear PI controllers such that to ensure the further improvement of the control system performance indices for the nonlinear process modeled in (2.17). The structure and the input membership functions of a simple T-S PI-FC are presented in Fig. 2.4, where q^{-1} is the backward shift operator.

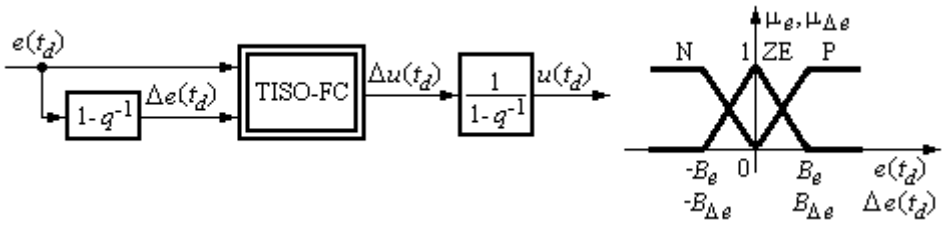

Fig. 2.4. Structure and input membership functions of Takagi-Sugeno PI-fuzzy controller.

More membership functions can be defined but they complicate the rule base. One solution to deal with such situations while focusing on the design of simple fuzzy controllers is represented by fuzzy rule interpolation [Bar95], [Bar96], [Koc97], [Yam06], [Joh10].

Fig. 2.4 points out the increment of control error $\Delta e(t_d) = e(t_d) - e(t_d - 1)$ and the increment of control signal $\Delta u(t_d) = u(t_d) - u(t_d - 1)$. These increments offer the dynamics of the T-S PI-FC and they result from discretizing the continuous-time PI controller. Tustin's method leads to the incremental form of the discrete-time PI controller:

$$\Delta u(t_d) = K_P[\Delta e(t_d) + \mu\, e(t_d)], \tag{2.25}$$

and to its parameters:

$$K_P = k_c(T_i - \frac{T_s}{2}),\ \mu = \frac{2\,T_s}{2\,T_i - T_s}, \tag{2.26}$$

where T_s is the sampling period set in accordance with the requirements of quasi-continuous digital control [Ise89].

The Two Inputs-Single Output fuzzy controller (TISO-FC) block presented in Fig. 2.4 is characterized by the weighted average method in the defuzzification module, and by the SUM and PROD operators in the inference engine. The rule base of the TISO-FC block is formulated as the decision table presented in Table 2.1, and the consequents of the fuzzy control rules are modeled by means of the two functions:

$$f_{C1}(t_d) = K_P[\Delta e(t_d) + \mu\, e(t_d)],\ f_{C2}(t_d) = \eta\, f_{C1}(t_d). \tag{2.27}$$

The parameter η is introduced in (2.27) to reduce the overshoot of the fuzzy control system when $e(t_d)$ and $\Delta e(t_d)$ have the same signs. Fig. 2.4 and Table 2.1 point out the tuning parameters of these simple T-S PI-FCs: β (for the linear part of the controllers design), and B_e, $B_{\Delta e}$ and η (for the fuzzy part of the controllers design).

The rule base presented in Table 2.1 can be formulated such that to contain only two rules because the tuning of simple T-S PI-FCs is targeted. The simplicity is ensured by the reduced number of input membership functions shown in Fig. 2.4, by the symmetry of the rule base and by the simple design method dedicated to T-S PI-FCs.

Table 2.1. Decision table of TISO-FC block.

$\Delta e(t)$	$e(t)$		
	N	ZE	P
P	$\Delta u(t_d) = f_{C1}(t_d)$	$\Delta u(t_d) = f_{C1}(t_d)$	$\Delta u(t_d) = f_{C2}(t_d)$
ZE	$\Delta u(t_d) = f_{C1}(t_d)$	$\Delta u(t_d) = f_{C1}(t_d)$	$\Delta u(t_d) = f_{C1}(t_d)$
N	$\Delta u(t_d) = f_{C2}(t_d)$	$\Delta u(t_d) = f_{C1}(t_d)$	$\Delta u(t_d) = f_{C1}(t_d)$

The modal equivalence principle [Gal95] results in the following tuning equation, which reduces the number of tuning parameters of the T-S PI-FC:

$$B_{\Delta e} = \mu\, B_e. \tag{2.28}$$

The application of the ESO method and of the modal equivalence principle yields only three tuning parameters for the T-S PI-FCs, $q = 3$. These parameters are included in the controller parameter vector involved in the optimization problems defined in (2.13) – (2.16):

$$\boldsymbol{\rho} = [\rho_1 \quad \rho_2 \quad \rho_3]^T,\ \rho_1 = \beta,\ \rho_2 = B_e,\ \rho_3 = \eta\ . \tag{2.29}$$

The design method dedicated to the simple T-S PI-FCs with the previously defined structure consists of the following steps that result in the optimal controller parameter vector $\boldsymbol{\rho}^*$ obtained by nature-inspired algorithms:

Step 1. Apply the ESO method to tune the parameters of continuous-time linear PI controllers, set the sampling period, apply Tustin's method that leads to (2.26), derive the state sensitivity models with respect to k_P and T_Σ, and insert the sensitivity models in the fuzzy control system structure involved in simulations and experiments in order to evaluate the objective functions.

Step 2. Set the weighting parameters $\gamma_{\alpha_\tau},\ \tau = 1..m_P$, the objective functions defined in (2.9) – (2.12), to meet the performance specifications of fuzzy control systems, set t_{df} to replace infinity in (2.9) – (2.12) such that the finite time horizon includes all transients of the fuzzy control systems until the objective functions reach the steady-state values, and set the feasible domains $D_{\boldsymbol{\rho}}$ to include all constraints imposed to the elements of $\boldsymbol{\rho}$.

Step 3. Map the optimization problems (2.13) – (2.16) onto the nature-inspired algorithms.

Step 4. Apply the nature-inspired algorithms that give the optimal parameter vector $\boldsymbol{\rho}^*$ and the optimal parameters:

$$\boldsymbol{\rho}^* = [\rho_1^* \quad \rho_2^* \quad \rho_3^*]^T,\ \beta^* = \rho_1^*,\ B_e^* = \rho_2^*,\ \eta^* = \rho_3^*\ , \tag{2.30}$$

and next the following tuning condition obtained from (2.28) using (2.23) and (2.26) for the optimal controller parameters:

$$B_{\Delta e}^* = \frac{2T_s}{2\beta^* T_\Sigma - T_s} B_e^*\ . \tag{2.31}$$

Several details concerning the application of this design method will be presented as follows. These details represent also the preparation for the implementation of the nature-inspired algorithms involved in the steps 3 and 4.

Accepting that the inputs *u* and *d* are changing at the discrete sampling intervals, the following discrete-time state-space model of the process is obtained from (2.17):

$$m(t_d) = \begin{cases} -1, & \text{if } u(t_d) \le -u_b, \\ \dfrac{u(t_d)+u_c}{u_b-u_c}, & \text{if } -u_b < u(t_d) < -u_c, \\ 0, & \text{if } -u_c \le |u(t_d)| \le u_a, \\ \dfrac{u(t_d)-u_a}{u_b-u_a}, & \text{if } u_a < u(t_d) < u_b, \\ 1, & \text{if } u(t_d) \ge u_b, \end{cases}$$

$$x_{P,1}(t_d+1) = x_{P,1}(t_d) + T_\Sigma[1-\exp(-\frac{T_s}{T_\Sigma})]x_{P,2}(t_d)$$

$$+ k_P[T_s + T_\Sigma \exp(-\frac{T_s}{T_\Sigma}) - T_\Sigma]m(t_d) + T_s d(t_d), \tag{2.32}$$

$$x_{P,2}(t_d+1) = [\exp(-\frac{T_s}{T_\Sigma})]x_{P,2}(t_d) + k_P[1-\exp(-\frac{T_s}{T_\Sigma})]m(t_d),$$

$$y(t_d) = x_{P,1}(t_d).$$

The state-space model (2.32) is a particular expression of the state-space model (2.2). The discretization of the process model given in (2.17) is done such that the models (2.17) and (2.32) should exhibit the same response at the discrete time moments defined by the discrete sampling intervals. The choice of T_s depends on the time constant(s) of the process, and it should fulfill, as mentioned before, the conditions of quasi-continuous digital control.

The derivation of the state-space model of the T-S PI-FC is supported by the definition of the state variables $x_{C,1}$ and $x_{C,2}$:

$$\begin{aligned} x_{C,1}(t_d) &= u(t_d - 1), \\ x_{C,2}(t_d) &= e(t_d - 1). \end{aligned} \tag{2.33}$$

These two state variables ($n_C = 2$ in the general state-space model (2.4)) are highlighted in Fig. 2.5. Fig. 2.5 and (2.33) are used in the derivation of the following discrete-time state-space model of the T-S PI-FC:

$$\begin{aligned} x_{C,1}(t_d + 1) &= x_{C,1}(t_d) + f_{FC}(e(t_d), e(t_d) - x_{C,2}(t_d)), \\ x_{C,2}(t_d + 1) &= e(t_d), \\ u(t_d) &= x_{C,1}(t_d) + f_{FC}(e(t_d), e(t_d) - x_{C,2}(t_d)), \end{aligned} \tag{2.34}$$

where the nonlinear input-output map of the TISO-FC block is:

$$\begin{aligned} & f_{FC} : \mathbf{R}^2 \to \mathbf{R},\ f_{FC}(e(t_d), \Delta e(t_d)) \\ & = f_{FC}(r_1(t_d) - x_{P,1}(t_d), r(t_d) - x_{P,1}(t_d) - x_{C,2}(t_d)). \end{aligned} \tag{2.35}$$

The state-space model (2.34) is a particular expression of (2.4).

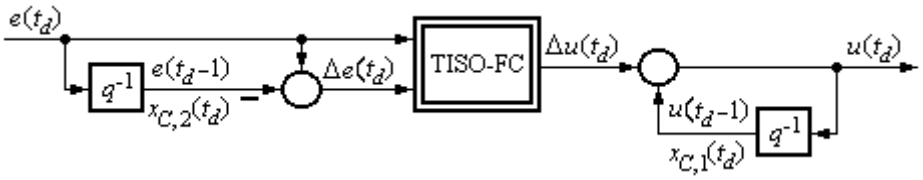

Fig. 2.5. Equivalent structure of Takagi-Sugeno PI-fuzzy controller.

Introducing the state variable of the filter x_F, the continuous-time state-space model of the set-point filter with the transfer function defined in (2.24) is:

$$\begin{aligned} \dot{x}_F(t) &= -(\frac{1}{\beta T_\Sigma})x_F(t) + (\frac{1}{\beta T_\Sigma})r(t), \\ r_1(t) &= x_F(t), \end{aligned} \tag{2.36}$$

because $n_F = 1$ in (2.3). Accepting again that the inputs *u* and *d* are changing at the discrete sampling intervals, the following discrete-time state-space model of the set-point filter results from (2.36):

$$\begin{aligned} x_F(t_d + 1) &= \exp(-\frac{T_s}{\beta T_\Sigma})x_F(t_d) + [1 - \exp(-\frac{T_s}{\beta T_\Sigma})]r(t_d), \\ r_1(t_d) &= x_F(t_d). \end{aligned} \tag{2.37}$$

The state-space model (2.37) is a particular expression of (2.3).

The state vector **x** of the control system is next obtained by merging the state variables of the process, of the T-S PI-FC and of the set-point filter:

$$\mathbf{x} = [x_1 \quad x_2 \quad x_3 \quad x_4 \quad x_5]^T = [\mathbf{x}_P^T \quad \mathbf{x}_C^T \quad \mathbf{x}_F^T] = [x_{P,1} \quad x_{P,2} \quad x_{C,1} \quad x_{C,2} \quad x_F]^T . \tag{2.38}$$

Equation (2.38) is a particular expression of equation (2.5) for $n + n_C + n_F = 2 + 2 + 1 = 5$.

Using the control system structure given in Fig. 2.1, the equations (2.32), (2.33) and (2.37), and the notations defined in (2.38), the expression of $e(t_d)$ and $\Delta e(t_d)$ are:

$$\begin{aligned} e(t_d) &= r_1(t_d) - x_1(t_d) = x_5(t_d) - x_1(t_d), \\ \Delta e(t_d) &= e(t_d) - e(t_d - 1) = x_5(t_d) - x_1(t_d) - x_4(t_d). \end{aligned} \tag{2.39}$$

The expression of the control signal results from (2.34) and (2.39):

$$u(t_d) = x_3(t_d) + f_{FC}(x_5(t_d) - x_1(t_d), x_5(t_d) - x_1(t_d) - x_4(t_d)) . \tag{2.40}$$

The state-space models of the process, of the T-S PI-FC and of the set-point filter expressed in (2.32), (2.34) and (2.37), with the set-point filter considered for the nominal process parameter $T_{\Sigma 0}$, are next merged using (2.39), (2.40) and the control system structure given in Fig. 2.1. Therefore, the discrete-time state-space model of the fuzzy control system is:

$$\begin{aligned} x_1(t_d + 1) &= x_1(t_d) + T_\Sigma[1 - \exp(-\frac{T_s}{T_\Sigma})]x_{P,2}(t_d) \\ &+ T_s d(t_d) + k_P[T_s + T_\Sigma \exp(-\frac{T_s}{T_\Sigma}) - T_\Sigma] \\ &\cdot \begin{cases} -1, & \text{if } u(t_d) \le -u_b, \\ \dfrac{x_3(t_d) + f_{FC}(x_5(t_d) - x_1(t_d), x_5(t_d) - x_1(t_d) - x_4(t_d)) + u_c}{u_b - u_c}, & \text{if } -u_b < u(t_d) < -u_c, \\ 0, & \text{if } -u_c \le\mid u(t_d) \mid\le u_a, \\ \dfrac{x_3(t_d) + f_{FC}(x_5(t_d) - x_1(t_d), x_5(t_d) - x_1(t_d) - x_4(t_d)) - u_a}{u_b - u_a}, & \text{if } u_a < u(t_d) < u_b, \\ 1, & \text{if } u(t_d) \ge u_b, \end{cases} \end{aligned} \tag{2.41}$$

$$\begin{aligned} x_2(t_d + 1) &= [\exp(-\frac{T_s}{T_\Sigma})]x_2(t_d) + k_P[1 - \exp(-\frac{T_s}{T_\Sigma})] \\ &\cdot \begin{cases} -1, & \text{if } u(t_d) \le -u_b, \\ \dfrac{x_3(t_d) + f_{FC}(x_5(t_d) - x_1(t_d), x_5(t_d) - x_1(t_d) - x_4(t_d)) + u_c}{u_b - u_c}, & \text{if } -u_b < u(t_d) < -u_c, \\ 0, & \text{if } -u_c \le\mid u(t_d) \mid\le u_a, \\ \dfrac{x_3(t_d) + f_{FC}(x_5(t_d) - x_1(t_d), x_5(t_d) - x_1(t_d) - x_4(t_d)) - u_a}{u_b - u_a}, & \text{if } u_a < u(t_d) < u_b, \\ 1, & \text{if } u(t_d) \ge u_b, \end{cases} \end{aligned} \tag{2.42}$$

$$x_3(t_d + 1) = x_3(t_d) + f_{FC}(x_5(t_d) - x_1(t_d), x_5(t_d) - x_1(t_d) - x_4(t_d)) , \tag{2.43}$$

$$x_4(t_d + 1) = x_5(t_d) - x_1(t_d) , \tag{2.44}$$

$$x_5(t_d + 1) = \exp(-\frac{T_s}{\beta T_{\Sigma 0}})x_5(t_d) + [1 - \exp(-\frac{T_s}{\beta T_{\Sigma 0}})]r(t_d) , \tag{2.45}$$

$$y(t_d) = x_1(t_d) . \tag{2.46}$$

Using the formulas (2.8) in the state-space model (2.41) – (2.46) for constant inputs of the control system, viz. $r(t) = r_0 = \text{const}$ and $d(t) = d_0 = \text{const}$, the discrete-time state sensitivity model of the fuzzy control system with respect to k_P is:

$$\lambda_{k_P,1}(t_d+1)=\lambda_{k_P,1}(t_d)+T_{\Sigma 0}[1-\exp(-\frac{T_s}{T_{\Sigma 0}})]\lambda_{k_P,2}(t_d)$$

$$+[T_s+T_{\Sigma 0}\exp(-\frac{T_s}{T_{\Sigma 0}})-T_{\Sigma 0}]$$

$$\cdot\begin{cases}-1, & \text{if } u(t_d)\le -u_b,\\ \dfrac{x_{30}(t_d)+f_{FC}(x_{50}(t_d)}{u_b-u_c}\dfrac{-x_{10}(t_d),x_{50}(t_d)-x_{10}(t_d)-x_{40}(t_d))+u_c}{}, & \text{if } -u_b<u(t_d)<-u_c,\\ 0, & \text{if } -u_c\le|u(t_d)|\le u_a,\\ \dfrac{x_{30}(t_d)+f_{FC}(x_{50}(t_d)}{u_b-u_a}\dfrac{-x_{10}(t_d),x_{50}(t_d)-x_{10}(t_d)-x_{40}(t_d))-u_a}{}, & \text{if } u_a<u(t_d)<u_b,\\ 1, & \text{if } u(t_d)\ge u_b,\end{cases}$$

$$+k_{P0}[T_s+T_{\Sigma 0}\exp(-\frac{T_s}{T_{\Sigma 0}})-T_{\Sigma 0}]$$

$$\cdot\begin{cases}0, & \text{if } u(t_d)\le -u_b,\\ \dfrac{\lambda_{k_P,3}(t_d)+\left[\dfrac{\partial f_{FC}(t_d)}{\partial e(t_d)}\right]_0(\lambda_{k_P,5}(t_d)-\lambda_{k_P,1}(t_d))}{u_b-u_c}\dfrac{+\left[\dfrac{\partial f_{FC}(t_d)}{\partial \Delta e(t_d)}\right]_0(\lambda_{k_P,5}(t_d)-\lambda_{k_P,1}(t_d)-\lambda_{k_P,4}(t_d))}{}, & \text{if } -u_b<u(t_d)<-u_c,\\ 0, & \text{if } -u_c\le|u(t_d)|\le u_a,\\ \dfrac{\lambda_{k_P,3}(t_d)+\left[\dfrac{\partial f_{FC}(t_d)}{\partial e(t_d)}\right]_0(\lambda_{k_P,5}(t_d)-\lambda_{k_P,1}(t_d))}{u_b-u_a}\dfrac{+\left[\dfrac{\partial f_{FC}(t_d)}{\partial \Delta e(t_d)}\right]_0(\lambda_{k_P,5}(t_d)-\lambda_{k_P,1}(t_d)-\lambda_{k_P,4}(t_d))}{}, & \text{if } u_a<u(t_d)<u_b,\\ 0, & \text{if } u(t_d)\ge u_b,\end{cases} \tag{2.47}$$

$$\lambda_{k_P,2}(t_d+1)=[\exp(-\frac{T_s}{T_{\Sigma 0}})]\lambda_{k_P,2}(t_d)+[1-\exp(-\frac{T_s}{T_{\Sigma 0}})]$$

$$\cdot\begin{cases}-1, & \text{if } u(t_d)\le -u_b,\\ \dfrac{x_{30}(t_d)+f_{FC}(x_{50}(t_d)}{u_b-u_c}\dfrac{-x_{10}(t_d),x_{50}(t_d)-x_{10}(t_d)-x_{40}(t_d))+u_c}{}, & \text{if } -u_b<u(t_d)<-u_c,\\ 0, & \text{if } -u_c\le|u(t_d)|\le u_a,\\ \dfrac{x_{30}(t_d)+f_{FC}(x_{50}(t_d)}{u_b-u_a}\dfrac{-x_{10}(t_d),x_{50}(t_d)-x_{10}(t_d)-x_{40}(t_d))+u_c}{}, & \text{if } u_a<u(t_d)<u_b,\\ 1, & \text{if } u(t_d)\ge u_b,\end{cases}$$

$$+k_{P0}[1-\exp(-\frac{T_s}{T_{\Sigma 0}})]$$

$$\cdot\begin{cases}0, & \text{if } u(t_d)\le -u_b,\\ \dfrac{\lambda_{k_P,3}(t_d)+\left[\dfrac{\partial f_{FC}(t_d)}{\partial e(t_d)}\right]_0(\lambda_{k_P,5}(t_d)-\lambda_{k_P,1}(t_d))}{u_b-u_c}\dfrac{+\left[\dfrac{\partial f_{FC}(t_d)}{\partial \Delta e(t_d)}\right]_0(\lambda_{k_P,5}(t_d)-\lambda_{k_P,1}(t_d)-\lambda_{k_P,4}(t_d))}{}, & \text{if } -u_b<u(t_d)<-u_c,\\ 0, & \text{if } -u_c\le|u(t_d)|\le u_a,\\ \dfrac{\lambda_{k_P,3}(t_d)+\left[\dfrac{\partial f_{FC}(t_d)}{\partial e(t_d)}\right]_0(\lambda_{k_P,5}(t_d)-\lambda_{k_P,1}(t_d))}{u_b-u_a}\dfrac{+\left[\dfrac{\partial f_{FC}(t_d)}{\partial \Delta e(t_d)}\right]_0(\lambda_{k_P,5}(t_d)-\lambda_{k_P,1}(t_d)-\lambda_{k_P,4}(t_d))}{}, & \text{if } u_a<u(t_d)<u_b,\\ 0, & \text{if } u(t_d)\ge u_b,\end{cases} \tag{2.48}$$

$$\lambda_{k_P,3}(t_d+1)=\lambda_{k_P,3}(t_d)+\left[\frac{\partial f_{FC}(t_d)}{\partial e(t_d)}\right]_0(\lambda_{k_P,5}(t_d)-\lambda_{k_P,1}(t_d))$$
$$+\left[\frac{\partial f_{FC}(t_d)}{\partial \Delta e(t_d)}\right]_0(\lambda_{k_P,5}(t_d)-\lambda_{k_P,1}(t_d)-\lambda_{k_P,4}(t_d)), \tag{2.49}$$

$$\lambda_{k_P,4}(t_d+1)=\lambda_{k_P,5}(t_d)-\lambda_{k_P,1}(t_d)\,, \tag{2.50}$$

$$\lambda_{k_P,5}(t_d+1)=\exp(-\frac{T_s}{\beta T_{\Sigma 0}})\lambda_{k_P,5}(t_d)\,, \tag{2.51}$$

$$\sigma_{k_P}(t_d)=\lambda_{k_P,1}(t_d)\,, \tag{2.52}$$

and the discrete-time state sensitivity model of the fuzzy control system with respect to T_Σ is:

$$\lambda_{T_\Sigma,1}(t_d+1)=\lambda_{T_\Sigma,1}(t_d)+T_{\Sigma 0}[1-\exp(-\frac{T_s}{T_{\Sigma 0}})]\lambda_{T_\Sigma,2}(t_d)$$
$$+[1-\exp(-\frac{T_s}{T_{\Sigma 0}})-(\frac{T_s}{T_{\Sigma 0}})\exp(-\frac{T_s}{T_{\Sigma 0}})]x_{20}(t_d)+k_{P0}[(\frac{T_s}{T_{\Sigma 0}})\exp(-\frac{T_s}{T_{\Sigma 0}})-1]$$
$$\cdot\begin{cases}-1, & \text{if } u(t_d)\le -u_b,\\ \dfrac{x_{30}(t_d)+f_{FC}(x_{50}(t_d))}{u_b-u_c}, & \text{if } -u_b<u(t_d)<-u_c,\\ \dfrac{-x_{10}(t_d),x_{50}(t_d)-x_{10}(t_d)-x_{40}(t_d))+u_c}{u_b-u_c}, & \text{if } -u_b<u(t_d)<-u_c,\\ 0, & \text{if } -u_c\le|u(t_d)|\le u_a,\\ \dfrac{x_{30}(t_d)+f_{FC}(x_{50}(t_d))}{u_b-u_a}, & \text{if } u_a<u(t_d)<u_b,\\ \dfrac{-x_{10}(t_d),x_{50}(t_d)-x_{10}(t_d)-x_{40}(t_d))-u_a}{u_b-u_a}, & \text{if } u_a<u(t_d)<u_b,\\ 1, & \text{if } u(t_d)\ge u_b,\end{cases}$$
$$+k_{P0}[T_s+T_{\Sigma 0}\exp(-\frac{T_s}{T_{\Sigma 0}})-T_{\Sigma 0}]$$
$$\cdot\begin{cases}0, & \text{if } u(t_d)\le -u_b,\\ \dfrac{\lambda_{T_\Sigma,3}(t_d)+\left[\frac{\partial f_{FC}(t_d)}{\partial e(t_d)}\right]_0(\lambda_{T_\Sigma,5}(t_d)-\lambda_{T_\Sigma,1}(t_d))}{u_b-u_c}, & \text{if } -u_b<u(t_d)<-u_c,\\ \dfrac{+\left[\frac{\partial f_{FC}(t_d)}{\partial \Delta e(t_d)}\right]_0(\lambda_{T_\Sigma,5}(t_d)-\lambda_{T_\Sigma,1}(t_d)-\lambda_{T_\Sigma,4}(t_d))}{u_b-u_c}, & \text{if } -u_b<u(t_d)<-u_c,\\ 0, & \text{if } -u_c\le|u(t_d)|\le u_a,\\ \dfrac{\lambda_{T_\Sigma,3}(t_d)+\left[\frac{\partial f_{FC}(t_d)}{\partial e(t_d)}\right]_0(\lambda_{T_\Sigma,5}(t_d)-\lambda_{T_\Sigma,1}(t_d))}{u_b-u_a}, & \text{if } u_a<u(t_d)<u_b,\\ \dfrac{+\left[\frac{\partial f_{FC}(t_d)}{\partial \Delta e(t_d)}\right]_0(\lambda_{T_\Sigma,5}(t_d)-\lambda_{T_\Sigma,1}(t_d)-\lambda_{T_\Sigma,4}(t_d))}{u_b-u_a}, & \text{if } u_a<u(t_d)<u_b,\\ 0, & \text{if } u(t_d)\ge u_b,\end{cases} \tag{2.53}$$

$$\lambda_{T_\Sigma,2}(t_d+1)=[\exp(-\frac{T_s}{T_{\Sigma 0}})]\lambda_{T_\Sigma,2}(t_d)+(\frac{T_s}{T_{\Sigma 0}^2})[\exp(-\frac{T_s}{T_{\Sigma 0}})]x_{20}(t_d)$$

$$-k_{P0}(\frac{T_s}{T_{\Sigma 0}^2})[\exp(-\frac{T_s}{T_{\Sigma 0}})]$$

$$\cdot\begin{cases}-1, & \text{if } u(t_d)\le -u_b,\\ x_{30}(t_d)+f_{FC}(x_{50}(t_d)) & \\ \dfrac{-x_{10}(t_d),x_{50}(t_d)-x_{10}(t_d)-x_{40}(t_d))+u_c}{u_b-u_c}, & \text{if } -u_b<u(t_d)<-u_c,\\ 0, & \text{if } -u_c\le|u(t_d)|\le u_a,\\ x_{30}(t_d)+f_{FC}(x_{50}(t_d)) & \\ \dfrac{-x_{10}(t_d),x_{50}(t_d)-x_{10}(t_d)-x_{40}(t_d))-u_a}{u_b-u_a}, & \text{if } u_a<u(t_d)<u_b,\\ 1, & \text{if } u(t_d)\ge u_b,\end{cases}$$

$$+k_{P0}[1-\exp(-\frac{T_s}{T_{\Sigma 0}})]$$

$$\cdot\begin{cases}0, & \text{if } u(t_d)\le -u_b,\\ \lambda_{T_\Sigma,3}(t_d)+\left[\dfrac{\partial f_{FC}(t_d)}{\partial e(t_d)}\right]_0(\lambda_{T_\Sigma,5}(t_d)-\lambda_{T_\Sigma,1}(t_d)) & \\ \dfrac{+\left[\dfrac{\partial f_{FC}(t_d)}{\partial \Delta e(t_d)}\right]_0(\lambda_{T_\Sigma,5}(t_d)-\lambda_{T_\Sigma,1}(t_d)-\lambda_{T_\Sigma,4}(t_d))}{u_b-u_c}, & \text{if } -u_b<u(t_d)<-u_c,\\ 0, & \text{if } -u_c\le|u(t_d)|\le u_a,\\ \lambda_{T_\Sigma,3}(t_d)+\left[\dfrac{\partial f_{FC}(t_d)}{\partial e(t_d)}\right]_0(\lambda_{T_\Sigma,5}(t_d)-\lambda_{T_\Sigma,1}(t_d)) & \\ \dfrac{+\left[\dfrac{\partial f_{FC}(t_d)}{\partial \Delta e(t_d)}\right]_0(\lambda_{T_\Sigma,5}(t_d)-\lambda_{T_\Sigma,1}(t_d)-\lambda_{T_\Sigma,4}(t_d))}{u_b-u_a}, & \text{if } u_a<u(t_d)<u_b,\\ 0, & \text{if } u(t_d)\ge u_b,\end{cases} \tag{2.54}$$

$$\lambda_{T_\Sigma,3}(t_d+1)=\lambda_{k_P,3}(t_d)+\left[\frac{\partial f_{FC}(t_d)}{\partial e(t_d)}\right]_0(\lambda_{T_\Sigma,5}(t_d)-\lambda_{T_\Sigma,1}(t_d))$$
$$+\left[\frac{\partial f_{FC}(t_d)}{\partial \Delta e(t_d)}\right]_0(\lambda_{T_\Sigma,5}(t_d)-\lambda_{T_\Sigma,1}(t_d)-\lambda_{T_\Sigma,4}(t_d)), \tag{2.55}$$

$$\lambda_{T_\Sigma,4}(t_d+1)=\lambda_{T_\Sigma,5}(t_d)-\lambda_{T_\Sigma,1}(t_d)\,, \tag{2.56}$$

$$\lambda_{T_\Sigma,5}(t_d+1)=\exp(-\frac{T_s}{\beta\, T_{\Sigma 0}})\lambda_{T_\Sigma,5}(t_d)\,, \tag{2.57}$$

$$\sigma_{T_\Sigma}(t_d)=\lambda_{T_\Sigma,1}(t_d)\,, \tag{2.58}$$

where the nominal control system trajectory is set by the state vector $\mathbf{x}_0(t_d)=[x_1(t_d)\;\;x_2(t_d)\;\;x_3(t_d)\;\;x_4(t_d)\;\;x_5(t_d)]^T\in\mathbf{R}^5$. The subscript 0 in (2.47) – (2.58) indicates not just the nominal trajectory of the fuzzy control system, i.e., the trajectory for the nominal values of the process parameters k_P and T_Σ but also the nominal values of k_P and T_Σ.

Since the discrete-time state-space model of the fuzzy control system given in (2.41) – (2.46) is not differentiable with respect to the process parameters k_P and T_Σ because of the nonlinearity of the process and of the structure of the T-S PI-FC, the state sensitivity models (2.47) – (2.52) and (2.53) – (2.58) are not defined at the break points $u(t_d)=-u_b$, $u(t_d)=-u_c$, $u(t_d)=u_a$ and $u(t_d)=u_b$. Therefore, the closed intervals in (2.47), (2.48), (2.53) and (2.54) should be replaced by open intervals. The closed intervals are actually used in practical implementations in order to obtain values of the state sensitivity functions at those points.

The structure of the T-S PI-FC does not ensure the differentiability of the function f_{FC} with respect to e and Δe. This is not a problem because the nature-inspired algorithms are in fact derivative-free optimization algorithms. The following finite difference formulas are applied to carry out the numerical differentiations that lead to the estimated derivatives $\left[\frac{\partial f_{FC}(t_d)}{\partial e(t_d)}\right]_0$ and $\left[\frac{\partial f_{FC}(t_d)}{\partial \Delta e(t_d)}\right]_0$ which are used in the implementation of the state sensitivity models:

$$\left[\frac{\partial f_{FC}(t_d)}{\partial e(t_d)}\right]_0 \approx \begin{cases} \dfrac{f_{FC0}(t_d)-f_{FC0}(t_d-1)}{e_0(t_d)-e_0(t_d-1)}, & \text{if } e_0(t_d)\neq e_0(t_d-1), \\ 0, & \text{if } e_0(t_d)=e_0(t_d-1), \end{cases} \tag{2.59}$$

$$\left[\frac{\partial f_{FC}(t_d)}{\partial \Delta e(t_d)}\right]_0 \approx \begin{cases} \dfrac{f_{FC0}(t_d)-f_{FC0}(t_d-1)}{\Delta e_0(t_d)-\Delta e_0(t_d-1)}, & \text{if } \Delta e_0(t_d)\neq \Delta e_0(t_d-1), \\ 0, & \text{if } \Delta e_0(t_d)=\Delta e_0(t_d-1). \end{cases} \tag{2.60}$$

The formulas given in (2.59) and (2.60) are justified because of the quasi-continuous digital control design and implementation of the T-S PI-FCs.

The dynamic regimes considered in solving the optimization problems (2.13) – (2.16) by nature-inspired algorithms are characterized by the step-type modification of magnitude r_0 of the angular position reference input. These regimes employ the initial state vector which sets the initial point of the nominal fuzzy control system trajectory that is set to the origin of the state-space $\mathbf{x}_0(0)=[0 \quad 0 \quad 0 \quad 0 \quad 0]^T \in \mathbf{R}^5$. Other dynamic regimes characterized by different modifications of the reference input and/or of the disturbance input yield similar results but different controller tuning parameters.

The design method and the nature-inspired algorithms are applied to the design of T-S PI-FCs for a case study that deals with the angular position of the experimental setup built around a DC servo system laboratory equipment [Int07b]. The experimental setup is illustrated in Fig. 2.6 and in Fig. 2.7. An optical encoder is used for the measurement of the angle and a tacho-generator for the measurement of the angular speed. The speed can also be estimated from the angle measurements. The PWM signals that are proportional with the control signal are produced by the actuator in the power interface. The main features of the experimental setup are [Int07b]: rated amplitude of $24\,\mathrm{V}$, rated current of $3.1\,\mathrm{A}$, rated torque of $15\,\mathrm{N\,cm}$, rated speed of $3000\,\mathrm{rpm}$, and weight of inertial load of $2.03\,\mathrm{kg}$. The nominal values of the parameters of the process model given in (2.17) and (2.20), obtained by a least squares algorithm, are $u_a=0.15$, $u_b=1$, $u_c=0.15$, $k_{P0}=k_{EP0}=140$, and $T_{\Sigma 0}=0.92\,\mathrm{s}$.

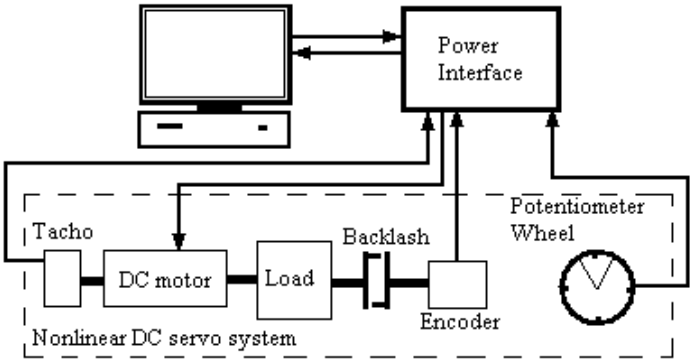

Fig. 2.6. Structure of experimental setup.

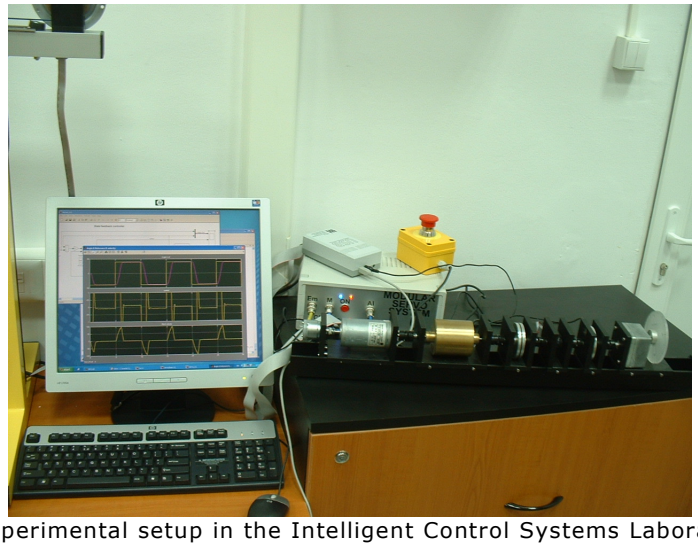

Fig. 2.7. Experimental setup in the Intelligent Control Systems Laboratory of the Politehnica University of Timisoara.

The weighting parameters in the objective functions (2.9) – (2.12) were set such that to obtain a ratio of {0, 0.1, 1, 10} of the initial values of the first and second terms in the sums. The following values were obtained and used in the case study:

- for $J_{1,k_P}(\boldsymbol{\rho})$:

$$(\gamma_{k_P})^2 \in \{0,0.0021357,0.021357,0.21357\}, \tag{2.61}$$

- for $J_{1,T_\Sigma}(\boldsymbol{\rho})$:

$$(\gamma_{T_\Sigma})^2 \in \{0,0.17187,1.7187,17.187\}, \tag{2.62}$$

- for $J_{2,k_P}(\boldsymbol{\rho})$:

$$(\gamma_{k_P})^2 \in \{0,0.006858,0.06858,0.6858\}, \tag{2.63}$$

- for $J_{2,T_\Sigma}(\boldsymbol{\rho})$:

$$(\gamma_{T_\Sigma})^2 \in \{0,0.0066695,0.066695,0.66695\}, \quad (2.64)$$

- for $J_{3,k_P}(\boldsymbol{\rho})$:

$$(\gamma_{k_P})^2 \in \{0,3.9187,39.187,391.87\}, \quad (2.65)$$

- for $J_{3,T_\Sigma}(\boldsymbol{\rho})$:

$$(\gamma_{T_\Sigma})^2 \in \{0,3.8693,38.693,386.93\}, \quad (2.66)$$

- for $J_{4,k_P}(\boldsymbol{\rho})$:

$$(\gamma_{k_P})^2 \in \{0,0.142,1.42,14.2\}, \quad (2.67)$$

- for $J_{4,T_\Sigma}(\boldsymbol{\rho})$:

$$(\gamma_{T_\Sigma})^2 \in \{0,0.15885,1.5885,15.885\}. \quad (2.68)$$

The variables of the objective function were initialized taking into consideration the following boundaries which define the search domain $D_{\boldsymbol{\rho}}$, which is also the feasible domain of $\boldsymbol{\rho}$:

$$D_{\boldsymbol{\rho}} = \{\beta \mid 3 \le \beta \le 17\} \times \{B_e \mid 20 \le B_e \le 40\} \times \{\eta \mid 0.25 \le \eta \le 0.75\}. \quad (2.69)$$

The nature-inspired optimization algorithms presented in the next chapter were run for the dynamic regimes characterized by the $r = r_0 = 40$ rad step type modification of the reference input and zero disturbance input, $d = d_0 = 0$.

In order to guarantee the stability of the fuzzy control systems for every potential solution belonging to the search domain $D_{\boldsymbol{\rho}}$ with the obtained fuzzy controller tuning parameters, an additional inequality-type constraint is enforced in order to ensure the convergence of the objective function:

$$|y(t_d) - r(t_d)| \le \varepsilon_y |r(t_d) - r(t_0)|. \quad (2.70)$$

where t_0 is the initial time moment, t_d is the final time moment, and $\varepsilon_y = 0.001$ for a 2% settling time. The condition (2.70) is checked in steady-state regimes, so theoretically $t_d \to \infty$ as shown in (2.9) – (2.12), but t_d takes practically a finite value to capture the transients in the fuzzy control systems' response. The condition (2.68) guarantees the stability of the fuzzy control systems, and it also ensures the zero steady-state control error.

2.2. State-of-the-art analysis for the optimal tuning of fuzzy controllers based on nature-inspired algorithms

Nature-inspired algorithms proved to be successful solutions to optimization problems in many applications [Che08], [Jaj11], [Kav13a], [Pan13]. Optimal tuning of fuzzy controllers is one of these problems, as they can cope with non-convex or non-differentiable objective functions because of controllers' structures and nonlinearities, of process's complexity in industrial applications and of performance specifications that can lead to multi-objective optimization problems [Guo07], [Mar11], [Nik13].

The analysis of the state-of-the-art concerning the optimal tuning of fuzzy controllers based on nature-inspired algorithms is organized as follows from the point of view of the specific algorithms considered with this regard. The most important algorithms from the point of view of validation by real-time experimental results will be pointed out as follows and treated in the next chapter. Having in mind the point of view of real-time experimental results has resulted in a total of seven algorithms; that is the reason why genetic algorithms are not considered in this thesis and analyzed in this sub-chapter.

Simulated annealing was recently applied to solve similar problems with non-convex objective functions in various domains: traffic control [Hai10], biomedical applications [Kar88], economy theory [Oli14], routing problems [Cir14], image processing [Asa12], [San12], material molding [Wan12a], cellular manufacturing [Ark07] or supply management [Gol13]. Simulated annealing is involved in finding the optimal parameters of a robust proportional-integral-derivative (PID) controller in [Abd08], which is used in a power system stabilizer. The geometrical dimension and section parameter of a robot mechanism is optimized in [Chu04] by a fuzzy self-tuning PID controller tuned by simulated annealing for suppressing residual vibration. A trajectory tracking algorithm of a mobile robot developed based on a combined control scheme with proportional-derivative (PD)-fuzzy controller and separate integral component with parameters tuned using simulated annealing is proposed in [Lia10].

Simulated annealing performed well in combination with other algorithms. Optimal integral gains for integral gain control, and proportional-integral-derivative gains for PID control, are computed by a genetic algorithm and by hybrid genetic algorithm-simulated annealing algorithms in [Gho04] and applied to the optimization of certain transient responses of interconnected three equal generating areas in power systems.

Particle swarm optimization (PSO) has emerged as one of the most successful and versatile nature-inspired algorithms. The application domains for this algorithm include: microwave applications [Deb14], supply chain management [Sad14], structural control [Nom07] or economic dispatch [Nik11]. PSO algorithms have proven successful results in the optimal tuning of fuzzy controllers as shown in the following applications: induction motor drives [Wai07], mobile robot navigation [Jua11], radio frequency identification [Kuo14], stock index forecasting [Sin14], backlight compensation [Lin09a], signal validation [Oli09], fuzzy systems design [Cas12], train lateral suspension model [Li12a], photovoltaic systems [Kha10a], robot manipulation [Sol13], linear induction motor [Wai07], voltage control strategy [Zir13] and functional-link-based neural fuzzy network [Lin09b]. Another successful application of PSO is presented in [Sak13] as an optimal fuzzy control system is proposed to reduce frequency deviations in a simulated PV-diesel hybrid system. In [Jua05] an adaptive recurrent fuzzy controller is suggested using a Takagi-Sugeno recurrent fuzzy network tuned offline by PSO, and the results are validated on a water bath temperature system. A new PID-type fuzzy logic controller tuning strategy is proposed using a PSO-based approach in [Bou12] with confirmed results using simulated and experimental tests involving an electrical DC drive benchmark. The paper [Zir13] suggests the use of interval type-2 fuzzy logic controller to control a flexible-joint robot with voltage control strategy, with the parameters of the primary membership functions optimally tuned using PSO. A valve with nonlinear dynamic behavior is controlled in [Coe08] using a PSO-based optimized PID-fuzzy controller. A combination of fuzzy logic and PSO for the optimal tuning of the most popular existing proportional-integral (PI) frequency controllers in the AC microgrid systems

is introduced in [Bev12], and the control system performance is compared with PI-fuzzy and Ziegler-Nichols PI-based control structures. Other examples of successful applications of PSO algorithms to the tuning of fuzzy controllers are given in [Cas10], where the results are verified through simulated results and in [Mal13], with results validated using real experiments.

In a pursuit to improve the performance of PSO algorithms, several adaptive versions of the initial PSO algorithm emerged, and they are briefly discussed as follows. The paper [Yan10] describes a fuzzy backstepping controller design for permanent magnet synchronous motor with the parameters of nonlinear controller based on backstepping technique which is adjusted by fuzzy logic control, and the fuzzy logic control is optimized by adaptive weighted PSO; the proposed optimal controller is verified by simulation, and the results show that the controller has robust and good dynamic response.

In addition to the adaptive versions, algorithm hybridization has also been employed as a solution for increasing the algorithm's performance. The paper [Tal11a] proposes a PSO algorithm combined with tabu search in order to generate fuzzy controller with only three rules by adjusting the membership functions and fuzzy rules according to different environments and validate the results using the control of angle of an inverted pendulum. A hybrid PSO and pattern search optimized PI-fuzzy controller is proposed in [Sah15] and applied to the automatic generation control of multi-area power systems; simulation results are offered.

A more recent nature-inspired algorithm is the Gravitational Search Algorithm (GSA), which although is a fairly new addition it has already proven as a viable solution with solid performance. Successful application domains of GSAs include: edge detection [Der14], feature selection [Lia13a], pattern recognition [Gon15], image segmentation [Kum14], task scheduling [Zar14], data mining [Hat12], anomaly detection [She14], supply chains [Pei14], hydrothermal systems [Yua14], water turbines regulation [Che14], optimal reactive power dispatch [Sha14] or wind power [Ji14]. An optimal solution using GSA for path planning of mobile robots operating in static environments, such that to ensure the collision avoidance of potential environmental obstacles and danger zones, is proposed in [Pur13a]. Solutions for embedding nature-inspired algorithms combined with the classical backpropagation algorithm in the training of convolutional neural networks for optical character recognition systems with improved performance are described in [Fed12a], [Fed12b]. Promising results were obtained when the GSA was employed for fuzzy control optimization problems, discussed as follows. In [She13] one of the parameters of GSA is controlled using a fuzzy logic controller to achieve better optimization results and to increase the convergence rate. An optimization approach of a PID-fuzzy controller using genetic algorithms, a bacterial foraging optimization algorithm and a GSA is introduced in [Aza13] for load frequency control in power systems, validated by simulation results. In [Roy13] a hybrid design methodology for stable adaptive fuzzy controllers dedicated to a certain nonlinear system is proposed, with the GSA-based design and hybrid GSA-Lyapunov concurrent design methodologies, and simulation results are included.

In recent publications adaptive versions of the GSA have appeared along with the standard version of the algorithm. An adaptive variant of GSA developed using the 5E learning model [Bal06] exhibits significant performance increases for the optimal tuning of T-S PI-FCs [Dav12a], [Pre12a], [Pre13b], [Pre13c], [Dav14a]. The optimal tuning of PI controllers using adaptive GSA for a class of servo systems characterized by saturation and dead zone static nonlinearities and second-order

models with an integral component is suggested in [Pre14a]; the optimal tuning of an anti-windup block is carried out as well.

Out of the hybridization attempts concerning the GSA, the most successful one is with the PSO algorithm. This hybrid algorithm shows promising results in [Mir10], and it is applied in various domains: flow-based anomaly detection [Jad13], emission load dispatch [Jia14], economic and emission dispatch [Dub13], landslide displacement [Lia13b], voltage instability [Man14], supply chain [Pei14] and path planning [Pur13b]. As in the case of GSA, an adaptive version using the 5E learning model [Bal06] is developed in [Pre14b] for the hybrid PSO-GSA algorithm, and applied to controller tuning in order to offer control systems with T-S PI-FCs that ensure a reduced process parametric sensitivity.

One of the latest nature-inspired algorithms that show a solid performance is Charged System Search (CSS). The applications domain of CSS algorithms include: neural networks training [Per13], optimization of concrete structures [Kav12a], seismic design of steel frames [Kav14a], design of structures [Kav13b], cost optimization [Kav12a], power dispatch problems [Ozy12], frame structures [Kav12b] and optimal power flow problems [Nik12]. CSS algorithms are successfully applied for the optimal tuning of PI controllers dedicated to a class of second-order processes with an integral component and variable parameters [Pre11b], [Pre12d].

An adaptive version based on the 5E learning model [Bal06] is applied in [Pre14c] to the parameter tuning of the CSS algorithm. This adaptive CSS algorithm shows the control system performance improvement when used to give a solution to the optimization problems that aim the minimization of objective functions in the optimal tuning of T-S PI-FCs.

2.3. CHAPTER CONCLUSIONS

This sub-chapter is dedicated to summarizing the information presented throughout this chapter and highlighting new contributions based on these materials.

The first part of this chapter introduces the definition of optimization problems, which will be solved in the next chapter with the aid of nature-inspired algorithms, together with the presentation of the process models, state sensitivity models, definition of discrete-time objective functions and a design method for optimal fuzzy controllers with a reduced parametric sensitivity tuned by the Extended Symmetrical Optimum method.

The second part of the chapter was dedicated to a bibliographic analysis of nature-inspired algorithms applications with regard to the optimization of fuzzy controllers. The focus of this analysis included the following algorithms: Simulated Annealing, Particle Swarm Optimization, Gravitational Search Algorithm, Hybrid Particle Swarm Optimization - Gravitational Search Algorithm and Charged System Search. The rationale for this nature-inspired algorithm selection was their application for solving the optimization problems introduced in the sub-chapter 2.1, in the course of the following chapter. This selection is not permanent as other algorithms might be employed for solving these optimization problems in the potential scope of a future research, as mentioned in the dedicated sub-chapter of Chapter 5.

The new **contributions** extracted from this chapter are presented as follows.

1. New discrete-time state-space models of T-S PI-FCs characterized by the manipulation of the dynamics elements in the structure of these controllers such that to define two state variables. The models proposed in the framework of this contribution are published in:

*R.-E. Precup, **R.-C. David**, E. M. Petriu, M.-B. Rădac, S. Preitl, J. Fodor, Evolutionary optimization-based tuning of low-cost fuzzy controllers for servo systems, Knowledge-Based Systems, vol. 38, pp. 74-84, Jan. 2013, impact factor (IF) = 3.058, IF according to 2013 Journal Citation Reports (JCR) released by Thomson Reuters in 2014 = 3.058.*

2. New discrete-time state sensitivity models of fuzzy control systems with respect to two parameters of the controlled process represented by a class of nonlinear servo systems. The fuzzy control systems include T-S PI-FCs, and the class of nonlinear servo systems is structured as a series connection of second-order dynamics with an integral component, and saturation and dead zone static nonlinearity placed on the process input. The models proposed in the framework of this contribution are published in:

*R.-E. Precup, **R.-C. David**, S. Preitl, E. M. Petriu, J. K. Tar, Optimal control systems with reduced parametric sensitivity based on particle swarm optimization and simulated annealing, in Intelligent Computational Optimization in Engineering Techniques and Applications, editors: M. Köppen, G. Schaefer, A. Abraham, Studies in Computational Intelligence, vol. 366, Springer-Verlag, Berlin, Heidelberg, pp. 177-207, 2011, indexed in Thomson Reuters Web of Science (formerly ISI Web of Knowledge).*

3. A novel design method dedicated to the simple T-S PI-FCs for servo systems with a reduced parametric sensitivity, namely with a reduced process gain sensitivity and with a reduced process small time constant sensitivity. The design method ensures the parameter tuning of the fuzzy controllers by solving four types of optimization problems using nature-inspired optimization algorithms. The design method proposed in the framework of this contribution is published and organized in several versions in:

***R.-C. David**, R.-E. Precup, S. Preitl, J. K. Tar, J. Fodor, Parametric sensitivity reduction of PI-based control systems by means of evolutionary optimization algorithms, Proceedings of 6th IEEE International Symposium on Applied Computational Intelligence and Informatics (SACI 2011), Timisoara, Romania, pp. 241-246, 2011, indexed in IEEE Xplore, INSPEC, SCOPUS.*

3. NATURE-INSPIRED ALGORITHMS FOR THE OPTIMAL TUNING OF FUZZY CONTROLLERS WITH A REDUCED PROCESS PARAMETRIC SENSITIVITY

3.1. SIMULATED ANNEALING ALGORITHMS

Simulated Annealing (SA) is a random-search technique, derived from a metallurgy process which describes the way in which the metal cools and freezes into a minimum energy crystalline structure and the search for a minimum in a more general system. For this process, the selected cooling schedule has a decisive role in the final properties of the substance: if a fast cooling schedule is used the resulting substance will be easily broken due to an imperfect structure, so as to avoid this scenario an appropriate cooling schedule has to be employed, for the resulting structure to be well organized and strong.

According to [Kir83], the operating mechanism of the SA algorithm mimics a ball that can bounce over mountains from valley to valley. The process begins at a high temperature, which enables the ball to make very high bounces, thus enabling it to access any valley, given enough bounces. As the temperature declines, the ball cannot bounce so high and it can settle to become trapped in relatively small ranges of valleys [Led07]. A generating distribution produces possible valleys or states to be explored. An acceptance distribution is also defined, which depends on the difference between the function value corresponding to the explored valley and the last saved lowest valley. The decision making on staying in the valley is based on the acceptance distribution in a probabilistic framework. The generating and acceptance distributions depend on the current temperature value.

With the purpose of decreasing the computational complexity of the SA algorithm, two additional iteration indices are introduced in [Pre11c], namely the success rate s_r and the rejection rate r_r. The success rate s_r aims the acceleration of the cooling process by forcing a jump in temperature when the minimum value of the fitness function changes for a preset number of times at the same temperature level. The rejection rate r_r is proposed as an alternative index to assess and set the convergence of the algorithm, and it is reset only when small values of the fitness function are found and not when the temperature cools.

Using the SA algorithm implies the following steps described in [Pre13a] and [Pre11c]:

Step 1. Generate the initial solution, in line with (2.29), conduct the following operations: generate a random initial solution ζ and calculate its fitness value $f(\zeta)$ according to (2.9) – (2.12), set the minimum temperature $\theta_{\min}$, using the notation k for the current iteration index, initialize the maximum allowed number of

iterations $k_{\max}$ for each temperature step, the maximum accepted success rate $s_{r\max}$, the maximum accepted rejection rate $r_{r\max}$, and the minimum accepted value of the fitness function $f_{\min}$, set the initial temperature θ_0, i.e., the temperature θ_k for $k=0$, and set the initial rejection rate $r_r=0$.

Step 2. Set the initial value of the iteration index $k=0$ and the initial success rate $s_r=0$.

Step 3. Generate a new probable solution ψ in the vicinity of ζ by disturbing ζ, and calculate its fitness value $f(\psi)$.

Step 4. Accept or not the new solution by means of the change of fitness expressed as the difference $\Delta f_{\psi\zeta}$:

$$\Delta f_{\psi\zeta} = f(\psi) - f(\zeta) . \tag{3.1}$$

If $\Delta f_{\psi\zeta} \le 0$, accept $\zeta = \psi$ as the new vector solution. Otherwise, set the random parameter q_k, $0 \le q_k \le 1$, and calculate the probability p_ψ of ψ to be the next solution:

$$p_\psi = \exp(-\frac{\Delta f_{\psi\zeta}}{\theta_k}) . \tag{3.2}$$

If $p_\psi > q_k$, $\zeta = \psi$ is the new solution.

Step 5. If the new solution is accepted, then update the new solution and *f*, increment k and reset $r_r=0$. Otherwise, increment r_r. If r_r has reached its maximum value $r_{r\max}$, go to step 8; otherwise, continue with the next step. Increment s_r. If s_r has reached its maximum value $s_{r\max}$, continue with the next step; otherwise, increment k. If k has reached its maximum value $k_{\max}$, continue with the next step; otherwise, go to step 2.

Step 6. The temperature is decreased in terms of the temperature decrement rule, referred to also as the cooling schedule, which gives the next temperature θ_{k+1}:

$$\theta_{k+1} = \alpha_{cs}\theta_k . \tag{3.3}$$

where $\alpha_{cs} = \text{const},\ \alpha_{cs} < 1$.

Step 7. If $\theta_k > \theta_{\min}$ or $f(\zeta) > f_{\min}$, go to step 2. Otherwise, continue with the next step.

Step 8. The algorithm is stopped, and the last vector solution ζ is the final solution.

The steps described before are displayed in Fig. 3.1.1.

The SA algorithm described above was employed as a nature-inspired algorithm in the step 4 of the design method dedicated to the simple T-S PI-FCs presented in Sub-chapter 2.1. In order to obtain an efficient cooling schedule for solving the optimization problems described by the objective (fitness) functions $J_{1\ldots4,k_P}$ and $J_{1\ldots4,T_\Sigma}$ from (2.9) – (2.12) the parameter α_{cs} in (3.3) was set to $\alpha_{cs}=0.9$. This value was not arbitrarily chosen, as it was previously selected in [Pre11c] as a trade-off between convergence accuracy and the probability of avoiding being trapped into a local minimum. The values of the parameters set in the step 1 of the SA algorithm are: maximum success rate $s_{r\max}=50$, maximum rejection rate $r_{r\max}=1000$, maximum allowed number of iterations for each temperature step

$k_{\max} = 300$ with the initial temperature set to $\theta_0 = 1$ and the minimum temperature $\theta_{\min} = 10^{-8}$.

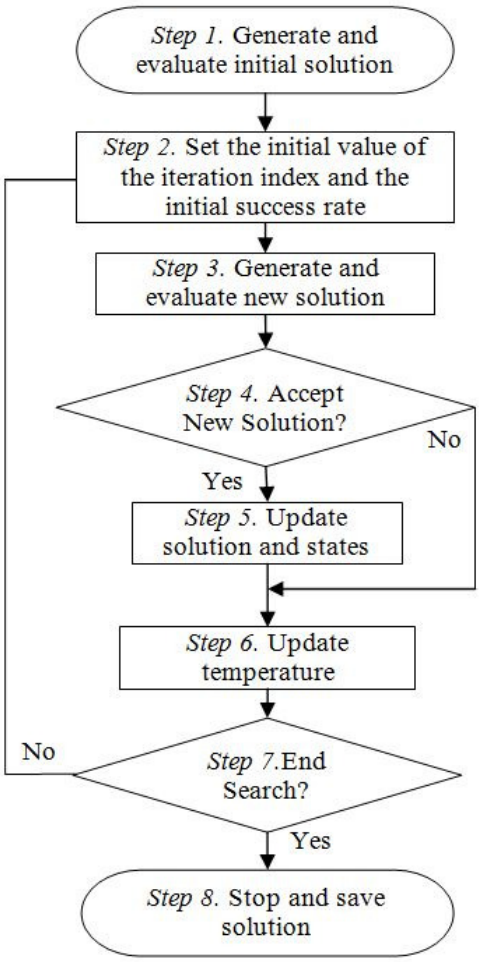

Fig. 3.1.1. Flowchart of Simulated Annealing algorithm.

The values of the optimal controller tuning parameters and the minimum values of the objective functions $J_{1...4,k_P}$ and $J_{1...4,T_\Sigma}$ (i.e., $J_{1...4,k_P \min}$ and $J_{1...4,T_\Sigma \min}$) are presented in Tables 3.1.1 – 3.1.8.

Due to the stochastic characteristic of the SA algorithm, several runs of the algorithm were required before drawing a final result for each of the objective functions. Fig. 3.1.2 illustrates the evolutions of the parameters of the T-S PI-FC (i.e., the variables of the objective functions) and of the objective function during the iterations of the SA algorithm. This parameter progression graphics correspond to the objective function J_{2,k_P} and to the weighting parameter $\gamma_{k_P} = 0$. A comprehensive analysis of the SA convergence based on the average values of the optimal

objective function values along with two newly defined performance indices will be presented in Sub-chapter 3.8.

Table 3.1.1. Results for the SA-based minimization of J_{1,k_P}.

$(\gamma_{k_P})^2$	$B^*_{\Delta e}$	B^*_e	η^*	β^*	k_c^*	T_i^*	$J_{1,k_P\min}$
0	0.1386	39.9986	0.74998	3.1430	0.0044	2.8916	390462
0.0021357	0.1384	39.9998	0.74996	3.1473	0.0044	2.8955	393513
0.021357	0.1398	39.9973	0.74993	3.1158	0.0044	2.8665	420962
0.21357	0.1372	39.9681	0.74901	3.1724	0.0044	2.9186	695455

Table 3.1.2. Results for the SA-based minimization of J_{1,T_Σ}.

$(\gamma_{T_\Sigma})^2$	$B^*_{\Delta e}$	B^*_e	η^*	β^*	k_c^*	T_i^*	$J_{1,T_\Sigma\min}$
0	0.1386	39.9956	0.7497	3.14236	0.0044	2.891	390483
0.17187	0.1397	39.4088	0.7441	3.07071	0.0044	2.8251	639539
1.7187	0.1261	39.739	0.7482	3.43036	0.0042	3.1559	2865980
17.187	0.0128	20.0221	0.2507	16.9996	0.0019	15.64	22808700

Table 3.1.3. Results for the SA-based minimization of J_{2,k_P}.

$(\gamma_{k_P})^2$	$B^*_{\Delta e}$	B^*_e	η^*	β^*	k_c^*	T_i^*	$J_{2,k_P\min}$
0	0.085591	39.9994	0.7498	5.0852	0.0034	4.6784	22980.3
0.006858	0.085575	39.9974	0.7499	5.0858	0.0034	4.679	32597.7
0.06858	0.081367	38.4081	0.7339	5.1363	0.0034	4.7254	118869
0.6858	0.012814	20.0137	0.2573	16.9816	0.0019	15.6231	874238

Table 3.1.4. Results for the SA-based minimization of J_{2,T_Σ}.

$(\gamma_{T_\Sigma})^2$	$B^*_{\Delta e}$	B^*_e	η^*	β^*	k_c^*	T_i^*	$J_{2,T_\Sigma\min}$
0	0.0856	39.9916	0.7494	5.0857	0.0034	4.67887	22990.2
0.0066695	0.0855	39.9921	0.7499	5.0875	0.0034	4.68046	32518.2
0.066695	0.0779	36.6549	0.7496	5.1209	0.0034	4.71122	117383
0.66695	0.0128	20.0285	0.2501	16.995	0.0019	15.6354	865024

Table 3.1.5. Results for the SA-based minimization of J_{3,k_P}.

$(\gamma_{k_P})^2$	$B^*_{\Delta e}$	B^*_e	η^*	β^*	k_c^*	T_i^*	$J_{3,k_P\min}$
0	0.0856	39.9908	0.7494	5.0853	0.0034	4.6785	2986410
3.9187	0.0853	39.8962	0.7467	5.0867	0.0034	4.6798	8480520
39.187	0.0842	39.5241	0.7464	5.1093	0.0034	4.7005	57590600
391.87	0.0337	39.8288	0.7424	12.8479	0.0022	11.8201	527966000

Table 3.1.6. Results for the SA-based minimization of J_{3,T_Σ}.

$(\gamma_{T_\Sigma})^2$	$B^*_{\Delta e}$	B^*_e	η^*	β^*	k_c^*	T_i^*	$J_{3,T_\Sigma\,\min}$
0	0.0856	39.9908	0.7494	5.0853	0.0034	4.6785	2986410
3.8693	0.0836	39.6254	0.7375	5.158	0.0034	4.7454	8208700
38.693	0.0827	39.2911	0.7303	5.1673	0.0034	4.7539	54280900
386.93	0.0286	34.5289	0.7477	13.1202	0.0021	12.0706	527790000

Table 3.1.7. Results for the SA-based minimization of J_{4,k_P}.

$(\gamma_{k_P})^2$	$B^*_{\Delta e}$	B^*_e	η^*	β^*	k_c^*	T_i^*	$J_{4,k_P\,\min}$
0	0.085594	39.9994	0.7499	5.085	0.0034	4.6782	153104
0.142	0.081086	38.3744	0.7491	5.1495	0.0034	4.7378	328330
1.42	0.077329	36.6807	0.715	5.1614	0.0034	4.7485	2056520
14.2	0.023008	20.4916	0.2511	9.6863	0.0025	8.9114	19284900

Table 3.1.8. Results for the SA-based minimization of J_{4,T_Σ}.

$(\gamma_{T_\Sigma})^2$	$B^*_{\Delta e}$	B^*_e	η^*	β^*	k_c^*	T_i^*	$J_{4,T_\Sigma\,\min}$
0	0.0856	39.9994	0.7499	5.085	0.0034	4.6782	153104
0.15885	0.0827	39.1723	0.7298	5.152	0.0034	4.7398	354836
1.5885	0.0424	20.1246	0.6618	5.1617	0.0034	4.7488	2200250
15.885	0.0202	20.2201	0.2531	10.9026	0.0024	10.0304	21605800

Fig. 3.1.3 illustrates the evolution of the vector solution $\boldsymbol{\rho}$ to the optimization problem (2.14) in the search domain $D_{\boldsymbol{\rho}}$, which is also the feasible domain of $\boldsymbol{\rho}$ during several iterations of the SA algorithm.

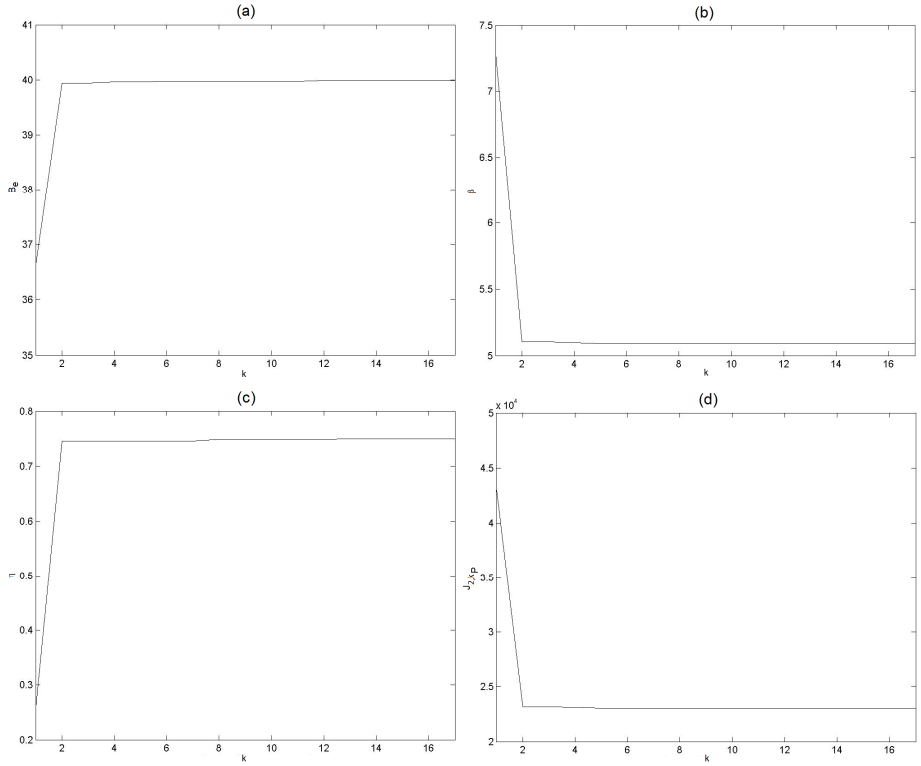

Fig. 3.1.2. T-S PI-FC tuning parameters and objective function evolution vs. iteration index: B_e versus *k* (a), β versus *k* (b), η versus *k* (c), and J_{2,k_P} versus *k* (d).

The solution obtained from the implementation of the SA for the optimization problems presented in Chapter 2 was tested on the experimental setup described in Chapter 2. Several experimental results are reported in [Pre12b]. As used in the evaluations of the objective functions presented in this Sub-chapter, the dynamic regimes characterized by the $r_0 = 40$ rad step type modification of the reference input and zero disturbance input, $d_0 = 0$, the real-time experimental results are obtained in the same conditions. In addition, a step type disturbance input of $d_0 = -20$ was applied at the time moment 25 s. An example of real-time experimental results of the fuzzy control system with the T-S PI-FC and the optimal parameters obtained by the SA-based minimization of the objective function J_{2,k_P} for the value of the weighting parameter $(\gamma_{k_P})^2 = 0.006858$ is presented in Fig. 3.1.4.

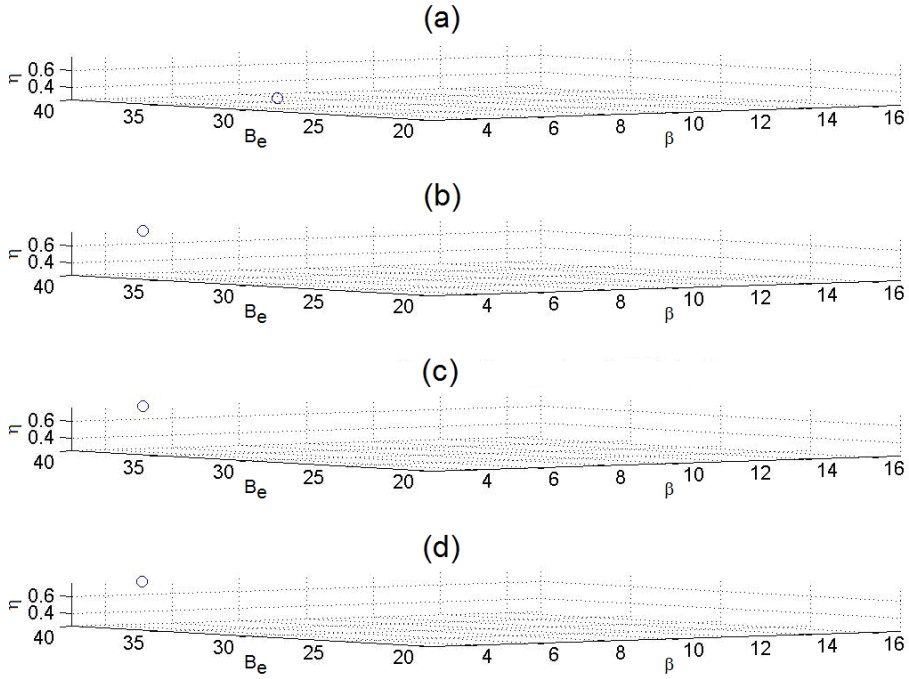

Fig. 3.1.3. Vector solution $\boldsymbol{\rho}$ to the optimization problem (2.14) in the search domain $D_{\boldsymbol{\rho}}$ for four values of iteration index k: $k=1$ (a), $k=4$ (b), $k=9$ (c), and $k=17$ (d).

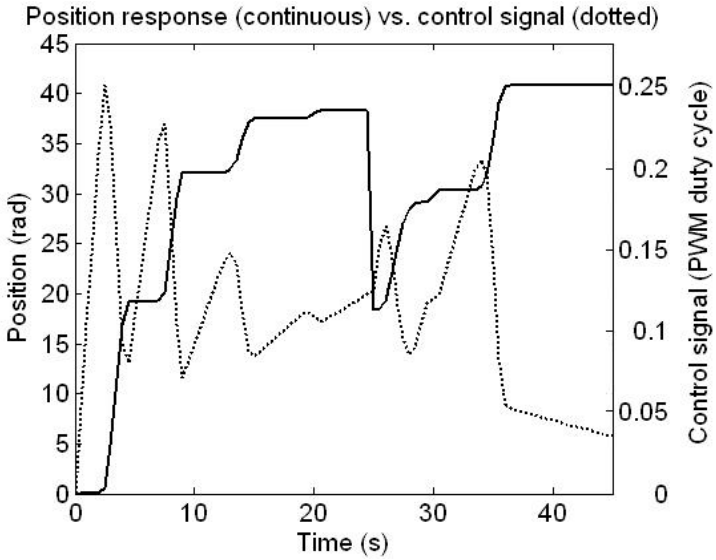

Fig. 3.1.4. Real-time experimental results of the fuzzy control system with the SA-based optimized T-S PI-FC.

The results of the real-time experiments present the output of the system and of the controller and prove the disturbance rejection and the presence of the insensitivity zone in the real-world controlled plant. An insensitivity zone of such magnitude in the actuator is therefore difficult to use for precise positioning because the control signal is subjected to oscillations.

3.2. PARTICLE SWARM OPTIMIZATION ALGORITHMS

Particle Swarm Optimization (PSO) is a population based stochastic optimization technique that was developed and initially introduced by Kennedy and Eberhard [Ken95a], [Ken95b]. As one of the most recognized nature-inspired algorithms, PSO is inspired by the behavior of entities observed in flocks of birds or schools of fishes. The movement of the population, characterized by agents, in PSO is guided by simple laws that repeat at each iteration, helping these agents, which represent candidate solutions, flow through the search-domain. Each agent has assigned a multidimensional vector that is updated according to the calculated velocity which takes into consideration the best position explored by the agent and best solution explored by the swarm.

As shown in [Ken95a], [Ken95b], PSO is based on two fundamental disciplines, social science and computer science. Social concepts like evaluation, comparison and imitations of other individuals are typically associated with intelligent agents that interact in order to adapt to the environment and develop optimal patterns of behavior. Mutual learning allows individuals to become similar and transgress to more adaptive patterns of behavior. The swarm intelligence is based on the following principles [Val08]:

1. The proximity principle, i.e., the population should be able to carry out simple time and space calculations.
2. The quality principle, i.e., the population should be able to respond to quality factors in the environment.
3. The diverse response principle, i.e., the population should not commit its activity to excessively long narrow channels.
4. The stability principle, i.e., the population should not change its behavior every time the environment changes.
5. The adaptability principle, i.e., the population should be able to change its behavior when it is worth the computational price.

The PSO algorithm starts with a random generation of candidate solutions which are continuously improved toward the optimal solutions. From this point of view PSO can be considered as an evolutionary algorithm that is similar to the genetic algorithms. The PSO algorithm uses the following computational attributes: individual particles are updated in parallel, a new value depends on the previous and its neighbors, all updates are based on the same rules. In the PSO algorithm instead of evolutionary operators, the agents are set in the *D*-dimensional search space search space $\mathbf{R}^D$ with randomly chosen velocities and positions knowing their best values so far and the positions in the search space $\mathbf{R}^q$. For each particle in the search space there is data about the position and velocity at each step of the iteration. The velocity of each particle is adjusted according to its previous flying experience and the experience of the other particles.

A swarm particle can be represented by the two q-dimensional vectors $\mathbf{X}_i = [x_{i1} \quad x_{i2} \quad \dots \quad x_{iq}]^T \in \mathbf{R}^q$ standing for the particle position and the particle velocity $\mathbf{V}_i = [v_{i1} \quad v_{i2} \quad \dots \quad v_{iq}]^T$. In addition, the best position achieved by the particle is the vector $\mathbf{P}_{i,Best} = [p_{i1} \quad p_{i2} \quad \dots \quad p_{iq}]^T$ and the best position explored by the entire swarm so far is the vector $\mathbf{P}_{g,Best} = [p_{g1} \quad p_{g2} \quad \dots \quad p_{gq}]^T$. For our optimization problems defined in (2.13) – (2.16), $\mathbf{X}_i$ is defined in accordance to (2.29) resulting in a $q = 3$ dimensional search space. The particle velocity and position update equations that govern the PSO algorithm can be expressed in terms of the state-space equations also given in [Kha07]:

$$\mathbf{V}_i(k+1) = w(k)\mathbf{V}_i(k) + c_1 r_1 (\mathbf{P}_{g,Best} - \mathbf{X}_i(k)) + c_2 r_2 (\mathbf{P}_{i,Best} - \mathbf{X}_i(k)), \tag{3.4}$$

$$\mathbf{X}_i(k+1) = \mathbf{X}_i(k) + \mathbf{V}_i(k+1), \tag{3.5}$$

where: r_1, r_2 – random variables with uniform distribution between 0 and 1, $i, \ i = 1 \dots n$ – the index of the current particle in the swarm, n – the number of particles in the swarm, $k, \ k = 1 \dots k_{\max}$ – the index of the current iteration, $k_{\max}$ – the maximum number of iterations. The parameter $w(k)$ in (3.4) stands for the inertia weight, which shows the effect of the previous velocity vector on the new vector. Upper $w_{\max}$ and lower $w_{\min}$ limits are imposed to $w(k)$ in order to prevent the particle from moving too rapidly in the search space. The constants $c_1, \ c_2 > 0$ represent the weighting factors of the stochastic acceleration terms that pull each particle towards their end position. Low values allow particles to roam far from the target regions before being tugged back. On the other hand, high values result in an abrupt movement towards, or past, target regions.

The individuals (particles) within the swarm learn from each other, and based on the knowledge obtained then move to become similar to their "better" previously obtained position and their "better" neighbor. The individuals within a neighborhood communicate with each other. Different neighborhood topologies can emerge on the basis of the communication of a particle within the swarm. A star-type topology is created in the majority of cases. In that topology each particle can communicate with every other individual forming a fully connected social network, so that each particle could access the overall best position. The PSO algorithm can be expressed according to the following steps [Ken95a], [Ken95b], [Kha07], [Val08]:

Step 1. Initialize the swarm placing particles at random positions inside the search domain $D_{\mathbf{\rho}}$, set the iteration index $k = 0$, set the search process iteration limit $k_{\max}$, define the weighting factors $c_1, \ c_2$ and the inertia weight parameter $w(k)$:

$$w(k) = w_{\max} - k \frac{w_{\max} - w_{\min}}{k_{\max}}. \tag{3.6}$$

The best particle position vector $\mathbf{P}_{i,Best}$ is initialized with the initial positions of the agents and the best swarm position vector $\mathbf{P}_{g,Best}$ is initialized with the position of the first agent.

Step 2. Evaluate the fitness of each particle using the objective (fitness) functions (2.9) – (2.12) based on their current position.

Step 3. Compare the performance of each individual to its best performance so far, and eventually update the best particle position vector $\mathbf{P}_{i,Best}$:

$$\mathbf{P}_{i,Best} = \mathbf{X}_i(k), \text{ if } J_{1..4,\alpha_\tau}(\mathbf{X}_i(k)) < J_{1..4,\alpha_\tau}(\mathbf{P}_{i,Best}) . \quad (3.7)$$

Step 4. Compare the performance of each particle to the best global performance, and eventually update the best swarm position vector $\mathbf{P}_{g,Best}$:

$$\mathbf{P}_{g,Best} = \mathbf{X}_i(k), \text{ if } J_{1..4,\alpha_\tau}(\mathbf{X}_i(k)) < J_{1..4,\alpha_\tau}(\mathbf{P}_{g,Best}) . \quad (3.8)$$

Step 5. Change the velocity of each particle according to (3.4).

Step 6. Move each particle to its new position according to (3.5).

Step 7. Increment the iteration index k and go to step 2, until the search process iteration limit $k_{\max}$ is reached.

Step 8. The algorithm is terminated, and the swarm best position $\mathbf{P}_{g,Best}$ is the final solution.

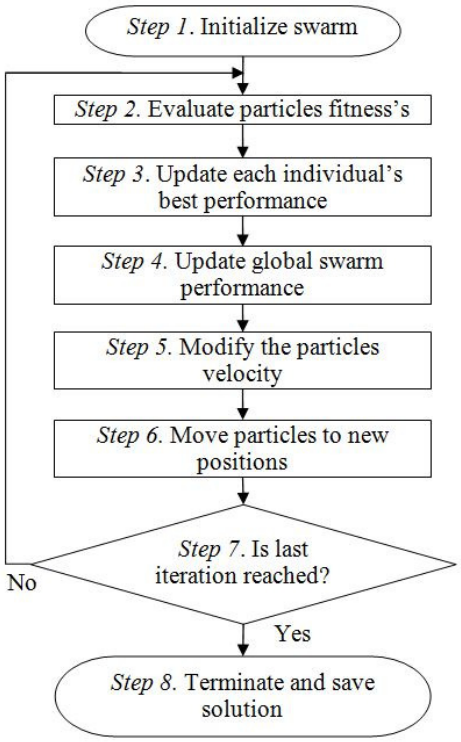

Fig. 3.2.1. Flowchart of Particle Swarm Optimization algorithm.

The simple model used in PSO has proven that it can cope with high complexity problems as shown in [Dav09], [Pre11c], [Dav12d], [Pre13a]. In addition to the initial version of PSO, which was developed to operate with real value search domains, an alternative version was introduced by Kennedy and Eberhart [Ken97] for the purpose of dealing with discrete valued search spaces. The binary version of PSO is required to deal with these finite domains.

The differences between the two versions of PSO are focused around the representation of particle position vector and movement definition. The position vector is constructed around the discrete values defined by the search domain, with the

movement represented by the agent's probability of changing state in for that dimension.

The flowchart of the PSO algorithm is presented in Fig. 3.2.1.

In order to integrate the PSO-based solution in the fourth step of the design method dedicated to the simple T-S PI-FCs presented in Sub-chapter 2.1, the PSO algorithm parameters, mentioned in the first step of the above algorithm description, had to be set in such a manner to achieve a prime search process. Based on the previous work presented in [Pre09b], [Dav11], [Pre11c], [Pre13a], the number of used agents $n = 20$ was set and the maximum number of iterations was set to $k_{\max} = 100$. In order to have a good balance between exploration and exploitation characteristics of the algorithm the weighting parameters were set as $c_1 = 0.3, c_2 = 0.9$. For the setup of the inertia weight parameter $w(k)$ a linear decrease was employed throughout the interval determined by $w_{\max} = 0.9$ and $w_{\min} = 0.5$ according to (3.6).

Table 3.2.1. Results for the PSO-based minimization of J_{1,k_P}.

$(\gamma_{k_P})^2$	$B_{\Delta e}^*$	B_e^*	η^*	β^*	k_c^*	T_i^*	$J_{1,k_P \min}$
0	0.145191	40	0.75	3	0.004483	2.76	392076
0.0021357	0.145191	40	0.75	3	0.004483	2.76	395143
0.021357	0.139548	40	0.75	3.12109	0.004395	2.8714	420966
0.21357	0.145191	40	0.75	3	0.004483	2.76	698859

Table 3.2.2. Results for the PSO-based minimization of J_{1,T_Σ}.

$(\gamma_{T_\Sigma})^2$	$B_{\Delta e}^*$	B_e^*	η^*	β^*	k_c^*	T_i^*	$J_{1,T_\Sigma \min}$
0	0.145191	40	0.75	3	0.004483	2.76	392076
0. 17187	0.145191	40	0.75	3	0.004483	2.76	641826
1.7187	0.144715	39.8689	0.75	3	0.004483	2.76	1007420
17.187	0.012792	20	0.25	17	0.001883	15.64	22809200

Table 3.2.3. Results for the PSO-based minimization of J_{2,k_P}.

$(\gamma_{k_P})^2$	$B_{\Delta e}^*$	B_e^*	η^*	β^*	k_c^*	T_i^*	$J_{2,k_P \min}$
0	0.085597	40	0.75	5.08485	0.003443	4.67806	22975.7
0.006858	0.085597	40	0.75	5.08485	0.003443	4.67806	32579.1
0.06858	0.085597	40	0.75	5.08485	0.003443	4.67806	119010
0.6858	0.012792	20	0.25	17	0.001883	15.64	874183

Table 3.2.4. Results for the PSO-based minimization of J_{2,T_Σ}.

$(\gamma_{T_\Sigma})^2$	$B_{\Delta e}^*$	B_e^*	η^*	β^*	k_c^*	T_i^*	$J_{2,T_\Sigma \min}$
0	0.085597	40	0.75	5.08485	0.003443	4.67806	22975.7
0.0066695	0.085597	40	0.75	5.08486	0.003443	4.67807	32481.3
0.066695	0.070551	33.4137	0.75	5.15341	0.00342	4.74114	108043
0.66695	0.012792	20	0.25	17	0.001883	15.64	864943

Table 3.2.5. Results for the PSO-based minimization of J_{3,k_P}.

$(\gamma_{k_P})^2$	$B^*_{\Delta e}$	B^*_e	η^*	β^*	k^*_c	T^*_i	$J_{3,k_P\min}$
0	0.085597	40	0.75	5.08485	0.003443	4.67806	2984780
3.9187	0.085597	40	0.75	5.08485	0.003443	4.67806	8472200
39.187	0.085003	40	0.75	5.12035	0.003431	4.71072	57631000
391.87	0.03284	40	0.75	13.2449	0.002133	12.1853	527908000

Table 3.2.6. Results for the PSO-based minimization of J_{3,T_Σ}.

$(\gamma_{T_\Sigma})^2$	$B^*_{\Delta e}$	B^*_e	η^*	β^*	k^*_c	T^*_i	$J_{3,T_\Sigma\min}$
0	0.085597	40	0.75	5.08485	0.003443	4.67806	2984780
3.8693	0.085597	40	0.75	5.08485	0.003443	4.67806	8499440
38.693	0.082991	39.3271	0.75	5.15624	0.003419	4.74374	57664100
386.93	0.032083	38.5553	0.75	13.0679	0.002148	12.0224	527679000

Table 3.2.7. Results for the PSO-based minimization of J_{4,k_P}.

$(\gamma_{k_P})^2$	$B^*_{\Delta e}$	B^*_e	η^*	β^*	k^*_c	T^*_i	$J_{4,k_P\min}$
0	0.085597	40	0.75	5.08485	0.003443	4.67806	152970
0.142	0.085597	40	0.75	5.08485	0.003443	4.67806	351814
1.42	0.084488	40	0.75	5.15154	0.003421	4.73942	1891650
14.2	0.02317	20	0.25	9.3881	0.002534	8.63706	19274400

Table 3.2.8. Results for the PSO-based minimization of J_{4,T_Σ}.

$(\gamma_{T_\Sigma})^2$	$B^*_{\Delta e}$	B^*_e	η^*	β^*	k^*_c	T^*_i	$J_{4,T_\Sigma\min}$
0	0.085597	40	0.75	5.08485	0.003443	4.67806	152970
0. 15885	0.084379	40	0.748922	5.15818	0.003419	4.74553	379355
1.5885	0.084508	40	0.75	5.15031	0.003421	4.73829	2123110
15.885	0.020733	20	0.25	10.4906	0.002397	9.65135	21595700

Tables 3.2.1 – 3.2.8 contain the values of the optimal controller tuning parameters and the minimum values of the objective functions $J_{1\ldots4,k_P}$ and $J_{1\ldots4,T_\Sigma}$ (i.e., $J_{1\ldots4,k_P\min}$ and $J_{1\ldots4,T_\Sigma\min}$). In order to overcome the uncertain characteristic of the PSO algorithm, several re-runs were required in order to obtain the desired results for each of the objective functions. The data presented in these tables was obtained after several re-runs of the algorithm, that were required in order to deal with the arbitrary characteristic of the PSO algorithm. A more detailed analysis based on the average values of the objective functions, together with two newly introduced algorithm performance indices is presented in Sub-chapter 3.8.

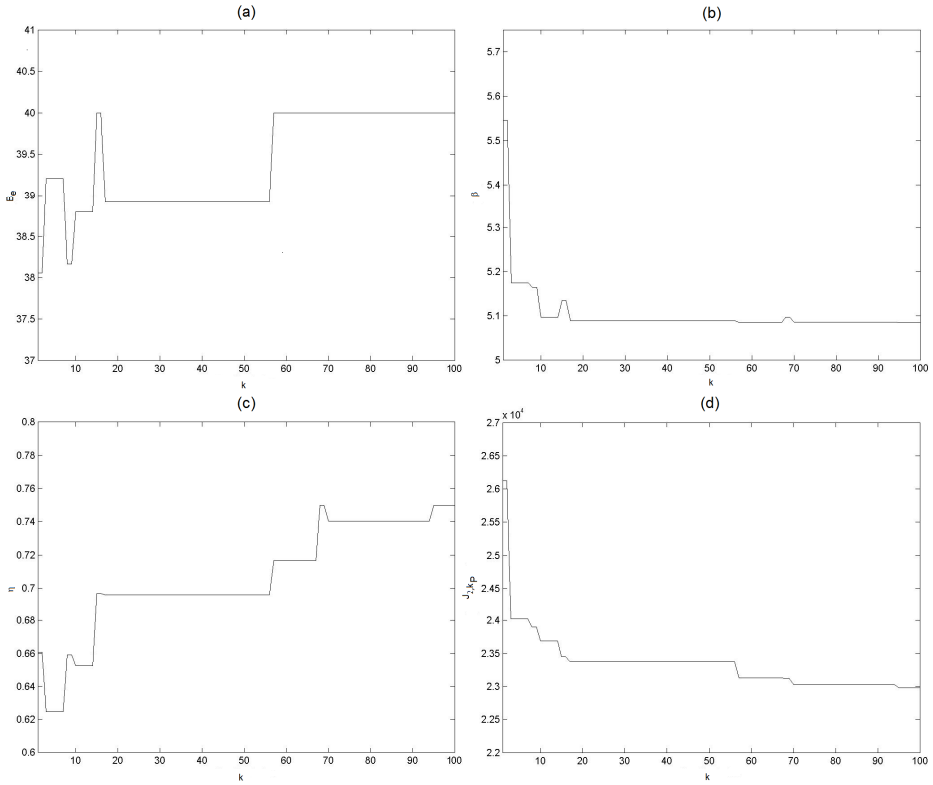

Fig. 3.2.2. T-S PI-FC tuning parameters and objective function evolution vs. iteration index: B_e versus k (a), β versus k (b), η versus k (c), and J_{2,k_P} versus k (d).

In order to have a better representation of the search process, Fig. 3.2.2 presents the evolution of parameters defined by the search domain in the case of objective function J_{2,k_P} and weighting parameter $\gamma_{k_P} = 0$.

An evolutionary display throughout the search process for all PSO's particles (agents), expressed as vector solutions $\boldsymbol{\rho}$ to the optimization problem (2.14) comprised in the search domain $D_{\boldsymbol{\rho}}$, is presented in Fig. 3.2.3.

The results of the PSO-based solution to the optimization problems presented in this thesis were verified using the experimental system presented in Chapter 2. A set of experimental results is given in [Pre13a]. The proposed approach presented in this Sub-chapter uses the digital simulation of the fuzzy control system behavior with respect to the step-type modification of the reference input $r_0 = 40$ rad, and zero disturbance input, $d_0 = 0$. The experiments were conducted using a similar setup with the control systems using an additional PI controller to the T-S PI-FCs for comparison purposes. A sample of the real-time experimental results that corresponds to the control systems with the controllers and the parameters given for the objective function J_{1,k_P} and for the value of the weighting parameter $(\gamma_{k_P})^2 = 0.0021357$ is presented in Fig. 3.2.4.

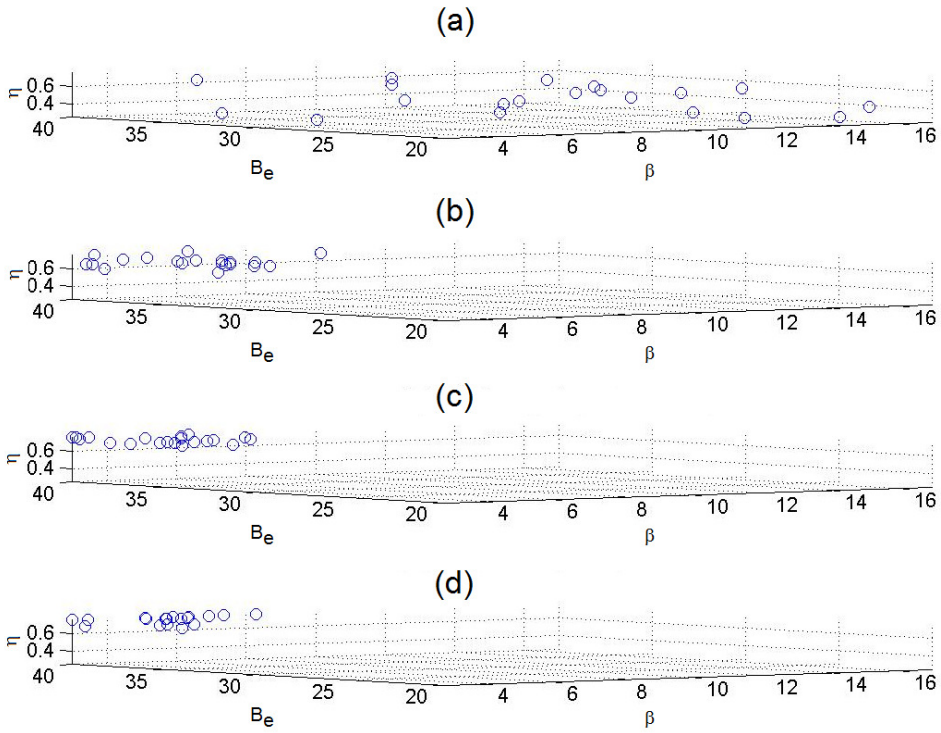

Fig. 3.2.3. Vector solution $\boldsymbol{\rho}$ to the optimization problem (2.14) in the search domain $D_{\boldsymbol{\rho}}$ for four values of iteration index k: $k=1$ (a), $k=15$ (b), $k=60$ (c), and $k=100$ (d).

For the additional PI controller mentioned in the experimental study case and used for comparison, the average value of the design parameter β taken into account was $\beta=7$. This controller was tuned by the ESO method.

Fig. 3.2.4 shows, as expected, the performance improvement exhibited by the control system with the fuzzy controller (T-S PI-FC) compared to the control system with the linear (PI) controller, namely the settling time is reduced. The proposed tuning approach has proved to be effective in reference input tracking and load disturbance regulation when controlling the real-world servo system targeting the reduced process gain sensitivity. The experimental results validate the solution offered by means of this nature-inspired optimization algorithm, the tuning approach and the fuzzy controllers.

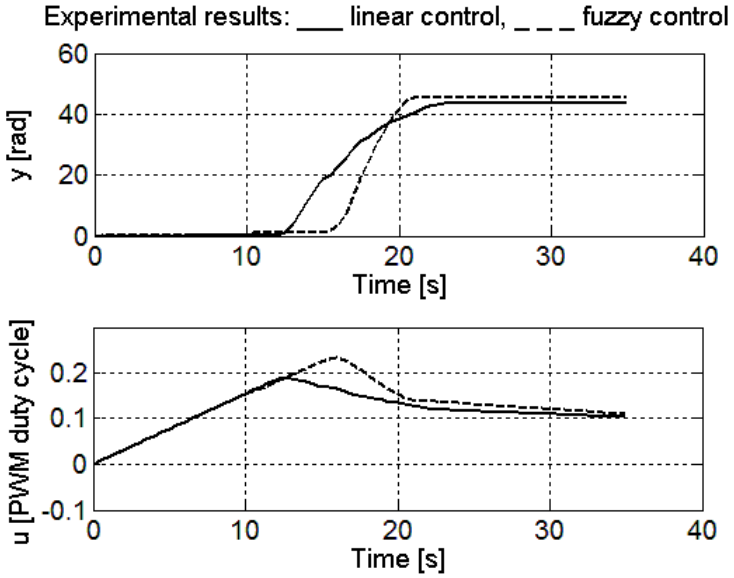

Fig. 3.2.4. Real-time experimental results: controlled output and control signal of the control system with the PI controller (dashed line) and of the control system with the T-S PI-FC (solid line).

3.3. GRAVITATIONAL SEARCH ALGORITHMS

The Gravitational Search Algorithm (GSA) [Ras07], [Ras09] is inspired by Newtonian physics principals of gravity and interaction between masses [Sch03], [Hol05]. As described by the law of gravity, each agent, also referred to as object, interacts with the existing population. This interaction is proportional to each agent's mass, expressed in accordance to its fitness, and inversely proportional to the distance between them. Also, the attraction effect between the particles of the universe is introduced through the gravitational constant. The variation of the gravitational constant is modeled by the following decrease laws in relation with GSA's iterations:

$$g(k) = \psi(1 - \frac{k}{k_{\max}})g_0 \ , \tag{3.9}$$

$$g(k) = g_0 \exp(-\zeta \frac{k}{k_{\max}}) \ , \tag{3.10}$$

where $g(k)$ is the value of the gravitational constant at the current iteration index k, $k_{\max}$ is the maximum number of iterations, $g_0 = g(0)$, and $\psi > 0$, $\zeta > 0$ are parameters that are set in order to ensure GSA's convergence and to influence the search accuracy as well.

The decrease of the gravitational constant outlined in equations (3.9) and (3.10) targets the modeling and the simulation of the effect of decreasing gravity. These equations show the decrease of the gravitational constant with age, which in

GSA is represented by the iteration index. The GSA's convergence and search accuracy is influenced by the chosen values for parameters ψ and ζ for which the designer's experience is employed.

As mentioned in [Ras10], particles, referred to also as agents, are used in the GSA, and their performance is represented through their masses. The gravity force attracts each of these particles, leading to the global movement of all particles towards the particles with heavier masses. The exploitation step of the algorithm is guaranteed by the heavy masses (which correspond to good solutions, i.e., solutions close to the optimum) moving more slowly than the lighter ones.

Considering *N* agents and a *q*-dimensional search space, the position of i^{th} agent is defined by the vector $\mathbf{X}_i$:

$$\mathbf{X}_i = [x_i^1 \quad \dots \quad x_i^d \quad \dots \quad x_i^q]^T \in \mathbf{R}^q, \; i = 1 \dots N, \tag{3.11}$$

where x_i^d is the position of the i^{th} agent in d^{th} dimension, $d = 1 \dots q$. The position vector $\mathbf{X}_i$ will be replaced by the controller parameter vector (2.29) involved in the optimization problems described by (2.13) – (2.16).

The force acting on i^{th} agent from j^{th} agent is defined as follows at the iteration index k :

$$F_{ij}^d(k) = g(k) \frac{m_{Pi}(k) m_{Aj}(k)}{r_{ij}(k) + \varepsilon} x_j^d(k) - x_i^d(k)], \tag{3.12}$$

where $m_{Ai}(k)$ is the active gravitational mass related to i^{th} agent, $m_{Pj}(k)$ is the passive gravitational mass related to j^{th} agent, $\varepsilon > 0$ is a small constant, and $r_{ij}(k)$ is the Euclidian distance between i^{th} and j^{th} agents (used instead of the squared distance to simplify the GSA):

$$r_{ij}(k) = \| \mathbf{X}_i(k) - \mathbf{X}_j(k) \| . \tag{3.13}$$

To ensure the stochastic characteristic of the GSA the total force acting on i^{th} agent in d^{th} dimension, $F_i^d(k)$, is a randomly weighted sum of all forces exerted from the other agents:

$$F_i^d(k) = \sum_{j=1, j \neq i}^{N} \rho_j F_{ij}^d(k) , \tag{3.14}$$

where ρ_j, $0 \le \rho_j \le 1$, is a randomly generated number. The law of motion leads to the acceleration $a_i^d(k)$ of i^{th} agent at the iteration index k in d^{th} dimension:

$$a_i^d(k) = \frac{F_i^d(k)}{m_{Ii}(k)} , \tag{3.15}$$

where $m_{Ii}(t)$ is the inertia mass related to i^{th} agent.

The next velocity of an agent, $v_i^d(k+1)$, is considered as a fraction of its current velocity added to its acceleration. Therefore, the position and velocity of an agent are updated in terms of the following state-space equations [Ras07], [Ras09]:

$$\begin{aligned} v_i^d(k+1) &= \rho_i v_i^d(k) + a_i^d(k), \\ x_i^d(k+1) &= x_i^d(k) + v_i^d(k+1), \end{aligned} \tag{3.16}$$

where ρ_i, $0 \le \rho_i \le 1$, is a uniform random variable.

The gravitational and inertial masses are [Ras07], [Ras09]:

$$n_i(k)=\frac{f_i(k)-w(k)}{b(k)-w(k)},$$
$$m_i(k)=\frac{n_i(k)}{\sum_{j=1}^{N} n_j(k)}, \tag{3.17}$$
$$m_{Ai}=m_{Pi}=m_{Ii}=m_i,$$

where $f_i(k)$ is the fitness value of i^{th} agent at the iteration index k, and the terms $b(k)$ (corresponding to the best agent) and $w(k)$ (corresponding to the worst agent) are defined as follows:

$$b(k)=\min_{j=1\ldots n} f_j(k),$$
$$w(k)=\max_{j=1\ldots n} f_j(k). \tag{3.18}$$

GSA consists of the following steps illustrated in Fig. 3.3.1 as the GSA's flowchart:

Step 1. Generate the initial population of agents, i.e., initialize the *q*-dimensional search space, the number of agents *N*, set the iteration index $k=0$, set the search process iteration limit $k_{\max}$ and initialize randomly the agents' position vector $\mathbf{x}_i(0)$.

Step 2. Evaluate the agents' fitness according to (2.9) – (2.12).

Step 3. Update the population of agents, i.e., compute the terms $g(k)$, $b(k)$, $w(k)$ and $m_i(k)$ using equations (3.9) or (3.10), (3.17) and (3.18) for $i=1\ldots N$.

Step 4. Calculate the total force in all directions $F_i^d(k)$, $i=1\ldots N$, using equation (3.14).

Step 5. Calculate the agents' accelerations $a_i^d(k)$ according to (3.15).

Step 6. Update the agents' velocities $v_i^d(k+1)$ and positions $x_i^d(k+1)$ using (3.16) for $i=1\ldots N$.

Step 7. Increment *k* and go to step 2 until the maximum number of iterations is reached, i.e., until $k=k_{\max}$.

Step 8. Stop and save the final solution in the vector $\mathbf{x}_i$ obtained so far.

A GSA-based solution for the optimization problems (2.13) – (2.16) is implemented with the introduction of the GSA in the fourth step of the design method detailed in Sub-chapter 2.1. Employing the experience of [Dav11], [Pre11d], [Pre11e], [Dav12d], [Pre12a], [Dav13], the GSA parameters were chosen in order to achieve the best search performance. The number of agents was set to $N=20$ with a maximum number of iterations $k_{\max}=100$. Using the search domain $D_{\boldsymbol{\rho}}$ defined in (2.67) the dimension size was set as $d=3$. The decrease law (3.10) of the gravitational constant was applied, with the initial value $g_0=g(0)$ set to $g_0=100$ and $\zeta=8.5$. The ε value from (3.12) was set to $\varepsilon=10^{-4}$ in order to avoid possible divisions by zero. The results corresponding to the objective functions are presented in Tables 3.3.1 – 3.3.8.

As in the case of other nature-inspired algorithms, the GSA solution required several re-runs before obtaining the final results for each of the $J_{1\ldots4,k_P}$ and $J_{1\ldots4,T_\Sigma}$ objective functions. This aspect will be approached in Sub-chapter 3.8 using the average values of the objective functions together with three algorithm performance indices.

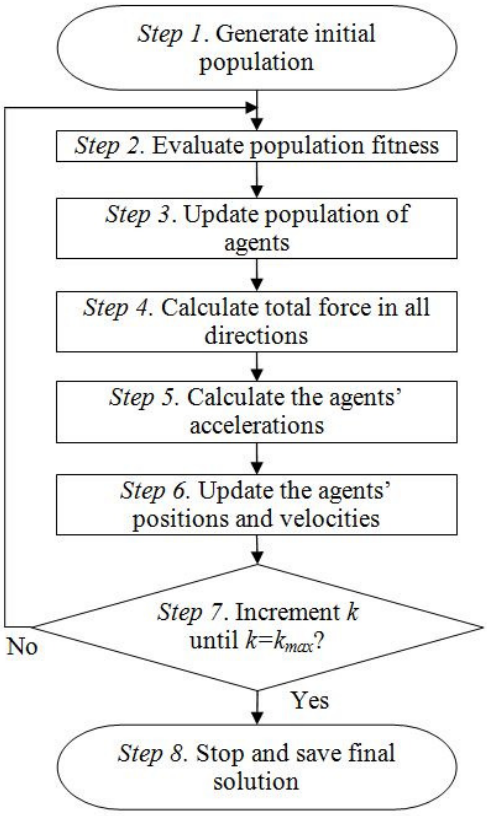

Fig. 3.3.1. Flowchart of Gravitational Search Algorithm.

Table 3.3.1. Results for the GSA-based minimization of J_{1,k_P}.

$(\gamma_{k_P})^2$	$B^*_{\Delta e}$	B^*_e	η^*	β^*	k^*_c	T^*_i	$J_{1,k_P \min}$
0	0.138541	40	0.75	3.14374	0.004379	2.89224	390459
0.0021357	0.138462	39.9979	0.75	3.14537	0.004378	2.89374	393520
0.021357	0.139267	40	0.75	3.12737	0.00439	2.87718	421083
0.21357	0.134318	39.7505	0.75	3.2222	0.004325	2.96442	695544

Table 3.3.2. Results for the GSA-based minimization of J_{1,T_Σ}.

$(\gamma_{T_\Sigma})^2$	$B^*_{\Delta e}$	B^*_e	η^*	β^*	k^*_c	T^*_i	$J_{1,T_\Sigma \min}$
0	0.138541	40	0.75	3.14374	0.004379	2.8922	390459
0.17187	0.142008	39.3697	0.75	3.01888	0.004469	2.7774	618429
1.7187	0.129304	36.4119	0.75	3.0663	0.004434	2.821	2861380
17.187	0.01281	20	0.287	16.9763	0.001884	15.618	22794600

Table 3.3.3. Results for the GSA-based minimization of J_{2,k_P}.

$(\gamma_{k_P})^2$	$B^*_{\Delta e}$	B^*_e	η^*	β^*	k^*_c	T^*_i	$J_{2,k_P\min}$
0	0.085582	40	0.7384	5.08576	0.003443	4.6789	23041.8
0.006858	0.081221	37.9584	0.75	5.08532	0.003443	4.6785	32718
0.06858	0.085461	40	0.75	5.09296	0.00344	4.6855	119183
0.6858	0.0128	20.0057	0.25	16.9947	0.001883	15.635	874127

Table 3.3.4. Results for the GSA-based minimization of J_{2,T_Σ}.

$(\gamma_{T_\Sigma})^2$	$B^*_{\Delta e}$	B^*_e	η^*	β^*	k^*_c	T^*_i	$J_{2,T_\Sigma\min}$
0	0.081626	38.1835	0.75	5.09006	0.003441	4.6829	23167.7
0.0066695	0.080257	37.8053	0.75	5.1256	0.003429	4.7156	32814.3
0.066695	0.078426	36.8115	0.75	5.10741	0.003435	4.6988	117880
0.66695	0.013045	20.3962	0.25	17	0.001883	15.64	864208

Table 3.3.5. Results for the GSA-based minimization of J_{3,k_P}.

$(\gamma_{k_P})^2$	$B^*_{\Delta e}$	B^*_e	η^*	β^*	k^*_c	T^*_i	$J_{3,k_P\min}$
0	0.0845	39.5685	0.6933	5.0948	0.0034	4.6872	3086210
3.9187	0.0807	37.7003	0.75	5.0851	0.00344	4.6782	8513560
39.187	0.0627	29.7309	0.75	5.1586	0.00342	4.746	57875400
391.87	0.032	38.8976	0.7161	13.2043	0.00214	12.148	527538000

Table 3.3.6. Results for the GSA-based minimization of J_{3,T_Σ}.

$(\gamma_{T_\Sigma})^2$	$B^*_{\Delta e}$	B^*_e	η^*	β^*	k^*_c	T^*_i	$J_{3,T_\Sigma\min}$
0	0.0845	39.5685	0.6933	5.09481	0.00344	4.6872	3086210
3.8693	0.0853	40	0.75	5.10019	0.003438	4.6922	8521880
38.693	0.0773	36.9454	0.75	5.20265	0.003404	4.7864	58013600
386.93	0.0318	38.5452	0.7434	13.1971	0.002137	12.141	527719000

Table 3.3.7. Results for the GSA-based minimization of J_{4,k_P}.

$(\gamma_{k_P})^2$	$B^*_{\Delta e}$	B^*_e	η^*	β^*	k^*_c	T^*_i	$J_{4,k_P\min}$
0	0.0848	40	0.75	5.1325	0.003427	4.72191	155631
0.142	0.0855	40	0.75	5.0851	0.003443	4.67833	352168
1.42	0.083	39.5146	0.75	5.1788	0.003412	4.76449	2142170
14.2	0.0269	22.0776	0.25316	8.9187	0.0026	8.20516	19276900

Table 3.3.8. Results for the GSA-based minimization of J_{4,T_Σ}.

$(\gamma_{T_\Sigma})^2$	$B_{\Delta e}^*$	B_e^*	η^*	β^*	k_c^*	T_i^*	$J_{4,T_\Sigma \min}$
0	0.0848	40	0.75	5.1325	0.003427	4.7219	155631
0.15885	0.0847	40	0.75	5.1357	0.003426	4.7248	381779
1.5885	0.0783	36.887	0.75	5.1242	0.00343	4.7142	2409020
15.885	0.0216	20.3656	0.25	10.234	0.002427	9.415	21602000

Fig. 3.3.2 presents a description of the evolution of the variables of the objective function and of the objective function J_{2,k_P} during the search process. The weighting parameter $\gamma_{k_P}=0$ was considered.

In addition to Fig. 3.3.2, which gives a representation focused on the best position of the algorithm iterations, Fig. 3.3.3 exemplifies the movements of all agents used in GSA during the search process in order to better recognize the exploration and exploitation capabilities of the algorithm.

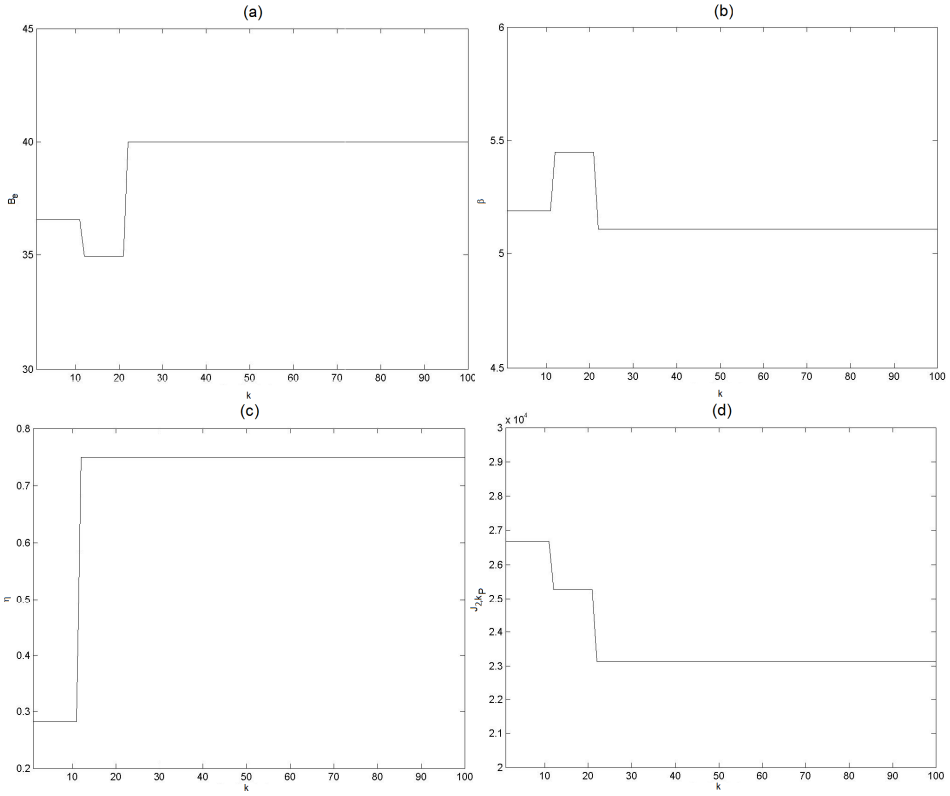

Fig. 3.3.2. T-S PI-FC tuning parameters and objective function evolution vs. iteration index: B_e versus k (a), β versus k (b), η versus k (c), and J_{2,k_P} versus k (d).

The results obtained for the GSA-based solution to the optimization problems described in Chapter 2, were validated in [Pre11e] using the experimental set-up described in Chapter 2. The presentation of the real-time experimental results is organized in terms of plotting the evolutions of the control signal (representing the PWM duty cycle, *u*) and of the controlled output (representing the angular position, *y*) versus time, and of evaluating the objective functions for the control systems on the real-world process represented by the experimental setup. The experimental results were obtained for the step-type angular position reference input of $r_0 = 40 \text{ rad}$. The experiments were conducted for the control systems with both the PI controller and the T-S PI-FC. The parameters used on the real-world process in order to evaluate the objective function J_{1,k_P} and the value of the weighting parameter $(\gamma_{k_P})^2 = 0.06858$ in order to record the control systems' responses (i.e., the control signals and the controlled outputs) in a comparative manner.

The average value of the design parameter β of the PI controller was $\beta = 7$. This controller was tuned by the ESO method.

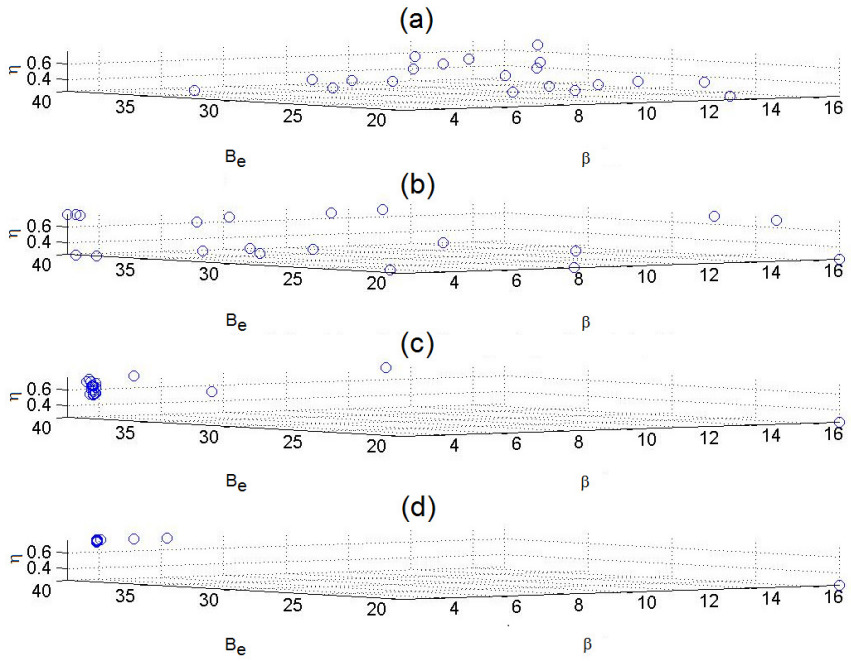

Fig. 3.3.3. Vector solution $\boldsymbol{\rho}$ to the optimization problem (2.14) in the search domain $D_{\boldsymbol{\rho}}$ for four values of iteration index *k*: $k = 1$ (a), $k = 15$ (b), $k = 60$ (c), and $k = 100$ (d).

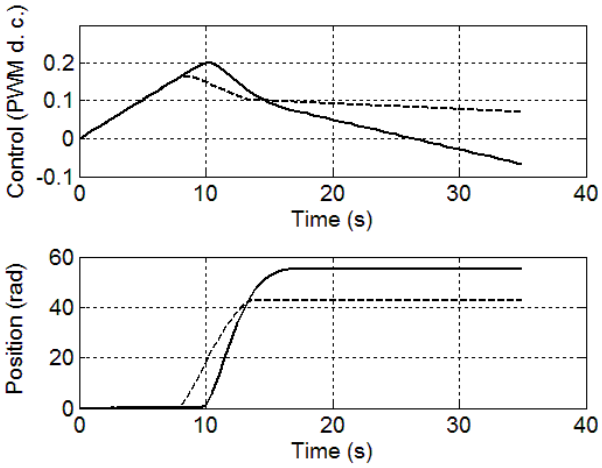

Fig. 3.3.4. Control signal and controlled output (angular position) of the control system with the PI controller (dashed) and of the control system with the T-S PI-FC (solid).

It can be observed from Fig. 3.3.4 that the differences between the results are somehow similar because of the equivalence between the PI controller and the T-S PI-FC. However, the control systems appear to be sensitive to different random disturbances that act as static friction which has a different unpredictable value each time. Even more insight can be gained when the objective functions are analyzed. They have different values than those from the simulations and the corresponding time responses are different. The reason for these is represented by the same aspects mentioned before and in addition to the uncertainty in the model. However it will be discussed and shown as follows that the tuning parameters of the T-S PI-FCs obtained through the implementation of the GSA-based solution ensures the strong decrease of the objective functions.

3.4. Hybrid Particle Swarm Optimization-Gravitational Search algorithms

The hybridization of nature-inspired algorithms evolved as a solution necessary in overcoming certain shortcomings observed during the use of original conventional of these classical algorithms. In [Mir10] a hybridization of PSO and GSA algorithms is proposed with the objective of obtaining an improved search technique, which aims to incorporate the advances of both algorithms. In order to achieve this goal, the ability of social thinking in PSO is interrelated with the local search capability of GSA.

The operating mechanism of the PSO algorithm, based on the use of swarm particles, also called agents, is employed in the framework of the hybrid Particle Swarm Optimization-Gravitational Search Algorithm (PSOGSA). The agents continue

to be characterized by the vectors $\mathbf{X}_i$ (the particle position vector) and $\mathbf{V}_i$ (the particle velocity vector) [Ken95a], [Ken95b]:

$$\begin{aligned} \mathbf{X}_i &= [x_i^1 \quad \dots \quad x_i^d \quad \dots \quad x_i^q]^T, \\ \mathbf{V}_i &= [v_i^1 \quad \dots \quad v_i^d \quad \dots \quad v_i^q]^T, \end{aligned} \tag{3.19}$$

where $i,\ i = 1 \dots N$, is the index of current agent in the swarm, *N* represents the size of the swarm, and *q* represents the dimension of search space. The particle position vector will have a $q = 3$ dimension in order to suit (2.29) for optimization problems (2.13) – (2.16). Assume $\mathbf{P}_{g,Best}$ be the best swarm position vector:

$$\mathbf{P}_{g,Best} = [p_g^1 \quad \dots \quad p_g^d \quad \dots \quad p_g^q]^T. \tag{3.20}$$

$\mathbf{P}_{g,Best}$ is used as in the case of PSO, and they is updated according to (3.8). The computation of the initial values of $\mathbf{P}_{g,Best}$ will be presented as follows in the first step of the hybrid PSOGSA.

The integration of PSO's exploitation capabilities and GSA's exploration abilities is highlighted during the agents velocities and positions update according to:

$$\begin{aligned} v_i^d(k+1) &= \begin{cases} w(k)\, v_i^d(k) + c_1 r_1 [\mathbf{P}_{g,Best}(k) - x_i^d(k)] + c_2\, r_2 a_i^d(k) & \text{if } m_i(k) > 0, \\ w(k)\, v_i^d(k) + c_1 r_1 [\mathbf{P}_{g,Best}(k) - x_i^d(k)] & \text{otherwise,} \end{cases} \\ x_i^d(k+1) &= x_i^d(k) + v_i^d(k+1),\ d = 1 \dots q,\ i = 1 \dots N, \end{aligned} \tag{3.21}$$

where $r_{1..2}$ are uniformly distributed random variables, $0 \le r_{1,2} \le 1$, and $c_{1,2}$, $c_{1,2} \ge 0$, are represent weighting factors; parameter $w(k)$ stands for the inertia weight and $a_i^d(k)$ is the acceleration expressed in (3.15).

The hybrid PSOGSA algorithm consists of the following steps, presented also in Fig. 3.4.1:

Step 1. Generate the initial population of agents, i.e., initialize the *q*-dimensional search space, the number of agents *N*, set the iteration index $k = 0$, set the search process iteration limit $k_{\max}$, the weighting factors $c_1,\ c_2$ the inertia weight parameter $w(k)$ according to (3.6) and initialize randomly the agents' position vector $\mathbf{X}_i(0)$. Define the gravitational constant decrease law.

The best particle position vector $\mathbf{P}_{i,Best}$ is initialized with the initial positions of the agents and the best swarm position vector $\mathbf{P}_{g,Best}$ is initialized with the position of the first agent.

Step 2. Evaluate the agents' fitness described by (2.9) – (2.12).

Step 3. Compare the performance of each particle to the best global performance, and eventually update the best swarm position vector $\mathbf{P}_{g,Best}$ according to (3.8).

Step 4. Calculate the agents' accelerations $a_i^d(k)$ according to (3.15).

Step 5. Update the agents' velocities $v_i^d(k+1)$ and positions $x_i^d(k+1)$ using (3.21) for $i = 1 \dots N$.

Step 6. Continue incrementing *k* and go to step 2 until the maximum number of iterations is reached, i.e., until $k = k_{\max}$.

Step 7. Terminate and retrieve the final solution in the vector $\mathbf{X}_i$ obtained so far.

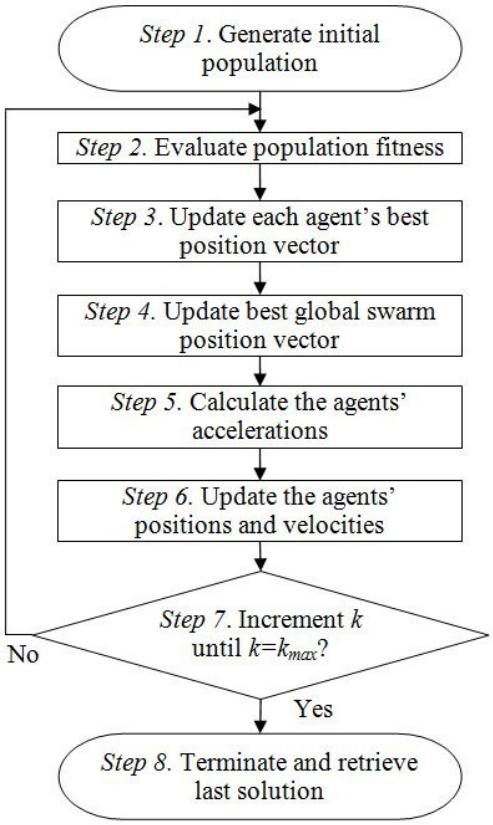

Fig. 3.4.1. Flowchart of hybrid Particle Swarm Optimization-Gravitational Search Algorithm.

In accordance with the fourth step of the design method dedicated to the simple T-S PI-FCs detailed in Sub-chapter 2.1, the hybrid PSOGSA was involved in this step in order to solve the optimization problems corresponding to the objective functions $J_{1...4,k_P}$ and $J_{1...4,T_\Sigma}$ from (2.9) – (2.12). Employing the hybrid PSOGSA requires the definition of all algorithm's parameters specified in step 1, and these values are presented as follows. The number of agents was set to $N = 20$. The maximum number of iterations of the search process was set to $k_{\max} = 100$. As in the case of GSA, the decrease law (3.10) of the gravitational constant was used, with the initial value g_0 set to $g_0 = 100$ and $\zeta = 8.5$. The ε value from (3.12), introduced to avoid possible divisions by zero, was set to $\varepsilon = 10^{-4}$. From the PSO part, the weighting parameters were set to $c_1 = c_2 = 0.3$ in order to ensure a good balance between exploration and exploitation characteristics. The inertia weight parameters outlined in (3.6) were set to $w_{\max} = 0.9$ and $w_{\min} = 0.5$.

Table 3.4.1. Results for the PSOGSA-based minimization of J_{1,k_P}.

$(\gamma_{k_P})^2$	$B^*_{\Delta e}$	B^*_e	η^*	β^*	k^*_c	T^*_i	$J_{1,k_P\min}$
0	0.1362	40	0.75	3.19747	0.004342	2.94168	390671
0.0021357	0.1384	40	0.75	3.14728	0.004376	2.8955	393510
0.021357	0.1379	40	0.75	3.15765	0.004369	2.90504	420934
0.21357	0.1353	40	0.75	3.21885	0.004327	2.96134	695405

Table 3.4.2. Results for the PSOGSA-based minimization of J_{1,T_Σ}.

$(\gamma_{T_\Sigma})^2$	$B^*_{\Delta e}$	B^*_e	η^*	β^*	k^*_c	T^*_i	$J_{1,T_\Sigma\min}$
0	0.1362	40	0.75	3.19747	0.004342	2.94168	390671
0.17187	0.1382	40	0.75	3.15222	0.004373	2.90005	636904
1.7187	0.1443	40	0.75	3.01759	0.004469	2.77618	2480870
17.187	0.0128	20	0.2511	17	0.001883	15.64	22790300

Table 3.4.3. Results for the PSOGSA-based minimization of J_{2,k_P}.

$(\gamma_{k_P})^2$	$B^*_{\Delta e}$	B^*_e	η^*	β^*	k^*_c	T^*_i	$J_{2,k_P\min}$
0	0.0809	37.8291	0.75	5.0852	0.003443	4.67842	23119.3
0.006858	0.0781	36.5224	0.75	5.0869	0.003442	4.67999	32844.2
0.06858	0.0834	39.009	0.75	5.0867	0.003442	4.67976	119057
0.6858	0.0128	20	0.2502	17	0.001883	15.64	873204

Table 3.4.4. Results for the PSOGSA-based minimization of J_{2,T_Σ}.

$(\gamma_{T_\Sigma})^2$	$B^*_{\Delta e}$	B^*_e	η^*	β^*	k^*_c	T^*_i	$J_{2,T_\Sigma\min}$
0	0.073	34.639	0.75	5.164	0.00349	4.75094	23691.9
0.0066695	0.0686	32.4755	0.75	5.1505	0.00349	4.73854	32207.1
0.066695	0.0841	39.8589	0.3458	5.1571	0.0034	4.74457	109204
0.66695	0.0128	20	0.25	17	0.0019	15.64	864943

Table 3.4.5. Results for the PSOGSA-based minimization of J_{3,k_P}.

$(\gamma_{k_P})^2$	$B^*_{\Delta e}$	B^*_e	η^*	β^*	k^*_c	T^*_i	$J_{3,k_P\min}$
0	0.0756	35.561	0.8835	5.1202	0.0034	4.71054	2903740
3.9187	0.0856	40	0.75	5.0849	0.0034	4.67807	8472280
39.187	0.0845	39.7112	0.75	5.1164	0.0034	4.70705	57920700
391.87	0.0315	40	0.75	13.7866	0.002	12.6836	528181000

Table 3.4.6. Results for the PSOGSA-based minimization of J_{3,k_P}.

$(\gamma_{T_\Sigma})^2$	$B^*_{\Delta e}$	B^*_e	η^*	β^*	k_c^*	T_i^*	$J_{3,k_P\min}$
0	0.075573	35.561	0.8835	5.1201	0.0034	4.7105	2903740
3.8693	0.084103	40	0.75	5.1751	0.0034	4.7611	8632620
38.693	0.082147	39.9614	0.75	5.293	0.0034	4.8696	56738000
386.93	0.031254	40	0.75	13.9168	0.002	12.804	528146000

Table 3.4.7. Results for the PSOGSA-based minimization of J_{4,k_P}.

$(\gamma_{k_P})^2$	$B^*_{\Delta e}$	B^*_e	η^*	β^*	k_c^*	T_i^*	$J_{4,k_P\min}$
0	0.0856	40	0.75	5.08538	0.003443	4.67855	153530
0.142	0.0856	40	0.73	5.0852	0.003443	4.67839	353343
1.42	0.0841	40	0.75	5.16972	0.003415	4.75615	2132880
14.2	0.0229	20	0.25	9.50746	0.002518	8.74686	19274000

Table 3.4.8. Results for the PSOGSA-based minimization of J_{4,T_Σ}.

$(\gamma_{T_\Sigma})^2$	$B^*_{\Delta e}$	B^*_e	η^*	β^*	k_c^*	T_i^*	$J_{4,T_\Sigma\min}$
0	0.0855	40	0.75	5.085	0.0034	4.6785	153530
0.15885	0.0855	40	0.75	5.085	0.0034	4.678	379380
1.5885	0.1344	37.0232	0.75	3	0.0045	2.76	1003440
15.885	0.0194	20	0.25	11.2378	0.0023	10.3387	21610900

The results containing the minimized values of the objective functions $J_{1...4,k_P}$ and $J_{1...4,T_\Sigma}$ (i.e., $J_{1...4,k_P\min}$ and $J_{1...4,T_\Sigma\min}$) are presented in Tables 3.4.1 – 3.4.8 together with the optimal controller tuning parameters.

Despite the hybridization of two nature-inspired algorithms, the random characteristic was not eliminated, and several simulations were required before obtaining the final results. An analysis centered on average values of the objective functions and two newly introduced performance indices will be detailed in Subchapter 3.8.

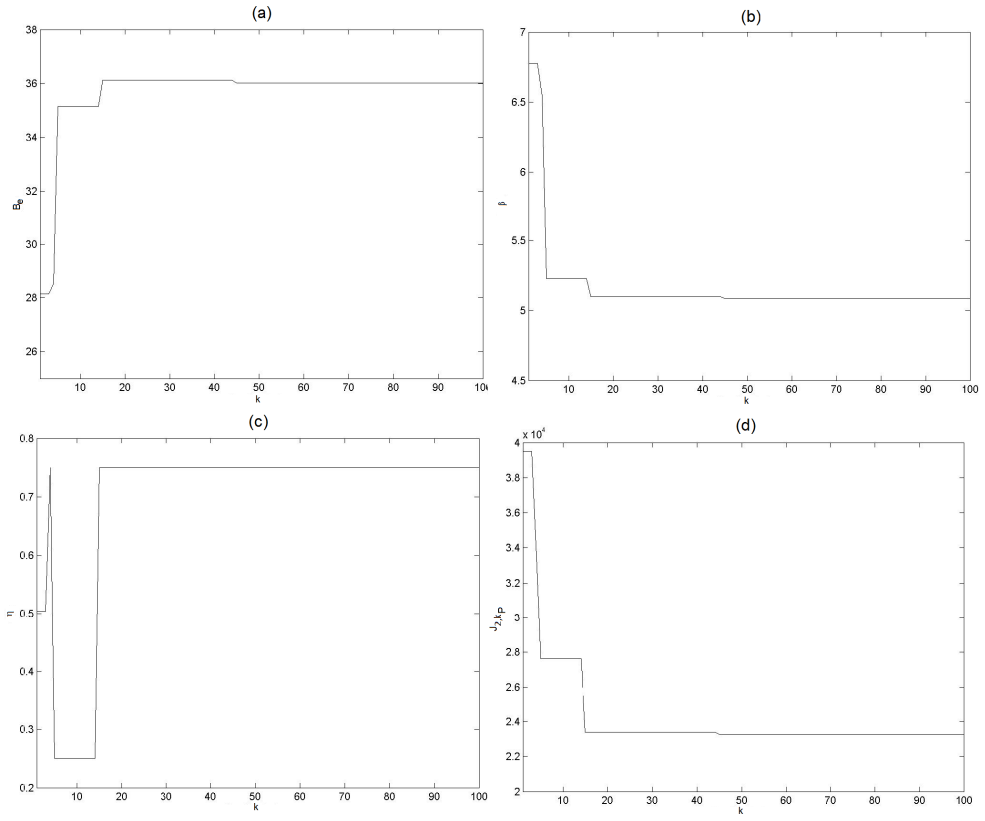

Fig. 3.4.2. T-S PI-FC tuning parameters and objective function evolution vs. iteration index: B_e versus k (a), β versus k (b), η versus k (c), and J_{2,k_P} versus k (d).

Fig. 3.4.2 describes the evolution of the controller tuning parameters and of the intermediate values of objective function J_{2,k_P} during the search process. The weighting parameter $\gamma_{k_P}=0$ was considered in the optimization problem.

Fig. 3.4.3 illustrates the evolution of all agents during the search process is presented at four steps: $k=1$, $k=15$, $k=60$ and $k=100$.

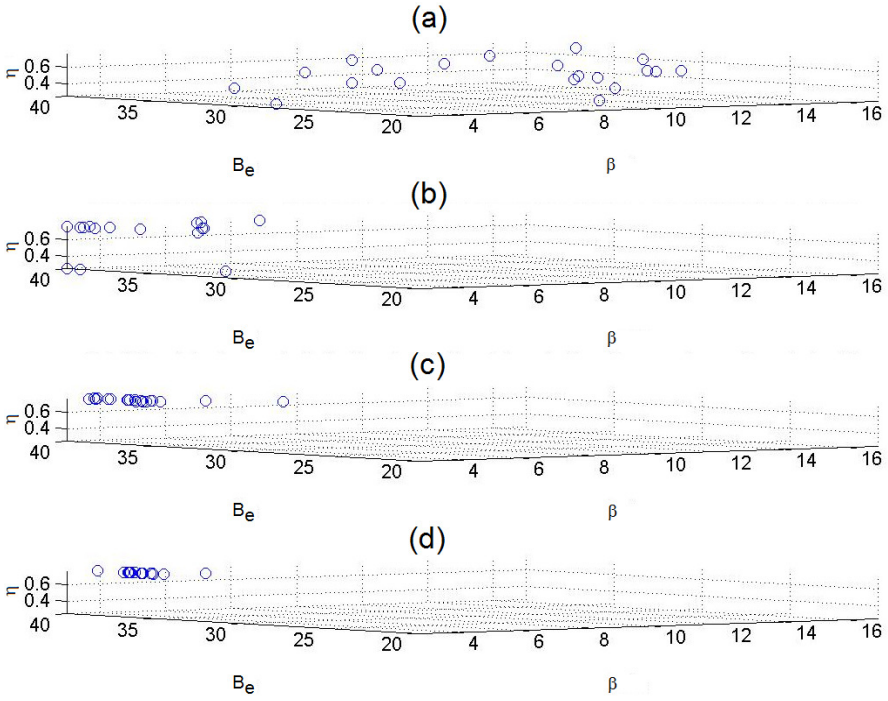

Fig. 3.4.3. Vector solution $\boldsymbol{\rho}$ to the optimization problem (2.14) in the search domain $D_{\boldsymbol{\rho}}$ for four values of iteration index k: $k=1$ (a), $k=15$ (b), $k=60$ (c), and $k=100$ (d).

For the sake of comparison, Fig. 3.4.4 includes a comparison with the T-S PI-FC tuned by PSO and with the T-S PI-FC tuned by GSA in the same conditions. The same values of the parameters of PSO and GSA are used (taken from the parameters of PSOGSA), and the parameters corresponding to the objective J_{1,T_Σ} and weighting parameter $(\gamma_{T_\Sigma})^2 = 0.17187$ from Table 3.2.2 and Table 3.3.2 are used. The performance improvement ensured by the PSOGSA algorithm is highlighted in Fig. 3.4.4.

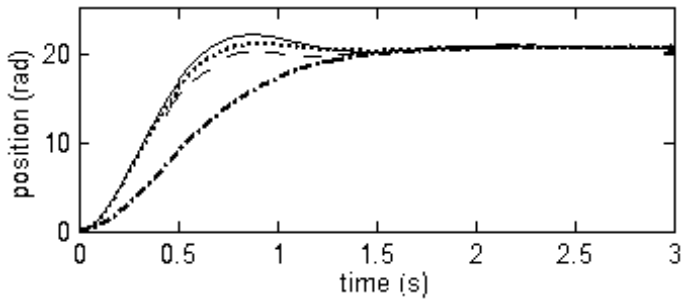

Fig. 3.4.4. Fuzzy control system responses: with initial T-S PI-FC (line-dotted), PSO-based T-S PI-FC (solid), GSA-based T-S PI-FC (discontinuous line), hybrid PSOGSA-based T-S PI-FC (dotted).

3.5. CHARGED SYSTEM SEARCH ALGORITHMS

The specific features of Charged System Search (CSS) algorithms concern the random determination of the initial positions of charged particles (CPs) and the initial velocities of CPs set to zero. Each CP has an associated magnitude of charge $q_{c,i}$ and as a result it creates an electrical field around its space. The magnitude of the charge at iteration *k* is defined considering the quality of its solution as:

$$q_{c,i}(k)=\frac{g_i(k)-g_{best}(k)}{g_{best}(k)-g_{worst}(k)},\ i=1...N\ , \tag{3.22}$$

where $g_{best}(k)$ and $g_{worst}(k)$ are the so far best and the worst fitness of all CPs at iteration *k*, $g_i(k)$ is the objective function value or the fitness function value of i^{th} CP at iteration *k*, and N is the total number of CPs. The separation distance r_{ij} between two CPs at iteration *k* is defined as [Pre12d]:

$$r_{ij}(k)=\frac{\|\mathbf{X}_i(k)-\mathbf{X}_j(k)\|}{\|\frac{(\mathbf{X}_i(k)+\mathbf{X}_j(k))}{2}-\mathbf{X}_{best}(k)\|+\varepsilon}\mathbf{X}_i(k),\ \mathbf{X}_o(k)\in\mathbf{R}^{q_s},\ o\in\{i,j,best\}\ , \tag{3.23}$$

where q_s is the dimension of the search space, $\mathbf{X}_i(\mathrm{k})$ and $\mathbf{X}_j(\mathrm{k})$ are the position vectors of i^{th} and j^{th} CP at iteration *k*, respectively, $\mathbf{X}_{best}(\mathrm{k})$ is the position of the best current CP at iteration *k*, $\varepsilon,\ \varepsilon>0$, is a constant introduced to avoid singularities, and the Euclidean norm is considered in (3.23).

For the optimization problems presented in (2.13) – (2.16), a $q=3$-dimensional search space is required, according to (2.19).

The electric forces between any two CPs are used in increasing CSS algorithm's exploitation ability. The good CPs can attract the other CPs and the bad ones repel the others, proportional to their rank c_{ij} [Kav10a], [Kav10b], [Kav10c], [Pre12d]:

$$c_{ij}=\begin{cases}-1, & \text{if } g_i<g_j,\\ 1, & \text{otherwise,}\end{cases} \tag{3.24}$$

where the parameter c_{ij} determines the type and the degree of influence of each CP on the other CPs, considering their fitness apart from their charges.

The value of the resultant electrical force $\mathbf{F}_i$ acting on i^{th} CP at iteration *k* is [Kav10a]:

$$\mathbf{F}_i(k)=q_i(k)\sum_{i,i\neq j}\left(\frac{q_j(k)r_{ij}(k)i_1}{a^3}+\frac{q_j(k)i_2}{r_{ij}^2(k)}\right)c_{ij}(\mathbf{X}_i(k)-\mathbf{X}_j(k)),\ (i_1,i_2)=\begin{cases}(0,1), & \text{if } r_{ij}(k)\geq a,\\ (1,0), & \text{otherwise,}\end{cases} \tag{3.25}$$

where $i,j=1...N$. Equation (3.25) shows that each CP is considered as a charged sphere with radius a having a uniform volume charge density.

The new position (vector) $\mathbf{X}_i(k+1)$ and velocity (vector) $\mathbf{V}_i(k+1)$ of each CP is determined in terms of [Kav10a], [Kav10b], [Kav10c], [Pre14c]:

$$\mathbf{X}_i(k+1) = r_{i1} k_a(k)(\frac{\mathbf{F}_i}{m_i})(\Delta k)^2 + r_{i2} k_v(k)\mathbf{V}_i(k)\Delta k + \mathbf{X}_i(k),$$
$$\mathbf{V}_i(k+1) = \frac{\mathbf{X}_i(k+1) - \mathbf{X}_i(k)}{\Delta k}, \tag{3.26}$$

where k is the current iteration index which is dropped out at certain variables for the sake of simplicity, $k_a(k)$ is the acceleration parameter at iteration k, $k_v(k)$ is the velocity parameter at iteration k, which controls the influence of the previous velocity, r_{i1} and r_{i2} are two random numbers uniformly distributed in the range $0 < r_{i1}, r_{i2} < 1$, m_i is the mass of i^{th} CP, $i = 1...N$, which is set here as equal to $q_{c,j}$, and Δk is the time step set to 1.

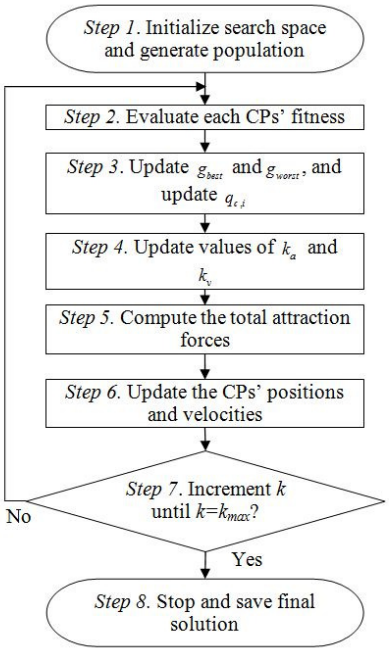

Fig. 3.5.1. Flowchart of Charged System Search algorithm.

The effect of the pervious velocity and the resultant force acting on a CP can be decreased or increased based on the values of $k_a(k)$ and $k_v(k)$, respectively. Since $k_a(k)$ is the parameter related to the attracting forces; selecting a large value of $k_a(k)$ may cause a fast convergence and choosing a small value can increase the computational time. $k_v(k)$ controls the exploration process. The following modifications of $k_v(k)$ and $k_v(k)$ with respect to the iteration index are applied [Pre14c]:

$$k_a(k) = 3(1 - \frac{k}{k_{\max}}),\ k_v(k) = 0.5(1 + \frac{k}{k_{\max}}), \tag{3.27}$$

where $k_{\max}$ is the maximum number of iterations.

The CSS algorithm consists of the following steps [Pre12d]:

Step 1. Initialize the dimensional search space, the number of CPs N, set the iteration index $k=0$, set the search process iteration limit $k_{\max}$ and randomly generate the CPs' position vector $\mathbf{X}_i(0)$, $i=1...N$.

Step 2. Evaluate the CPs' fitness in line with (2.9) – (2.12).

Step 3. Update $g_{best}(k)$ and $g_{worst}(k)$, and update $q_{c,i}(k)$ using (3.22) for $i=1...N$.

Step 4. Update the values of $k_a(k)$ and $k_v(k)$ according to (3.27).

Step 5. Compute the total force in different directions using (3.23), (3.24) and (3.25).

Step 6. Update the CPs' velocities and positions using (3.26).

Step 7. Increment k and go to step 2 until the maximum number of iterations is reached, i.e., $k=k_{\max}$.

Step 8. Save the optimal parameter vector as the position vector corresponding to the minimum value of objective (fitness) function.

These steps are included in the flowchart of the CSS algorithm as presented in Fig. 3.5.1.

Table 3.5.1. Results for the CSS-based minimization of J_{1,k_P}.

$(\gamma_{k_P})^2$	$B^*_{\Delta e}$	B^*_e	η^*	β^*	k_c^*	T_i^*	$J_{1,k_P\min}$
0	0.1408	40	0.75	3.0937	0.0044	2.846	390621
0.0021357	0.1452	40	0.75	3	0.0045	2.76	395143
0.021357	0.142	40	0.75	3.0664	0.0044	2.821	421548
0.21357	0.1452	40	0.7434	3	0.0045	2.76	698489

Table 3.5.2. Results for the CSS-based minimization of J_{1,T_Σ}.

$(\gamma_{T_\Sigma})^2$	$B^*_{\Delta e}$	B^*_e	η^*	β^*	k_c^*	T_i^*	$J_{1,T_\Sigma\min}$
0	0.1452	40	0.75	3	0.0042	2.76	392076
0.17187	0.1342	40	0.75	3.2453	0.0043	2.9857	640415
1.7187	0.1418	39.0736	0.75	3	0.0045	2.76	2867160
17.187	0.0128	20	0.25	17	0.0019	15.64	22809200

Table 3.5.3. Results for the CSS-based minimization of J_{2,k_P}.

$(\gamma_{k_P})^2$	$B^*_{\Delta e}$	B^*_e	η^*	β^*	k_c^*	T_i^*	$J_{2,k_P\min}$
0	0.0856	40	0.75	5.085	0.0034	4.6784	22979.9
0.006858	0.0852	40	0.75	5.111	0.0034	4.7024	32749.4
0.06858	0.0844	39.5179	0.75	5.097	0.0034	4.689	119197
0.6858	0.0129	20	0.25	17	0.0019	15.64	874183

Table 3.5.4. Results for the CSS-based minimization of J_{2,T_Σ}.

$(\gamma_{T_\Sigma})^2$	$B^*_{\Delta e}$	B^*_e	η^*	β^*	k_c^*	T_i^*	$J_{2,T_\Sigma \min}$
0	0.0856	40	0.75	5.0852	0.0034	4.6784	22979.9
0.0066695	0.085	40	0.75	5.1183	0.0034	4.7088	32661.5
0.066695	0.0853	40	0.75	5.1007	0.0034	4.6927	118170
0.66695	0.0128	20	0.25	17	0.0019	15.64	864943

Table 3.5.5. Results for the CSS-based minimization of J_{3,k_P}.

$(\gamma_{k_P})^2$	$B^*_{\Delta e}$	B^*_e	η^*	β^*	k_c^*	T_i^*	$J_{3,k_P \min}$
0	0.0779	36.563	0.75	5.1096	0.003435	4.701	3089410
3.9187	0.0854	40	0.75	5.0961	0.003439	4.688	8491810
39.187	0.0849	40	0.75	5.1447	0.0034	4.7332	57665900
391.87	0.0369	40	0.75	11.7966	0.0023	10.8529	528840000

Table 3.5.6. Results for the CSS-based minimization of J_{3,k_P}.

$(\gamma_{T_\Sigma})^2$	$B^*_{\Delta e}$	B^*_e	η^*	β^*	k_c^*	T_i^*	$J_{3,k_P \min}$
0	0.0851	40	0.75	5.1167	0.0034	4.70733	3033090
3.8693	0.0855	39.9368	0.7282	5.1026	0.0034	4.69442	8555190
38.693	0.1449	40	0.75	3.0066	0.0045	2.76606	52611000
386.93	0.0339	40	0.75	12.8174	0.0022	11.792	530435000

Table 3.5.7. Results for the CSS-based minimization of J_{4,k_P}.

$(\gamma_{k_P})^2$	$B^*_{\Delta e}$	B^*_e	η^*	β^*	k_c^*	T_i^*	$J_{4,k_P \min}$
0	0.0845	40	0.75	5.1497	0.003421	4.73768	155252
0.142	0.0845	40	0.75	5.151	0.003421	4.7389	354007
1.42	0.084	39.8938	0.75	5.1678	0.003415	4.75435	2142920
14.2	0.0225	20	0.25	9.6546	0.002499	8.88227	19379100

Table 3.5.8. Results for the CSS-based minimization of J_{4,T_Σ}.

$(\gamma_{T_\Sigma})^2$	$B^*_{\Delta e}$	B^*_e	η^*	β^*	k_c^*	T_i^*	$J_{4,T_\Sigma \min}$
0	0.0845	40	0.75	5.1497	0.003421	4.73768	155252
0.15885	0.0847	40	0.75	5.1365	0.003426	4.72559	380819
1.5885	0.085	40	0.75	5.1216	0.003431	4.7119	2419410
15.885	0.0207	20	0.25	10.4964	0.002396	9.65673	21711500

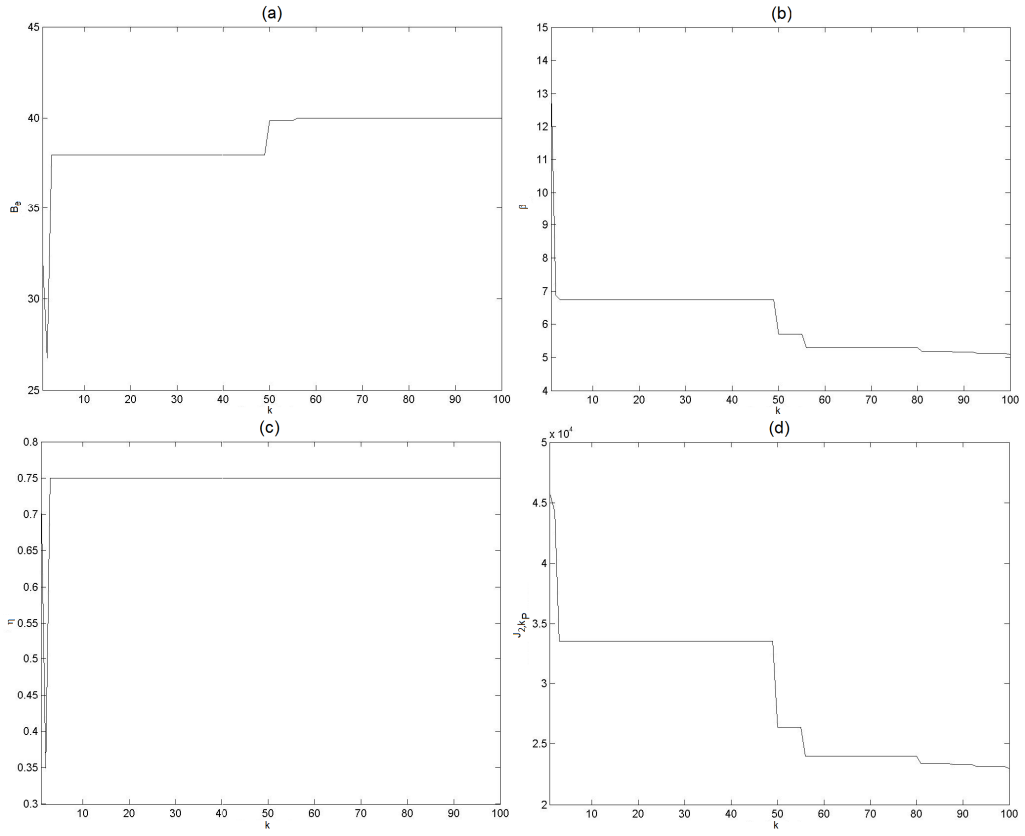

Fig. 3.5.2. T-S PI-FC tuning parameters and objective function evolution vs. iteration index: B_e versus k (a), β versus k (b), η versus k (c), and J_{2,k_P} versus k (d).

The CSS algorithm previously descried was employed in the step 4 of the design method dedicated to the simple T-S PI-FCs presented in Sub-chapter 2.1. Before a CSS-based solution could be used, all algorithm parameters required initialization. The number of used CPs was set as $N = 20$, the maximum number of iterations was set to $k_{\max} = 100$. For the sake of simplicity each CP is considered as a charged sphere with radius $a = 1$ having a uniform volume charge density. The constant ε in (3.23) was set to $\varepsilon = 10^{-4}$.

The results representing the optimal controller tuning parameters and the minimized values of the objective functions $J_{1...4,k_P}$ and $J_{1...4,T_\Sigma}$ (i.e., $J_{1...4,k_P \min}$ and $J_{1...4,T_\Sigma \min}$) are presented in Tables 3.5.1 – 3.5.8. A consequence of the degrees of freedom represented by the arbitrary CSS parameters requires several restarts of the search process before a final solution can be obtained. This aspect will be analyzed in Sub-chapter 3.8 based on the average values of the objective functions and two newly introduced performance indices.

Fig. 3.5.2 illustrates an evolutionary representation of the controller tuning parameters and of the objective function J_{2,k_P} along the algorithm's iterations. The weighting parameter $\gamma_{k_P} = 0$ was considered.

Several snapshots of all CPs during the search process are shown in Fig. 3.5.3 in order to give a better representation of algorithm's exploration and exploitation capabilities.

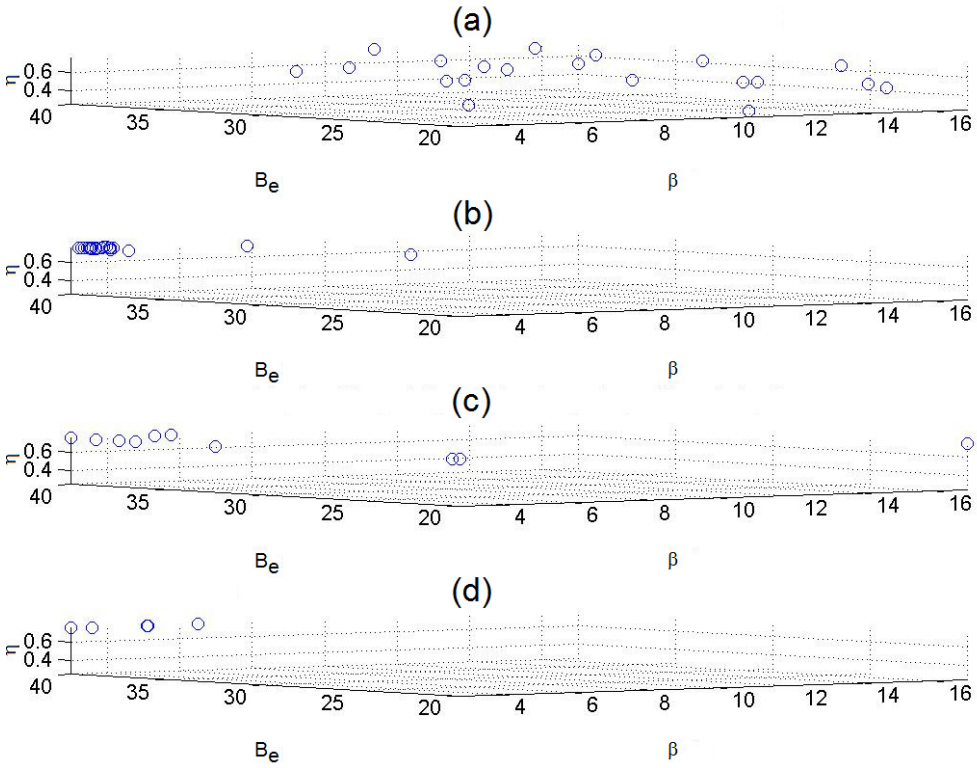

Fig. 3.5.3. Vector solution $\boldsymbol{\rho}$ to the optimization problem (2.14) in the search domain $D_{\boldsymbol{\rho}}$ for four values of iteration index k: $k=1$ (a), $k=15$ (b), $k=60$ (c), and $k=100$ (d).

The solution based on the CSS algorithm to the optimization problems presented in Chapter 2 is validated in [Pre12d] through experimental results for the experimental setup presented in Chapter 2. The experimental results were obtained for the step-type angular position reference input of $r_0 = 40 \text{ rad}$, and they were conducted for the control systems with both the PI controller and the T-S PI-FC. A sample of the real-time experimental that corresponds to the objective function J_{1,k_P} and for the $(\gamma_{k_P})^2 = 0.006858$ value of the weighting parameter is presented in Fig. 3.5.4.

The additional PI controller mentioned in this experimental study had the value of the design parameter β set to $\beta = 7$. This controller was tuned by the ESO method.

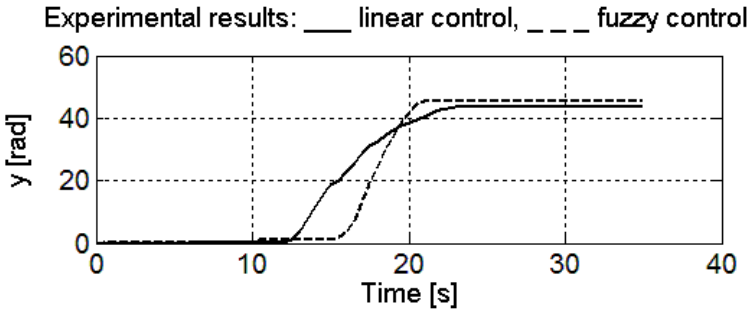

Fig. 3.5.4. Controlled output of the control system with the PI controller (solid line) and of the fuzzy control system (dashed line).

The objective function measured for the fuzzy control system is smaller compared to that of the control system with the linear (PI) controller [Pre12d]. In addition, the improvements of the settling time and of the overshoot ensured by the fuzzy control system are highlighted in Fig. 3.5.4. Therefore, the use of the CSS algorithm in the optimal tuning of fuzzy controllers is justified.

3.6. Adaptive Gravitational Search Algorithms

Although the standard GSA has already shown promising results illustrated in [Pre13a], a good computational efficiency and ease of implementation, it uses several predefined parameters and schedules which fail to take into consideration the state of the search process. Hence, the algorithm can become computationally inefficient as the exploration-exploitation ratio could become inefficient and the algorithm might get trapped in local minima situations.

Therefore, the most important and interesting goals in GSA development are optimal resource usage and avoiding local optima. The adaptive GSA proposed in [Pre12a], [Pre13d] offers a superior search process compared to the standard GSA by improving the exploration of the search space as it continues the development of the stage based adaptation of algorithm parameters [Liu10a]. This improvement is ensured by the use of a learning model for the algorithm, inspired by the 5E learning cycle discussed in [Byb02] and [Bal06].

As the standard GSA, the adaptive version is governed by the same operating mechanism which is based on the use of agents (i.e., particles) and on Newton's law of gravity [Ras09], [Ras10]. The algorithm consists of the following stages:

I. *Engagement*. The initial N agents number is defined and their positions are generated randomly:

$$\mathbf{X}_i = [x_i^1 \quad \dots \quad x_i^d \quad \dots \quad x_i^q]^T,\ \mathbf{X}_i = \boldsymbol{\rho},\ i = 1 \dots N\ , \tag{3.28}$$

where $\mathbf{X}_i$ is agents' position vector, x_i^d is the position of i^{th} agent in d^{th} dimension of the $q = 3$-dimensional search space, as results from (2.29) in order to solve the optimization problems (2.13) – (2.16). The maximum number of iterations $k_{\max}$ of the search process is set and the iteration index k is set to $k = 0$ and will be incremented at the end of the iteration according to step 7 in Fig. 3.6.1.

II. *Exploration*. This stage allows the algorithm to discover the extent of the search space. The following linear decrease law of the gravitational constant is employed:

$$g(k) = g_0(1 - \psi \frac{k}{k_{\max}}), \tag{3.29}$$

where $g(k)$ is the value of gravitational constant at current iteration index *k*, g_0 is the initial $g(k)$, and $\psi > 0$ is an a priori set parameter which ensures a trade-off to GSA's convergence and search accuracy.

The agent's velocities and positions are updated using:

$$\begin{aligned} v_i^d(k+1) &= \rho_i v_i^d(k) + a_i^d(k), \\ x_i^d(k+1) &= x_i^d(k) + v_i^d(k+1), \end{aligned} \tag{3.30}$$

where ρ_i, $0 \le \rho_i \le 1$, is a uniform random variable; $a_i^d(k)$ is the acceleration of i^{th} agent in d^{th} dimension:

$$a_i^d(k) = \frac{1}{m_{Ii}(k)} \sum_{j=1, j\neq i}^{N} \sigma_j \frac{g(k) m_{Pi}(k) m_{Aj}(k)[x_j^d(k) - x_i^d(k)]}{(r_{ij}(k) + \varepsilon x_j^d(k))}, \tag{3.31}$$

where σ_j, $0 \le \sigma_j \le 1$, is a random generated number, $m_{Ii}(k)$, $m_{Pi}(k)$ and $m_{Aj}(k)$ are the inertial, passive and active gravitational masses related to i^{th} and j^{th} agent, $\varepsilon > 0$ is a relatively small constant, and $r_{ij}(k)$ is the Euclidian distance between i^{th} and j^{th} agents:

$$r_{ij}(k) = \| \mathbf{X}_i(k) - \mathbf{X}_j(k) \|. \tag{3.32}$$

The expressions of the active gravitational mass and of the inertial mass are calculated in terms of:

$$\begin{aligned} n_i(k) &= \frac{f_i(k) - \max\limits_{j=1\ldots n} f_j(k)}{\min\limits_{j=1\ldots n} f_j(k) - \max\limits_{j=1\ldots n} f_j(k)}, \\ m_i(k) &= \frac{n_i(k)}{\sum\limits_{j=1}^{N} n_j(k)}, \\ m_{Ai} &= m_{Ii} = m_i. \end{aligned} \tag{3.33}$$

Stage II of the adaptive GSA is carried out for the first 15% iterations (i.e., runs) in the search process.

III. *Explanation*. Algorithm's parameters restrict agents' movement during the next 45% iterations in the search process, by the introduction of a more aggressive decrease law of $g(k)$ according to:

$$g(k) = g_0 \exp(-\zeta \frac{k}{k_{\max}}), \tag{3.34}$$

where $\zeta > 0$ is an a priori set parameter which affects GSA's convergence and search accuracy.

IV. *Elaboration*. The remaining 40% of iterations are characterized by setting the general position for the optimal value of the fitness function and leaving the remaining time to refine the obtained results. The value of $g(k)$ stops decreasing, and during this stage the worst agents' positions are reset to the best values obtained so far after each run.

V. *Evaluation*. The tuned parameters, obtained at the end of the search process, are applied to the real-world optimization problem in order to evaluate the quality of the solution.

Fig. 3.6.1 illustrates the adaptive GSA's stages.

The five stages of the proposed adaptive GSA are different to those ones presented in the non-adaptive GSA in several formulations [Ras09], [Pre11d], [Pre11e], that consist of the stages I, III and V, but with a single and fixed constant decrease law of the gravitational constant and without resetting the worst fitness and position.

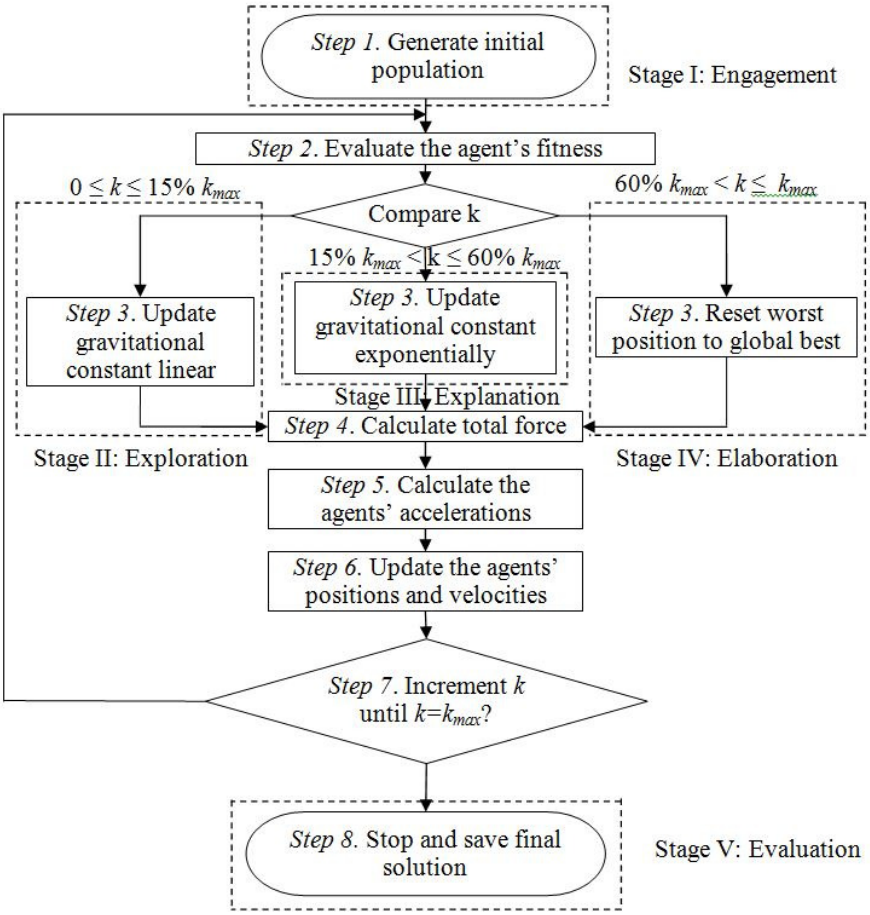

Fig. 3.6.1. Flowchart of Adaptive Gravitational Search Algorithm.

The computational complexity of this optimization algorithm is influenced by the complexity of the evaluation of the objective function (viz., the fitness function) and by the number of runs of the GSA. For the objective functions considered in this thesis, each variable (i.e., tuning parameter of the fuzzy controller) is altered separately at every stage and a new evaluation of the objective function is required in order to determine the variation impact. This results in an increase of the number of evaluations of the objective functions, which is proportional to the number of variables. In case of this adaptive GSA the computational complexity varies as function of which stage the search process is involved. Stage III is the most computationally intensive one because two parameters are modified simultaneously.

Introducing this adaptive GSA in the fourth step of the design method dedicated to the simple T-S PI-FCs presented in Sub-chapter 2.1 required the setting of algorithm's parameters. The number of used agents $N = 20$ was set and the maximum number of iterations was set to $k_{\max} = 100$. The ψ and g_0 parameters in (3.29) were set as $\psi = 0.5$ and $g_0 = 100$. The ε parameter in (3.31) was set to $\varepsilon = 10^{-4}$ in order to avoid possible divisions by zero. The ζ parameter in (3.34) was set to $\zeta = 8.5$, and g_0 was kept the same as in (3.29).

The simulation results for the optimal controller tuning parameters and the minimized values of the objective functions are presented in Tables 3.6.1 – 3.6.8. As in case of the normal GSA, the adaptive version required repeated runs of the simulations before obtaining the final results. The Sub-chapter 3.8 contains an analysis focused on this algorithm arbitrary characteristic based on the average values of the objective functions and three performance indices.

Table 3.6.1. Results for the adaptive GSA-based minimization of J_{1,k_P}.

$(\gamma_{k_P})^2$	$B^*_{\Delta e}$	B^*_e	η^*	β^*	k_c^*	T_i^*	$J_{1,k_P\min}$
0	0.1386	40	0.75	3.143	0.004379	2.8917	390459
0.0021357	0.1379	40	0.75	3.1576	0.004369	2.90502	393510
0.021357	0.1379	40	0.75	3.1573	0.004369	2.90467	421036
0.21357	0.1374	39.8401	0.75	3.1566	0.00437	2.90404	695019

Table 3.6.2. Results for the adaptive GSA-based minimization of J_{1,T_Σ}.

$(\gamma_{T_\Sigma})^2$	$B^*_{\Delta e}$	B^*_e	η^*	β^*	k_c^*	T_i^*	$J_{1,T_\Sigma\min}$
0	0.1386	40	0.75	3.1432	0.004379	2.8917	390459
0.17187	0.1393	40	0.75	3.1261	0.004391	2.87602	637573
1.7187	0.1387	39.5837	0.75	3.1074	0.004404	2.85879	2856930
17.187	0.0128	20.0053	0.25	17	0.001883	15.64	22806100

Table 3.6.3. Results for the adaptive GSA-based minimization of J_{2,k_P}.

$(\gamma_{k_P})^2$	$B^*_{\Delta e}$	B^*_e	η^*	β^*	k_c^*	T_i^*	$J_{2,k_P\min}$
0	0.0843	39.4214	0.75	5.0872	0.0034	4.6802	23042.5
0.006858	0.0848	39.6633	0.75	5.0918	0.0034	4.6844	32704.3
0.06858	0.0849	40	0.75	5.1263	0.0034	4.7161	119101
0.6858	0.0128	20.0052	0.25	17	0.0019	15.64	874136

Table 3.6.4. Results for the adaptive GSA-based minimization of J_{2,T_Σ}.

$(\gamma_{T_\Sigma})^2$	$B^*_{\Delta e}$	B^*_e	η^*	β^*	k_c^*	T_i^*	$J_{2,T_\Sigma\min}$
0	0.0843	39.4214	0.75	5.0872	0.003442	4.6802	23042.5
0.0066695	0.0855	40	0.75	5.0928	0.00344	4.6854	32599.4
0.066695	0.084	39.803	0.75	5.1574	0.003419	4.7448	116083
0.66695	0.0128	20.0053	0.25	17	0.001883	15.64	864596

Table 3.6.5. Results for the adaptive GSA-based minimization of J_{3,k_P}.

$(\gamma_{k_P})^2$	$B^*_{\Delta e}$	B^*_e	η^*	β^*	k_c^*	T_i^*	$J_{3,k_P\min}$
0	0.0851	40	0.75	5.1118	0.0034	4.70288	3025720
3.9187	0.0849	39.6832	0.75	5.0876	0.0034	4.68074	8483290
39.187	0.0712	35.1788	0.75	5.3772	0.0033	4.947	57354700
391.87	0.0323	40	0.75	13.471	0.0021	12.3934	527357000

Table 3.6.6. Results for the adaptive GSA-based minimization of J_{3,k_P}.

$(\gamma_{T_\Sigma})^2$	$B^*_{\Delta e}$	B^*_e	η^*	β^*	k_c^*	T_i^*	$J_{3,k_P\min}$
0	0.0856	39.9958	0.75	5.0849	0.0034	4.678	2984880
3.8693	0.0856	40	0.75	5.087	0.0034	4.68	8502740
38.693	0.0812	40	0.3804	5.3617	0.0034	4.9328	57918400
386.93	0.0324	38.6831	0.75	12.978	0.0022	11.9398	527683000

Table 3.6.7. Results for the adaptive GSA-based minimization of J_{4,k_P}.

$(\gamma_{k_P})^2$	$B^*_{\Delta e}$	B^*_e	η^*	β^*	k_c^*	T_i^*	$J_{4,k_P\min}$
0	0.0845	40	0.75	5.1528	0.0034	4.7406	155249
0.142	0.083	38.7878	0.75	5.0857	0.0034	4.6788	353686
1.42	0.084	39.9504	0.415	5.1342	0.0034	4.7234	2143540
14.2	0.023	20.3629	0.25	9.5955	0.0025	8.8279	19277500

Table 3.6.8. Results for the adaptive GSA-based minimization of J_{4,k_P}.

$(\gamma_{T_\Sigma})^2$	$B^*_{\Delta e}$	B^*_e	η^*	β^*	k_c^*	T_i^*	$J_{4,k_P\min}$
0	0.0845	40	0.75	5.1529	0.0034	4.7407	155249
0.15885	0.0846	40	0.75	5.1431	0.0034	4.7316	380396
1.5885	0.0491	23.2926	0.75	5.1583	0.0034	4.7456	2337150
15.885	0.0207	20.0066	0.25	10.5253	0.0024	9.6833	21600800

Fig. 3.6.2 presents the evolution of the tuning parameters of the T-S PI-FC and of the objective function J_{2,k_P} along the iterations of the optimization process. The weighting parameter $\gamma_{k_P}=0$ was considered.

Fig. 3.6.3 illustrates the evolution of all agents' positions for the adaptive GSA after the first four stages of the search process.

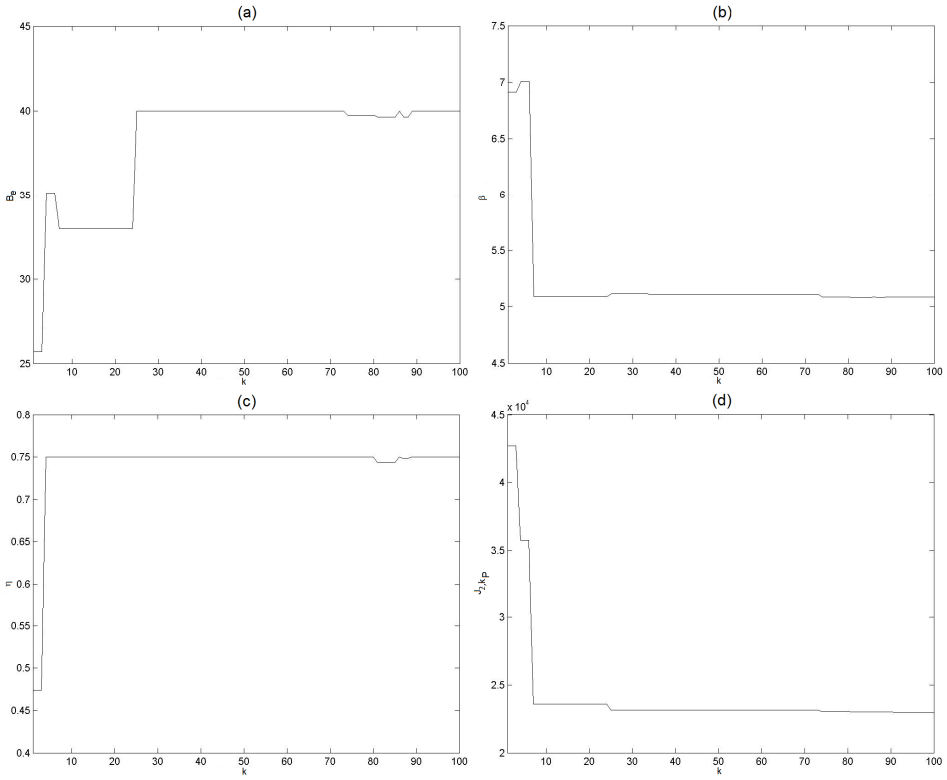

Fig. 3.6.2. T-S PI-FC tuning parameters and objective function evolution vs. iteration index: B_e versus k (a), β versus k (b), η versus k (c), and J_{2,k_P} versus k (d).

The solution obtained by the presented adaptive GSA algorithm to the optimization problems presented in Chapter 2 was also validated by the use of the experimental setup presented in Chapter 2. The real-time experimental results with dynamic regimes characterized by the $r_0 = 40$ rad step type modification presented in [Pre12a], show the performance improvement ensured by the fuzzy controller in case of the objective function J_{1,T_Σ} and the weighting parameter $(\gamma_{T_\Sigma})^2 = 0.17187$. The experiments were conducted for the control systems with both the PI controller (i.e., the linear control system) and the T-S PI-FC.

The PI controller used for comparison was tuned by the ESO method. The design parameter β was set to $\beta = 4$.

The real-time experimental results show the performance improvement ensured by the fuzzy controller. Although the differences between the outputs are rather small (overshoots and settling times), they are important because the values of the objective function are significantly different. The values of the objective function measured during all experiments show the reduction of the objective function of the fuzzy control system compared to the linear one although this is not visible in the control systems responses.

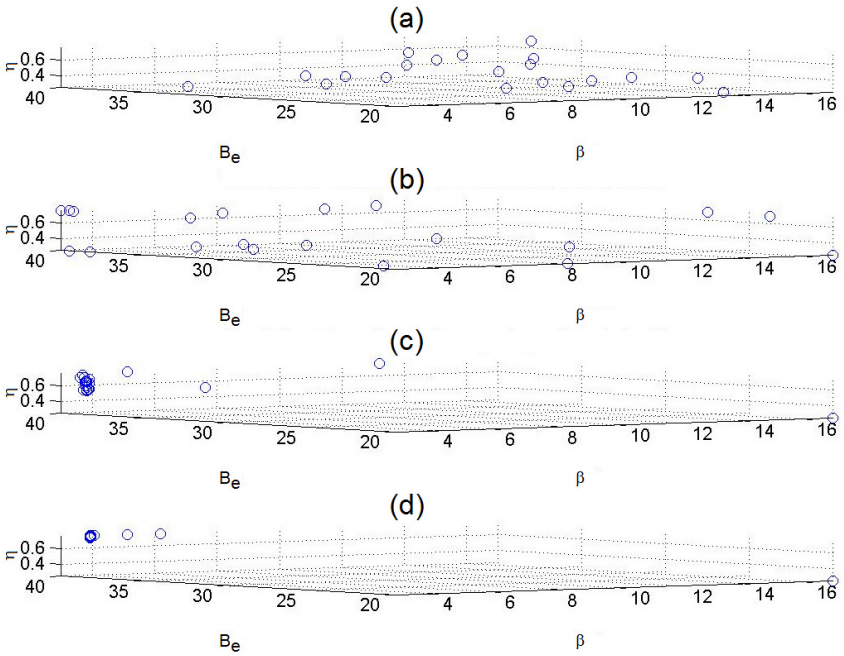

Fig. 3.6.3. Vector solution $\boldsymbol{\rho}$ to the optimization problem (2.14) in the search domain $D_{\boldsymbol{\rho}}$ for four values of iteration index k: $k=1$ (a), $k=15$ (b), $k=60$ (c), and $k=100$ (d).

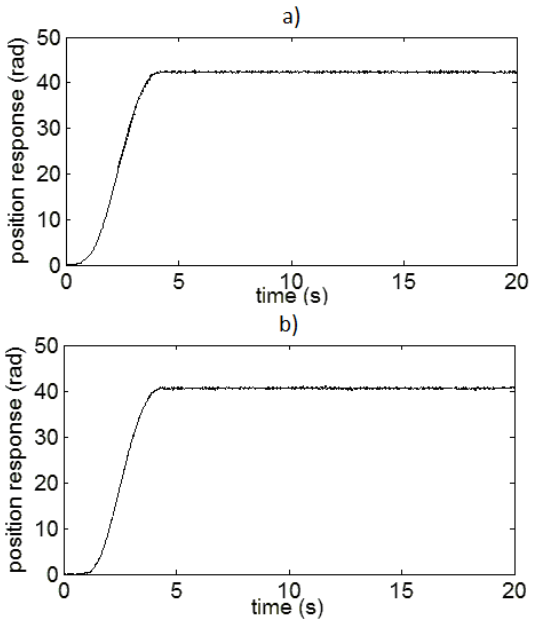

Fig. 3.6.4. Real-time experimental results of control system with PI controller a); and the fuzzy control system with T-S PI-FC b).

3.7. Adaptive Charged System Search algorithms

As in the case of adaptive GSA, the same framework can be integrated for the classical version of the CSS algorithm. The adaptation uses the specific features of CSS algorithms, which are based on the interactions between charged particles (CP) as they are moving through a predefined search domain, starting with arbitrarily determined initial positions with zero initial velocities. The CP is characterized by an associated magnitude of charge q_i and as a result it creates an electrical field around its space. The magnitude of the charge at iteration *k* is defined considering the quality of its solution as:

$$q_{c,i}(k)=\frac{g_i(k)-g_{best}(k)}{g_{best}(k)-g_{worst}(k)},\ i=1...N\ , \tag{3.35}$$

where $g_{best}(k)$ and $g_{worst}(k)$ are the so far best and the worst fitness of all CPs at iteration *k*, $g_i(k)$ is the objective function value or the fitness function value of i^{th} CP at iteration *k*, and *N* is the total number of CPs. The separation distance r_{ij} between two CPs at iteration *k* is defined as:

$$r_{ij}(k)=\frac{\|\mathbf{X}_i(k)-\mathbf{X}_j(k)\|}{\|\frac{(\mathbf{X}_i(k)+\mathbf{X}_j(k))}{2}-\mathbf{X}_{best}(k)\|+\varepsilon\mathbf{X}_i(k)},\ \mathbf{X}_o(k)\in\mathbf{R}^{q_s},\ o\in\{i,j,best\}\ , \tag{3.36}$$

where $\mathbf{X}_i(k)$ and $\mathbf{X}_j(k)$ are the positions of i^{th} and j^{th} CP at iteration *k*, respectively, $\mathbf{X}_{best}(k)$ is the position of the best current CP at iteration *k*, and the relative small parameter $\varepsilon>0$ is introduced to avoid singularities.

For the optimization problems described by (2.13) – (2.16), R^q will be defined in accordance to (2.29) resulting in a $q=3$-dimensional search space.

The exploitation ability of CSS algorithms is increased by the electric forces between CPs. When a search space is a noisy domain, having a complete search before converging to a result is necessary. In such a condition, the addition of the ability of repelling forces to the algorithm may improve its performance. Good CPs can attract the other agents and bad CPs repel the others, proportional to their rank c_{ij}:

$$c_{ij}=\begin{cases}-1 & \text{if } f_i<f_j,\\ 1 & \text{otherwise.}\end{cases} \tag{3.37}$$

The rank c_{ij} sets the type and the degree of influence of each CP on the other CPs considering their fitness function values apart from their charges. This means that good agents are awarded the capability of attraction and bad ones are given the repelling feature, resulting in the improvement of the exploration and exploitation abilities of the algorithm. When a good agent attracts a bad one, the exploitation ability is provided for the algorithm; on the other hand, when a bad agent repels a good CP, the exploration is provided.

The value of the resultant electrical force F_i acting on i^{th} CP at iteration *k* is:

$$\mathbf{F}_i(k)=q_i(k)\sum_{i,i\neq j}\left(\frac{q_j(k)r_{ij}(k)i_1}{a^3}+\frac{q_j(k)i_2}{r_{ij}^2(k)}\right)c_{ij}(\mathbf{X}_i(k)-\mathbf{X}_j(k)),\ (i_1,i_2)=\begin{cases}(0,1), & \text{if } r_{ij}(k)\geq a,\\ (1,0), & \text{otherwise,}\end{cases} \tag{3.38}$$

Equation (3.25) shows that each CP is considered as a charged sphere with radius *a* having a uniform volume charge density.

The new position of i^{th} CP, $\mathbf{X}_i(k+1)$, and the new velocity of i^{th} CP, $\mathbf{V}_i(k+1)$, are obtained in terms of [Kav10a], [Kav10b], [Pre12a], [Kav12e]:

$$\begin{aligned}\mathbf{X}_i(k+1) &= r_{i1}(k)k_a(k)\left(\frac{\mathbf{F}_i(k)}{m_i(k)}\right)(\Delta k)^2 + r_{i2}k_v(k)\mathbf{V}_i(k)\Delta k + \mathbf{X}_i(k),\\ \mathbf{V}_i(k+1) &= \frac{\mathbf{X}_i(k+1)-\mathbf{X}_i(k)}{\Delta k},\end{aligned} \tag{3.39}$$

where *k* is the current iteration index, $k_a(k)$ is the acceleration parameter, k_v is the velocity parameter, r_{i1} and r_{i2} are two random numbers uniformly distributed in the range of (0, 1), m_i is the mass of i^{th} CP, $i=1\ldots N$, $m_i = q_i$ in the sequel, and Δk is the time step set to 1.

The effect of previous velocity and the resultant force acting on a CP can be decreased or increased on the basis of the values of $k_v(k)$ and $k_a(k)$, respectively. Excessive search in the early iterations may improve the exploration ability; however, a gradual decrease is advised in [Kav10a], [Kav10b], [Kav10c]. Since $k_a(k)$ is the parameter related to the attracting forces, selecting a large value for this parameter may cause a fast convergence and choosing a small value can increase the computational time. In fact, $k_a(k)$ is a control parameter of the exploitation; therefore, choosing an incremental function can improve the performance of the algorithm. In addition, the direction of the pervious velocity of a CP is not necessarily the same as the resultant force. Thus, it can be concluded that the velocity parameter k_v controls the exploration process, so an increasing function can be selected. Therefore, based on extended experimental practice, we suggest the following modifications of $k_a(k)$ and $k_v(k)$ with respect to the iteration index *k*:

$$k_a(k) = 3\left(1-\frac{k}{k_{\max}}\right),\ k_v(k) = 0.5\left(1+\frac{k}{k_{\max}}\right), \tag{3.40}$$

where $k_{\max}$ is the maximum number of iterations.

The adaptive CSS algorithm is expressed in terms of the following five stages, I, II, III, IV and V, illustrated in Fig. 3.7.1 and described as follows.

I. *Engagement*. This stage is dedicated to the initialization of adaptive CSS algorithm's population and parameters.

II. *Exploration*. The adaptive CSS algorithm is run with no modifications of $k_a(k)$ and $k_v(k)$, so no constraints are applied to charged particles' movements. This stage accounts for the first 20% out of $k_{\max}$ iterations.

III. *Explanation*. The adaptive CSS algorithm is run using the linear modifications of k_a and k_v according to (3.40).

The next 40% out of $k_{\max}$ iterations are assigned to this stage. The adaptation is obtained on the basis of experience in adaptive GSA algorithm [Pre12d].

IV. *Elaboration*. This stage uses the last 40% out of $k_{\max}$ iterations in adaptive CSS algorithm's search process runs. In addition, at each run the agent's position with the worst fitness is reset to the position of the agent with the best fitness.

V. *Evaluation*. Charged particles' positions are mapped onto the variables of the optimization problem, and the objective functions are evaluated using the real-world model of the optimization problem to evaluate the obtained solution.

Some aspects concerning the stages of this algorithm are presented as follows. The search process in CSS algorithms depends generally on the number of agents *N*, on the maximum number of iterations $k_{\max}$, and on the parameters $k_a(k)$ and $k_v(k)$ and ε. Stage I concerns the generation of the initial population of CPs, i.e., the initialization of the *q*-dimensional search space, of *N*, the initialization of the iteration index k to $k=0$ and will be incremented at the end of the iteration according to step 7 in Fig. 3.7.1., the random initialization of charged particles' position vector $\mathbf{x}_i$, and the initialization of $k_{\max}$. Since *N* and $k_{\max}$ are constant, the adaptive CSS algorithm presented in this sub-chapter carries out the adaptation of $k_a(k)$ and $k_v(k)$ to k.

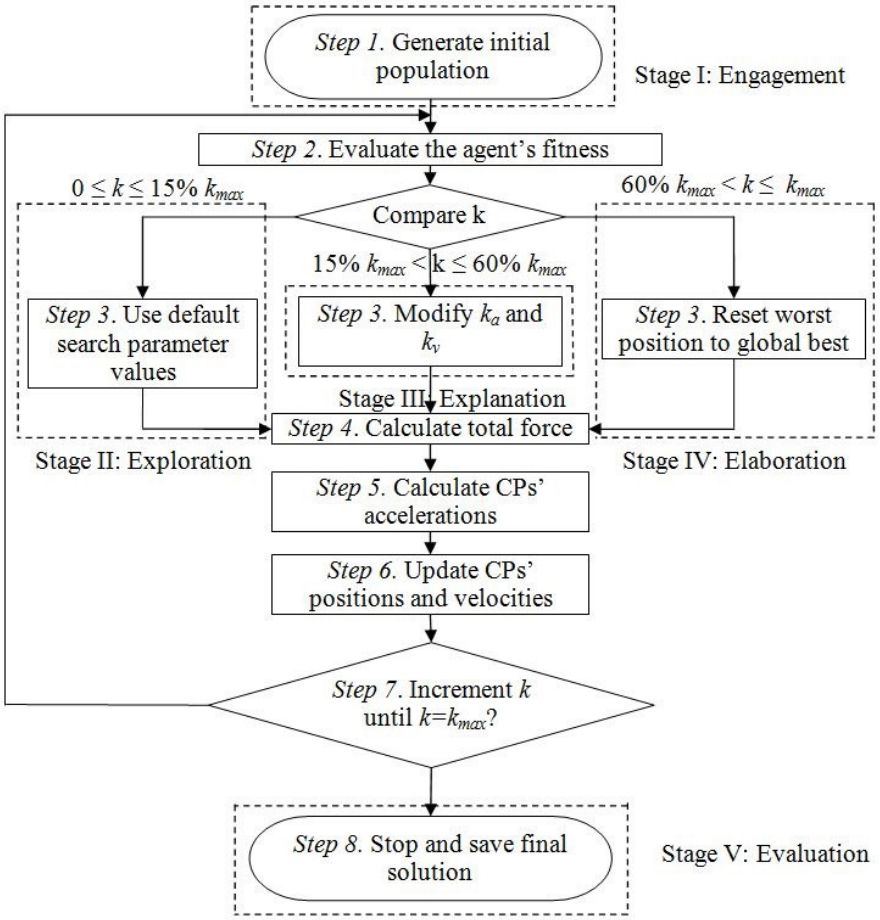

Fig. 3.7.1. Flowchart of adaptive Charged System Search algorithm.

Stage II allows the algorithm to discover the extent of the search space. This stage is characterized by conserving the initial parameters values during the first 20% out of $k_{\max}$ runs of the search process.

This adaptive CSS algorithm restricts charged particles' movements in stage III by the introduction of the modification laws for $k_a(k)$ and $k_v(k)$ in terms of (3.40) in order to reduce inter-CP distances.

Stage IV is characterized by setting the general position for the optimal value of fitness function and leaving the remaining time to refine the obtained results. The values of all parameters are frozen, and only the worst charged particles' positions are reset to the best values obtained so far after each run.

Stage V focuses on the evaluation of real-world optimization problem's performance for the location of the best position vector obtained during the search process. The obtained solution is mapped onto the real-world optimization problem and tested at this stage.

The adaptive CSS was employed as a nature-inspired algorithm in the step 4 of the design method dedicated to the simple T-S PI-FCs presented in Sub-chapter 2.1. The introduction of the solution based adaptive CSS required the priori setting of the algorithm's parameters given as follows. The number of CPs was set to $N = 20$. The maximum number of iterations of the search process was set to $k_{\max} = 100$. As in the case of the standard version of CSS, each CP has a uniform volume charge density and is considered as a charged sphere with radius $a = 1$. In order to avoid a possible division be zero ε parameter in (3.36) was set to $\varepsilon = 10^{-4}$.

Table 3.7.1. Results for the adaptive CSS-based minimization of J_{1,k_P}.

$(\gamma_{k_P})^2$	$B_{\Delta e}^*$	B_e^*	η^*	β^*	k_c^*	T_i^*	$J_{1,k_P\min}$
0	0.1385	40	0.75	3.1435	0.0044	2.892	390459
0.0021357	0.1337	40	0.75	3.2567	0.0043	2.996	394347
0.021357	0.1409	40	0.75	3.092	0.0044	2.8446	421167
0.21357	0.1427	40	0.7402	3.053	0.0044	2.8087	698092

Table 3.7.2. Results for the adaptive CSS-based minimization of J_{1,T_Σ}.

$(\gamma_{T_\Sigma})^2$	$B_{\Delta e}^*$	B_e^*	η^*	β^*	k_c^*	T_i^*	$J_{1,T_\Sigma\min}$
0	0.1385	40	0.75	3.1441	0.0044	2.8926	390460
0.17187	0.1452	40	0.74804	3	0.0045	2.76	638752
1.7187	0.1435	39.5422	0.75	3	0.0045	2.76	2857120
17.187	0.0128	20	0.25	17	0.0019	15.64	22809200

Table 3.7.3. Results for the adaptive CSS-based minimization of J_{2,k_P}.

$(\gamma_{k_P})^2$	$B_{\Delta e}^*$	B_e^*	η^*	β^*	k_c^*	T_i^*	$J_{2,k_P\min}$
0	0.0859	40	0.75	5.0849	0.0034	4.678	22975.7
0.006858	0.0858	40	0.75	5.0914	0.0034	4.68	32684.9
0.06858	0.0855	40	0.75	5.0899	0.0034	4.6827	118951
0.6858	0.0128	20	0.25	17	0.0019	15.64	874183

Table 3.7.4. Results for the adaptive CSS-based minimization of J_{2,T_Σ}.

$(\gamma_{T_\Sigma})^2$	$B^*_{\Delta e}$	B^*_e	η^*	β^*	k_c^*	T_i^*	$J_{2,T_\Sigma \min}$
0	0.0856	40	0.75	5.0849	0.0034	4.6781	22976
0.0066695	0.0853	40	0.7480	5.1049	0.0034	4.6965	32647.4
0.066695	0.1414	38.9685	0.3229	3	0.0045	2.76	117239
0.66695	0.0128	20	0.25	16.9989	0.0019	15.6389	864126

Table 3.7.5. Results for the adaptive CSS-based minimization of J_{3,k_P}.

$(\gamma_{k_P})^2$	$B^*_{\Delta e}$	B^*_e	η^*	β^*	k_c^*	T_i^*	$J_{3,k_P \min}$
0	0.0850	39.7528	0.75	5.0866	0.0034	4.6797	2991580
3.9187	0.0853	40	0.75	5.1002	0.00344	4.6922	8488570
39.187	0.0843	40	0.7249	5.1617	0.0034	4.7487	57651100
391.87	0.0176	20	0.75	12.3501	0.0022	11.3621	528696000

Table 3.7.6. Results for the adaptive CSS-based minimization of J_{3,k_P}.

$(\gamma_{T_\Sigma})^2$	$B^*_{\Delta e}$	B^*_e	η^*	β^*	k_c^*	T_i^*	$J_{3,k_P \min}$
0	0.0856	40	0.7496	5.0848	0.0034	4.6781	2985290
3.8693	0.0781	36.9602	0.4503	5.1486	0.0034	4.7367	8452010
38.693	0.0845	39.9978	0.7498	5.1492	0.0034	4.7373	50884400
386.93	0.0332	40	0.75	13.1011	0.0021	12.053	527661000

Table 3.7.7. Results for the adaptive CSS-based minimization of J_{4,k_P}.

$(\gamma_{k_P})^2$	$B^*_{\Delta e}$	B^*_e	η^*	β^*	k_c^*	T_i^*	$J_{4,k_P \min}$
0	0.0845	40	0.75	5.1529	0.0034	4.7407	155249
0.142	0.0845	40	0.75	5.1515	0.0034	4.7394	353981
1.42	0.0797	37.5427	0.75	5.1246	0.0034	4.7146	2132650
14.2	0.0379	20	0.5719	5.7422	0.0032	5.2828	19046800

Table 3.7.8. Results for the adaptive CSS-based minimization of J_{4,k_P}.

$(\gamma_{T_\Sigma})^2$	$B^*_{\Delta e}$	B^*_e	η^*	β^*	k_c^*	T_i^*	$J_{4,k_P \min}$
0	0.0856	40	0.75	5.0861	0.0034	4.6792	154343
0.15885	0.0856	40	0.7498	5.0853	0.0034	4.6785	379823
1.5885	0.0844	40	0.4389	5.1568	0.0034	4.7443	2406310
15.885	0.0209	20	0.25	10.3913	0.0024	9.56	21595900

Results pertaining to the simulations required for the objective functions $J_{1\ldots4,k_P}$ and $J_{1\ldots4,T_\Sigma}$ (i.e., $J_{1\ldots4,k_P \min}$ and $J_{1\ldots4,T_\Sigma \min}$) are presented in Tables 3.7.1 – 3.7.8. The results from the mentioned tables were obtained after several restarts of

the adaptive CSS algorithm for every objective function, that were imposed as a consequence for the degrees of freedom of the arbitrary variables contained by the search process, with the aim of ensuring the optimal controller tuning parameters and the minimized values of the objective functions. An in-depth analysis of this aspect is presented in Sub-chapter 3.8 with the focus on the average values of the objective functions along with three performance indices.

In Fig. 3.7.2, the progress of the search process is tracked for the best CP results. Each graph corresponds to the parameters given by the algorithm together with the values corresponding to the objective function J_{2,k_P}. The weighting parameter $\gamma_{k_P}=0$ was considered.

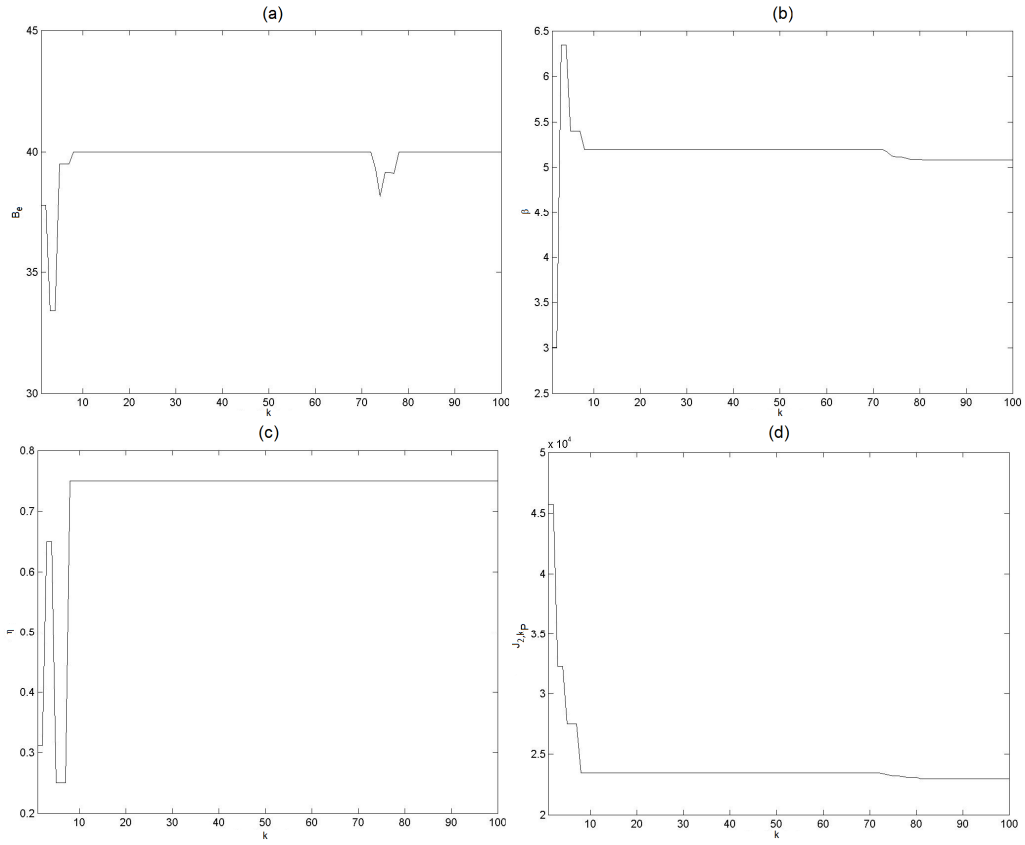

Fig. 3.7.2. T-S PI-FC tuning parameters and objective function evolution vs. iteration index: B_e versus k (a), β versus k (b), η versus k (c), and J_{2,k_P} versus k (d).

Fig. 3.7.3 displays the movement of all CPs employed by the adaptive CSS at the end of the first four stages of the algorithm.

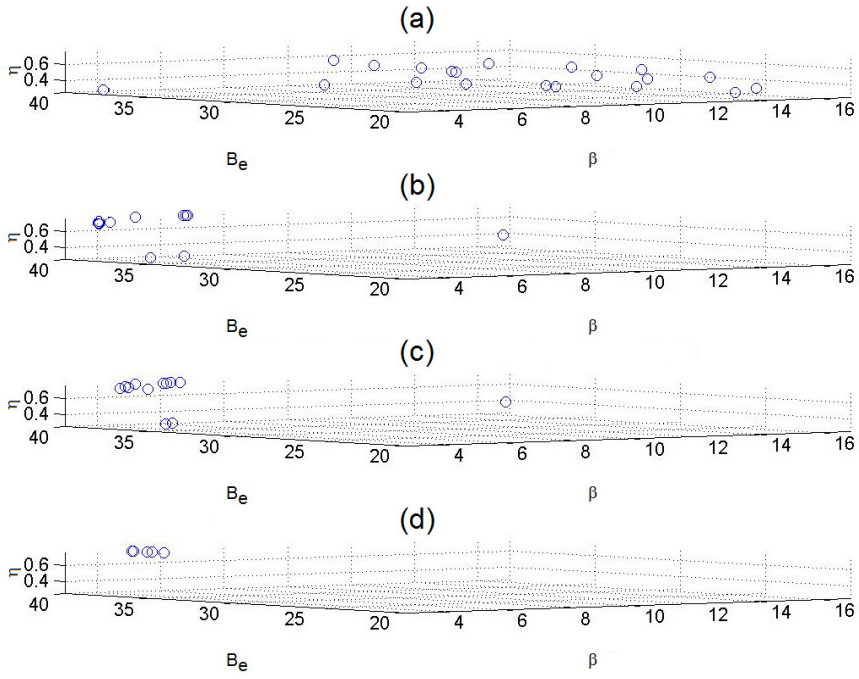

Fig. 3.7.3. Vector solution $\boldsymbol{\rho}$ to the optimization problem (2.14) in the search domain $D_{\boldsymbol{\rho}}$ for four values of iteration index k: $k=1$ (a), $k=15$ (b), $k=60$ (c), and $k=100$ (d).

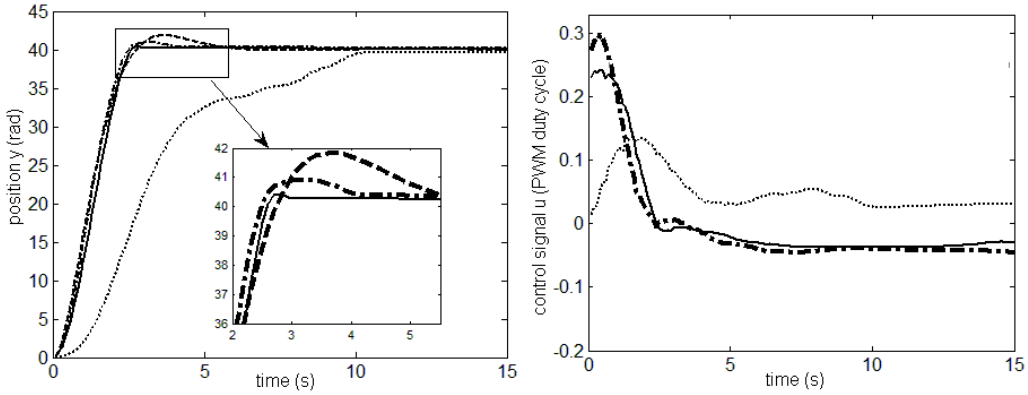

Fig. 3.7.4. Real-time experimental results of control systems with initial PI controller (dotted), initial T-S PI-FC (dashed), standard CSS-based tuned T-S PI-FC (dash-dotted) and adaptive CSS-based tuned T-S PI-FC (solid).

The adaptive CSS algorithm-based solution for the optimization problems presented in Chapter 2 is also validated by an experimental case study dealing with the optimal tuning of a T-S PI-FC for the position control of a nonlinear servo sys-

tem in [Pre14c]. The experiments were conducted for a $r_0 = 40$ rad step-type modification of the angular position reference and for both PI and T-S PI-FC controllers. The experimental results for four controller architectures corresponding to the objective function J_{2,k_P} and the value of the weighting parameter $(\gamma_{k_P})^2 = 0.006858$ are represented in Fig. 3.7.4: (i) a linear control system with PI controller tuned by the ESO method, (ii) a fuzzy control system with T-S PI-FC obtained from the PI controller by the modal equivalence principle, (iii) a fuzzy control system with T-S-PI-FC tuned by the standard CSS algorithm, and (iv) the fuzzy control system with T-S-PI-FC tuned by the adaptive CSS algorithm.

The control system with PI controller, with the responses presented in Fig. 3.7.4, uses a PI controller tuned by the ESO method for $\beta = 4$. The experimental results illustrate the performance improvements offered by the adaptive CSS algorithm. The non-adaptive CSS algorithm was tested in the same conditions using the parameters taken from the parameters of the adaptive CSS algorithm.

3.8. CHAPTER CONCLUSIONS

If the previous sections were dedicated to the introduction of several nature-inspired algorithms and presenting the solutions they provided for the optimization problems defined in Chapter 2, this section proposes a performance comparison of these algorithms with regards to the values of the objective functions in the optimization problems.

As previously mentioned, the algorithms required several restarts before the optimal values were obtained in order to overcome the random characteristic common to all nature-inspired algorithms. Therefore, the averages of the best obtained values for each combination of objective function and weighting parameter are taken into consideration. The best values are the smallest values in the context of the optimization problems (2.13) – (2.16) that target the minimization of several objective functions.

The first comparison criterion is represented by the average value of each objective function (2.9) – (2.12) obtained by running a certain nature-inspired optimization algorithm. The notation for this criterion is $Avg(J_{i,\alpha_\tau \min})$, and it is calculated in terms of:

$$Avg(J_{i,\alpha_\tau \min}) = \frac{1}{N_{best}} \sum_{j=1}^{N_{best}} J_{i,\alpha_\tau \min}{}^{(j)}, \tag{3.41}$$

where $J_{i,\alpha_\tau \min}$ is the value of the objective function obtained by running a certain nature-inspired optimization algorithm considering one of the four expressions given in (2.9) – (2.12) and one weighting parameter, the subscript $i,\ i = 1...4,$ describes one of the four objective functions defined in (2.9) – (2.12), the process parameter is $\alpha_\tau,\ \tau = 1...m_P$, $m_P = 2$ for the process considered in this thesis, $\alpha_\tau \in \{k_P, T_\Sigma\}$ according to (2.21), N_{best} represents the number of best values (i.e., the smallest values) obtained for each of objective function and weighting parameter, and the superscript $j,\ j = 1...N_{best},$ indicates the value of the objective function $J_{i,\alpha_\tau \min}$ ob-

tained by one of the best N_{best} runs of a certain nature-inspired optimization algorithm, so $J_{i,\alpha_\tau \min}{}^{(j)}$ is the value of the objective function $J_{i,\alpha_\tau \min}$ obtained by the run $j,\ j=1...N_{best}$, of a certain nature-inspired optimization algorithm.

The results given in Tables 3.8.1.1 – 3.8.1.8 represent the average of the best $N_{best}=5$ obtained values for each combination of objective function and weighting parameter. However, different values but the same qualitative conclusions can be drawn for other values of N_{best}.

By analyzing the performance of all proposed nature-inspired algorithms it can be observed that no algorithm has a dominant position compared to the others, as the values of the proposed comparison criterion are relatively close. In addition, the best values for each combination of objective function and weighting parameter may be given by different algorithms in each of these cases. If the comparison is restricted to the adaptive and regular versions of GSA and CSS algorithms, it can be observed that the adaptive version of each algorithm outperforms the regular version.

Table 3.8.1.1. Average values of objective function after the minimization of J_{1,k_P}.

$(\gamma^{k_P})^2$	SA	PSO	GSA	PSOGSA	CSS	Adaptive GSA	Adaptive CSS
0	390491	392076	390478	391608	391275	390459	391151
0.0021357	393539	395143	393695	394638	395143	393514	394878
0.021357	421009	422158	421134	421547	422273	421053	421965
0.21357	696481	698859	696247	697464	698736	695394	697879

Table 3.8.1.2. Average values of objective function after the minimization of J_{1,T_Σ}.

$(\gamma^{T_\Sigma})^2$	SA	PSO	GSA	PSOGSA	CSS	Adaptive GSA	Adaptive CSS
0	390506	392076	390478	391608	392076	390459	390519
0.17187	639824	641826	631780	638308	640890	638372	639991
1.7187	2869153	1234553	2867530	2116253	2867807	2862040	2860877
17.187	22810300	22809200	22803933	22802567	22809200	22807400	22809200

Table 3.8.1.3. Average values of objective function after the minimization of J_{2,k_P}.

$(\gamma^{k_P})^2$	SA	PSO	GSA	PSOGSA	CSS	Adaptive GSA	Adaptive CSS
0	23017	23012	23511	23965	23129	23129	22976
0.006858	32647	32579	32817	36335	37931	32749	32847
0.06858	118967	119048	119306	119807	119467	119375	119075
0.6858	874484	874183	874149	873857	874183	874162	874183

Table 3.8.1.4. Average values of objective function after the minimization of J_{2,T_Σ}.

$(\gamma^{T_\Sigma})^2$	SA	PSO	GSA	PSOGSA	CSS	Adaptive GSA	Adaptive CSS
0	22992	22976	23238	24518	23129	23144	22978
0.0066695	32522	32481	32951	32773	33555	32642	32660
0.066695	117587	114650	118230	114712	118173	117630	118078
0.66695	865200	864943	864579	864943	864943	864770	864661

Table 3.8.1.5. Average values of objective function after the minimization of J_{3,k_P}.

$(\gamma^{k_P})^2$	SA	PSO	GSA	PSOGSA	CSS	Adaptive GSA	Adaptive CSS
0	2990690	2988143	3091163	31451967	3733680	3088620	3062597
3.9187	8487570	8472373	8574770	8537903	9310780	8514653	8530910
39.187	57650267	57839600	57974500	57972133	57848667	57655800	57765700
391.87	528113333	527919000	528306666	529213333	530061000	527891667	528767000

Table 3.8.1.6. Average values of objective function after the minimization of J_{3,T_Σ}.

$(\gamma^{T_\Sigma})^2$	SA	PSO	GSA	PSOGSA	CSS	Adaptive GSA	Adaptive CSS
0	2990690	2988143	3109277	3145197	37149067	3024803	3054703
3.8693	8402737	8499467	8666530	8659013	9265960	8524953	8584443
38.693	56659057	57975700	58157367	57705200	56420533	57987133	51137567
386.93	528041333	527755000	527868666	529023333	530442000	527702667	527876333

Table 3.8.1.7. Average values of objective function after the minimization of J_{4,k_P}.

$(\gamma^{k_P})^2$	SA	PSO	GSA	PSOGSA	CSS	Adaptive GSA	Adaptive CSS
0	153815	152975	160314	161796	178955	157367	155518
0.142	344696	352223	354148	385251	356694	354547	354712
1.42	2105230	1982330	2145623	2147777	2150850	2143730	2140853
14.2	19291467	19274833	19278100	19291867	19396400	19278667	19206067

Table 3.8.1.8. Average values of objective function after the minimization of J_{4,T_Σ}.

$(\gamma^{T_\Sigma})^2$	SA	PSO	GSA	PSOGSA	CSS	Adap-tive GSA	Adaptive CSS
0	153815	152975	160314	161796	167011	157382	154753
0.15885	371836	379400	384154	397527	418335	381176	381516
1.5885	2324983	2161323	2415300	2305900	2428513	2359830	2413023
15.885	21641033	21596000	21623233	21674533	21732867	21610633	21634533

The second comparison criterion is based on a newly introduced performance indices referred to as convergence speed (c_s). As defined in [Pre13a], the convergence speed represents the number of evaluations of the objective functions until their minimum value is found.

This approach is extremely important for the nature-inspired optimization algorithms applied to the optimal tuning of the parameters of controllers. The algorithm complexity analysis is generally used in the analysis of numerical algorithms including optimization ones in the general context of computer science, where assessing the amount of required resources to execute these algorithms is discussed. The algorithm complexity analysis is not carried out in this thesis, since:

- the optimization algorithms treated in this thesis are designed to work with a fixed number of inputs (i.e., the variables of the objective functions, namely the tuning parameters of the controllers), however the algorithms used in computer science are designed to work with inputs of arbitrary length, the number of inputs set in the algorithms treated in this thesis is fixed to three in order to have a reasonable dimension of the search space,

- the optimization algorithms are executed offline and only the evaluation of the objective function, conducted by simulations and/or experiments, requires strong time resources on the control system side, which are much more costly compared to the resources on the algorithm execution side.

In this context, the convergence speed c_s is an indication on the complexity of these algorithms. However, in the general application of these algorithms to various applications involving different objective functions with several numbers of variables, the algorithm complexity analysis becomes strictly necessary. The data corresponding to this second performance criterion represents the degree of algorithm iterations coverage before finding the final solution.

The results presented in Tables 3.8.2.1 – 3.8.2.8 contain the average values of the convergence speed c_s calculated for the best five runs, used for the previous comparison criterion as well. Each algorithm was considered, for each combination of objective function from (2.9) – (2.12) and weighting parameter.

Tables 3.8.2.1 – 3.8.2.8 show that the results obtained when the adaptive GSA and CSS algorithms were used are consistently superior to those offered by the non-adaptive algorithm versions. Local minima traps are also avoided when using the adaptive algorithm versions by the introduction of improved exploration and exploitation capabilities. On the negative side, finding the solution after a predefined number of iterations may results in longer time runs for the adaptive GSA and CSS algorithms.

Table 3.8.2.1. Average values of convergence speed c_s for the minimization of J_{1,k_P}.

$(\gamma^{k_P})^2$	c_s SA	c_s PSO	c_s GSA	c_s PSOGSA	c_s CSS	c_s Adaptive GSA	c_s Adaptive CSS
0	4143	218	1554	190	757	1298	1306
0.0021357	2595	141	932	356	118	1421	1406
0.021357	3072	485	477	1072	246	1749	1207
0.21357	975	134	1186	1287	347	1777	455

Table 3.8.2.2. Average values of convergence speed c_s for the minimization of J_{1,T_Σ}.

$(\gamma^{k_P})^2$	c_s SA	c_s PSO	c_s GSA	c_s PSOGSA	c_s CSS	c_s Adaptive GSA	c_s Adaptive CSS
0	2370	218	1554	190	99	1298	1004
0.17187	437	217	1511	696	918	1695	1317
1.7187	470	1451	1142	1802	729	1677	1364
17.187	2291	223	1528	785	76	1421	215

Table 3.8.2.3. Average values of convergence speed c_s for the minimization of J_{2,k_P}.

$(\gamma^{k_P})^2$	c_s SA	c_s PSO	c_s GSA	c_s PSOGSA	c_s CSS	c_s Adaptive GSA	c_s Adaptive CSS
0	3035	1906	1399	1660	1358	1718	1905
0.006858	2894	1704	1172	400	609	1839	1135
0.06858	165	1623	915	1613	973	1142	1935
0.6858	2748	105	1846	678	53	891	78

Table 3.8.2.4. Average values of convergence speed c_s for the minimization of J_{2,T_Σ}.

$(\gamma^{k_P})^2$	c_s SA	c_s PSO	c_s GSA	c_s PSOGSA	c_s CSS	c_s Adaptive GSA	c_s Adaptive CSS
0	3919	1766	391	1097	1358	1667	1963
0.0066695	4144	1728	1160	942	1607	1514	1049
0.066695	1890	1496	828	1348	1360	1675	1821
0.66695	2102	118	1421	128	60	1809	765

Table 3.8.3.5. Average values of convergence speed c_s for the minimization of J_{3,k_P}.

$(\gamma^{k_P})^2$	c_s SA	c_s PSO	c_s GSA	c_s PSOGSA	c_s CSS	c_s Adaptive GSA	c_s Adaptive CSS
0	1494	1647	596	723	136	1777	1816
3.9187	1149	1832	1359	1090	1596	1768	828
39.187	865	1270	803	1132	1549	1396	1411
391.87	465	755	1443	1039	834	1722	1449

Table 3.8.2.6. Average values of convergence speed c_s for the minimization of J_{3,T_Σ}.

$(\gamma^{k_P})^2$	c_s SA	c_s PSO	c_s GSA	c_s PSOGSA	c_s CSS	c_s Adaptive GSA	c_s Adaptive CSS
0	1494	1647	769	723	617	1739	1863
3.8693	3256	1832	690	520	1260	1685	1145
38.693	860	1268	670	1344	1384	1534	1751
386.93	835	1510	1288	935	1091	1335	1403

Table 3.8.2.7. Average values of convergence speed c_s for the minimization of J_{4,k_P}.

$(\gamma^{k_P})^2$	c_s SA	c_s PSO	c_s GSA	c_s PSOGSA	c_s CSS	c_s Adaptive GSA	c_s Adaptive CSS
0	2233	1618	499	1826	1325	1480	1659
0.142	2411	1634	694	1053	1168	1234	1457
1.42	1012	1804	545	1223	1286	1696	1581
14.2	612	1398	1530	1434	319	1848	199

Table 3.8.2.8. Average values of convergence speed c_s for the minimization of J_{4,T_Σ}.

$(\gamma^{k_P})^2$	c_s SA	c_s PSO	c_s GSA	c_s PSOGSA	c_s CSS	c_s Adaptive GSA	c_s Adaptive CSS
0	2233	1618	499	1826	1167	1711	1984
0.15885	1344	1366	766	1361	1479	1714	1585
1.5885	381	1672	725	1644	1267	1727	1649
15.885	632	1371	1580	1685	492	1852	1735

As the performance index c_S focuses on how fast a solution is found, it can miss other relevant information on the overall solution's quality. This limitation can be mitigated by the introduction of the third performance index, namely the accuracy rate a_r defined as follows as the percent standard deviation of the objective functions obtained by running a certain optimization algorithm divided to the average value $Avg(J_{i,\alpha_\tau \min})$ of each objective function (2.9) – (2.12) obtained by running a certain nature-inspired optimization algorithm:

$$a_r = StDev^{\%}(J_{i,\alpha_\tau \min}) = 100\frac{StDev(J_{i,\alpha_\tau \min})}{Avg(J_{i,\alpha_\tau \min})},\ i = 1...4\ , \tag{3.42}$$

where the average value $Avg(J_{i,\alpha_\tau \min})$ of each objective function (2.9) – (2.12) obtained by running a certain nature-inspired optimization algorithm is defined in (3.41), and the standard deviation $StDev(J_{i,\alpha_\tau \min})$ is calculated in terms of:

$$StDev(J_{i,\alpha_\tau \min}) = \sqrt{\frac{1}{N_{best}-1}\sum_{j=1}^{N_{best}}(J_{i,\alpha_\tau \min}{}^{(j)} - Avg(J_{i,\alpha_\tau \min}))^2}\ , \tag{3.43}$$

and the other notations are explained in relation with (3.41).

Tables 3.8.3.1 – 3.8.3.8 show the average values based on the best $N_{best} = 5$ runs that are in the case of previous comparison indices as well. These values correspond to the values of a_r presented comparatively for all proposed nature-inspired algorithms discussed up to now and each combination of objective function and weighting parameter.

The results outline that PSO and adaptive GSA and CSS algorithms have an improved search process which lead to the convergence to the optimal solution at the end of the search process. The accuracy rate values clearly show that the adaptive version of the algorithms have a higher accuracy rate of finding closer optimal solutions thus increasing the confidence in the solutions provided. Therefore, all search iterations are used compared to the non-adaptive GSA and CSS algorithms, which converge too early, leading to an unnecessary computational cost.

Table 3.8.3.1. Average values of accuracy rate a_r for the minimization of $J_{1,k_P \min}$.

$(\gamma^{k_P})^2$	a_r SA	a_r PSO	a_r GSA	a_r PSOGSA	a_r CSS	a_r Adaptive GSA	a_r Adaptive CSS
0	0.0069	0	0.0044	0.2071	0.1887	0.000148	0.2131
0.0021357	0.0058	0	0.0731	0.2481	0	0.001761	0.1164
0.021357	0.0114	0.2445	0.0202	0.248	0.1513	0.0049	0.1881
0.21357	0.1306	0	0.0881	0.261	0.03057	0.0748	0.1579

Table 3.8.3.2. Average values of accuracy rate a_r for the minimization of J_{1,T_Σ}.

$(\gamma^{k_P})^2$	a_r SA	a_r PSO	a_r GSA	a_r PSOGSA	a_r CSS	a_r Adaptive GSA	a_r Adaptive CSS
0	0.0058	0	0.0044	0.2071	0	0.0001	0.0256
0.1.7187	0.0483	0	1.8307	0.2431	0.1265	0.1592	0.2395
1.7187	0.1208	30.0018	0.1889	46.4322	0.0262	0.2249	0.1836
17.187	0.0072	0	0.0355	0.0466	0	0.005	0

Table 3.8.3.3. Average values of accuracy rate a_r for the minimization of J_{2,k_P}.

$(\gamma^{k_P})^2$	a_r SA	a_r PSO	a_r GSA	a_r PSOGSA	a_r CSS	a_r Adaptive GSA	a_r Adaptive CSS
0	0.1379	0.2702	2.1778	5.6485	0.5706	0.6448	0.0012
0.006858	0.1871	0.0007	0.431	13.1324	12.232	0.1393	0.5406
0.06858	0.0859	0.0386	0.0995	0.604	0.217	0.296	0.0947
0.6858	0.0356	0	0.0022	0.0647	0	0.0027	0

Table 3.8.3.4. Average values of accuracy rate a_r for the minimization of J_{2,T_Σ}.

$(\gamma^{k_P})^2$	a_r SA	a_r PSO	a_r GSA	a_r PSOGSA	a_r CSS	a_r Adaptive GSA	a_r Adaptive CSS
0	0.0153	0	0.3492	3.5956	0.57057	0.5949	0.0158
0.0066695	0.0166	0.0002	0.4084	1.7745	3.62334	0.1992	0.0391
0.066695	0.1663	5.008	0.2566	4.2211	0.0044	1.1587	0.6747
0.66695	0.0182	0	0.0402	0	0	0.0174	0.0536

Table 3.8.3.5. Average values of accuracy rate a_r for the minimization of J_{3,k_P}.

$(\gamma^{k_P})^2$	a_r SA	a_r PSO	a_r GSA	a_r PSOGSA	a_r CSS	a_r Adaptive GSA	a_r Adaptive CSS
0	0.124	0.1947	0.2775	7.6804	15.7606	2.5354	2.922
3.9187	0.0828	0.0023	0.8176	0.9114	14.3521	0.3981	0.6518
39.187	0.1057	0.3247	0.1682	0.1196	0.2858	0.4541	0.1772
391.87	0.0278	0.0024	0.126024	0.2839	0.1999	0.0968	0.013

Table 3.8.3.6. Average values of accuracy rate a_r for the minimization of J_{3,T_Σ}.

$(\gamma^{k_P})^2$	a_r SA	a_r PSO	a_r GSA	a_r PSOGSA	a_r CSS	a_r Adaptive GSA	a_r Adaptive CSS
0	0.1239	0.1947	0.9032	7.6804	16.6725	1.305	1.9679
3.8693	1.9998	0.0004	2.1453	0.3398	12.3669	0.2309	1.8345
38.693	3.6376	0.4655	0.2552	1.5364	5.8569	0.1364	0.7596
386.93	0.078	0.0169	0.0449	0.2351	0.0012	0.0035	0.0586

Table 3.8.3.7. Average values of accuracy rate a_r for the minimization of J_{4,k_P}.

$(\gamma^{k_P})^2$	a_r SA	a_r PSO	a_r GSA	a_r PSOGSA	a_r CSS	a_r Adaptive GSA	a_r Adaptive CSS
0	0.4009	0.0036	4.7067	8.6845	22.7708	1.5897	0.2075
0.142	4.1121	0.1977	0.5175	9.3238	1.3021	0.2964	0.1918
1.42	2.0071	6.5054	0.2305	0.8542	0.4006	0.0154	0.3384
14.2	0.0345	0.0035	0.0055	0.1564	0.154	0.0096	0.7184

Table 3.8.3.8. Average values of accuracy rate a_r for the minimization of J_{4,T_Σ}.

$(\gamma^{k_P})^2$	a_r SA	a_r PSO	a_r GSA	a_r PSOGSA	a_r CSS	a_r Adaptive GSA	a_r Adaptive CSS
0	0.4009	0.0036	4.7067	8.6845	12.0122	1.606	0.4585
0.15885	3.9602	0.0171	0.7031	3.9545	13.0819	0.1772	0.3969
1.5885	4.7276	2.4878	0.2899	6.8972	0.4505	1.3744	0.2548
15.885	0.1503	0.0012	0.1241	0.4167	0.1695	0.04186	0.155

The results show the reduced sensitivity of the initial conditions associated to the sensitivity models of the optimization problems solved by the nature-inspired algorithms. Therefore, the optimal values of the controller tuning parameters exhibit reduced sensitivity with respect to the initial conditions of the sensitivity models.

Figs. 3.8.1 – 3.8.8 highlight the controlled output (y) versus time and the behavior of the control systems optimized by the minimization of the objective functions J_{i,α_τ}, $i=1...4,\ \ \alpha_\tau \in \{k_P, T_\Sigma\}$, and the parameters of the optimal T-S PI-FCs obtained by the nature-inspired algorithms. The simulation scenario is characterized by the application of a $r_0 = 40$ rad unit step reference input, followed by a 0.1 step disturbance input after 500 s from the total 1000 s simulation time.

The results shown in Figs. 3.8.1 – 3.8.8 were obtained using only one set of fuzzy controller parameters because the nature-inspired algorithms applied in solving the same optimization problems lead to very close solutions. The fuzzy controller parameters were chosen arbitrarily from all proposed nature-inspired algorithms.

The nature-inspired algorithms are treated randomly in Figs. 3.8.1 – 3.8.8. However, Figs. 3.8.1 – 3.8.8 are presented in the ascending order of the objective functions. This style of presentation has been chosen in order to highlight the fact that the empirical control system performance indices (overshoot and settling time) are very close for the same objective function that is minimized and for the same process parameter that is considered in the sensitivity models.

As expected, Figs. 3.8.1 – 3.8.8 illustrate that the overshoot and the settling time depend on the objective function and on the process parameter that is considered in the sensitivity models. These results are justified by different dynamical regimes of the fuzzy control systems.

Fig. 3.8.1 presents the simulation results corresponding to the objective function J_{1,k_P} and to the following controller parameters obtained by the GSA: $B_e^* = 40$, $\eta^* = 0.75$, $\beta^* = 3.14374$ and weighting parameter $(\gamma_{k_P})^2 = 0$ for a); $B_e^* = 39.9979$, $\eta^* = 0.75$, $\beta^* = 3.14537$ and weighting parameter $(\gamma_{k_P})^2 = 0.0021357$ for

b); $B_e^* = 40$, $\eta^* = 0.75$, $\beta^* = 3.12737$ and weighting parameter $(\gamma_{k_P})^2 = 0.021357$ for c); $B_e^* = 39.7505$, $\eta^* = 0.75$, $\beta^* = 3.2222$ and weighting parameter $(\gamma_{k_P})^2 = 0.21357$ for d) as retrieved from Table 3.3.1.

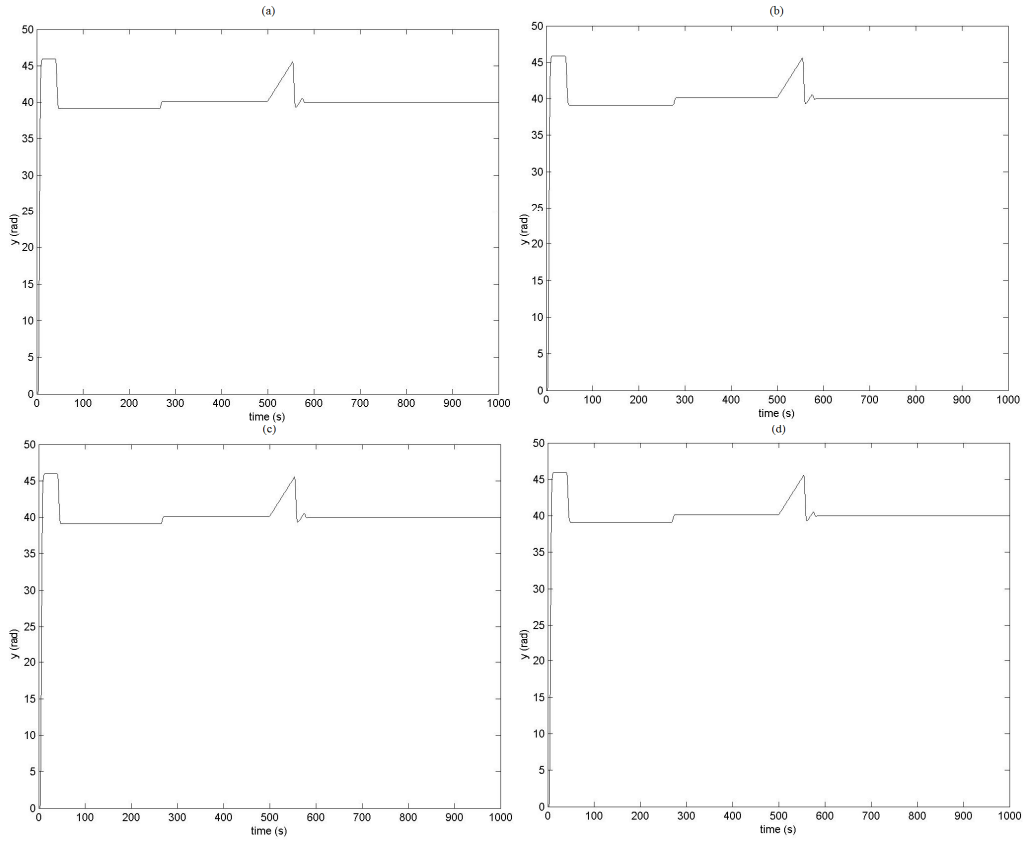

Fig. 3.8.1. Simulation results of optimal fuzzy control systems obtained for objective function J_{1,k_P} and different values of the weighting parameter γ_{k_P} : $\gamma_{k_P} = 0$ (a), $(\gamma_{k_P})^2 = 0.0021357$ (b), $(\gamma_{k_P})^2 = 0.021357$ (c), and $(\gamma_{k_P})^2 = 0.21357$ (d).

Fig. 3.8.2 illustrates the simulation results corresponding to the objective function J_{1,T_Σ} and to the controller parameters obtained by the adaptive CSS algorithm with the parameters from Table 3.7.2: $B_e^* = 40$, $\eta^* = 0.75$, $\beta^* = 5.08485$ and weighting parameter $\gamma_{k_P} = 0$ for (a); $B_e^* = 40$, $\eta^* = 0.748044$, $\beta^* = 5.08485$ and weighting parameter $(\gamma_{T_\Sigma})^2 = 0.17187$ for (b); $B_e^* = 39.5422$, $\eta^* = 0.75$, $\beta^* = 5.08485$ and weighting parameter $(\gamma_{T_\Sigma})^2 = 1.7187$ for (c); $B_e^* = 20$, $\eta^* = 0.25$, $\beta^* = 17$ and weighting parameter $(\gamma_{T_\Sigma})^2 = 17.187$ for (d).

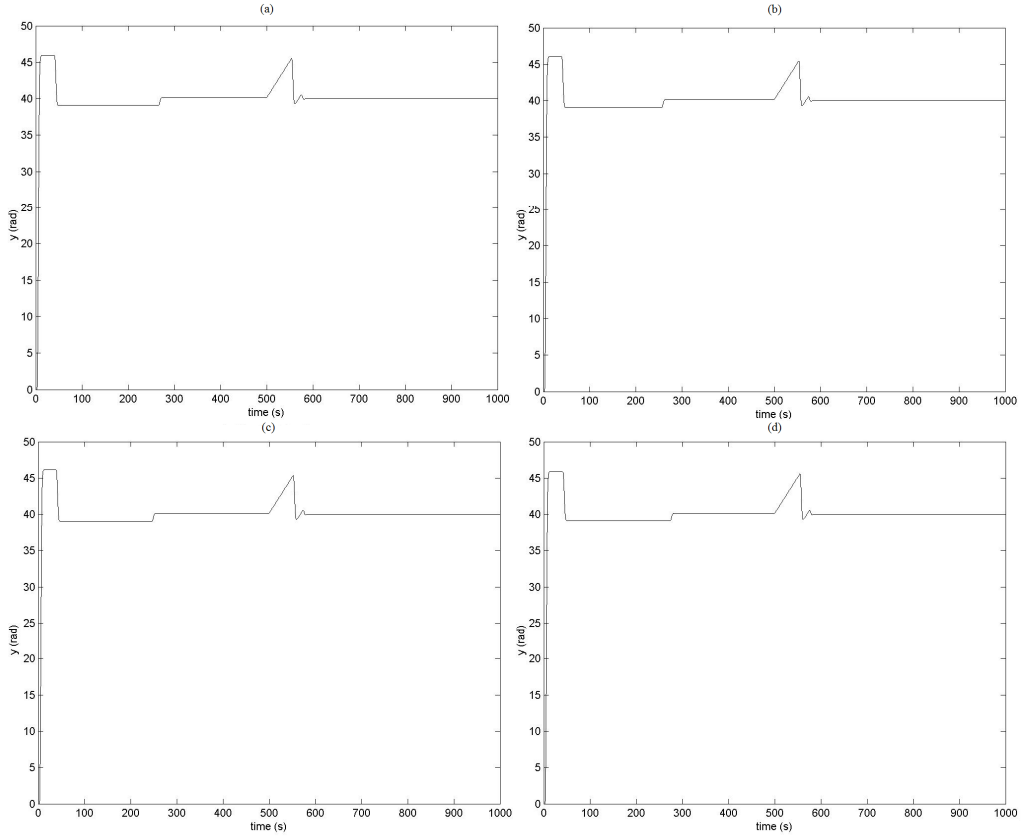

Fig. 3.8.2. Simulation results of optimal fuzzy control systems obtained for objective function J_{1,T_Σ} and different values of the weighting parameter γ_{T_Σ}: $\gamma_{T_\Sigma}=0$ (a), $(\gamma_{T_\Sigma})^2=0.17187$ (b), $(\gamma_{T_\Sigma})^2=1.7187$ (c), and $(\gamma_{T_\Sigma})^2=17.187$ (d).

In Fig. 3.8.3 the simulation results corresponding to the objective function J_{2,k_P} and to the following controller parameters obtained by the PSO algorithm: $B_e^*=40$, $\eta^*=0.75$, $\beta^*=5.08485$ and weighting parameter $\gamma_{k_P}=0$ for (a); $B_e^*=40$, $\eta^*=0.75$, $\beta^*=5.08485$ and weighting parameter $(\gamma_{k_P})^2=0.006858$ for (b); $B_e^*=40$, $\eta^*=0.75$, $\beta^*=5.08485$ and weighting parameter $(\gamma_{k_P})^2=0.06858$ for (c); $B_e^*=20$, $\eta^*=0.25$, $\beta^*=17$ and weighting parameter $(\gamma_{k_P})^2=0.6858$ for (d), as found in Table 3.2.3 are given.

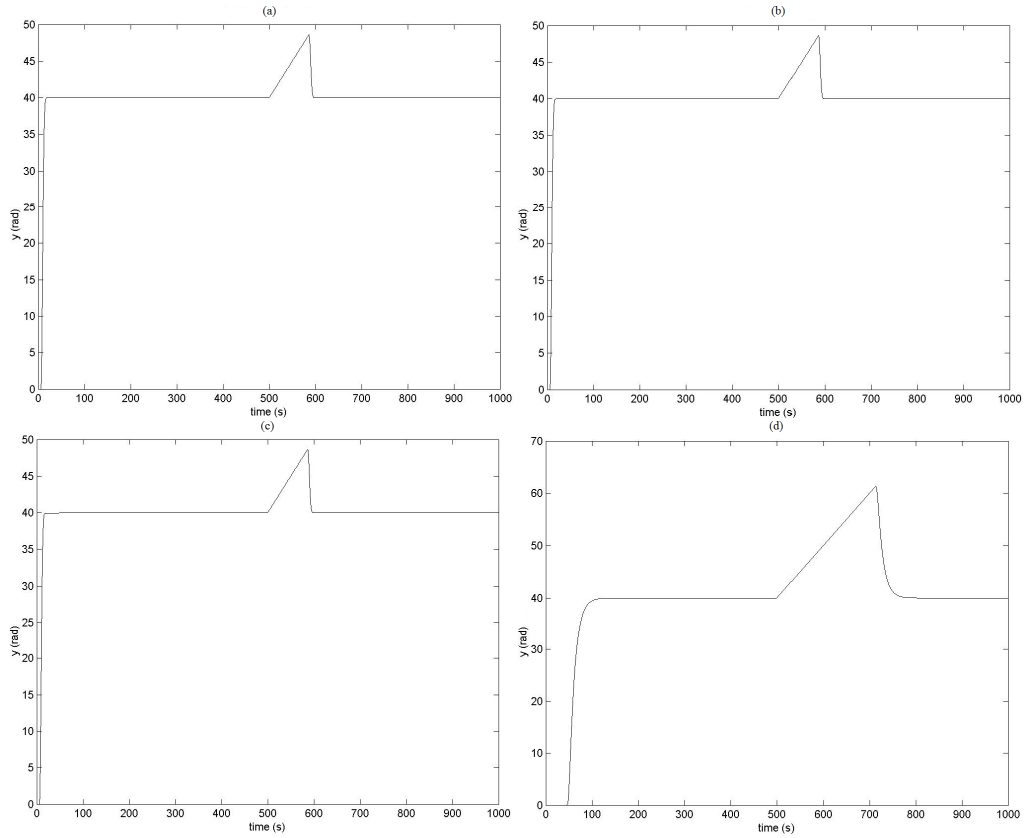

Fig. 3.8.3. Simulation results of optimal fuzzy control systems obtained for objective function J_{2,k_P} and different values of the weighting parameter γ_{k_P} : $\gamma_{k_P} = 0$ (a), $(\gamma_{k_P})^2 = 0.006858$ (b), $(\gamma_{k_P})^2 = 0.06858$ (c), and $(\gamma_{k_P})^2 = 0.6858$ (d).

In Fig. 3.8.4 the simulation results corresponding to the objective function J_{2,T_Σ} and to the following controller parameters obtained by the adaptive GSA algorithm: $B_e^* = 39.4214$, $\eta^* = 0.75$, $\beta^* = 5.08716$ and weighting parameter $\gamma_{k_P} = 0$ for (a); $B_e^* = 40$, $\eta^* = 0.75$, $\beta^* = 5.09279$ and weighting parameter $(\gamma_{T_\Sigma})^2 = 0.0066695$ for (b); $B_e^* = 39.803$, $\eta^* = 0.75$, $\beta^* = 5.15735$ and weighting parameter $(\gamma_{T_\Sigma})^2 = 0.066695$ for (c); $B_e^* = 20.0053$, $\eta^* = 0.25$, $\beta^* = 17$ and weighting parameter $(\gamma_{T_\Sigma})^2 = 0.66695$ for (d), matching Table 3.3.4 are shown.

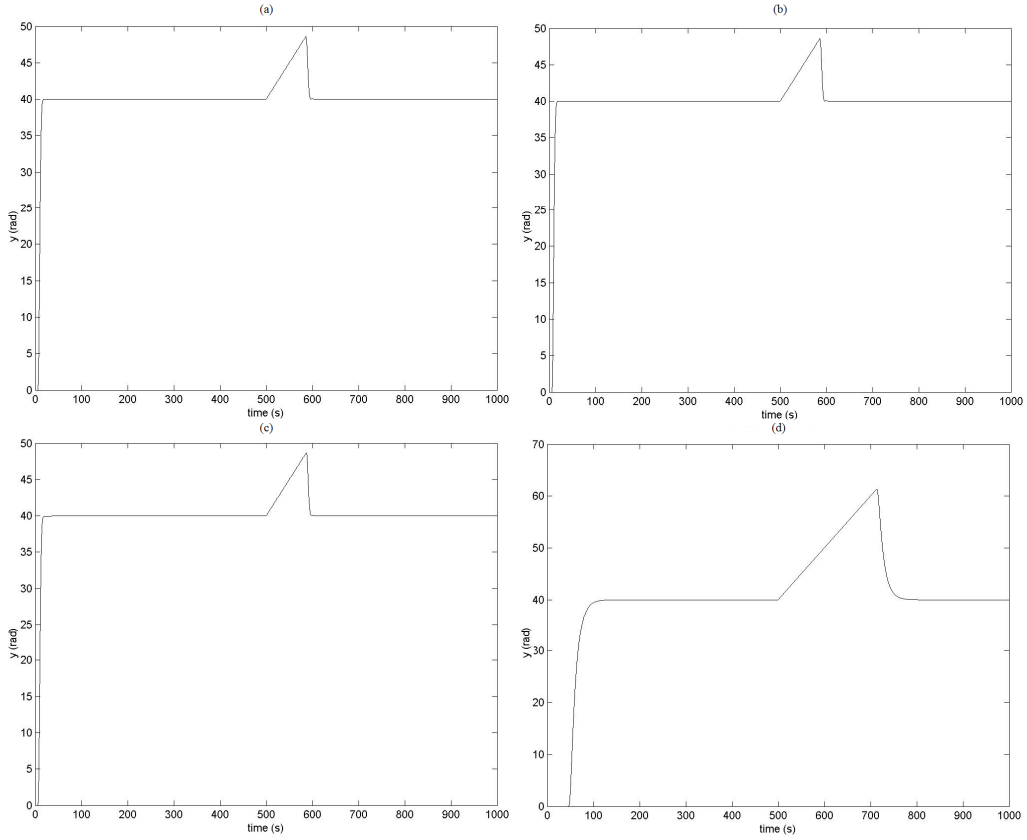

Fig. 3.8.4. Simulation results of optimal fuzzy control systems obtained for objective function J_{2,T_Σ} and different values of the weighting parameter γ_{T_Σ}: $\gamma_{T_\Sigma} = 0$ (a), $(\gamma_{T_\Sigma})^2 = 0.0066695$ (b), $(\gamma_{T_\Sigma})^2 = 0.066695$ (c), and $(\gamma_{T_\Sigma})^2 = 0.66695$ (d).

The simulation results corresponding to the objective function J_{3,k_P} based on the results retrieved from Table 3.1.5 and on the following controller parameters obtained by the SA algorithm: $B_e^* = 39.9908$, $\eta^* = 0.749364$, $\beta^* = 5.08527$ and weighting parameter $\gamma_{k_P} = 0$ for (a); $B_e^* = 39.8962$, $\eta^* = 0.746735$, $\beta^* = 5.0867$ and weighting parameter $(\gamma_{k_P})^2 = 3.9187$ for (b); $B_e^* = 39.5241$, $\eta^* = 0.746393$, $\beta^* = 5.10925$ and weighting parameter $(\gamma_{k_P})^2 = 39.5241$ for (c); $B_e^* = 39.8288$, $\eta^* = 0.742363$, $\beta^* = 12.8479$ and weighting parameter $(\gamma_{k_P})^2 = 39.8288$ for (d), are highlighted in Fig. 3.8.5.

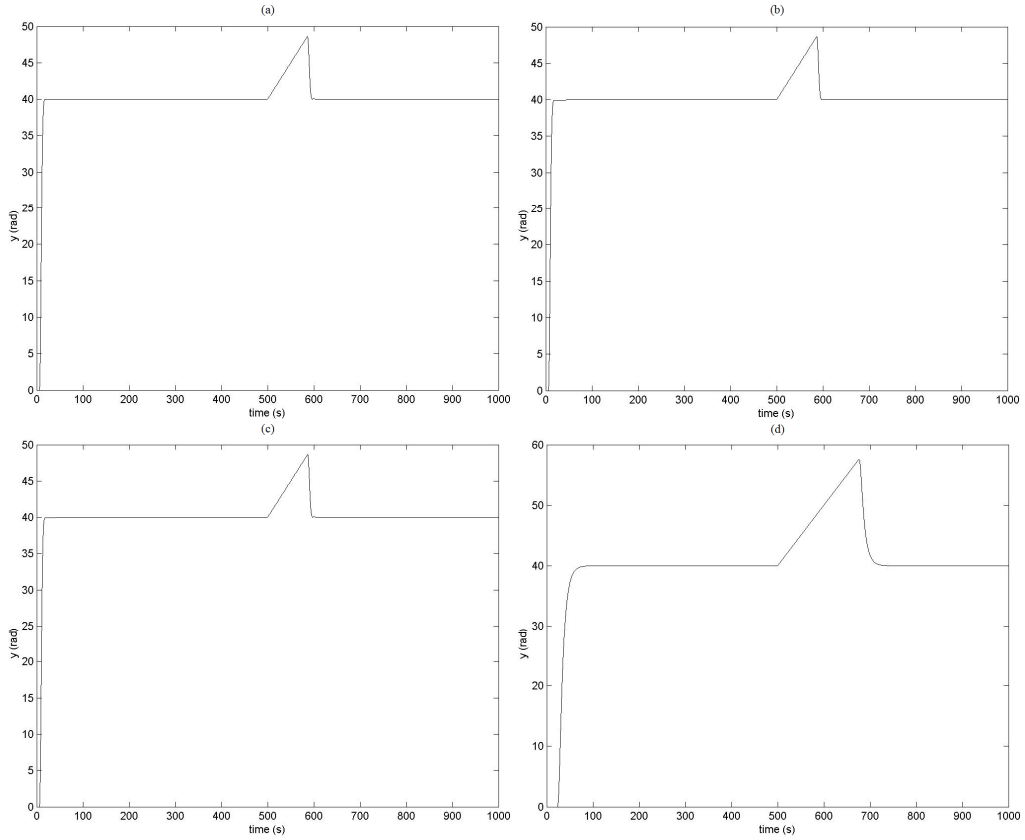

Fig. 3.8.5. Simulation results of optimal fuzzy control systems obtained for objective function J_{3,k_P} and different values of the weighting parameter γ_{k_P} : $\gamma_{k_P}=0$ (a), $(\gamma_{k_P})^2=3.9187$ (b), $(\gamma_{k_P})^2=39.187$ (c), and $(\gamma_{k_P})^2=391.87$ (d).

Fig. 3.8.6 presents the simulation results corresponding to the objective function J_{3,T_Σ} and to the controller parameters obtained by the GSA algorithm: $B_e^*=39.5685$, $\eta^*=0.693304$, $\beta^*=5.09481$ and weighting parameter $\gamma_{k_P}=0$ for (a); $B_e^*=40$, $\eta^*=0.75$, $\beta^*=5.10019$ and weighting parameter $(\gamma_{T_\Sigma})^2=3.8693$ for (b); $B_e^*=36.9454$, $\eta^*=0.75$, $\beta^*=5.20265$ and weighting parameter $(\gamma_{T_\Sigma})^2=38.693$ for (c); $B_e^*=38.5452$, $\eta^*=0.743411$, $\beta^*=13.1971$ and weighting parameter $(\gamma_{T_\Sigma})^2=386.93$ for (d), as presented in Table 3.3.6.

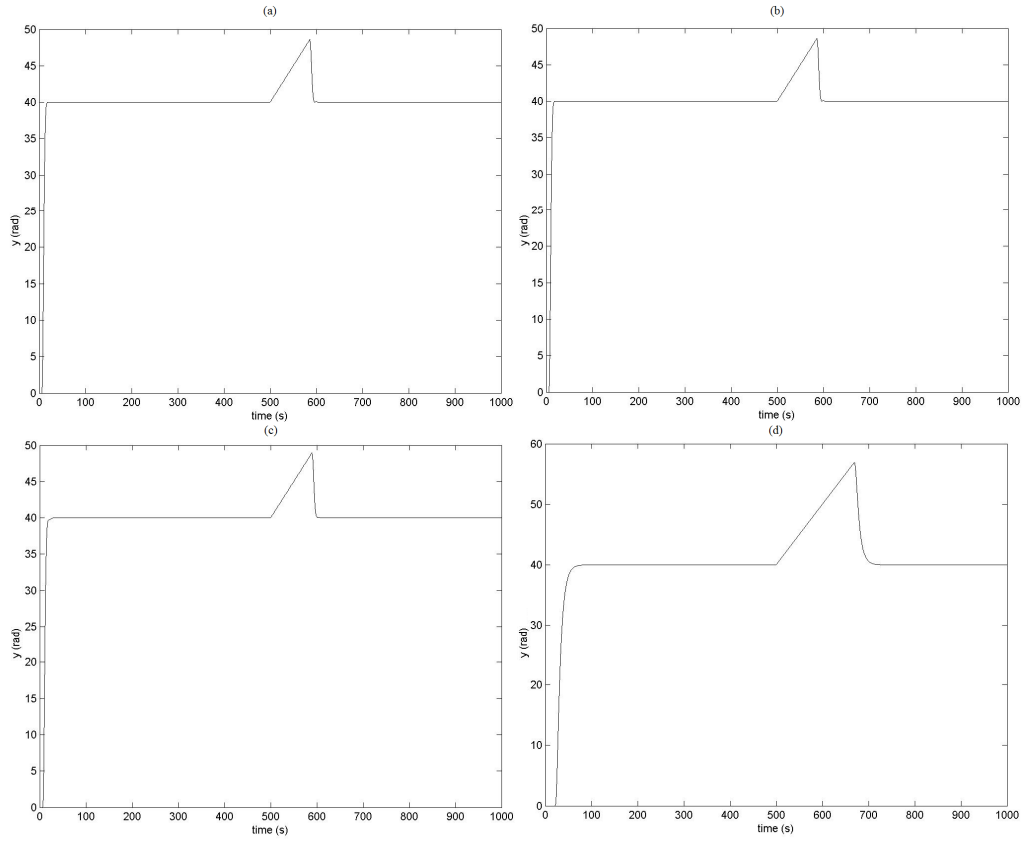

Fig. 3.8.6. Simulation results of optimal fuzzy control systems obtained for objective function J_{3,T_Σ} and different values of the weighting parameter γ_{T_Σ}: $\gamma_{T_\Sigma} = 0$ (a), $(\gamma_{T_\Sigma})^2 = 3.8693$ (b), $(\gamma_{T_\Sigma})^2 = 38.693$ (c), and $(\gamma_{T_\Sigma})^2 = 386.93$ (d).

Fig. 3.8.7 offers the simulation results obtained for the objective function J_{4,k_P}, as found in Table 3.5.7 for the following controller parameters computed by the CSS algorithm: $B_e^* = 40$, $\eta^* = 0.75$, $\beta^* = 5.14965$ and weighting parameter $\gamma_{k_P} = 0$ for (a); $B_e^* = 40$, $\eta^* = 0.75$, $\beta^* = 5.15098$ and weighting parameter $(\gamma_{k_P})^2 = 0.142$ for (b); $B_e^* = 39.8938$, $\eta^* = 0.75$, $\beta^* = 5.16777$ and weighting parameter $(\gamma_{k_P})^2 = 1.42$ for (c); $B_e^* = 20$, $\eta^* = 0.25$, $\beta^* = 9.65464$ and weighting parameter $(\gamma_{k_P})^2 = 14.2$ for (d).

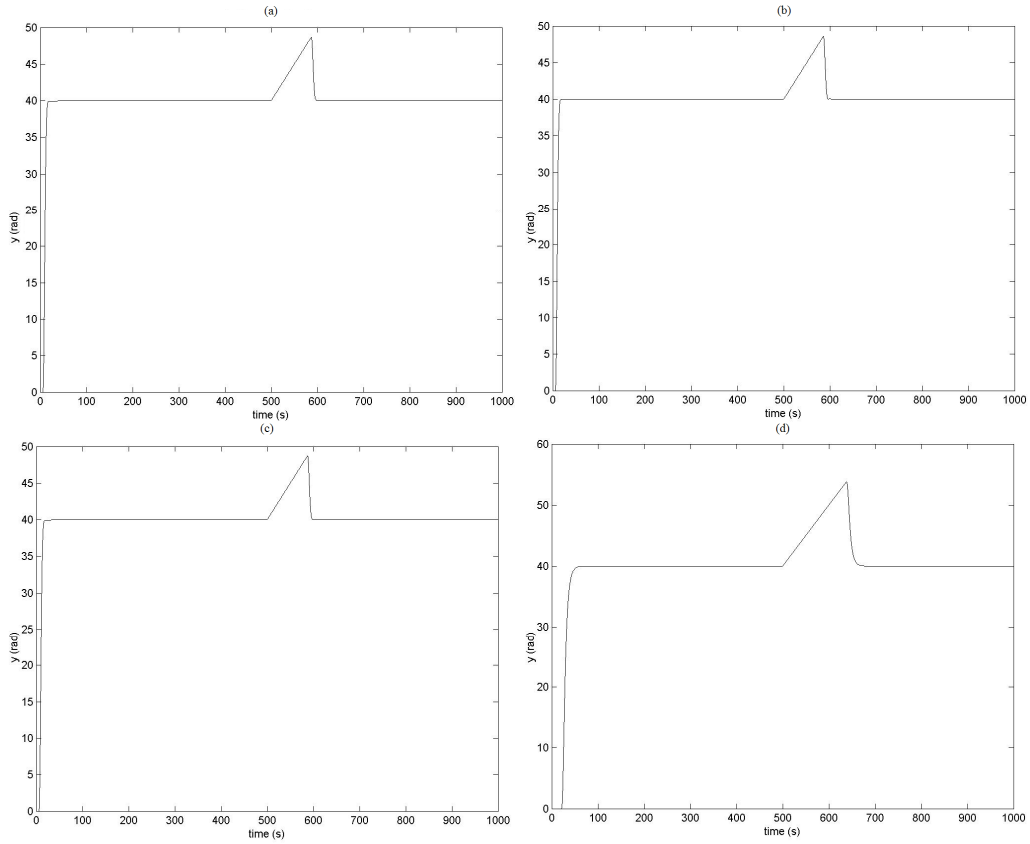

Fig. 3.8.7. Simulation results of optimal fuzzy control systems obtained for objective function J_{4,k_P} and different values of the weighting parameter γ_{k_P} : $\gamma_{k_P}=0$ (a), $(\gamma_{k_P})^2=0.142$ (b), $(\gamma_{k_P})^2=1.42$ (c), and $(\gamma_{k_P})^2=14.2$ (d).

Fig. 3.8.8 presents the simulation results for the objective function J_{4,T_Σ} using the following controller parameters obtained from by the PSOGSA algorithm: $B_e^*=40$, $\eta^*=0.75$, $\beta^*=5.08538$ and weighting parameter $\gamma_{k_P}=0$ for (a); $B_e^*=40$, $\eta^*=0.75$, $\beta^*=5.08486$ and weighting parameter $(\gamma_{T_\Sigma})^2=0.15885$ for (b); $B_e^*=37.0232$, $\eta^*=0.75$, $\beta^*=3$ and weighting parameter $(\gamma_{T_\Sigma})^2=1.5885$ for (c); $B_e^*=20$, $\eta^*=0.25$, $\beta^*=11.2378$ and weighting parameter $(\gamma_{T_\Sigma})^2=15.885$ for (d) as described in Table 3.4.8.

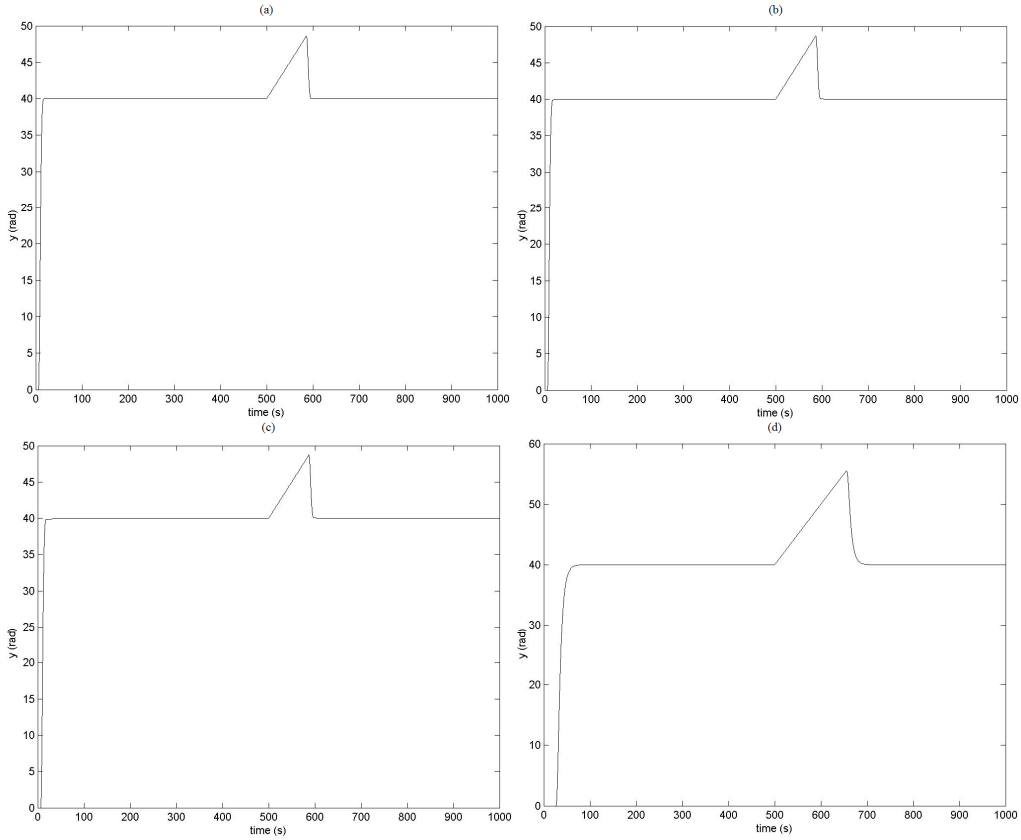

Fig. 3.8.8. Simulation results of optimal fuzzy control systems obtained for objective function J_{4,T_Σ} and different values of the weighting parameter γ_{T_Σ}: $\gamma_{T_\Sigma} = 0$ (a), $(\gamma_{T_\Sigma})^2 = 0.15885$ (b), $(\gamma_{T_\Sigma})^2 = 1.5885$ (c), and $(\gamma_{T_\Sigma})^2 = 15.885$ (d).

The parametric sensitivity reduction will be proved as follows by conducting the digital simulation of the fuzzy control system behaviors for different values of the process parameters k_P and T_Σ with respect to the nominal values $k_{P0} = k_{EP0} = 140$ and $T_{\Sigma 0} = 0.92\,\mathrm{s}$, respectively. Experiments are not conducted as the laboratory experimental setup does not allow for modifications of these process parameters.

The demonstration is based on simulations involving the variation of process parameters in conjunction with the initial and optimal values of the T-S PI-FCs. Two aspects regarding the variation of the process parameters will be presented for each objective function and process parameter: first is the variation of the values of objective function for different values of the process parameter handled in the current optimization and the second aspect is the output variation of the fuzzy control system.

The results corresponding to the first aspect of this demonstration for each objective function given in (2.9) – (2.12) and for the process parameter k_P are

presented in Figs. 3.8.9, 3.8.13, 3.8.17 and 3.8.21. Figs. 3.8.11, 3.8.15, 3.8.19 and 3.8.23 give the results for the process parameter T_Σ. For simplicity, the presented figures describe only the case of unitary ratio for the weighting parameter.

The output variation of the fuzzy control system that minimizes the objective functions (2.9) – (2.12) for the process parameter k_P is illustrated in Figs. 3.8.10, 3.8.14, 3.8.18 and 3.8.22. The results for the process parameter T_Σ are presented in Figs. 3.8.12, 3.8.16, 3.8.20 and 3.8.24. As in the case of the previous aspect, only the case of unitary ratio for the weighting parameter was considered.

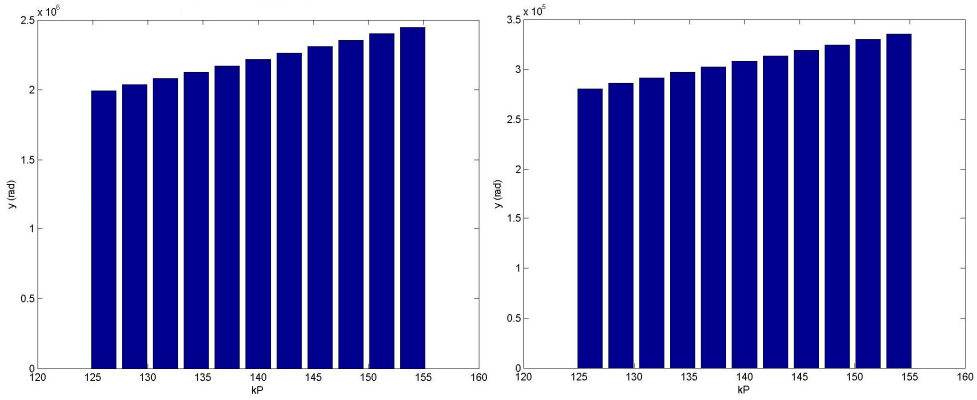

Fig. 3.8.9. Objective function J_{1,k_P} values for weighting parameter $(\gamma_{k_P})^2 = 0.021357$ and different values of the process parameter $k_P \in \{126, 128.8, 131.6, 134.4, 137.2, 140, 142.8, 145.6, 148.4, 151.2, 154\}$.

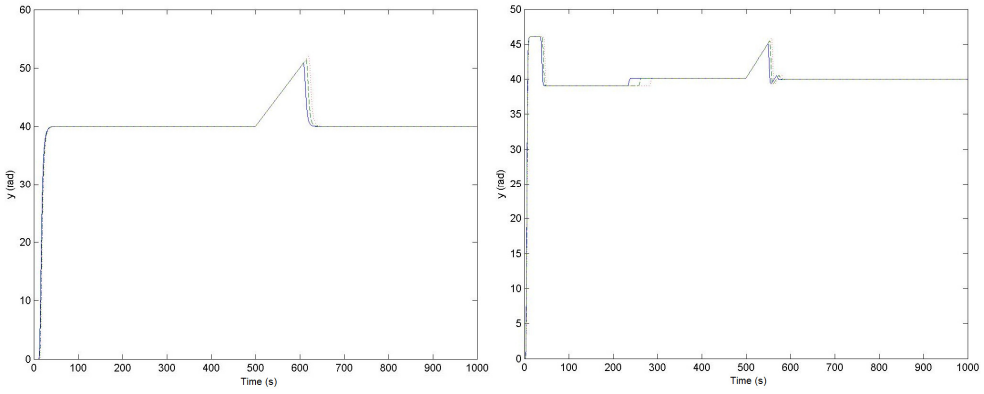

Fig. 3.8.10. Simulation results of fuzzy control systems with different values of k_P parameter: $k_P = 126$ (solid), $k_P = 140$ (dashed) and $k_P = 156$ (dotted) for objective function J_{1,k_P} and weighting parameter $(\gamma_{k_P})^2 = 0.021357$.

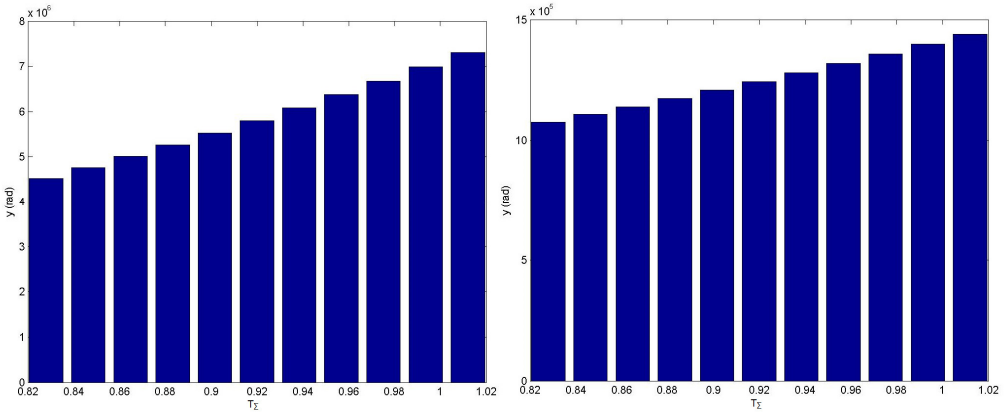

Fig. 3.8.11. Objective function J_{1,T_Σ} values for weighting parameter $(\gamma_{T_\Sigma})^2 = 1.7187$ and different values of the process parameter $T_\Sigma \in \{0.828, 0.8464, 0.8648, 0.8832, 0.9016, 0.92, 0.9384, 0.9568, 0.9752, 0.9936, 1.012\}$.

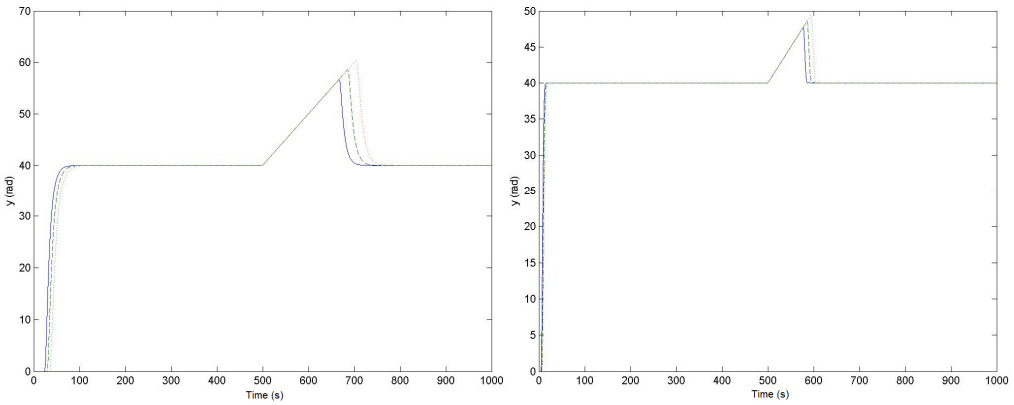

Fig. 3.8.12. Simulation results of fuzzy control systems with different values of T_Σ parameter: $T_\Sigma = 0.828$ (solid), $T_\Sigma = 0.92$ (dashed) and $T_\Sigma = 1.012$ (dotted) for objective function J_{1,T_Σ} and weighting parameter $(\gamma_{T_\Sigma})^2 = 1.7187$.

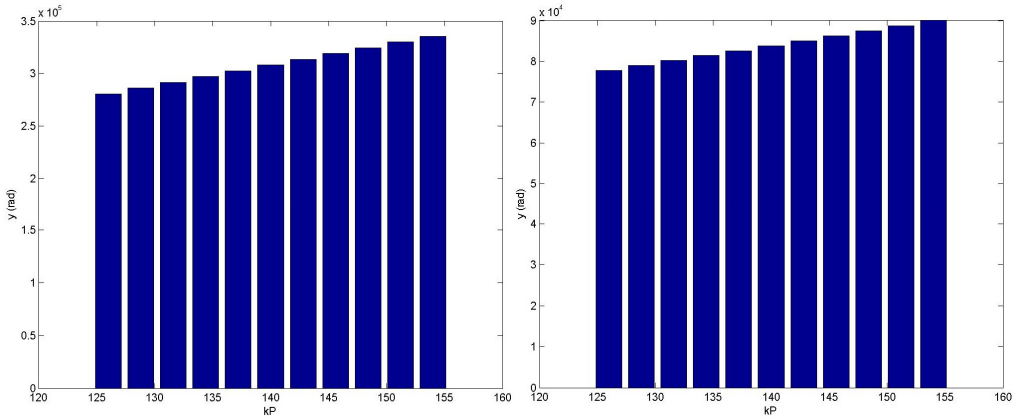

Fig. 3.8.13. Objective function J_{2,k_P} values for weighting parameter $(\gamma_{k_P})^2 = 0.06858$ and different values of the process parameter $k_P \in \{126,128.3,131.6,134.4,137.2,140,142.8,145.6,148.4,151.2,154\}$.

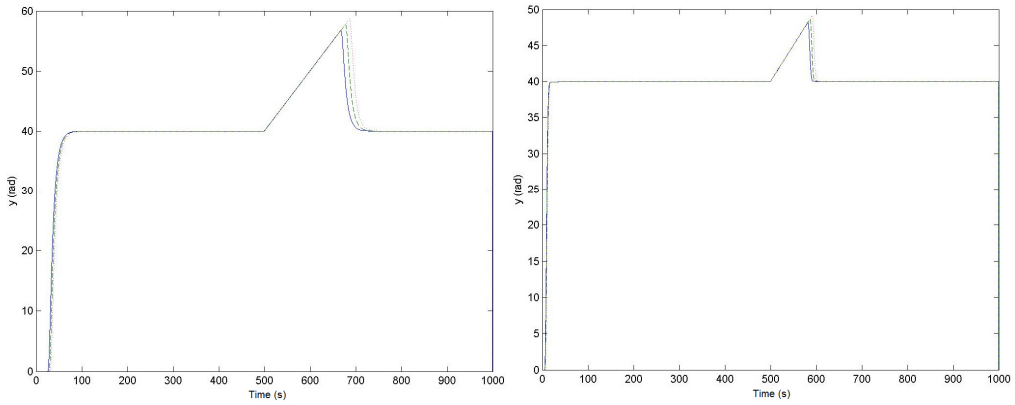

Fig. 3.8.14. Simulation results of fuzzy control systems with different values of k_P parameter: $k_P = 126$ (solid), $k_P = 140$ (dashed) and $k_P = 156$ (dotted) for objective function J_{2,k_P} and weighting parameter $(\gamma_{T_\Sigma})^2 = 0.06858$.

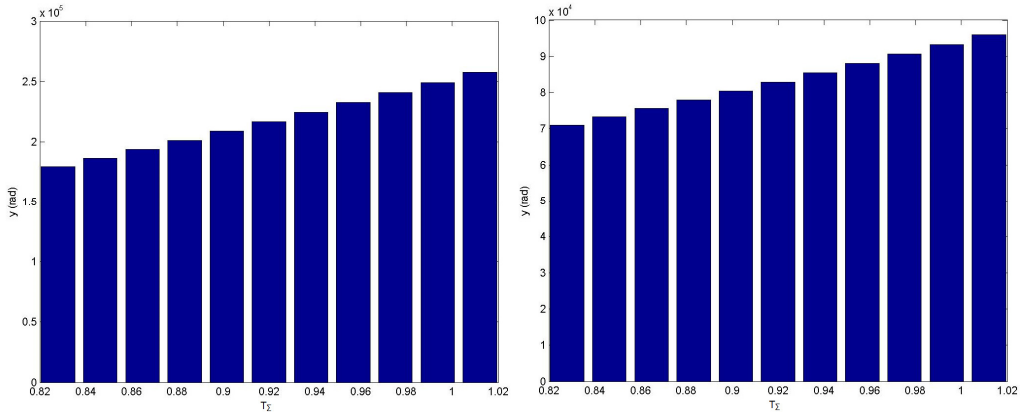

Fig. 3.8.15. Objective function J_{2,T_Σ} values for weighting parameter $(\gamma_{T_\Sigma})^2 = 0.066695$ and different values of the process parameter $T_\Sigma \in \{0.828, 0.8464, 0.8648, 0.8832, 0.9016, 0.92, 0.9384, 0.9568, 0.9752, 0.9936, 1.012\}$.

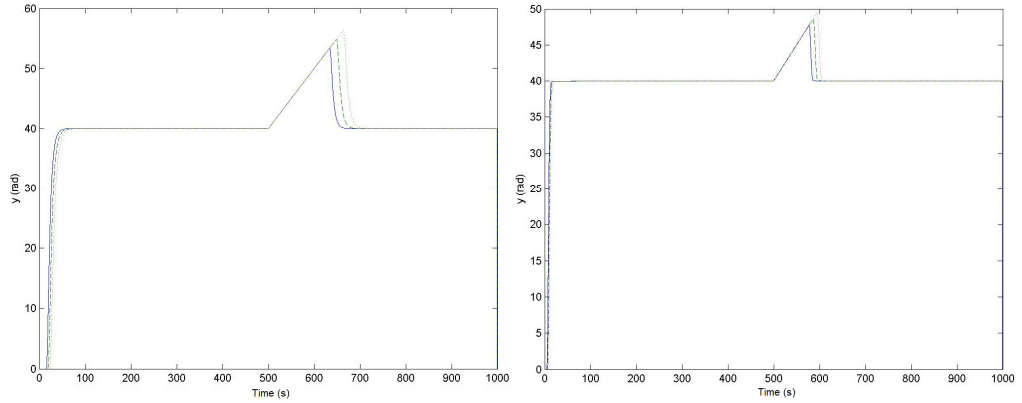

Fig. 3.8.16. Simulation results of fuzzy control systems with different values of T_Σ parameter: $T_\Sigma = 0.828$ (solid), $T_\Sigma = 0.92$ (dashed) and $T_\Sigma = 1.012$ (dotted) for objective function J_{2,T_Σ} and weighting parameter $(\gamma_{T_\Sigma})^2 = 0.066695$.

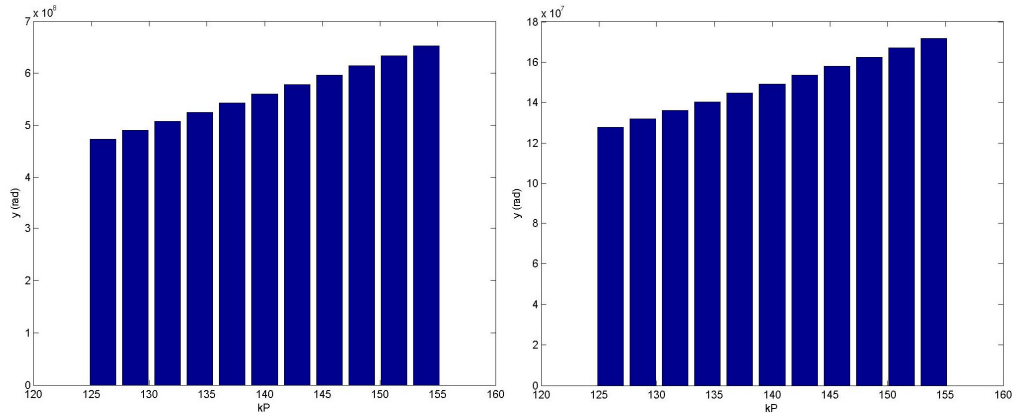

Fig. 3.8.17. Objective function J_{3,k_P} values for weighting parameter $(\gamma_{k_P})^2 = 39.187$ and different values of the process parameter $k_P \in \{126, 128.8, 131.6, 134.4, 137.2, 140, 142.8, 145.6, 148.4, 151.2, 154\}$.

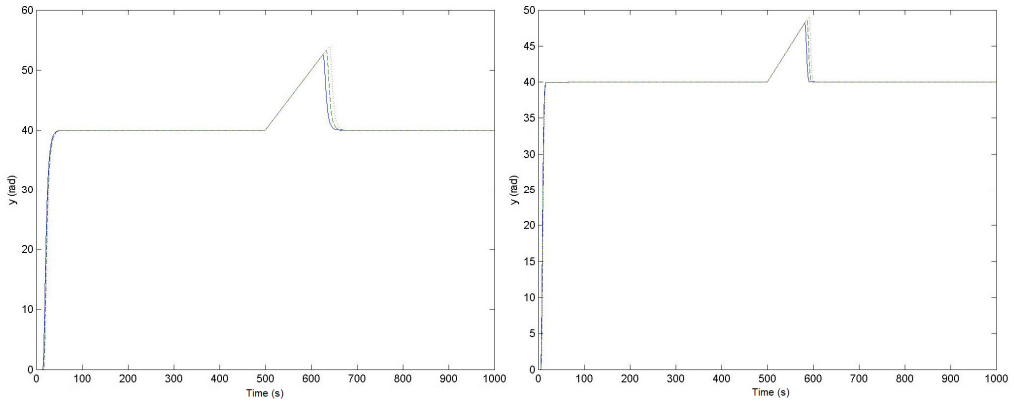

Fig. 3.8.18. Simulation results of fuzzy control systems with different values of k_P parameter: $k_P = 126$ (solid), $k_P = 140$ (dashed) and $k_P = 156$ (dotted) for objective function J_{3,k_P} and weighting parameter $(\gamma_{k_P})^2 = 39.187$.

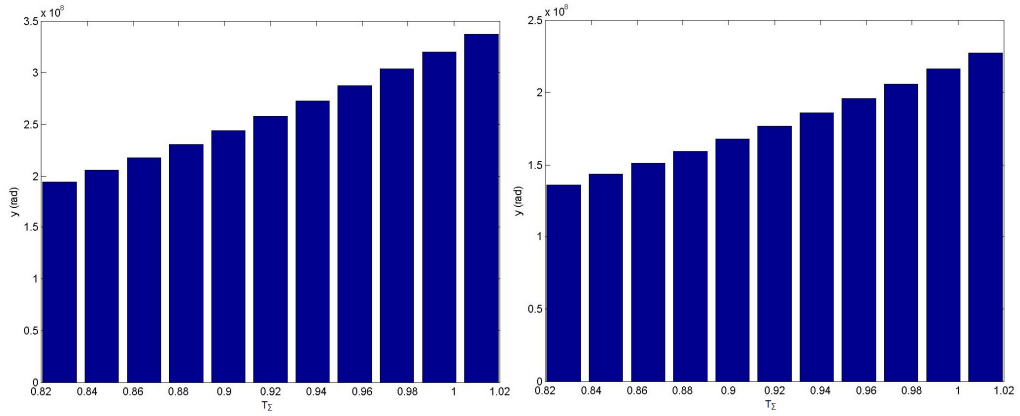

Fig. 3.8.19. Objective function J_{3,T_Σ} values for weighting parameter $(\gamma_{T_\Sigma})^2 = 38.693$ and different values of the process parameter $T_\Sigma \in \{0.828, 0.8464, 0.8648, 0.8832, 0.9016, 0.92, 0.9384, 0.9568, 0.9752, 0.9936, 1.012\}$.

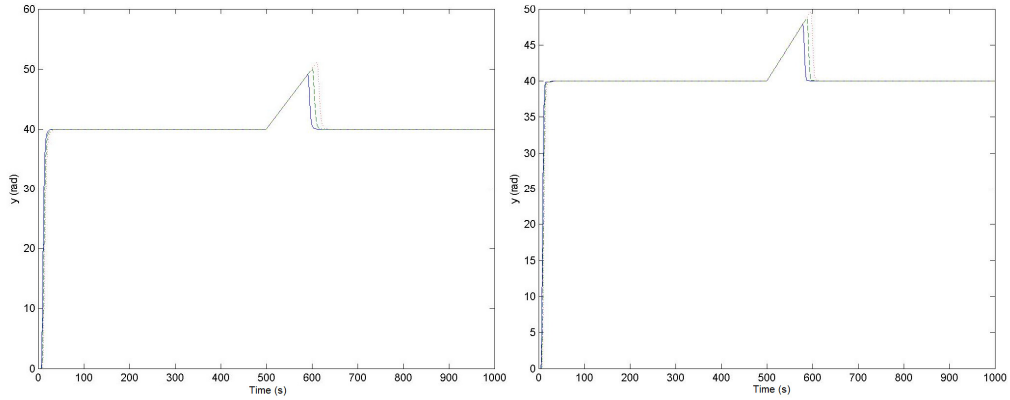

Fig. 3.8.20. Simulation results of fuzzy control systems with different values of T_Σ parameter: $T_\Sigma = 0.828$ (solid), $T_\Sigma = 0.92$ (dashed) and $T_\Sigma = 1.012$ (dotted) for objective function J_{3,T_Σ} and weighting parameter $(\gamma_{T_\Sigma})^2 = 38.693$.

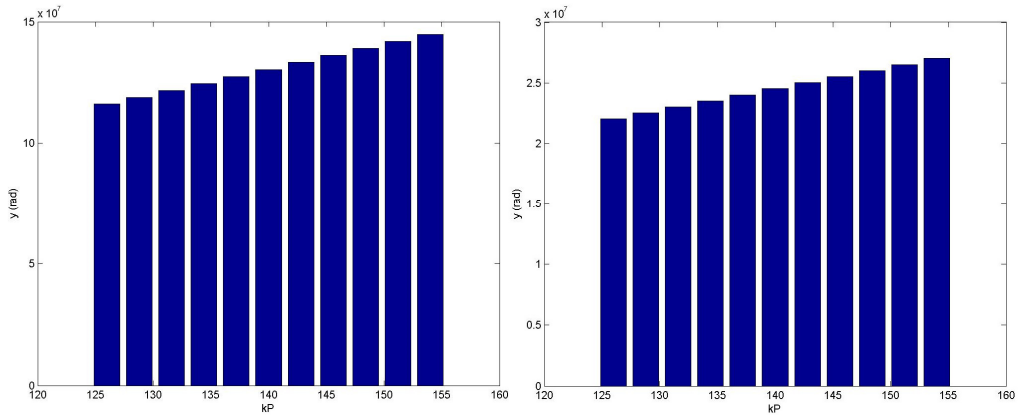

Fig. 3.8.21. Objective function J_{4,k_P} values for weighting parameter $(\gamma_{k_P})^2 = 1.42$ and different values of the process parameter $k_P \in \{126, 128.8, 131.6, 134.4, 137.2, 140, 142.8, 145.6, 148.4, 151.2, 154\}$.

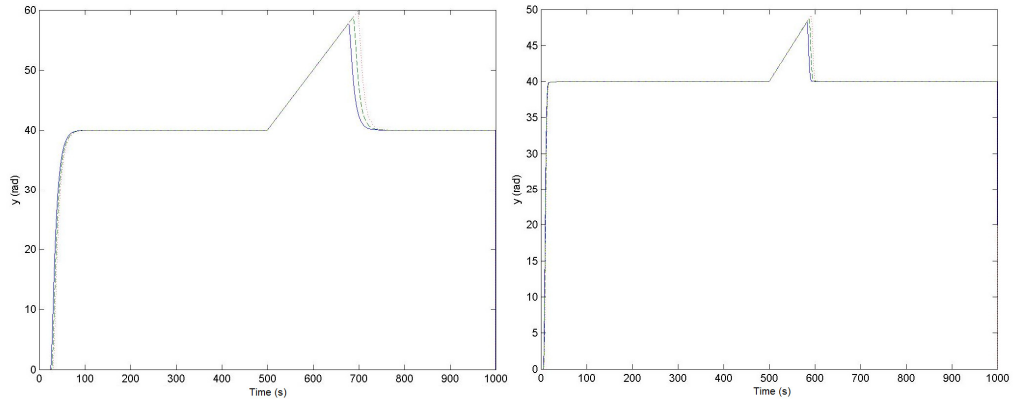

Fig. 3.8.22. Simulation results of fuzzy control systems with different values of k_P parameter: $k_P = 126$ (solid), $k_P = 140$ (dashed) and $k_P = 156$ (dotted) for objective function J_{4,k_P} and weighting parameter $(\gamma_{k_P})^2 = 1.42$.

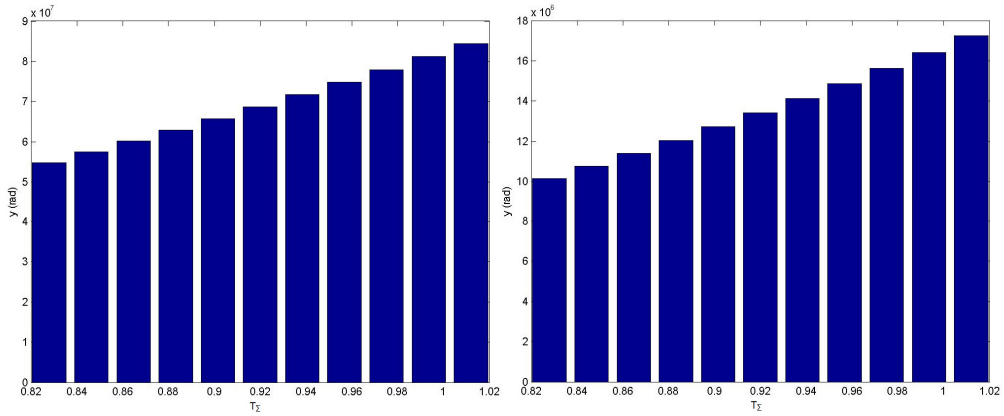

Fig. 3.8.23. Objective function J_{4,T_Σ} values for weighting parameter $(\gamma_{T_\Sigma})^2 = 1.5885$ and different values of the process parameter $T_\Sigma \in \{0.828, 0.8464, 0.8648, 0.8832, 0.9016, 0.92, 0.9384, 0.9568, 0.9752, 0.9936, 1.012\}$.

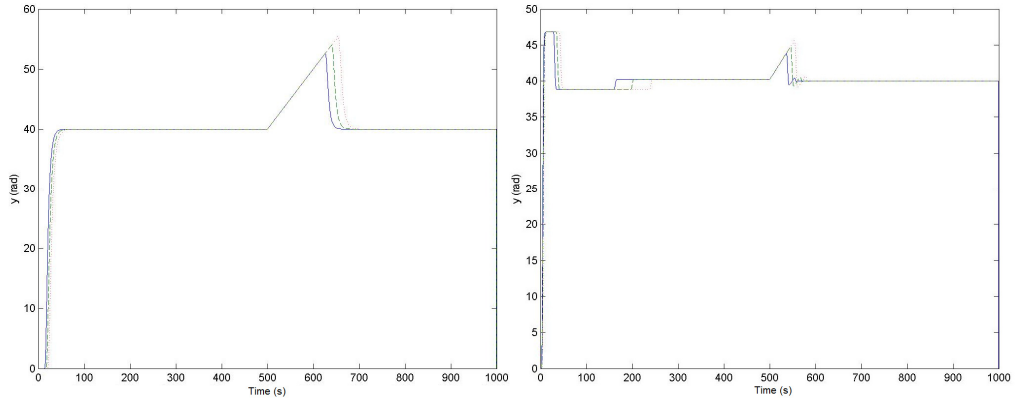

Fig. 3.8.24. Simulation results of fuzzy control systems with different values of T_Σ parameter: $T_\Sigma = 0.828$ (solid), $T_\Sigma = 0.92$ (dashed) and $T_\Sigma = 1.012$ (dotted) for objective function J_{4,T_Σ} and weighting parameter $(\gamma_{T_\Sigma})^2 = 1.5885$.

In a similar test setup as for Figs. 3.8.1 – 3.8.8, the results presented here clearly demonstrate the reduced sensitivity of the fuzzy control systems when the optimal tuning parameters were applied. The performance improvement is consistent in the case of process parameter variations, as showed by the reduced values of the objective functions and better responses for the fuzzy control systems in all scenarios.

In this chapter, five nature-inspired optimization algorithms were presented in subchapters 3.1 – 3.5 and applied to the optimal tuning of the parameters of fuzzy controllers, along with two newly developed adaptive versions for two of them

in subchapters 3.6 and 3.7. Based on these proposed algorithms, optimal solutions were obtained to each of the optimization problems (2.13) – (2.16) described in the previous chapter by finding the near minimal values of the objective functions (2.9) – (2.12). For every algorithm a parameter evolution analysis was presented, focused on two points of view: the first presented the best solution evolution for each step of the search process and the later a global view of all agents' positions in the search domain at certain stages.

Further on, three indices were defined in order to assess the performance of these algorithms. Each index corresponds to a performance criterion: the average value of the objective functions presents the algorithms' capabilities to overcome local minima situations, the convergence speed describes how fast the final solutions are found in the search process, and the accuracy rate measures the precision of the algorithms' solutions.

Finally, the solutions obtained based on the nature-inspired algorithms were validated through simulations and experiments that proved the reduced sensitivity with respect to the process parameters considered in the derivation of the sensitivity models.

The new **contributions** of this chapter can be summed up as follows:

1. The original application of Simulated Annealing algorithms to solve four types of optimization problems such that to carry out the optimal tuning of the parameters of T-S PI-FCs dedicated to the control of a class of nonlinear servo systems. The results concerning the application of these algorithms are published in:

*R.-E. Precup, **R.-C. David**, E. M. Petriu, S. Preitl, M.-B. Rădac, Fuzzy control systems with reduced parametric sensitivity based on simulated annealing, IEEE Transactions on Industrial Electronics, vol. 59, no. 8, pp. 3049-3061, Aug. 2012, impact factor (IF) = 5.165, IF according to 2013 Journal Citation Reports (JCR) released by Thomson Reuters in 2014 = 6.500.*

2. The original application of Particle Swarm Optimization algorithms to solve four types of optimization problems such that to carry out the optimal tuning of the parameters of T-S PI-FCs dedicated to the control of a class of nonlinear servo systems. The results concerning the application of these algorithms are published in:

*R.-E. Precup, **R.-C. David**, S. Preitl, E. M. Petriu, Design aspects of optimal PI controllers with reduced sensitivity for a class of servo systems using PSO algorithms, Facta Universitatis Series: Automatic Control and Robotics, vol. 8, no. 1, pp. 1-12, 2009.*

3. The original application of Gravitational Search Algorithms to solve four types of optimization problems such that to carry out the optimal tuning of the parameters of T-S PI-FCs dedicated to the control of a class of nonlinear servo systems. The results concerning the application of these algorithms are published in:

***R.-C. David**, R.-E. Precup, E. M. Petriu, M.-B. Rădac, S. Preitl, Gravitational search algorithm-based design of fuzzy control systems with a reduced parametric sensitivity, Information Sciences (Elsevier Science), vol. 247, pp. 154-173, Oct. 2013, impact factor (IF) = 3.893, IF according to 2013 Journal Citation Reports (JCR) released by Thomson Reuters in 2014 = 3.893.*

4. The original application of a version of hybrid Particle Swarm Optimization-Gravitational Search Algorithms to solve four types of optimization problems

such that to carry out the optimal tuning of the parameters of T-S PI-FCs dedicated to the control of a class of nonlinear servo systems. The results concerning the application of these algorithms are published in:

R.-C. David, *R.-E. Precup, E. M. Petriu, C. Purcaru, S. Preitl, PSO and GSA algorithms for fuzzy controller tuning with reduced process small time constant sensitivity, Proceedings of 2012 16th International Conference on System Theory, Control and Computing (ICSTCC 2012), Sinaia, Romania, 6 pp., 2012, indexed in IEEE Xplore, INSPEC, SCOPUS*.

5. The original application of Charged System Search algorithms to solve four types of optimization problems such that to carry out the optimal tuning of the parameters of T-S PI-FCs dedicated to the control of a class of nonlinear servo systems. The results concerning the application of these algorithms are published in:

*R.-E. Precup, **R.-C. David**, E. M. Petriu, S. Preitl, M.-B. Rădac, Charged system search algorithms for optimal tuning of PI controllers, Proceedings of 1st IFAC Conference on Embedded Systems, Computational Intelligence and Telematics in Control (CESCIT 2012), editors: K. Schilling, E. Leutert, Würzburg, Germany, pp. 115-120, 2012, indexed in SCOPUS.*

6. A novel class of adaptive GSAs with improved exploration and exploitations capabilities inspired by the 5E learning model used in education. The adaptive GSAs are developed around the basic version of GSA, and their three new functions are:

- the adaptation of two depreciation laws of the gravitational constant to the iteration index,
- the adaptation of a parameter in the weighted sum of all forces exerted from the other agents to the iteration index,
- the resetting at each run of adaptive GSA agents' worst fitnesses and positions to their best values.

These new adaptive GSAs are published in:

*R.-E. Precup, **R.-C. David**, E.M. Petriu, S. Preitl, M.-B. Rădac, Novel adaptive gravitational search algorithm for fuzzy controlled servo systems, IEEE Transactions on Industrial Informatics, vol. 8, no. 4, pp. 791-800, Nov. 2012, impact factor (IF) = 3.381, IF according to 2013 Journal Citation Reports (JCR) released by Thomson Reuters in 2014 = 8.785.*

7. The original application of the new adaptive GSAs to solve four types of optimization problems such that to carry out the optimal tuning of the parameters of T-S PI-FCs dedicated to the control of a class of nonlinear servo systems. The results concerning the application of these algorithms are published in:

*R.-E. Precup, **R.-C. David**, E. M. Petriu, S. Preitl, M.-B. Rădac, Experiments in fuzzy controller tuning based on an adaptive gravitational search algorithm, Proceedings of the Romanian Academy, Series A: Mathematics, Physics, Technical Sciences, Information Science, vol. 14, no. 4, pp. 360-367, Dec. 2013, impact factor (IF) = 1.115, IF according to 2013 Journal Citation Reports (JCR) released by Thomson Reuters in 2014 = 1.115.*

8. A novel class of adaptive CSS algorithms with improved exploration and exploitations capabilities inspired by the 5E learning model used in education. The adaptive CSS algorithms are developed around the basic version of CSS algorithms, and their two new functions are:

- the adaptation of the acceleration, velocity, and separation distance parameters to the iteration index,
- the substitution of the worst charged particles' fitness function values and positions with the best performing particle data.

These new adaptive CSS algorithms are published in:

*R.-E. Precup, **R.-C. David**, E. M. Petriu, St. Preitl and M.-B. Radac, Novel adaptive charged system search algorithm for optimal tuning of fuzzy controllers, Expert Systems with Applications, vol. 41, no. 4, part 1, pp. 1168-1175, March 2014, impact factor (IF) = 1.965, IF according to 2013 Journal Citation Reports (JCR) released by Thomson Reuters in 2014 = 1.965.*

9. The original application of the new adaptive CSS algorithms to solve four types of optimization problems such that to carry out the optimal tuning of the parameters of T-S PI-FCs dedicated to the control of a class of nonlinear servo systems. The results concerning the application of these algorithms are published in:

***R.-C. David**, R.-E. Precup, E. M. Petriu, St. Preitl, M.-B. Rădac, L.-O. Fedorovici, Adaptive evolutionary optimization algorithms for simple fuzzy controller tuning dedicated to servo systems, in: Fuzzy Modeling and Control: Theory and Applications, F. Matia, G. N. Marichal and E. Jimenez, Eds., Atlantis Computational Intelligence Systems, vol. 9, Atlantis Press and Springer International Publishing, Cham, Heidelberg, New York, Dordrecht, London, pp. 159-173, 2014, indexed in Springer Link.*

10. The definition of three original performance indices to assess the quality of nature-inspired optimization algorithms:

- the average value of each objective function,
- the convergence speed,
- the accuracy rate.

A part of these indices is proposed in:

*R.-E. Precup, **R.-C. David**, E. M. Petriu, S. Preitl, M.-B. Rădac, Gravitational search algorithms in fuzzy control systems tuning, Proceedings of 18th IFAC World Congress, Milano, Italy, pp. 13624-13629, 2011, indexed in SCOPUS.*

11. The quality assessment of the performance of nature-inspired optimization algorithms based on three original performance indices considering a certain number of runs (five in these thesis) of each nature-inspired optimization algorithm. The results concerning the quality assessment of the nature-inspired optimization algorithms applied to PI controller tuning are published in:

***R.-C. David**, R.-E. Precup, S. Preitl, J. K. Tar, J. Fodor, Three evolutionary optimization algorithms in PI controller tuning, in: Applied Computational Intelligence in Engineering and Information Technology, editors: R.-E. Precup, S. Kovacs, S. Preitl, E. M. Petriu, Topics in Intelligent Engineering and Informatics, vol. 1, Springer-Verlag, Berlin, Heidelberg, pp. 95-106, 2012, indexed in Springer Link.*

12. The validation of all new results by simulations using the detailed fuzzy control system models and by experiments conducted on the real-world laboratory servo system. Simulation results are presented in all publications. Experimental results are published in:

*R.-E. Precup, **R.-C. David**, E. M. Petriu, S. Preitl, M.-B. Rădac, Fuzzy logic-based adaptive gravitational search algorithm for optimal tuning of fuzzy*

controlled servo systems, IET Control Theory and Applications, vol. 7, no. 1, pp. 99-107, Jan. 2013, impact factor (IF) = 1.844, IF according to 2013 Journal Citation Reports (JCR) released by Thomson Reuters in 2014 = 1.844.

4. OPTIMAL TUNING OF INPUT MEMBERSHIP FUNCTIONS OF TAKAGI-SUGENO FUZZY MODELS BASED ON SIMULATED ANNEALING ALGORITHMS

4.1. PROBLEM SETTING CONCERNING THE OPTIMAL TUNING OF INPUT MEMBERSHIP FUNCTIONS OF TAKAGI-SUGENO FUZZY MODELS BASED ON NATURE-INSPIRED ALGORITHMS

As mentioned in Sub-chapter 1.1, several parameters that belong to the blocks in the structure of Takagi-Sugeno (T-S) fuzzy models can be optimally tuned. The optimal tuning of a part of the parameters of the input membership functions is treated in this thesis. This is organized in terms of the modeling approach that consists of the following steps:

Step 1. The structure of the dynamic T-S fuzzy model is set, namely the number of operating points that is equal to the number of rules, the number of input linguistic terms (LTs) of the input variables, the shapes of the membership functions (m.f.s) of the input LTs, the operators in the inference engine, and the method for defuzzification.

Step 2. The nonlinear continuous-time state-space model of the process is linearized at a number of important operating points, and this number is equal to the number of rules of the dynamic T-S fuzzy model. This leads to a set of linearized continuous-time local process models, which are placed in the rule consequents of the continuous-time T-S fuzzy model, and they related to the modal values of the input m.f.s, which are exactly the coordinates of the operating points in terms of the modal equivalence principle [Gal95]. The sampling period is set, and the models in the consequents of the T-S fuzzy model are discretized accounting for the zero-order hold resulting in the rule base of the discrete-time T-S fuzzy model.

Step 3. Considering the parameter vector $\boldsymbol{\rho}$ that consists of a part of the parameters of the input membership functions of the dynamic T-S fuzzy model, the following optimization problem is defined:

$$\boldsymbol{\rho}^* = \arg\min_{\boldsymbol{\rho}\in D} J(\boldsymbol{\rho}), \tag{4.1}$$

where $\boldsymbol{\rho}^*$ is the optimal parameter vector of the fuzzy model and the solution to the optimization problem, and D is the feasible domain of $\boldsymbol{\rho}$. The objective function $J(\boldsymbol{\rho})$ in (4.1) is defined as:

$$J(\boldsymbol{\rho}) = \frac{1}{N}\sum_{k=1}^{N}(y_k(\boldsymbol{\rho}) - y_{k,m}(\boldsymbol{\rho}))^2 = \frac{1}{N}\sum_{k=1}^{N}(e_{k,m}(\boldsymbol{\rho}))^2, \tag{4.2}$$

where $y_k(\boldsymbol{\rho}) = \lambda_k(\boldsymbol{\rho})$ is the process output at k^{th} sampling interval, $y_{k,m}(\boldsymbol{\rho})$ is the fuzzy model output, $e_{k,m}(\boldsymbol{\rho}) = y_k(\boldsymbol{\rho}) - y_{k,m}(\boldsymbol{\rho})$ is the modeling error, and *N* is the length of the time horizon. The optimization problem (4.1), with the objective function (4.2), aims the minimization of the mean square modeling error.

Step 4. A nature-inspired optimization algorithm is applied to solve the optimization problem (4.1), i.e., to obtain the optimal input membership function parameters, which lead to the optimal dynamic T-S fuzzy model of the process.

The input variables specified in the step 1 of the modeling approach are in fact the scheduling variables that are involved in the premise part of the dynamic T-S fuzzy model rules.

The steps 1 and 2 produce the initial dynamic T-S fuzzy model of the process, and the step 4 produces the optimized dynamic T-S fuzzy model of the process. These two steps of the fuzzy modeling approach can be replaced by an appropriate fuzzy model identification technique.

Some recent applications of fuzzy model identification techniques are discussed as follows. An attractive result is formulated in [Anh12] as an inverse adaptive fuzzy model trained by PSO algorithm. An extended allied fuzzy C-means algorithm is introduced in [Moh13] and optimized using PSO. A hyperplane prototype fuzzy clustering model is proposed in [Li12b] using a GSA-based hyperplane clustering algorithm to improve the performance of the fuzzy clustering algorithm in the fuzzy space partition of the fuzzy model identification technique. A fuzzy model identification technique for a nonlinear model predictive control is optimized in [Sy08] using the branch and bound method and genetic algorithm. An interval fuzzy model identification technique is developed in [Kha10b] using the interval fuzzy model that is based on lower and upper fuzzy models or a fuzzy model with a set of lower and upper parameters. A method to obtain computationally efficient low-order process models for large-scale processes based on the combination of orthogonal decompositions, black-box system identification techniques and non-linear spline-based blending is described in [Wat10]. A self-extracting rules fuzzy control method is introduced in [Lu10] for dealing with complex thermal processes.

The approach presented in this sub-chapter is applied in the next sub-chapters to the fuzzy modeling of two nonlinear processes using the Simulated Annealing (SA) algorithm as the nature-inspired optimization algorithm in the step 4. These processes are an Anti-lock Braking System (ABS) and a magnetic levitation system, and the proposed dynamic T-S fuzzy models are validated by real-time experimental results on laboratory equipment.

4.2. State-of-the-art analysis for the optimal tuning of input membership functions of Takagi-Sugeno fuzzy models based on nature-inspired algorithms

The analysis of the state-of-the-art concerning the optimal tuning of input membership functions of Takagi-Sugeno fuzzy models based on nature-inspired al-

gorithms is first considered in a more general framework of the optimal tuning of parameters of Takagi-Sugeno fuzzy models. This bibliographic analysis presents a general view of different approaches concerning the optimization of fuzzy control systems in the first part, from the point of view of the fuzzy model structure, and later focuses on applications of nature-inspired algorithms with regard to general optimization of fuzzy systems.

Since the structure of fuzzy models consists of the well-known fuzzification module, rule base and inference engine and defuzzification module, the analysis will be organized in three separate categories because the optimal tuning of the parameters in the defuzzification module is not carried out in the literature as far as the author knows:

(i) The optimal tuning of the parameters in the fuzzification module with focus on the optimal tuning of the parameters of the input membership functions.

(ii) The optimal tuning of the rule base and of the parameters in the inference engine.

(iii) Cross-module optimization, i.e., the optimal tuning of several parameters that belong to different blocks in the structure of the Takagi-Sugeno fuzzy models.

(i) A first result containing the optimal tuning of the membership functions, is represented in [Esm02] as a learning algorithm based on PSO for the membership functions automatic adjustment. The tuning of Gaussian membership functions is carried out in [Tay11]. An adaptive fuzzy logic controller based on genetic algorithms used for optimizing the internal parameters of fuzzy membership functions is described in [Far07]. The shape of membership functions is adjusted in [Mer11] using a clonal selection algorithm. [Kha08] propose a method for optimizing the membership functions of a fuzzy logic controller using genetic algorithms. A hybrid procedure based on PSO and gradient descent algorithms is proposed in [Kha10c] to obtain membership functions with a superior performance.

(ii) One of the results concerning the optimal tuning of the rule base and of the parameters in the inference engine is given in [Bod05], where evolutionary optimization tools are employed in the optimization of normalized root mean square error of the training data which is minimized for the fine-tuning of the fuzzy rule base parameters. Hybrid tabu search and PSO algorithms are used in [Tal11b] to dynamically adjust the membership functions and fuzzy rules according to different environments. A bacterial evolutionary algorithm is applied in [Cab06] to determine the fuzzy rule base of fuzzy systems. A PSO algorithm is employed in [Zha12] to deal with fuzzy rule interpolation with fuzzy measure-based antecedent variables and fuzzy rule interpolation based on polygonal membership functions. A bacterial foraging optimization algorithm is used in [Kam12] to determine the rule base of fuzzy models. The structure and the parameters of a fuzzy rule base are generate automatically by a PSO algorithm in [Che12]. A method to build a T-S fuzzy model with optimal rules using a combination of chaotic PSO and Gustafson-Kessel clustering algorithm is proposed in [Coe07]. An Ant Colony Optimization algorithm is used in [Jua08] for rule base optimization in fuzzy controller design. A method for optimizing the rule base of a Mamdani-type fuzzy controller using an integer evolutionary algorithm is described [Meg13].

A partitioning of the fuzzy inference system is carried out in [Jua09] on the basis of ant colony optimization combined with fuzzy-Q learning for finding the best pheromone trail. A neuro-fuzzy system using a PSO algorithm is proposed in [Tur12] to optimize fuzzy systems with the use of neuro-fuzzy techniques emerged

from the fusion of neural networks and fuzzy inference systems. A soft computing optimizer is introduced in [Fuj07] to obtain a fuzzy inference system with the use of genetic algorithms.

(iii) An example of cross-module optimization by nature inspired algorithms is presented in [Abo13], where a self-tuning fuzzy PID controller based on PSO is proposed; the PSO algorithm optimally tunes the rule base, the scaling factors, the membership function parameters and the optimal range of the tuning parameters of the linear PID controller. The rule base and the membership functions of a hierarchical fuzzy control system are optimized in [Xia10] with the use of genetic algorithm.

Several applications of fuzzy models optimized by nature-inspired algorithms are discussed as follows. These applications are organized on the algorithms considered, focusing, as mentioned in Sub-chapter 2.2, the validation of the results (namely, the fuzzy models) by real-time experiments.

Popular applications of simulated annealing include the optimal tuning of fuzzy models for robotic systems [Hos14], performance drilling [Hab07], [Hab09], autonomous robot path planning [Mar98], data mining [Moh08], inventory management [Mil12], network topology [Kha09], project scheduling [Shu08] or renewable energy [Gar13]. A variation called orthogonal simulated annealing algorithm is used in an optimization problem that optimizes a fuzzy neural network model for the tuning of PID controllers in [Ho06]; various test plants with under-damped responses are considered. Simulated annealing showed a strong performance when combined with other algorithms. For example, in [Tor11] the fuzzy classifier is a cooperation of the simulated annealing and the subtractive clustering method as the simulated annealing is used in order to optimize the subtractive clustering parameters. Along with the standard version of simulated annealing, different adaptive versions emerged. A fuzzy adaptive simulated annealing is introduced in [Agu12]. A fuzzy adaptive simulated annealing-genetic algorithm is proposed in [Pen14].

A PSO-based example of T-S neuro-fuzzy network optimization using is presented in [Lin08]. A neuro-fuzzy inference system is tuned in [Oli09] by a PSO algorithm and applied to monitoring the relevant sensor in a nuclear power plant. The paper [Ma10] introduces an algorithm for T-S fuzzy modeling based on PSO, in which the solution is represented by both a binary value vector and a real value vector with corresponding equations for parameters update. The rule base of a T-S fuzzy model is optimized in [Jos12] using a PSO algorithm in order to minimize the output error surface of a nonlinear water level tank process. A fuzzy adaptive PSO algorithm is introduced in [Wu11] in order to identify a subset of features embedded out of a large dataset that is contaminated with high dimensional noise; the approach is divided into three stages, namely core feature subset selection, feature subset selection and spam filtering, leading to an optimal feature subset. An improved PSO algorithm is suggested in [Tan08] using a self-adaptive idea, which introduces the concept of dynamic learning factor.

A hybridization of cooperative PSO and cultural algorithm is suggested in [Lin09b] with the scope of increasing the global search capacity using the belief space; experimental results concerning the prediction of the number of sunspots are presented. A combination of PSO and black stork foraging process used in functional neural fuzzy networks is proposed in [Ham12], with experimental results related to solving the Iris and Breast cancer benchmark classification problems. A fuzzy PSO is introduced in [Alf11], with the PSO algorithm enhanced by a fuzzy inertia weight to rationally balance the global and local exploitation abilities. A chaos PSO algorithm is proposed in [Jia12]; this algorithm combines the strengths of chaos optimization

algorithm and PSO, and it optimizes T-S fuzzy models that are employed in constrained predictive control and validated by simulation tests.

A swarm intelligence-based classifier is described in [Ask12] using a fuzzy system designed for intelligently updating the effective parameters of GSA, which are used to construct a decision function estimation algorithm from feature space; the classifier is applied to a pattern recognition problem with nonlinear, overlapping class boundaries and different feature space dimensions. A T-S fuzzy model identification problem is solved in [Xue14] using an improved GSA based on silhouette index considered for both the intra-cluster cohesion and the inter-cluster separation, one cluster representing a fuzzy rule; cluster center is regarded as the Gaussian membership function center parameter, which is identified by this GSA. The paper [Jas14] deals with the problem of contact-state recognition for force-controlled robotic tasks by developing the corresponding contact formation classifiers using a GSA-based search fuzzy clustering algorithm that is validated through experimental results. A T-S fuzzy model identification method based on chaotic GSA is proposed in [Li13] and applied to the modeling of hydraulic turbine governing system with experimental results. A stochastic optimization approach to solve optimal bidding strategy problem in a pool based electricity market using fuzzy adaptive GSA is presented in [Vij13] and validated through simulations. A solution to feature selection using fuzzy grids-based association rules mining whose training parameters are optimized by GSA is presented in [She13] and validated using experimental results.

In recent publications adaptive versions of the GSA have appeared along with the standard version of the algorithm. One such adaptive version is characterized in [Vij13] by fuzzy rule-based systems applied to design the gravitational constant. Another adaptive quantum-inspired GSA is proposed in [Ibr14]. The combination with fuzzy logic leads to further performance improvement for this algorithm as shown in [Dum15], where simulations for several benchmark test functions are presented.

Along with the standard versions presented in Sub-chapter 2.4, improved versions for the standard form of the CSS algorithm have been developed with the scope of performance improvement. A combination of the CSS algorithm and the force method is applied to the simultaneous analysis and design of structures in [Kav14b]. A CSS-based approach that applies a construction factor to prevent converging to a local optimum is proposed in [Lin13]. A CSS algorithm is utilized in [Kav14c] as a search engine in combination with clustering and particle regeneration procedures. All these applications are validated by simulation results.

4.3. Simulated Annealing-based optimal tuning of input membership functions of Takagi-Sugeno fuzzy models for a laboratory anti-lock braking system

The development of Takagi-Sugeno fuzzy models for Anti-lock Braking Systems (ABSs) is a challenging task because of their process nonlinearities and the importance they impose to the automotive safety systems as they are used to prevent wheel locking. The INTECO ABS setup used in the experimental tests, consists

of two wheels as described in Fig. 4.3.1, which makes it different compared to the regular ABS setups based on electro-hydraulic actuators.

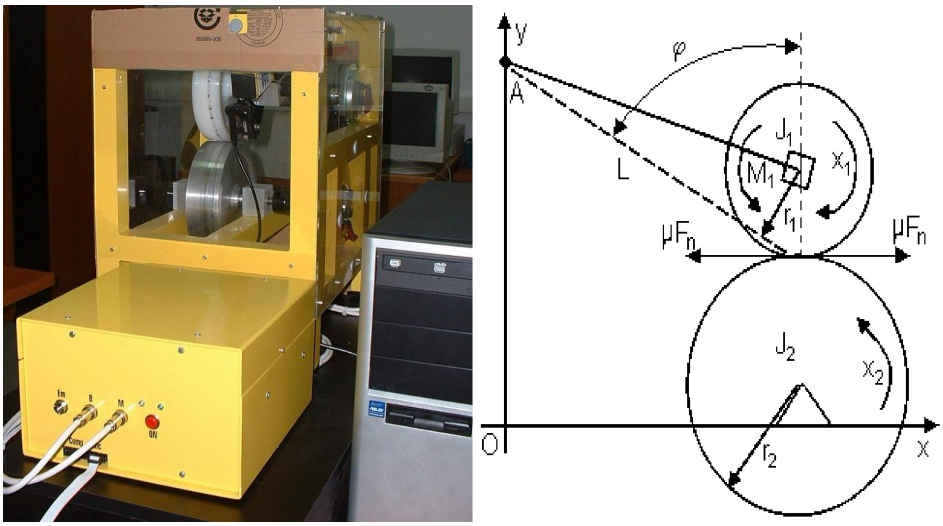

Fig. 4.3.1 INTECO ABS experimental setup and block diagram.

A simple approach to fuzzy modeling of ABSs will be presented in this sub-chapter following the methodology introduced in Sub-chapter 4.1. This approach starts with the T-S fuzzy model of the nonlinear state-space model of the ABS laboratory equipment [Int07a], which is derived by linear modal equivalence principle starting with the first-principle equations [Int07a], [Dav14b]:

$$\begin{aligned} J_1\dot{x}_1 &= F_n r_1 \mu(\lambda) - d_1 x_1 - M_{10} - M_1, \\ J_2\dot{x}_2 &= -F_n r_2 \mu(\lambda) - d_2 x_2 - M_{20}, \end{aligned} \tag{4.3}$$

where J_1 and J_2 are the moments of inertia of the wheels, x_1 and x_2 are the angular velocities, d_1 and d_2 are the friction coefficients in the wheels' axes, M_{10} and M_{20} are the static friction torques that oppose the normal rotation, M_1 is the brake torque, r_1 and r_2 are the radii of the wheels, F_n is the normal force that the upper wheel pushes upon the lower wheel, $\mu(\lambda)$ is the friction coefficient depending on the slip, and $\dot{x}_1$ and $\dot{x}_2$ are the angular accelerations of the wheels.

The identification by measurements and experiments leads to the following parameter values [Pre12c]:

$$\begin{aligned} &r_1 = r_2 = 0.99\,\text{m}, F_n = 58.214\,\text{N}, J_1 = 7.53\cdot 10^{-3}\,\text{kg m}^2, J_2 = 25.6\cdot 10^{-3}\,\text{kg m}^2, \\ &d_1 = 1.1874\cdot 10^{-4}\,\text{kg m}^2/\text{s}, d_2 = 2.1468\cdot 10^{-4}\,\text{kg m}^2/\text{s}, M_{10} = 0.0032\,\text{N m}, \\ &M_{20} = 0.0925\,\text{N m}. \end{aligned} \tag{4.4}$$

The definitions of the longitudinal slip λ which plays the role of controlled output in the slip control system and of the nonlinear factor $S(\lambda)$ are:

$$\lambda = \frac{r_2 x_2 - r_1 x_1}{r_2 x_2}, x_2 \neq 0, S(\lambda) = \frac{\mu(\lambda)}{L[\sin\varphi - \mu(\lambda)\cos\varphi]}, \tag{4.5}$$

where $L = 0.37\,\text{m}$ is arm's length, which fixes the upper wheel, and $\varphi = 65.61^{\circ}$ is the angle between the normal direction in wheels' contact point and L's direction.

The nonlinear state-space equations of the process are:

$$\begin{aligned}\dot{x}_1 &= S(\lambda)(c_{11}x_1 + c_{12}) + c_{13}x_1 + c_{14} + (c_{15}S(\lambda) + c_{16})s_1M_1,\\ \dot{x}_2 &= S(\lambda)(c_{21}x_1 + c_{22}) + c_{23}x_2 + c_{24} + c_{25}S(\lambda)s_1M_1,\\ \dot{M}_1 &= c_{31}(b(u) - M_1),\end{aligned} \tag{4.6}$$

where *u* is the control signal applied to the DC motor, which drives the upper wheel and the nonlinear model of the actuator, and the nonlinearity of the actuator is highlighted in the third equation. The expressions of the parameters in (4.6) are [Dav14b]:

$$\begin{aligned}&c_{11} = \frac{r_1 d_1}{J_1}, c_{12} = (M_{10} + M_g)\frac{r_1}{J_1}, c_{13} = -\frac{d_1}{J_1}, c_{14} = -\frac{M_{10}}{J_1},\\ &c_{15} = \frac{r_1}{J_1}, c_{16} = -\frac{1}{J_1}, c_{21} = -\frac{r_2 d_1}{J_2}, c_{22} = -(M_{10} + M_g)\frac{r_2}{J_2},\\ &c_{23} = -\frac{d_2}{J_2}, c_{24} = -\frac{M_{20}}{J_2}, c_{25} = -\frac{r_2}{J_2}.\end{aligned} \tag{4.7}$$

The introduction of λ as controlled output in the model (4.6) is done by the substitution of x_1 from (4.5). The state-space equations of ABS process are:

$$\begin{aligned}\dot{\lambda} &= Z_1(\lambda, x_2)\lambda + Z_3(\lambda, x_2)M_1 + Z_{20}(\lambda, x_2),\\ \dot{x}_2 &= Z_{40}(\lambda)x_2 + Z_5(\lambda_2)M_1 + Z_6(\lambda),\\ \dot{M}_1 &= c_{31}(b(u) - M_1),\end{aligned} \tag{4.8}$$

they point out the state vector **x**, which is also the scheduling vector of the dynamic T-S fuzzy model:

$$\mathbf{x} = [\lambda \quad x_2 \quad M_1]^T, \tag{4.9}$$

where *T* indicates the matrix transposition, and the first group of dynamic T-S fuzzy models of the process is characterized in [Pre12c], [Dav14b] by the four input variables Z_1, Z_3, Z_{40} and Z_5. These variables belong to the input (scheduling) vector:

$$\mathbf{z} = [Z_1 \quad Z_3 \quad Z_{40} \quad Z_5]^T, \tag{4.10}$$

The derivation of these dynamic T-S fuzzy models starts with the graphical calculation of the following sectors of the input variables:

$$\begin{aligned}&0.6148 \le z_1 \le 5.6851, 0.6167 \le z_3 \le 5.7135,\\ &-0.009 \le z_{40} \le -0.0084, -5.6139 \le z_5 \le -5.4132.\end{aligned} \tag{4.11}$$

Furthermore, in order to derive the T-S fuzzy model, the membership functions of input variables λ, x_2 and M_1 have to be defined. First, the domains of variation of the three state variables have to be set for all ABS operating regimes [Dav14b]:

$$0.1 \le \lambda \le 1, 20 \le x_2 \le 178, 0 \le M_1 \le 10. \tag{4.12}$$

In accordance with the first step of the T-S fuzzy modeling approach described in Sub-chapter 4.1, the first phase is represented by the fuzzification process, which is done with the aid of LTs assigned to the input variables, i.e., the scheduling variables. They are defined as: for the first input variable, λ, the following five linguistic terms with triangular membership functions are introduced: $LT_{\lambda,j}, j = 1...5$:

$$\mu_{LT_{\lambda,1}}:[0,0.2]\to[0,1],\ \mu_{LT_{\lambda,2}}:[0.1,0.4]\to[0,1],\ \mu_{LT_{\lambda,3}}:[0.2,0.8]\to[0,1],$$
$$\mu_{TL_{\lambda,4}}:[0.4,1]\to[0,1],\ \mu_{LT_{\lambda,5}}:[0.8,1.1]\to[0,1],$$
$$\mu_{LT_{\lambda,j}}(x)=\begin{cases}0, & x<a_{\lambda,j},\\ 1+\dfrac{x-b_{\lambda,j}}{b_{\lambda,j}-a_{\lambda,j}}, & x\in a_{\lambda,j}\le x<b_{\lambda,j},\\ 1-\dfrac{x-b_{\lambda,j}}{c_{\lambda,j}-b_{\lambda,j}}, & x\in b_{\lambda,j}\le x<c_{\lambda,j},\\ 0, & x\ge c_{\lambda,j},\end{cases}\qquad (4.13)$$
$$a_{\lambda,j}<b_{\lambda,j}<c_{\lambda,j},\ j=1...5,$$

where the variable vector $\boldsymbol{\rho}$ of the objective function contains the variable parameters $a_{\lambda,j},\ j=1...5$, and $c_{\lambda,j},\ j=1...5$; the parameters $b_{\lambda,j},\ j=1...5$, which represent modal values of membership functions, are fixed: $b_{\lambda,1}=0.1$, $b_{\lambda,2}=0.2$, $b_{\lambda,3}=0.4$, $b_{\lambda,4}=0.8$ and $b_{\lambda,5}=1$.

The second input variable, x_2, uses two linguistic terms $LT_{x_2,j},\ j=1...2$ with triangular shapes for the membership functions of the same type as the ones in (4.13): $\mu_{LT_{x_2,1}}:[0,150]\to[0,1]$ and $\mu_{LT_{x_2,2}}:[50,180]\to[0,1]$. As in the case of the first input variable, the variable parameters $a_{x_2,j},\ j=1...2$, and $c_{x_2,j},\ j=1...2$, belong to the variable vector $\boldsymbol{\rho}$, and the parameters $b_{x_2,j},\ j=1...2$, are fixed: $b_{x_2,1}=50$ and $b_{x_2,2}=150$.

For the remaining input variable M_1, one linguistic term, $LT_{M_1,1}$ with a triangular membership function type $\mu_{LT_{M_1,1}}:[0,11]\to[0,1]$ of same type as in (4.13), is used. Variable parameters $a_{M_1,1}$ and $c_{M_1,1}$ are included in vector $\boldsymbol{\rho}$, and the fixed parameter $b_{M_1,1}$ has the value: $b_{M_1,1}=10$.

For the second step of the modeling approach, the complete rule base of this set of dynamic T-S fuzzy models is defined as the rules $R^i,\ i=1...10$, with each resulting rule being assigned to a continuous-time state-space model (4.8) obtained for the modal values of the input membership functions and linearized at one of the ten operating points. The complete rule base of the continuous-time dynamic T-S fuzzy model is:

$$R^1:\text{IF }\lambda\text{ IS }LT_{\lambda,1}\text{ AND }x_2\text{ IS }LT_{x_2,1}\text{ AND }M_1\text{ IS }LT_{M_1,1}\text{ THEN}\begin{cases}\mathbf{x}_{k+1}=\mathbf{A}_{d,1}\mathbf{x}_k+\mathbf{B}_{d,1}u_k,\\ y_{k,m}=\mathbf{C}_{d,1}\mathbf{x}_k,\end{cases}\qquad (4.14)$$
$$...$$
$$R^{10}:\text{IF }\lambda\text{ IS }LT_{\lambda,5}\text{ AND }x_2\text{ IS }LT_{x_2,2}\text{ AND }M_1\text{ IS }LT_{M_1,1}\text{ THEN}\begin{cases}\mathbf{x}_{k+1}=\mathbf{A}_{d,10}\mathbf{x}_k+\mathbf{B}_{d,10}u_k,\\ y_{k,m}=\mathbf{C}_{d,10}\mathbf{x}_k.\end{cases}$$

The following matrices are next exemplified for the consequents of the rules R^1 and R^{10}:

$$\mathbf{A}_{d,1}=\begin{bmatrix}0.9441 & -0.0025 & 0.0194\\ -1.0335 & 1.0012 & -0.0601\\ 0 & 0 & 0.8157\end{bmatrix},\mathbf{B}_{d,1}=\begin{bmatrix}0.0021\\ -0.0059\\ 0.1843\end{bmatrix},\mathbf{C}_{d,1}=[1\quad 0\quad 0],\qquad (4.15)$$
$$\mathbf{A}_{d,10}=\begin{bmatrix}1.0041 & -0.0003 & 0.0069\\ -0.3192 & 1 & -0.0519\\ 0 & 0 & 0.8157\end{bmatrix},\mathbf{B}_{d,10}=\begin{bmatrix}0.0007\\ -0.0054\\ 0.1843\end{bmatrix},\mathbf{C}_{d,10}=[1\quad 0\quad 0].$$

The initial T-S fuzzy model in (4.14) is obtained by discretization of the continuous-time state-space models given in (4.8) accepting the zero-order hold and the sampling period set to $T_s=0.01\,\text{s}$ and by the application of the modal equivalence

principle to the rule consequent parameters from (4.15) as the coordinates of the operating points represent the modal values of the membership functions. For the inference engine the SUM and PROD operators are used and the weighted average method is employed for defuzzification.

In the third step of the modeling approach, the parameter vector of the fuzzy model is defined as:

$$\boldsymbol{\rho} = [a_{\lambda,1} \quad c_{\lambda,1} \quad a_{\lambda,2} \quad c_{\lambda,2} \quad a_{\lambda,3} \quad c_{\lambda,3} \quad a_{\lambda,4} \quad c_{\lambda,4} \quad a_{\lambda,5} \quad c_{\lambda,5} \quad a_{x_2,1} \quad c_{x_2,1} \quad a_{x_2,2} \quad c_{x_2,2} \quad a_{M_1,1} \quad c_{M_1,1}]^T. \tag{4.16}$$

The SA algorithm is applied in the last step of the modeling approach as a nature-inspired optimization algorithm employed to solve the optimization problem defined in (4.1). This algorithm, detailed in Sub-chapter 3.1, is implemented following the given description, using the following relations between the fitness function and the objective function defined in (4.2), and between the parameter vectors (the vector variables of the functions):

$$J(\boldsymbol{\rho}) = f(\boldsymbol{\psi}),\ J(\boldsymbol{\rho}) = f(\varphi),\ \boldsymbol{\rho} = \boldsymbol{\psi},\ \boldsymbol{\rho} = \varphi\ . \tag{4.17}$$

The original solution used in the initial stage of the SA algorithm [Dav14b] was:

$$\boldsymbol{\rho} = [0 \quad 0.2 \quad 0.1 \quad 0.4 \quad 0.2 \quad 0.8 \quad 0.4 \quad 1 \quad 0.8 \quad 1.1 \quad 0 \quad 150 \quad 50 \quad 180 \quad 0 \quad 11]^T \tag{4.18}$$

at the starting temperature $\theta_0 = 1$. The SA specific implementation parameters $r_{r\max}$ and of $s_{r\max}$ were set to $r_{r\max} = 100$ and $s_{r\max} = 50$.

The final solution vector:

$$\boldsymbol{\rho}^* = [0.008615 \quad 0.1614 \quad 0.09901 \quad 0.4067 \quad 0.2295 \quad 0.8471 \quad 0.4019 \quad 0.9578 \quad 0.847 \quad 1.12 \quad 0.02202 \quad 169 \quad 59.85 \quad 180.5 \quad -0.3227 \quad 11.04]^T \tag{4.19}$$

was found after 84 iterations of the algorithm at the temperature $\theta_{84} = 0.090235$.

The evolution of the control signal *u* versus time is taken from [Dav14b], and presented in Fig. 4.3.2. This control signal was generated in order to cover different ranges of magnitudes and shows 35000 input-output data points which are separated in the training data and the validation data set for cross-validation and to assess the performance of the T-S fuzzy models. The training set consists of the first $N = 10000$ data points and corresponds to 0 s to 100 s interval, with the remaining $N = 25000$ data points starting with 100 s to 350 s interval representing the validation data set.

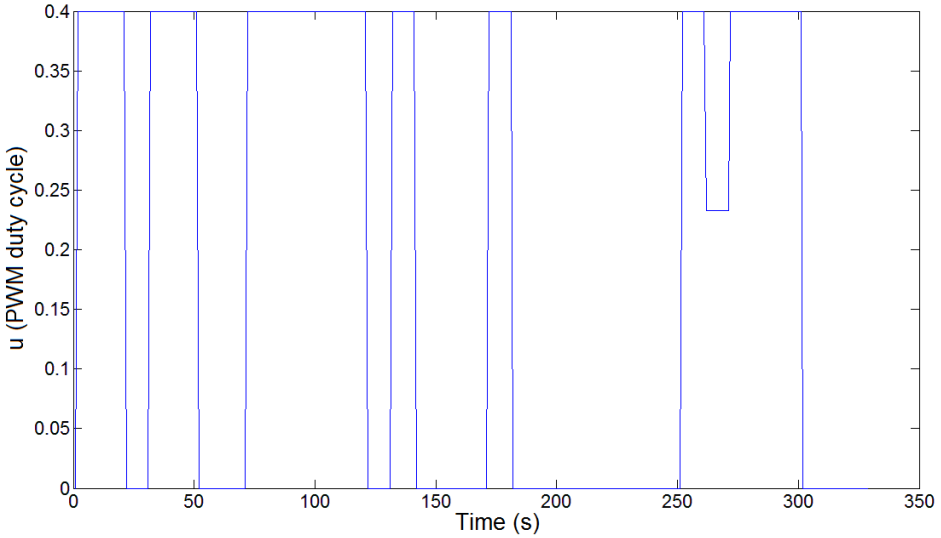

Fig. 4.3.2. Control signal *u* versus time, applied to real-world process and to T-S fuzzy model: training data from 0 s to 100 s, validation data starting with 100 s to 350 s.

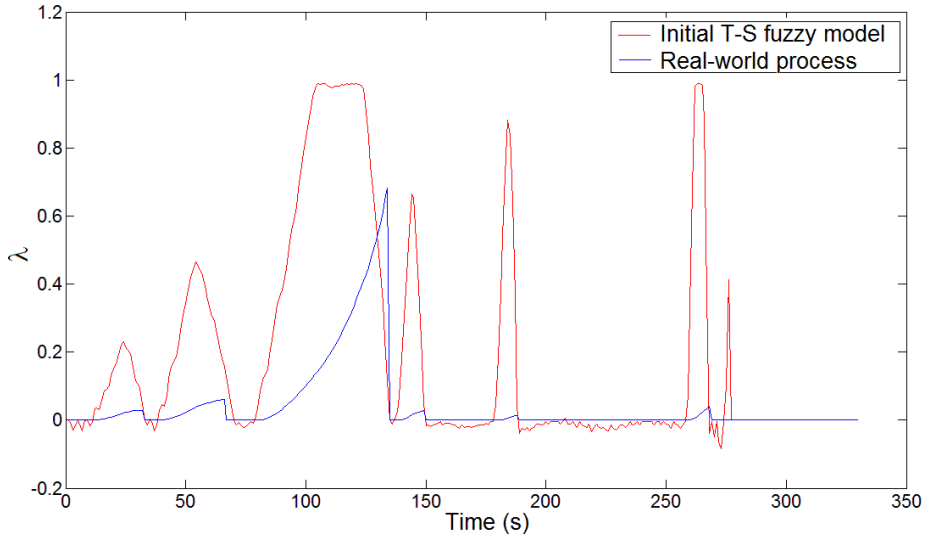

Fig. 4.3.3. Real-time experimental results: wheel slip λ versus time for initial T-S fuzzy model and for real-world process.

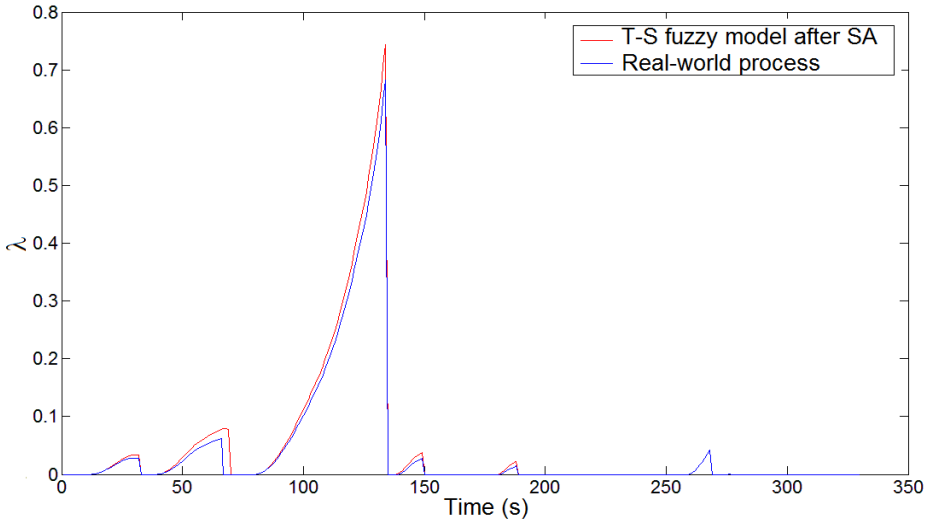

Fig. 4.3.4. Real-time experimental results: wheel slip λ versus time for T-S fuzzy model after optimization by SA algorithm and for real-world process.

The experimental results conducted in order to validate the obtained dynamic T-S fuzzy model are presented in Figs. 4.3.3 and 4.3.4 and represent the outputs of the ABS laboratory setup equipment. The graphs display the performance of the T-S fuzzy model before the application of the SA algorithm and of the T-S fuzzy model after the application of the SA algorithm. The performance improvement from the point of view the modeling errors is highlighted in Figs. 4.3.3 and 4.3.4, as it is significantly improved in training and validation data sets.

The objective function values evolution during the SA-based optimization is presented in Fig. 4.3.5. The data presented in this graphic relates to the training data set.

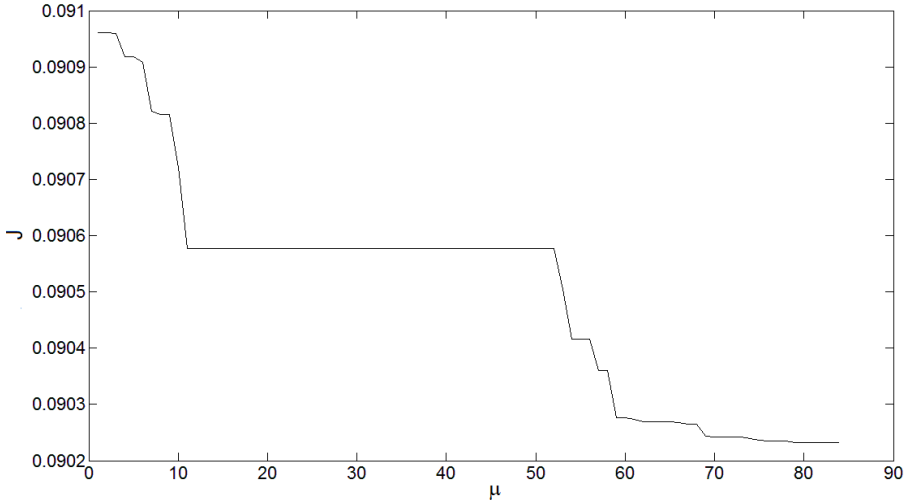

Fig. 4.3.5. Objective function J versus iteration number μ for validation data set.

4.4. SIMULATED ANNEALING-BASED OPTIMAL TUNING OF INPUT MEMBERSHIP FUNCTIONS OF TAKAGI-SUGENO FUZZY MODELS FOR A LABORATORY MAGNETIC LEVITATION SYSTEM

The application of T-S fuzzy models to the magnetic levitation problem for a metallic sphere maintained in an electromagnetic field resembling the block diagram presented in Fig. 4.4.1 is considered in this sub-chapter. The importance of precise model development for the magnetic levitation system consists in their extensibility to other systems with high performance [Dra11b], [Dra13]. For these types of magnetic levitation systems, the use of fuzzy models is justified by their process specific nonlinearity.

Additionally, the use of SA algorithm is introduced in the step 4 of the fuzzy modeling approach given in Sub-chapter 4.1. The application of the four steps of the fuzzy modeling approach is described as follows.

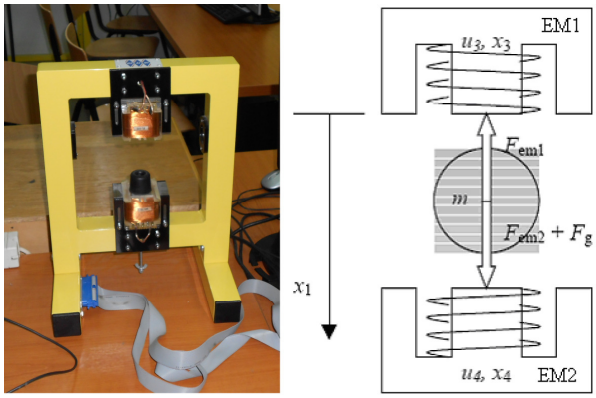

Fig. 4.4.1 INTECO magnetic levitation system with two electromagnets setup and block diagram.

The fuzzy modeling approach for the magnetic levitation problem starts with the first-principle state-space model of a magnetic levitation system with two electromagnets [Int08]:

$$\begin{aligned}
\dot{x}_1 &= x_2,\\
\dot{x}_2 &= -\frac{1}{m}\cdot\frac{F_{emP1}}{F_{emP2}}\cdot e^{-\frac{x_1}{F_{emP1}}}\cdot x_3^2 + g + \frac{1}{m}\cdot\frac{F_{emP1}}{F_{emP2}}\cdot e^{-\frac{x_d - x_1}{F_{emP2}}}\cdot x_4^2,\\
\dot{x}_3 &= \frac{1}{\frac{f_{iP1}}{f_{iP2}}\cdot e^{-\frac{x_1}{f_{iP2}}}}(k_i u_1 + c_i - x_3),\\
\dot{x}_4 &= \frac{1}{\frac{f_{iP1}}{f_{iP2}}\cdot e^{-\frac{x_d - x_1}{f_{iP2}}}}(k_i u_2 + c_i - x_4),\\
y &= x_1,
\end{aligned} \tag{4.20}$$

where: $u = u_1$ is the control signal (voltage applied to the upper electromagnet), the disturbance input is $d = u_2$ (voltage applied to the lower electromagnet), $0.0049 \le u_1, u_2 \le 1$, x_i are state variables: x_1 - sphere position, $0 \le x_1 \le 0.016m$; x_2 - sphere speed, x_3 and x_4 are currents in the upper and lower electromagnetic coil $0.038A \le x_3, x_4 \le 2.38A$, and y is the controlled output. The numerical values corresponding to these parameters are taken from [Int08] and given in Table 4.4.1.

Table 4.4.1. Numerical values of the parameters of the magnetic levitation system with two electromagnets [Int08].

Parameter	Numerical Value	Unit
m	0.0571 (for the big sphere)	[kg]
g	9.81	[m/s^2]
F_{em1}, F_{em2}	Functions of x_1 and x_3	[N]
F_{emP1}	$1.7521 \cdot 10^{-2}$	[H]
F_{emP2}	$5.8231 \cdot 10^{-3}$	[m]
$f_i(x_1)$	Function of x_1	[1/s]
f_{iP1}	$1.4142 \cdot 10^{-4}$	[m·s]
f_{iP2}	$4.5626 \cdot 10^{-3}$	[m]
c_i	0.0243	[A]
k_i	2.5165	[A]
x_d	The distance between electromagnets without the sphere diameter (depends on the sphere)	[m]
i_{MIN}	0.03884	[A]
u_{MIN}	0.00498	[V]

Two input variables, i.e., scheduling variables are considered for the T-S fuzzy model. The input variables are the first two state variables in (4.20), namely x_1 and x_2.

The fourth-order model (4.20) is next reduced to a third-order state-space model, for $u_2 = 0$:

$$\begin{cases} \dot{\mathbf{x}} = \mathbf{A}\,\mathbf{x} + \mathbf{B}\,\Delta u \\ y = \mathbf{C}^T\,\mathbf{x} \end{cases}, \quad \mathbf{x} = \begin{bmatrix} \Delta x_1 \\ \Delta x_2 \\ \Delta x_3 \end{bmatrix}, \quad \mathbf{A} = \begin{bmatrix} 0 & 1 & 0 \\ a_{21} & 0 & a_{23} \\ a_{31} & 0 & a_{33} \end{bmatrix}, \mathbf{B} = \begin{bmatrix} 0 \\ 0 \\ b_3 \end{bmatrix}, \quad \mathbf{c}^T = \begin{bmatrix} 1 & 0 & 0 \end{bmatrix}, \tag{4.21}$$

where the elements of the matrices $\mathbf{A}$ and $\mathbf{B}$ are [Dav12c]:

$$
\begin{aligned}
&a_{11}=0,\ a_{12}=1,\ a_{13}=0,\ a_{14}=0,\\
&a_{21}=\frac{x_{30}^2}{m}\frac{F_{emP1}}{F_{emP2}^2}e^{-\frac{x_{10}}{F_{emP2}}}+\frac{x_{40}^2}{m}\frac{F_{emP1}}{F_{emP2}^2}e^{-\frac{x_d-x_{10}}{F_{emP2}}},\ a_{22}=0,\\
&a_{23}=-\frac{2x_{30}}{m}\frac{F_{emP1}}{F_{emP2}}e^{-\frac{x_{10}}{F_{emP2}}},\ a_{24}=\frac{2x_{40}}{m}\frac{F_{emP1}}{F_{emP2}}e^{-\frac{x_d-x_{10}}{F_{emP2}}},\\
&a_{31}=\frac{f_{iP2}}{f_{iP1}}\cdot e^{\frac{x_{10}}{f_{iP2}}}\cdot(k_iu_1+c_i-x_{30}),\ a_{32}=0,\ a_{33}=-\frac{1}{f_{iP1}}\cdot e^{\frac{x_{10}}{f_{iP2}}},a_{34}=0,\\
&a_{41}=-\frac{1}{f_{iP1}}\cdot e^{\frac{x_d-x_{10}}{F_{emP2}}}\cdot(k_iu_2+c_i-x_{40}),\\
&a_{42}=0\ ,a_{43}=0,\ a_{44}=-\frac{f_{iP2}}{f_{iP1}}\cdot e^{\frac{x_d-x_{10}}{F_{emP2}}}\\
&b_{11}=0,\ b_{21}=0,\ b_{31}=k_i\cdot\frac{f_{iP2}}{f_{iP1}}\cdot e^{\frac{x_{10}}{f_{iP2}}},\ b_{41}=k_i\cdot\frac{f_{iP2}}{f_{iP1}}\cdot e^{\frac{x_d-x_{10}}{F_{emP2}}}.
\end{aligned}
\tag{4.22}
$$

In order to stabilize the sphere from the magnetic levitation system, a state feedback control structure is designed by the pole placement method to stabilize the unstable linearized state-space model in (4.21) with the state feedback gain matrix:

$$\mathbf{k}_c^T=[36\quad 5\quad 0.0075]\,. \tag{4.23}$$

This leads to the following closed-loop third order continuous-time state-space linearized model:

$$\begin{cases}\dot{\mathbf{x}}=\mathbf{A}\,\mathbf{x}+\mathbf{B}\,r_x\\ y=\mathbf{C}^T\mathbf{x}\end{cases},\ \mathbf{x}=\left[\Delta x_1\quad \Delta x_2\quad \Delta x_3\right]^T\,. \tag{4.24}$$

The input of the stabilized process represents the input of the stabilized process *u* from (4.20) extended with the state feedback matrix gain in (4.30), which is the same as the reference input of the control system.

The first step of the methodology presented in Sub-chapter 4.1 starts with the fuzzification phase, by setting the largest domains of variation for the two state variables in all operating regimes:

$$-0.2\le x_1\le 0.2,-8.757\le x_3\le 18.765\,. \tag{4.25}$$

Also, for fuzzification, linguistic terms assigned to the input variables are employed and defined as: the input variable x_1 has three linguistic terms, $LT_{x_1,j}$, $j=1...3$, with triangular m.f.s. They are defined and referred to as $LT_{x_1,1}$, with the universe of discourse $\left[-0.2\quad 0\right]$, $LT_{x_1,2}$, with the universe of discourse $\left[-0.1\quad 0.1\right]$, and $LT_{x_1,3}$, with the universe of discourse $\left[0\quad 0.2\right]$. These triangular m.f.s can be expressed as:

$$
\begin{aligned}
&\mu_{LT_{x_1,j}}(x_1)=\begin{cases}0, & x_1<a_{x_1,j},\\ 1+\dfrac{x_1-b_{x_1,j}}{b_{x_1,j}-a_{x_1,j}}, & x_1\in[a_{x_1,j},b_{x_1,j}),\\ 1-\dfrac{x_1-b_{x_1,j}}{c_{x_1,j}-b_{x_1,j}}, & x_1\in[b_{x_1,j},c_{x_1,j}),\\ 0, & x_1\ge c_{x_1,j}.\end{cases}\\
&a_{x1,j}<b_{x1,j}<c_{x1,j},\ j=1...3,
\end{aligned}
\tag{4.26}
$$

where the initial modal values of the m.f.s are the parameters $a_{x1,j}$, $b_{x1,j}$, and $c_{x1,j}$, $j=1...3$. The parameters $a_{x1,j},\ j=1...3$, and $c_{x1,j},\ j=1...3$, which indicate the modal values of the m.f.s, are fixed, with the values given in Table 4.4.2 [Dav12c]. The parameters $b_{x1,j},\ j=1...3$ are variable.

Table 4.4.2. Modal values of the linguistic terms.

Linguistic terms $LT_{x_1,j},\ j=1...3$	Triangular membership functions		
	$a_{x1,j}$	$b_{x1,j}$	$c_{x1,j}$
$TL_{x_1,1}$	-0.2	-0.1	0
$TL_{x_1,2}$	-0.1	0	0.1
$TL_{x_1,3}$	0	0.1	0.2

For the second input variable x_3, are defined three linguistic terms, $LT_{x_3,j},\ j=1...3$, with the first and third being modeled by trapezoidal membership functions, and the second one modeled by a Gaussian membership function. The universes of discourse of the membership functions of these linguistic terms are: $[-8.757 \quad 4.3785]$ for $LT_{x_3,1}$, $[3.753 \quad 4.3785]$ for $LT_{x_3,2}$, and $[4.3785 \quad 18.765]$ for $LT_{x_3,3}$. The expressions of the trapezoidal membership functions are:

$$\mu_{LT_{x_3,j}}(x)=\begin{cases}0, & x<a_{x3,j},\\ 1+\dfrac{x-b_{x3,j}}{b_{x3,j}-a_{x3,j}}, & x\in[a_{x3,j},b_{x3,j}),\\ 1, & x\in[b_{x3,j},c_{x3,j}),\\ 1-\dfrac{x-c_{x3,j}}{d_{x3,j}-c_{x3,j}}, & x\in[c_{x3,j},d_{x3,j}),\\ 0, & x\geq d_{x3,j},\end{cases} \tag{4.27}$$

$$a_{x3,j}<b_{x3,j}\leq c_{x3,j}<d_{x3,j},\ j\in\{1,3\},$$

and the second linguistic term is modeled by the Gaussian membership function:

$$\mu_{LT_{x_3,2}}(x_3)=\exp[-\frac{(x_3-a_{x3,2})^2}{2b_{x3,2}^2}]. \tag{4.28}$$

The parameters $a_{x3,2}$, $b_{x3,3}$ and $c_{x3,1}$ are variable. The parameters $a_{x3,j},\ j\in\{1,3\}$, $b_{x3,j},\ j\in\{1,3\}$, $b_{x3,2}$, $c_{x3,j},\ j\in\{1,3\}$, and $d_{x3,j},\ j\in\{1,3\}$, are fixed. The initial m.f.s of the fuzzy sets that correspond to the linguistic terms of the input variables x_1 and x_3 are given in Table 4.4.3 [Dav12c].

Table 4.4.3. Parameters of trapezoidal linguistic terms.

Linguistic terms, $LT_{x_3,j},\ j=\{1,3\}$	Trapezoidal membership functions			
	$a_{x3,j},\ j=\{1,3\}$	$b_{x3,j},\ j=\{1,3\}$	$c_{x3,j},\ j=\{1,3\}$	$d_{x3,j},\ j=\{1,3\}$
$TL_{x_3,1}$	-8.757	-8.757	-1.251	4.3785
$TL_{x_3,3}$	4.3785	11.259	18.765	18.765

Table 4.4.4. Operating points coordinates.

Co-ordi-nates	Operating points								
	A_1	A_2	A_3	A_4	A_5	A_6	A_7	A_8	A_9
x_{10}	0.007	0.007	0.008	0.008	0.009	0.009	0.007	0.008	0.009
x_{20}	0	0	0	0	0	0	0	0	0
x_{30}	0.285	0.6	0.3	0.6	0.3	0.285	0.3	0.285	0.6
x_{40}	0	0	0	0	0	0	0	0	0

The nine operating points $A_j(x_{10},x_{20},x_{30},x_{40}),\ j=1...9$, have the coordinates contained by Table 4.4.4.

The linearization of the nonlinear models (4.21) at these operating points is carried out in the step 2 of the fuzzy modeling approach. This results in nine continuous-time state-space models as described by Table 4.4.5.

Table 4.4.5. Numerical values of continuous-time state-space models.

Operating point	Continuous-time state-space models corresponding to operating point $A_j(x_{10},x_{20},x_{30},x_{40}),\ j=1...9$
A_1	$\mathbf{A}_1=\begin{bmatrix}0 & 1 & 0\\ 220.92 & 0 & -9.03\\ 15548 & 0 & -149.62\end{bmatrix};\mathbf{B}_1=\begin{bmatrix}0\\ 0\\ 376.53\end{bmatrix};\mathbf{c}_1^T=[1\quad 0\quad 0]$
A_2	$\mathbf{A}_2=\begin{bmatrix}0 & 1 & 0\\ 979.15 & 0 & -19.01\\ 5218.1 & 0 & -149.62\end{bmatrix};\mathbf{B}_2=\begin{bmatrix}0\\ 0\\ 376.53\end{bmatrix};\mathbf{c}_2^T=[1\quad 0\quad 0]$

A_3	$\mathbf{A}_3=\begin{bmatrix}0 & 1 & 0\\ 206.16 & 0 & -8\\ 18746 & 0 & -186.29\end{bmatrix};\mathbf{B}_3=\begin{bmatrix}0\\ 0\\ 468.80\end{bmatrix};\mathbf{c}_3^T=[1\quad 0\quad 0]$
A_4	$\mathbf{A}_4=\begin{bmatrix}0 & 1 & 0\\ 824.64 & 0 & -16.00\\ 6496.7 & 0 & -186.29\end{bmatrix};\mathbf{B}_4=\begin{bmatrix}0\\ 0\\ 468.80\end{bmatrix};\mathbf{c}_4^T=[1\quad 0\quad 0]$
A_5	$\mathbf{A}_5=\begin{bmatrix}0 & 1 & 0\\ 173.63 & 0 & -6.74\\ 23339 & 0 & -231.94\end{bmatrix};\mathbf{B}_5=\begin{bmatrix}0\\ 0\\ 583.67\end{bmatrix};\mathbf{c}_5^T=[1\quad 0\quad 0]$
A_6	$\mathbf{A}_6=\begin{bmatrix}0 & 1 & 0\\ 156.70 & 0 & -6.40\\ 24102 & 0 & -231.94\end{bmatrix};\mathbf{B}_6=\begin{bmatrix}0\\ 0\\ 583.67\end{bmatrix};\mathbf{c}_6^T=[1\quad 0\quad 0]$
A_7	$\mathbf{A}_7=\begin{bmatrix}0 & 1 & 0\\ 244.79 & 0 & -9.50\\ 15056 & 0 & -149.62\end{bmatrix};\mathbf{B}_7=\begin{bmatrix}0\\ 0\\ 376.53\end{bmatrix};\mathbf{c}_7^T=[1\quad 0\quad 0]$
A_8	$\mathbf{A}_8=\begin{bmatrix}0 & 1 & 0\\ 186.06 & 0 & -7.60\\ 19358 & 0 & -186.29\end{bmatrix};\mathbf{B}_8=\begin{bmatrix}0\\ 0\\ 468.80\end{bmatrix};\mathbf{c}_8^T=[1\quad 0\quad 0]$
A_9	$\mathbf{A}_9=\begin{bmatrix}0 & 1 & 0\\ 694.52 & 0 & -13.48\\ 8088.7 & 0 & -231.94\end{bmatrix};\mathbf{B}_9=\begin{bmatrix}0\\ 0\\ 583.67\end{bmatrix};\mathbf{c}_9^T=[1\quad 0\quad 0]$

These continuous-time state-space models are discretized using the sampling period $T_s=0.005\,\mathrm{s}$. The discrete-time state-space models are comprised in Table 4.4.6.

Table 4.4.6. Numerical values of discrete-time state-space models.

Operating point	Discrete-time state-space models corresponding to operating point $A_j(x_{10},x_{20},x_{30},x_{40})$, $j=1...9$

A_1	$\mathbf{A}_{d,1}=\begin{bmatrix}1 & 0.005 & -0.00009\\ -0.2833 & 1 & -0.03179\\ 54.75 & 0.1538 & 0.4712\end{bmatrix};\mathbf{B}_{d,1}=\begin{bmatrix}-0.00006\\ -0.03362\\ 1.325\end{bmatrix};\mathbf{C}_{d,1}=[1\quad 0\quad 0]$
A_2	$\mathbf{A}_{d,2}=\begin{bmatrix}1.011 & 0.005 & -0.00019\\ 3.931 & 1.011 & -0.0672\\ 18.45 & 0.0517 & 0.4718\end{bmatrix};\mathbf{B}_{d,2}=\begin{bmatrix}-0.00013\\ -0.07091\\ 1.325\end{bmatrix};\mathbf{C}_{d,2}=[1\quad 0\quad 0]$
A_3	$\mathbf{A}_{d,3}=\begin{bmatrix}1 & 0.005 & -0.00008\\ -0.3761 & 1 & -0.02604\\ 60.99 & 0.1758 & 0.392\end{bmatrix};\mathbf{B}_{d,3}=\begin{bmatrix}-0.00006\\ -0.03519\\ 1.524\end{bmatrix};\mathbf{C}_{d,3}=[1\quad 0\quad 0]$
A_4	$\mathbf{A}_{d,4}=\begin{bmatrix}1.009 & 0.005 & -0.00015\\ 3.159 & 1.009 & -0.05226\\ 21.21 & 0.061 & 0.3926\end{bmatrix};\mathbf{B}_{d,4}=\begin{bmatrix}-0.00012\\ -0.07049\\ 1.524\end{bmatrix};\mathbf{C}_{d,4}=[1\quad 0\quad 0]$
A_5	$\mathbf{A}_{d,5}=\begin{bmatrix}0.9997 & 0.005 & -0.00006\\ -0.5159 & 0.9997 & -0.01995\\ 69.07 & 2.053 & 0.3117\end{bmatrix};\mathbf{B}_{d,5}=\begin{bmatrix}-0.00006\\ -0.03462\\ 1.726\end{bmatrix};\mathbf{C}_{d,5}=[1\quad 0\quad 0]$
A_6	$\mathbf{A}_{d,6}=\begin{bmatrix}0.9995 & 0.005 & -0.00006\\ -0.5743 & 0.9995 & -0.01895\\ 71.33 & 0.2121 & 0.3117\end{bmatrix};\mathbf{B}_{d,6}=\begin{bmatrix}-0.00006\\ -0.03288\\ 1.726\end{bmatrix};\mathbf{C}_{d,6}=[1\quad 0\quad 0]$
A_7	$\mathbf{A}_{d,7}=\begin{bmatrix}1.001 & 0.005 & -0.00009\\ -0.1908 & 1.001 & -0.03347\\ 53.03 & 0.1489 & 0.4712\end{bmatrix};\mathbf{B}_{d,7}=\begin{bmatrix}-0.00006\\ -0.03539\\ 1.325\end{bmatrix};\mathbf{C}_{d,7}=[1\quad 0\quad 0]$
A_8	$\mathbf{A}_{d,8}=\begin{bmatrix}0.9999 & 0.005 & -0.00007\\ -0.4499 & 0.9999 & -0.02474\\ 62.98 & 0.1816 & 0.392\end{bmatrix};\mathbf{B}_{d,8}=\begin{bmatrix}-0.00006\\ -0.03343\\ 1.524\end{bmatrix};\mathbf{C}_{d,8}=[1\quad 0\quad 0]$
A_9	$\mathbf{A}_{d,9}=\begin{bmatrix}1.007 & 0.005 & -0.00012\\ 2.52 & 1.007 & -0.04002\\ 24.01 & 0.071 & 0.3123\end{bmatrix};\mathbf{B}_{d,9}=\begin{bmatrix}-0.00013\\ -0.06932\\ 1.726\end{bmatrix};\mathbf{C}_{d,9}=[1\quad 0\quad 0]$

The rule base of the discrete-time dynamic T-S fuzzy model is expressed on the basis of the modal equivalence principle [Gal95] that guarantees the equivalence between the fuzzy models and the set of discrete-time nonlinear state-space ones for the modal values of the inputs. Consequently, the complete rule base of the discrete-time dynamic T-S fuzzy model with the input m.f.s previously described, consists of the rules $R^i, i=1...9$:

$$\begin{aligned} &R^1: \text{IF } x_{1,k} \text{ IS } LT_{x_1,1} \text{ AND } x_{3,k} \text{ IS } LT_{x_3,1} \text{ THEN} \begin{cases} \mathbf{x}_{k+1} = \mathbf{A}_{d,1}\mathbf{x}_k + \mathbf{B}_{d,1}u_k \\ y_{k,m} = \mathbf{C}_{d,1}\mathbf{x}_k \end{cases}, \\ &\ldots \\ &R^9: \text{IF } x_{1,k} \text{ IS } LT_{x_1,3} \text{ AND } x_{3,k} \text{ IS } LT_{x_3,3} \text{ THEN} \begin{cases} \mathbf{x}_{k+1} = \mathbf{A}_{d,9}\mathbf{x}_k + \mathbf{B}_{d,9}u_k \\ y_{k,m} = \mathbf{C}_{d,9}\mathbf{x}_k \end{cases}, \end{aligned} \tag{4.29}$$

where *k* is the index of the current sampling interval, *i* is the index of the current rule, and *j* is the index of the current linguistic term.

For example, the matrices of the state-space models in the rule consequents of R^1 and R^9 are:

$$\begin{aligned} &\mathbf{A}_{d,1} = \begin{bmatrix} 0.9982 & 0.0047 & -0.00009 \\ -1.482 & 0.8350 & -0.02977 \\ 99.96 & 6.488 & 0.3488 \end{bmatrix}, \mathbf{B}_{d,1} = \begin{bmatrix} -0.00006 \\ -0.03263 \\ 1.24 \end{bmatrix}, \mathbf{C}_{d,1} = [1 \quad 0 \quad 0], \\ &\mathbf{A}_{d,9} = \begin{bmatrix} 1.002 & 0.0044 & -0.00011 \\ -0.1642 & 0.679 & -0.03415 \\ 90.37 & 7.633 & 0.09682 \end{bmatrix}, \mathbf{B}_{d,9} = \begin{bmatrix} -0.00012 \\ -0.06461 \\ 1.472 \end{bmatrix}, \mathbf{C}_{d,9} = [1 \quad 0 \quad 0]. \end{aligned} \tag{4.30}$$

The SUM and PROD operators are used in the inference engine, and the weighted average method is employed for defuzzification.

The SA algorithm is employed in the step 4 of the fuzzy modeling approach given in Sub-chapter 4.1 to solve the optimization problem defined in (4.1). For this, the SA algorithm presented in detail in Sub-chapter 3.1 is implemented following the steps presented there and by following relations between the fitness and objective functions and parameter vector as they are contained in the third step of our T-S fuzzy modeling approach:

$$J(\boldsymbol{\rho}) = f(\boldsymbol{\psi}),\ J(\boldsymbol{\rho}) = f(\varphi),\ \boldsymbol{\rho} = \boldsymbol{\psi},\ \boldsymbol{\rho} = \varphi\ . \tag{4.31}$$

The SA algorithm starts with a parameter vector $\boldsymbol{\rho}$ of the fuzzy model [Dav12c]:

$$\boldsymbol{\rho} = [-0.1 \quad 0 \quad 0.1 \quad -1.251 \quad 4.3785 \quad 11.26]^T \tag{4.32}$$

at the initial temperature $\theta_0 = 1$ and using maximum rejection and success rates of $r_{r\max} = 1000$ and $s_{r\max} = 50$, it finds the final solution vector $\boldsymbol{\rho}^*$ after 176 iterations at a temperature of $\theta_{176} = 9.82741 \cdot 10^{-9}$:

$$\boldsymbol{\rho}^* = [-0.0751 \quad 0.0001 \quad 0.0104 \quad -1.1094 \quad 5.9424 \quad 14.3821]^T\ . \tag{4.33}$$

Several experiments were conducted in order to validate this T-S fuzzy model and the fuzzy modeling approach. First the T-S fuzzy model was trained, as described in [Dra11b], [Dra13] using the control signal u that was generated such that to cover different ranges of magnitudes as high amplitude and high frequency (HAHF) signal presented in Fig. 4.4.1.

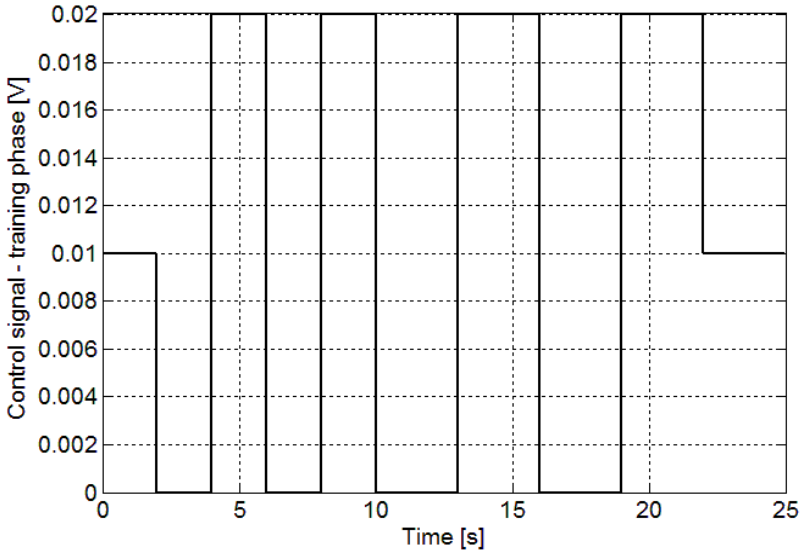

Fig. 4.4.1. Control signal *u* as HAHF signal versus time, applied to real-world process and to T-S fuzzy model in the training experiment.

The validation of the T-S fuzzy model was performed using the control signal *u,* that was generated to cover different ranges of magnitudes in two cases corresponding to two validation experiments, the low amplitude and low frequency (LALF) signal presented in Fig. 4.4.2, and the low amplitude, low frequency, high amplitude and high frequency (LALFHAHF) signal presented in Fig. 4.4.3.

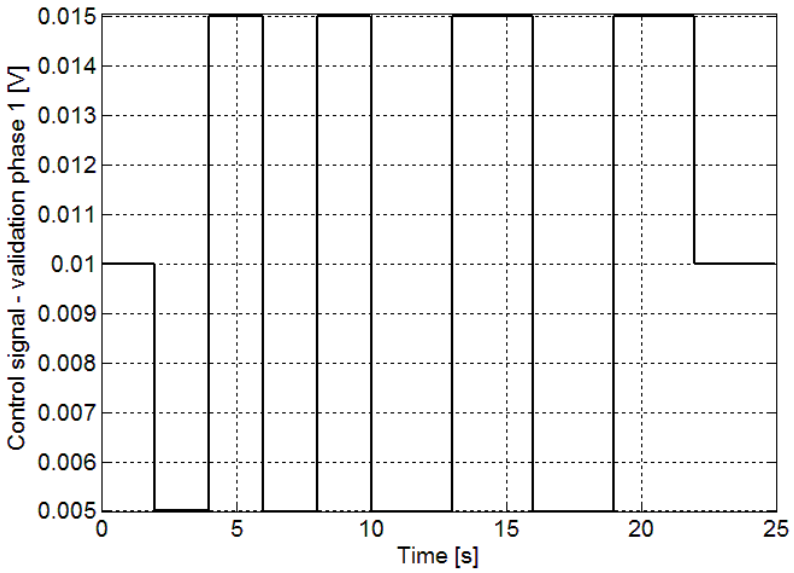

Fig. 4.4.2. Control signal *u* as LALF signal versus time, applied to real-world process and to T-S fuzzy model in the first validation experiment.

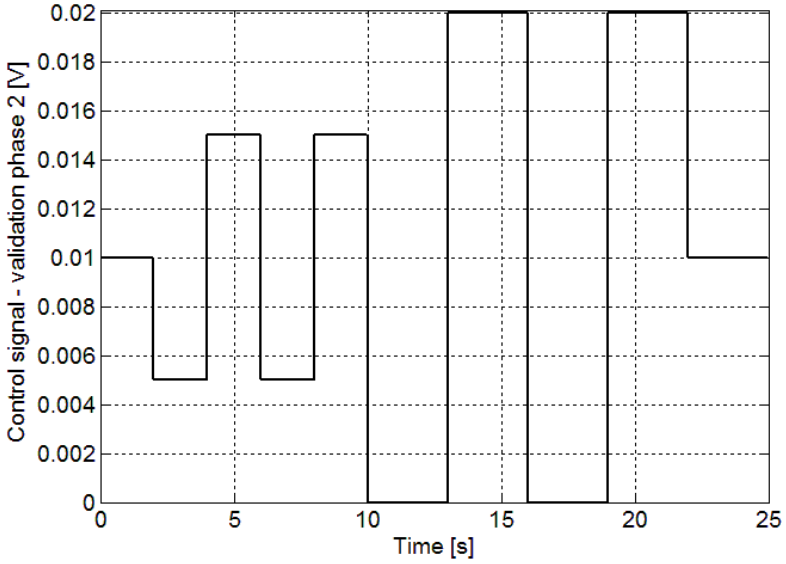

Fig. 4.4.3. Control signal *u* as LALFHAHF signal versus time, applied to real-world process and to T-S fuzzy model in the second validation experiment.

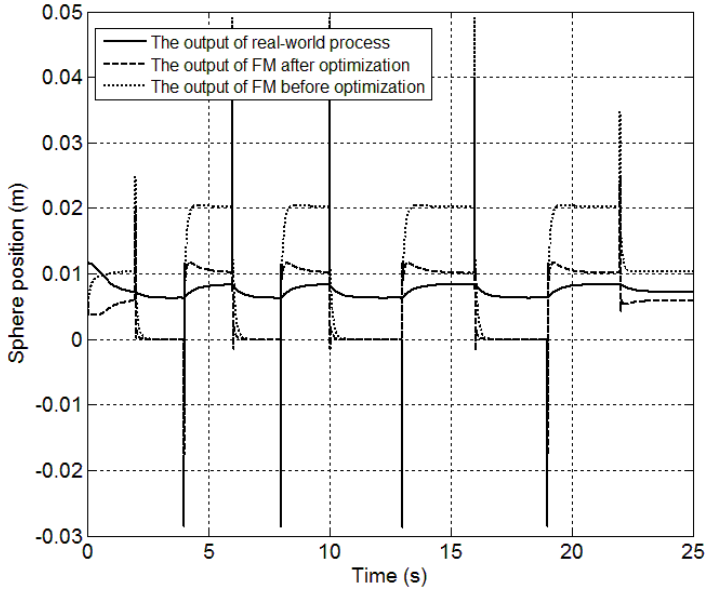

Fig. 4.4.4. Real-time experimental results for training data: output versus time for real-world process (solid), for initial T-S fuzzy model (dotted) and for optimized T-S fuzzy model (dashed). FM indicates fuzzy model.

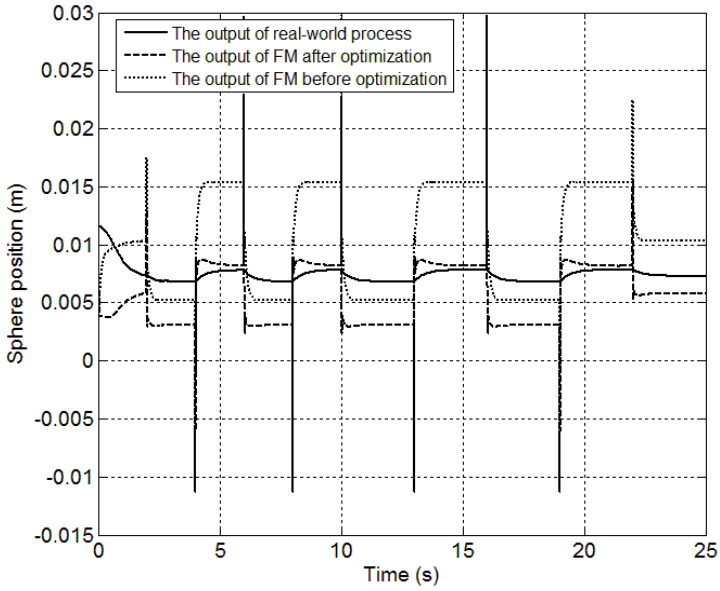

Fig. 4.4.5. Real-time experimental results for first validation data: output versus time for real-world process (solid), for initial T-S fuzzy model (dotted) and for optimized T-S fuzzy model (dashed). FM indicates fuzzy model.

The experimental results reported in [Dra11b] are presented in Fig. 4.4.4, Fig. 4.4.5 and Fig. 4.4.6 as follows:

- Fig. 4.4.4 illustrates the system response obtained for the training data set (Fig. 4.4.1).
- Fig. 4.4.5 and Fig. 4.4.6 illustrate the system response obtained for the two validation data sets (Fig. 2 and Fig. 3).
- The objective function versus the iteration index in SA algorithm is shown in Fig. 4.4.7.

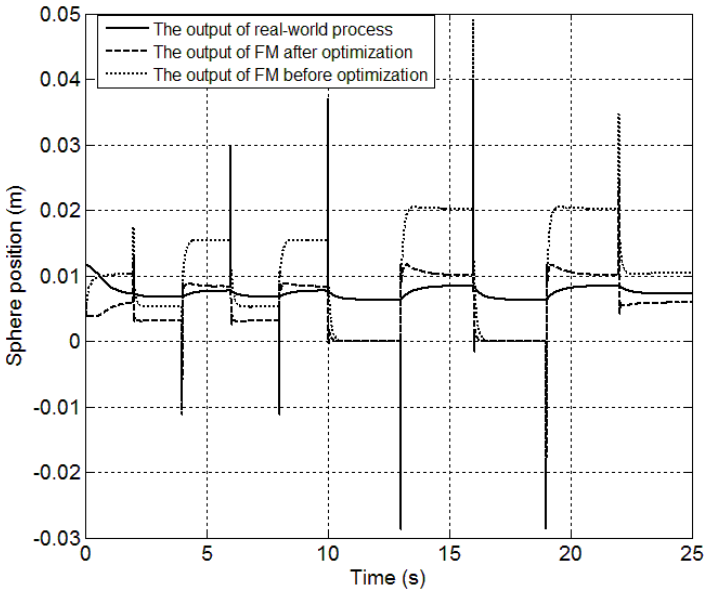

Fig. 4.4.6. Real-time experimental results for second validation data: output versus time for real-world process (solid), for initial T-S fuzzy model (dotted) and for optimized T-S fuzzy model (dashed). FM indicates fuzzy model.

Figs. 4.4.4 - 4.4.6 demonstrate the strong performance improvement of the T-S fuzzy model by the application of the SA algorithm from the point of view of the alleviation of the modeling errors. Starting the two validation experiments with the objective function $J = 0.00055$, the objective function measured after the application of the SA algorithm for the LALF control signal is $J_{LALF} = 0.000203$, and the objective function measured after the application of the SA algorithm for the LALFHAHF control signal is $J_{LALFHAHF} = 0.001197$.

The evolution of the objective function versus the iteration index illustrated in Fig. 4.4.7 shows that the solution to the optimization problem (4.1) obtained by the SA algorithm ensures a strong decrease of the objective function. Although the minimum of the objective function cannot be guaranteed, Fig. 4.4.7 suggests that the improvement can continue by considering a larger number of iterations.

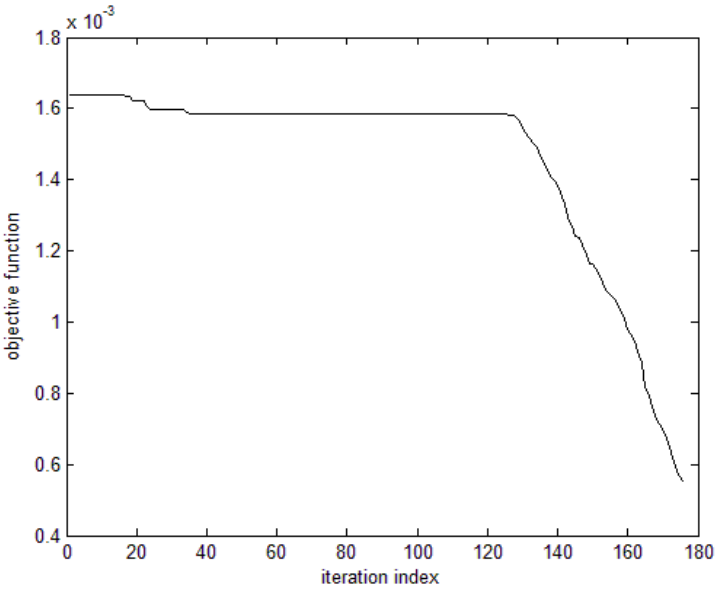

Fig. 4.4.7. Evolution of the objective function versus the iteration index in the SA algorithm.

4.5. CHAPTER CONCLUSIONS

This sub-chapter is dedicated to briefly summarize the information presented up to here during this chapter, together with the new contributions which are later supported by a list of disseminated publications.

In the course of this chapter an optimization problem concerning the input membership functions of T-S fuzzy models has been initially described in Sub-chapter 4.1. In Sub-chapter 4.2 a bibliographic research for optimal tuning of input membership functions of T-S fuzzy models was presented.

A novel method to obtain discrete-time T-S fuzzy models dedicated to ABSs has been introduced in Sub-chapter 4.3. The models are based on SA-based optimization of T-S fuzzy models initially obtained by the modal equivalence principle. One of the advantages of the proposed solution is the ease of implementation for the obtained models, which can be further adapted to other categories of industrial applications. The drawbacks of this method are restricted to the arbitrary behavior introduced by the SA algorithm.

In Sub-chapter 4.4 an approach to the fuzzy modeling of magnetic levitation systems is offered. This approach is based on the implementation of SA algorithms to optimize the parameters of T-S fuzzy models initially obtained in terms of the modal equivalence principle. A new T-S fuzzy model of a magnetic levitation system with two electromagnets laboratory equipment is offered. The new modeling approach is important because it is applicable with adequate but not complicated generalizations to a wide category of industrial applications. Similar other T-S fuzzy models can be obtained in order to be further used in the T-S fuzzy controller design and tuning.

The new **contributions** of this chapter are summarized as follows.

1. A modeling approach that ensures the optimal tuning of a part of the parameters of the input membership functions of T-S fuzzy models is presented in Sub-chapter 4.1. The approach is based on the definition of an optimization problem, which is solved using nature-inspired optimization algorithms.

2. An original approach to fuzzy modeling of Anti-lock Braking Systems using Simulated Annealing optimized variable parameters of input membership functions is proposed in:

***R.-C. David**, R.-B. Grad, R.-E. Precup, M.-B. Rădac, C.-A. Dragoş and E. M. Petriu, An approach to fuzzy modeling of anti-lock braking systems, in: Soft Computing in Industrial Applications, V. Snasel, P. Kromer, M. Koppen and G. Schaefer, Eds., Advances in Intelligent Systems and Computing, Springer International Publishing, Berlin, Heidelberg, vol. 223, pp. 83-93, 2014, indexed in Springer Link.*

3. An original approach to fuzzy modeling of magnetic levitation systems using Simulated Annealing optimized variable parameters of input membership functions is described in:

*C.-A. Dragoş, R.-E. Precup, **R.-C. David**, S. Preitl, A.-I. Stînean and E. M. Petriu, Simulated annealing-based optimization of fuzzy models for magnetic levitation systems, Proceedings of 2013 Joint IFSA World Congress and NAFIPS Annual Meeting IFSA/NAFIPS 2013, Edmonton, AB, Canada, pp. 286-291, 2013, indexed in Thomson Reuters Web of Science (formerly ISI Web of Knowledge or ISI Proceedings).*

***R.-C. David**, C.-A. Dragoş, R.-G. Bulzan, R.-E. Precup, E. M. Petriu and M.-B. Rădac, An approach to fuzzy modeling of magnetic levitation systems, International Journal of Artificial Intelligence, vol. 9, no. A12, pp. 1-18, 2012, indexed in SCOPUS.*

4. New discrete-time T-S fuzzy models for Anti-lock Braking Systems and for magnetic levitation systems, derived on the basis of the modal equivalence principle with rule consequents containing the state-space models of the local state feedback control system structures are proposed as initial fuzzy models, to be next optimized, in:

*R.-E. Precup, S. V. Spătaru, M.-B. Rădac, E. M. Petriu, S. Preitl, C.-A. Dragoş, **R.-C. David**, Experimental results of model-based fuzzy control solutions for a laboratory antilock braking system, in: Human-Computer Systems Interaction: Backgrounds and Applications 2, Part 2, Z. S. Hippe, J. L. Kulikowski and T. Mroczek, Eds., Advances in Intelligent and Soft Computing, vol. 99, Springer-Verlag, Berlin, Heidelberg, pp. 223-234, 2012, indexed in Thomson Reuters Web of Science (formerly ISI Web of Knowledge or ISI Proceedings).*

These contributions have the following advantages:

1) They give solutions with relatively reduced degree of complexity.
2) They have potential for generalization to a wide category of applications.
3) The performance improvement of the T-S fuzzy models is demonstrated by experimental results using laboratory equipment.

5. NEW CONTRIBUTIONS, FUTURE RESEARCH DIRECTIONS AND DISSEMINATION OF RESULTS

5.1. NEW CONTRIBUTIONS

The research direction of this thesis has been focused on the development of feasible solutions dedicated to the modeling and optimization of fuzzy control systems with reduced sensitivity. The rationale of this research is synthesized in the following concepts:

- Optimization of T-S PI-FCs through minimization of various objective functions;
- Computationally efficient control solutions by avoiding high complexity degree derivative calculations;
- Reduced implementations costs for the proposed solutions;
- Demonstration of control solutions' potential in various experimental test environments;
- Extensibility potential to other optimization problems.

The new contributions presented in the course of this thesis, also pointed out in chapters 2, 3, and 4, can be summarized as:

- New discrete-time state-space models of T-S PI-FCs characterized by the manipulation of the dynamics elements in the structure of these controllers such that to define two state variables;
- New discrete-time state sensitivity models of fuzzy control systems with respect to two parameters of the controlled process represented by a class of nonlinear servo systems. The fuzzy control systems include T-S PI-FCs, and the class of nonlinear servo systems is structured as a series connection of second-order dynamics with an integral component, and saturation and dead zone static nonlinearity placed on the process input;
- A novel design method dedicated to the simple T-S PI-FCs for servo systems with a reduced parametric sensitivity, namely with a reduced process gain sensitivity and with a reduced process small time constant sensitivity. The design method ensures the parameter tuning of the fuzzy controllers by solving four types of optimization problems using nature-inspired optimization algorithms;
- The original application of Simulated Annealing algorithms to solve four types of optimization problems such that to carry out the optimal tuning of the parameters of T-S PI-FCs dedicated to the control of a class of nonlinear servo systems;
- The original application of Particle Swarm Optimization algorithms to solve four types of optimization problems such that to carry out the op-

timal tuning of the parameters of T-S PI-FCs dedicated to the control of a class of nonlinear servo systems;

- The original application of Gravitational Search Algorithms to solve four types of optimization problems such that to carry out the optimal tuning of the parameters of T-S PI-FCs dedicated to the control of a class of nonlinear servo systems;
- The original application of a version of hybrid Particle Swarm Optimization-Gravitational Search Algorithms to solve four types of optimization problems such that to carry out the optimal tuning of the parameters of T-S PI-FCs dedicated to the control of a class of nonlinear servo systems;
- The original application of Charged System Search algorithms to solve four types of optimization problems such that to carry out the optimal tuning of the parameters of T-S PI-FCs dedicated to the control of a class of nonlinear servo systems;
- A novel class of adaptive GSAs with improved exploration and exploitations capabilities inspired by the 5E learning model used in education. The adaptive GSAs are developed around the basic version of GSA, and their three new functions are:
    - the adaptation of two depreciation laws of the gravitational constant to the iteration index,
    - the adaptation of a parameter in the weighted sum of all forces exerted from the other agents to the iteration index,
    - the resetting at each run of adaptive GSA agents' worst fitness's and positions to their best values;
- The original application of the new adaptive GSAs to solve four types of optimization problems such that to carry out the optimal tuning of the parameters of T-S PI-FCs dedicated to the control of a class of nonlinear servo systems;
- A novel class of adaptive CSS algorithms with improved exploration and exploitations capabilities inspired by the 5E learning model used in education. The adaptive CSS algorithms are developed around the basic version of CSS algorithms, and their two new functions are:
    - the adaptation of the acceleration, velocity, and separation distance parameters to the iteration index,
    - the substitution of the worst charged particles' fitness function values and positions with the best performing particle data;
- The original application of the new adaptive CSS algorithms to solve four types of optimization problems such that to carry out the optimal tuning of the parameters of T-S PI-FCs dedicated to the control of a class of nonlinear servo systems;
- The definition of three original performance indices to assess the quality of nature-inspired optimization algorithms:
    - the average value of each objective function,
    - the convergence speed,
    - the accuracy rate;
- The quality assessment of the performance of nature-inspired optimization algorithms based on three original performance indices considering a certain number of runs (five in these thesis) of each nature-inspired optimization algorithm;

- The validation of all new results by simulations using the detailed fuzzy control system models and by experiments conducted on the real-world laboratory servo system. Simulation results are presented in all publications;
- A modeling approach that ensures the optimal tuning of a part of the parameters of the input membership functions of T-S fuzzy models, based on the definition of an optimization problem, which is solved using nature-inspired optimization algorithms;
- An original approach to fuzzy modeling of Anti-lock Braking Systems using Simulated Annealing optimized variable parameters of input membership functions;
- An original approach to fuzzy modeling of magnetic levitation systems using Simulated Annealing optimized variable parameters of input membership functions;
- New discrete-time T-S fuzzy models for Anti-lock Braking Systems, derived on the basis of the modal equivalence principle with rule consequents containing the state-space models of the local state feedback control system structures are proposed as initial fuzzy models, to be next optimized.

5.2. FUTURE RESEARCH DIRECTIONS

Starting with the new contributions presented in the previous sub-chapter, the research contained in this thesis, can be extended in the following future research directions:

- Extending the presented solutions to other sensitivity-based optimization problems in the time domain and frequency domain;
- Fuzzy modeling of nonlinear dynamic processes by the parametric optimization using new nature-inspired algorithms;
- Extending the fuzzy controller tuning approach by including stability conditions;
- Introducing and extending fuzzy logic in the tuning of nature-inspired algorithms in order to limit the degrees of freedom represented by the free parameters;
- Developing new solutions based on algorithm hybridization for alleviating the drawbacks encountered in standard versions;
- Use of the proposed modeling approach in various industrial applications.
- Extension of the modeling approach to the optimal tuning of the parameters of the fuzzy models included in other modules of the fuzzy model structure (rule base, inference engine and/or defuzzification module).

5.3. DISSEMINATION OF RESULTS

The new contributions resulted from the research work presented in this thesis are included in the following publications list:

1. *R.-E. Precup,* ***R.-C. David****, E. M. Petriu, S. Preitl, M.-B. Rădac, Fuzzy control systems with reduced parametric sensitivity based on simulated annealing, IEEE Transactions on Industrial Electronics, vol. 59, no. 8, pp. 3049-3061, 2012, impact factor (IF) = 5.165, IF according to 2013 Journal Citation Reports (JCR) released by Thomson Reuters in 2014 =* ***6.500****.*

Cited in:

1. M. A. Hosen, A. Khosravi, S. Nahavandi, D. Creighton, Improving the Quality of Prediction Intervals through Optimal Aggregation, IEEE Transactions on Industrial Electronics, DOI: 10.1109/TIE.2014.2383994, 2014, impact factor (IF) = 6.500, IF according to 2013 Journal Citation Reports (JCR) released by Thomson Reuters in 2014 = **6.500**.
2. A. Saleem, B. Taha, T. Tutunji, A. Al-Qaisi, Identification and cascade control of servo-pneumatic system using Particle Swarm Optimization, Simulation Modelling Practice and Theory, vol. 52, pp. 164-179, 2015, impact factor (IF) = 1.050, IF according to 2013 Journal Citation Reports (JCR) released by Thomson Reuters in 2014 = **1.050**.
3. S. I. Han, J. M. Lee, Fuzzy Echo State Neural Networks and Funnel Dynamic Surface Control for Prescribed Performance of a Nonlinear Dynamic System, IEEE Transactions on Industrial Electronics, vol. 61, no. 2, pp. 1099-1112, 2014, impact factor (IF) = 6.500, IF according to 2013 Journal Citation Reports (JCR) released by Thomson Reuters in 2014 = **6.500**.
4. A. G.Yepes, A. Vidal, O. Lopez, J. Doval-Gandoy, Evaluation of Techniques for Cross-Coupling Decoupling Between Orthogonal Axes in Double Synchronous Reference Frame Current Control, IEEE Transactions on Industrial Electronics, vol. 61, no. 2, pp. 1099-1112, 2014, impact factor (IF) = 6.500, IF according to 2013 Journal Citation Reports (JCR) released by Thomson Reuters in 2014 = **6.500**.
5. S. Blazic, On Periodic Control Laws for Mobile Robots, IEEE Transactions on Industrial Electronics, vol. 61, no. 7, pp. 3660-3670, 2014, impact factor (IF) = 6.500, IF according to 2013 Journal Citation Reports (JCR) released by Thomson Reuters in 2014 = **6.500**.
6. J. M. Ojeda, J. M. Fuertes, E. Grisful, Holistic indices for productivity control assessment, applied to the comparative analysis of PID and fuzzy controllers within an Isasmelt furnace, IEEE Transactions on Industrial Informatics, vol. 10, no. 1, pp. 92-98, 2014, impact factor (IF) = 8.785, IF according to 2013 Journal Citation Reports (JCR) released by Thomson Reuters in 2014 = **8.785**.
7. H. Huang, Y. Jin, B. Huang, H.-G. Qiu, Mixed Replenishment Policy for ATO Supply Chain Based on Hybrid Genetic Simulated Annealing Al-

gorithm, Mathematical Problems in Engineering, article number 574827, 2014, impact factor (IF) = 1.082, IF according to 2013 Journal Citation Reports (JCR) released by Thomson Reuters in 2014 = **1.082**.

8. J.-C. Hung, Multichannel Time-Delay and Signal Model Estimation with Missing Observations, Circuits, Systems, and Signal Processing, vol. 33, no. 1, pp. 257-274, 2014, impact factor (IF) = 1.264, IF according to 2013 Journal Citation Reports (JCR) released by Thomson Reuters in 2014 = **1.264**.
9. D. Cai, Z. Zhuo, J. Wang, J. Wu, J. Tang, Distribution of thermo seeds in magnetic induction therapy based on the simulated annealing algorithm, Qinghua Daxue Xuebao/Journal of Tsinghua University, vol. 54, no. 2, pp. 153-158, 2014, indexed in **SCOPUS**.
10. B. Xing, W.-J. Gao, Gravitational Search Algorithm, Chapter 22 in Innovative Computational Intelligence: A Rough Guide to 134 Clever Algorithms, Intelligent Systems Reference Library, vol. 62, Springer International Publishing, Cham, Heidelberg, New York, Dordrecht, London, pp. 355-364, 2014, indexed in **Springer Link**.
11. F. Salem, E. H. E. Bayoumi, Robust Fuzzy-PID control of three-motor drive system using Simulated Annealing Optimization, Journal of Electrical Engineering, Vol. 13, Issue 3, 2013, pp. 284-292, indexed in **SCOPUS**.
12. X.-H. Yan, G.-B. Cai, B. Ning, W. Shangguan, Research on multi-objective high-speed train operation optimization based on differential evolution, Tiedao Xuebao/Journal of the China Railway Society, vol. 35, no. 9, pp. 65-71, 2013, indexed in **SCOPUS**.
13. A. Biswas, K. K. Mishra, S. Tiwari, A. K. Misra, Physics-Inspired Optimization Algorithms: A Survey, Journal of Optimization, vol. 2013, article ID 438152, 16 pp., 2013.
14. B. Yue, Z. Peng, Q. Zhang, A New Grouping Simulated Annealing Algorithm, International Journal of Digital Content Technology and its Applications, vol. 7, no. 8, pp. 218-228, 2013.
15. L. F. C. Figueredo, F. B. Cavalcanti, J. Y. Ishihara, G. A. Borges, Novel stabilization technique for the H_∞ control of systems with time-varying input delay, Proceedings of 2013 American Control Conference ACC 2013, Washington, DC (USA), pp. 1739-1744, 2013, indexed in **Thomson Reuters Web of Science** (formerly ISI Web of Knowledge or **ISI Proceedings**).
16. S. Chang, Y. Wang, X. Wei, Optimal soft lunar landing based on differential evolution, Proceedings of 2013 IEEE International Conference on Industrial Technology ICIT 2013, Cape Town, Western Cape (South Africa), pp. 152-156, 2013, indexed in **Thomson Reuters Web of Science** (formerly ISI Web of Knowledge or **ISI Proceedings**).
17. A. G. Yepes, A. Vidal Jano Malvar, O. Lopez, J. Doval-Gandoy, F. D. Freijedo, Ineffectiveness of orthogonal axes cross-coupling decoupling technique in dual sequence current control, Proceedings of 2013 IEEE Energy Conversion Congress and Exposition ECCE 2013, Denver, CO (USA), pp. 1047-1053, 2013, indexed in **Thomson Reuters Web of Science** (formerly ISI Web of Knowledge or **ISI Proceedings**).

18. D. S. Chivilikhin, V. I. Ulyantsev, A. A. Shalyto, Solving Five Instances of the Artificial Ant Problem with Ant Colony Optimization, Proceedings of 2013 IFAC Conference on Manufacturing, Modelling, Management, and Control IFAC MIM '2013, Saint Petersburg (Russia), pp. 1077-1082, 2013, indexed in **SCOPUS**.
19. F. Yao, Z. Dong, K. Meng, Z. Xu, H. Iu and K. Wong, Quantum-Inspired Particle Swarm Optimization for Power System Operations Considering Wind Power Uncertainty and Carbon Tax in Australia, IEEE Transactions on Industrial Informatics, vol. 8, no. 4, pp. 880-888, 2012, impact factor (IF) = 3.381, IF according to 2013 Journal Citation Reports (JCR) released by Thomson Reuters in 2014 = **8.785**.
20. Y. J. Liu, Y. D. Xie, H. Wang, Fuzzy PID Control for Valve-Controlled Cylinder Hydraulic System, Applied Mechanics and Materials, vol. 212-213, pp. 1244-1248, 2012, indexed in **Thomson Reuters Web of Science** (formerly ISI Web of Knowledge or **ISI Proceedings**).
21. P. C. Shill, Md. F. Amin, M. A. H. Akhand, K. Murase, Optimization of interval type-2 fuzzy logic controller using quantum genetic algorithms, Proceedings of 2012 IEEE International Conference on Fuzzy Systems FUZZ-IEEE 2012, Brisbane (Australia), 8 pp., 2012, indexed in **Thomson Reuters Web of Science** (formerly ISI Web of Knowledge or **ISI Proceedings**).
22. L.-O. Fedorovici, A comparison between two character recognition approaches, Facta Universitatis Series Automatic Control and Robotics, vol. 10, no. 2, pp. 125-140, 2011.

2. *R.-E. Precup,* ***R.-C. David****, E. M. Petriu, M.-B. Rădac, S. Preitl, J. Fodor, Evolutionary optimization-based tuning of low-cost fuzzy controllers for servo systems, Knowledge-Based Systems (Elsevier Science), vol. 38, pp. 74-84, 2013, impact factor (IF) = 3.058, IF according to 2013 Journal Citation Reports (JCR) released by Thomson Reuters in 2014 =* ***3.058****.*

Cited in:

1. P. Gil, C. Lucena, A. Cardoso, L. Palma, Gains Tuning of Fuzzy PID Controllers for MIMO Systems: A Performance-Driven Approach, IEEE Transactions on Fuzzy Systems, DOI: 10.1109/10.1109/TFUZZ.2014.2327990, 2014, impact factor (IF) = 6.306, IF according to 2013 Journal Citation Reports (JCR) released by Thomson Reuters in 2014 = **6.306**.
2. M. Tarkeshwar, V. Mukherjee, Quasi-oppositional harmony search algorithm and fuzzy logic controller for load frequency stabilisation of an isolated hybrid power system, IET Generation, Transmission & Distribution, 2015, impact factor (IF) = 1.307, IF according to 2013 Journal Citation Reports (JCR) released by Thomson Reuters in 2014 = **1.307**.
3. P. Baranyi, TP model transformation as a manipulation tool for qLPV analysis and design, Asian Journal of Control, vol. 17, no. 2, pp. 1-11, 2015, impact factor (IF) = 0.000, IF according to 2013 Journal Citation Reports (JCR) released by Thomson Reuters in 2014 = **0.000**.

4. A. Banerjee, V. Mukherjee, S. P. Ghoshal, Intelligent fuzzy-based reactive power compensation of an isolated hybrid power system, International Journal of Electrical Power & Energy Systems, vol. 57, pp. 164-177, 2014, impact factor (IF) = 0.000, IF according to 2013 Journal Citation Reports (JCR) released by Thomson Reuters in 2014 = **0.000**.
5. B. Shaw, V. Mukherjee, S. P. Ghoshal, Solution of reactive power dispatch of power systems by an opposition-based gravitational search algorithm, International Journal of Electrical Power & Energy Systems, vol. 55, pp. 29-40, 2014, impact factor (IF) = 0.000, IF according to 2013 Journal Citation Reports (JCR) released by Thomson Reuters in 2014 = **0.000**.
6. J. Sun, Q. Zhang, X. Yao, Meta-Heuristic Combining Prior Online and Offline Information for the Quadratic Assignment Problem, IEEE Transactions on Cybernetics, vol. 44, no. 3, pp. 429-444, 2014, impact factor (IF) = 0.000, IF according to 2013 Journal Citation Reports (JCR) released by Thomson Reuters in 2014 = **0.000**.
7. J.C. Cortes-Rios, E. Gomez-Ramirez, H.A. Ortiz-de-la-Vega, O. Castillo, P. Melin, Optimal design of interval type 2 fuzzy controllers based on a simple tuning algorithm, Applied Soft Computing, vol. 23, pp. 270-285, 2014, impact factor (IF) = 2.679, IF according to 2013 Journal Citation Reports (JCR) released by Thomson Reuters in 2014 = **2.679**.
8. T. Nakashima-Paniagua, J. Doucette, W. Moussa, Fabrication Process Suitability Ranking for Micro-Electro-Mechanical Systems Using a Fuzzy Inference System, Expert Systems with Applications, vol. 41, no. 9, pp. 4123-4138, 2014, impact factor (IF) = 1.965, IF according to 2013 Journal Citation Reports (JCR) released by Thomson Reuters in 2014 = **1.965**.
9. C. Li, J. Zhou, Semi-supervised weighted kernel clustering based on gravitational search for fault diagnosis, ISA Transactions, DOI: 10.1016/j.isatra.2014.05.019, 2014, impact factor (IF) = 2.256, IF according to 2013 Journal Citation Reports (JCR) released by Thomson Reuters in 2014 = **2.256**.
10. T. Chenaina, A. Alraddadi, Identifying Fuzzy Controllers Parameters by Fuzzy Clustering Technique, Journal of Universal Computer Science, vol. 20, no. 2, pp. 107-134, 2014, impact factor (IF) = 0.401, IF according to 2013 Journal Citation Reports (JCR) released by Thomson Reuters in 2014 = **0.401**.
11. A. Kulanthaisamy, R. Vairamani, N. K. Karunamurthi, C. Koodalsamy, A Multi-objective PMU Placement Method Considering Observability and Measurement Redundancy using ABC Algorithm, Advances in Electrical and Computer Engineering, vol. 14, no. 2, pp. 117-128, 2014, impact factor (IF) = 0.642, IF according to 2013 Journal Citation Reports (JCR) released by Thomson Reuters in 2014 = **0.642**.
12. K. Kampouropoulos, F. Andrade, A. Garcia, L Romeral, A Combined Methodology of Adaptive Neuro-Fuzzy Inference System and Genetic Algorithm for Short-term Energy Forecasting, Advances in Electrical and Computer Engineering, vol. 14, no. 1, pp. 9-14, 2014, impact

factor (IF) = 0.642, IF according to 2013 Journal Citation Reports (JCR) released by Thomson Reuters in 2014 = **0.642**.

13. I. Kecskes, P. Odry, Optimization of PI and Fuzzy-PI Controllers on Simulation Model of Szabad(ka)-II Walking Robot, International Journal of Advanced Robotic Systems, vol. 11, DOI: 10.5772/59102, 13 pp., 2014, impact factor (IF) = 0.497, IF according to 2013 Journal Citation Reports (JCR) released by Thomson Reuters in 2014 = **0.497**.
14. S. K. Tharun, B. J. Pandian, Tuning and Implementation of Fuzzy Logic Controller using Simulated Annealing in a Non-linear Real-time System, Proceedings of 2014 International Conference on Circuit, Power and Computing Technologies ICCPCT 2014, Nagercoil (India), pp. 916-921, 2014.
15. I. Kecskes, E. Burkus, P. Odry, Swarm-Based Optimizations in Hexapod Robot Walking, Proceedings of 9th IEEE International Symposium on Applied Computational Intelligence and Informatics SACI 2014, Timisoara (Romania), pp. 123-127, 2014, indexed in **Thomson Reuters Web of Science** (formerly ISI Web of Knowledge or **ISI Proceedings**).
16. T. N. T. Ibrahim, T. Marapan, S. H. Hasim, A. F. Z. Abidin, N. Omar, N. A. Nordin, H. I. Jaafar, K. Osman, Z. A. Ghani and S. F. M. Hussein, A Brief Analysis of Gravitational Search Algorithm (GSA) Publication from 2009 to May 2013, Proceedings of International Conference Recent treads in Engineering & Technology ICRET'2014, Batam (Indonesia), 9 pp., 2014.
17. B. Xing, W.-J. Gao, Gravitational Search Algorithm, Chapter 22 in the book Innovative Computational Intelligence: A Rough Guide to 134 Clever Algorithms, authored by B. Xing and W.-J. Gao, Intelligent Systems Reference Library, vol. 62, Springer International Publishing, Cham, Heidelberg, New York, Dordrecht, London, pp. 355-364, 2014, indexed in **Springer Link**.
18. C.-H. Hsu, C.-F. Juang, Multi-Objective Continuous-Ant-Colony-Optimized FC for Robot Wall-Following Control, IEEE Computational Intelligence Magazine, vol. 8, no. 3, pp. 28-40, 2013, impact factor (IF) = 2.706, IF according to 2013 Journal Citation Reports (JCR) released by Thomson Reuters in 2014 = **2.706**.
19. P. Husek and O. Cerman, Fuzzy model reference control with adaptation of input fuzzy sets, Knowledge-Based Systems, vol. 49, pp. 116-122, 2013, impact factor (IF) = 3.058, IF according to 2013 Journal Citation Reports (JCR) released by Thomson Reuters in 2014 = **3.058**.
20. M.-F. Han, C.-T. Lin and J.-Y. Chang, Differential Evolution with Local Information for Neuro-Fuzzy Systems Optimisation, Knowledge-Based Systems, vol. 44, pp. 78-89, 2013, impact factor (IF) = 3.058, IF according to 2013 Journal Citation Reports (JCR) released by Thomson Reuters in 2014 = **3.058**.
21. S. Szenasi, Genetic algorithm for parameter optimization of image segmentation algorithm, Proceedings of IEEE 14th International Symposium on Computational Intelligence and Informatics CINTI 2013, Budapest (Hungary), pp. 351-354, 2013, indexed in **Thom-**

son Reuters Web of Science (formerly ISI Web of Knowledge or **ISI Proceedings**).

22. E. Toth-Laufer, M. Takacs and Z. Keresztenyi, Current physical status evaluation subsystem using user-specific tuned membership functions in sport activity risk calculation, Proceedings of 2013 IEEE 9th International Conference on Computational Cybernetics ICCC 2013, Tihany (Hungary), pp. 185-190, 2013, indexed in **Thomson Reuters Web of Science** (formerly ISI Web of Knowledge or **ISI Proceedings**).
23. P. C. Shill, Md. F. Amin, M. A. H. Akhand and K. Murase, Optimization of interval type-2 fuzzy logic controller using quantum genetic algorithms, Proceedings of 2012 IEEE International Conference on Fuzzy Systems FUZZ-IEEE 2012, Brisbane (Australia), 8 pp., 2012, indexed in **Thomson Reuters Web of Science** (formerly ISI Web of Knowledge or **ISI Proceedings**).
24. R. K. Sahu, S. Panda, S. Padhan, A novel hybrid gravitational search and pattern search algorithm for load frequency control of nonlinear power system, Applied Soft Computing, January 2015, impact factor (IF) = 2.679, IF according to 2013 Journal Citation Reports (JCR) released by Thomson Reuters in 2014 = **2.679**.

3. *R.-E. Precup,* ***R.-C. David****, E.M. Petriu, S. Preitl, M.-B. Rădac, Novel adaptive gravitational search algorithm for fuzzy controlled servo systems, IEEE Transactions on Industrial Informatics, vol. 8, no. 4, pp. 791-800, 2012, impact factor (IF) = 3.381, IF according to 2013 Journal Citation Reports (JCR) released by Thomson Reuters in 2014 =* ***8.785****.*

Cited in:

1. J. Pei, X. Liu, P. M. Pardalos, W. Fan, S. Yang, L. Wang, Application of an effective modified gravitational search algorithm for the coordinated scheduling problem in a two-stage supply chain, The International Journal of Advanced Manufacturing Technology, vol. 70, no. 1-4, pp. 335-348, 2014, impact factor (IF) = 1.779, IF according to 2013 Journal Citation Reports (JCR) released by Thomson Reuters in 2014 = **1.779**.
2. X. Feng, R. Zou, H. Yu, A novel optimization algorithm inspired by the creative thinking process, Soft Computing, DOI: 10.1007/s00500-014-1459-6, 2014, impact factor (IF) = 1.304, IF according to 2013 Journal Citation Reports (JCR) released by Thomson Reuters in 2014 = **1.304**.
3. S. Md Rozali, M. F. Rahmat, A. R. Husain, Performance Comparison of Particle Swarm Optimization and Gravitational Search Algorithm to the Designed of Controller for Nonlinear System, Journal of Applied Mathematics, vol. 2014, article ID 679435, 9 pp., 2014, impact factor (IF) = 0.720, IF according to 2013 Journal Citation Reports (JCR) released by Thomson Reuters in 2014 = **0.720**.
4. B. B. Lu, J. Liu, C. Wang, H. J. Xu, Q. Wang, Capacity and Power Optimization for Collaborative Beamforming with Two Relay Clusters, in: Advances in Swarm Intelligence, Y. Tan, Y. Shi and C. A. Coello Coello, Eds., Lecture Notes in Computer Science, vol. 8795, Springer International Publishing, Cham, Heidelberg, New York, Dordrecht,

London, pp. 155-162, 2014, indexed in **Thomson Reuters Web of Science** (formerly ISI Web of Knowledge or **ISI Proceedings**).
5. S. Blažič, I. Škrjanc and D. Matko, A robust fuzzy adaptive law for evolving control systems, Evolving Systems, vol. 5, no. 1, pp. 3-10, 2014, indexed in **SCOPUS**.
6. J. Fiosina, M. Fiosins, Resampling based Modelling of Individual Routing Preferences in a Distributed Traffic Network, International Journal of Artificial Intelligence, vol. 12, no. 1, pp. 79-103, 2014, indexed in **SCOPUS**.
7. L. F. Castillo, M. G. Bedia, G. Isaza, J. Velez, F. Seron, Development of Believable Bots in Videogames Capable of Learning During Runtime, International Journal of Artificial Intelligence, vol. 12, no. 1, pp. 117-128, 2014, indexed in **SCOPUS**.
8. K. Panagidi, K. Kolomvatsos, S. Hadjiefthymiades, An Intelligent Scheme for Concurrent Multi-Issue Negociations, International Journal of Artificial Intelligence, vol. 12, no. 1, pp. 129-149, 2014, indexed in **SCOPUS**.
9. J. L. Guerrero, A. Berlanga, J. M. Molina, Multiobjective Local Search as an Initialization Procedure for Evolutionary Approaches to Polygonal Approximation, International Journal of Artificial Intelligence, vol. 12, no. 1, pp. 150-165, 2014, indexed in **SCOPUS**.
10. S. M. Rozali, M. F. Rahmat, A. R. Husain, M. N. Kamarudin, Design of adaptive backstepping with gravitational search algorithm for nonlinear system, Journal of Theoretical and Applied Information Technology, vol. 59, no. 2, pp. 460-468, 2014, indexed in **SCOPUS**.
11. L.-T. Huang, S.-S. Jhan, Y.-J. Li, C.-C. Wu, Solving the Permutation Problem Efficiently for Tabu Search on CUDA GPUs, in: Computational Collective Intelligence. Technologies and Applications, D. Hwang, J. J. Jung and N.-T. Nguyen, Eds., Lecture Notes in Computer Science, vol. 8733, Springer International Publishing, Cham, Heidelberg, New York, Dordrecht, London, pp. 342-352, 2014, indexed in **Springer Link**.
12. A. Bagheri, M. Saraee, Persian Sentiment Analyzer: A Framework based on a Novel Feature Selection Method, International Journal of Artificial Intelligence, vol. 12, no. 2, pp. 115-129, 2014.
13. Y. Kumar, G. Sahoo, A Review on Gravitational Search Algorithm and its Applications to Data Clustering & Classification, International Journal of Intelligent Systems and Applications, vol. 6, no. 6, pp. 79-93, 2014.
14. L. Andre, R. S. Parpinelli, Tutorial Sobre o Uso de Tecnicas para Controle Online de Parametros em Algoritmos de Inteligencia de Enxame e Computacao Evolutiva, Revista de Informatica Teorica e Aplicada, vol. 2, no. 2, pp. 90-135, 2014
15. F. Wang, P. L. H. Yu, D. W. Cheung, Combining technical trading rules using parallel particle swarm optimization based on Hadoop, Proceedings of International Joint Conference on Neural Networks IJCNN 2014, Beijing (China), pp. 3987-3994, 2014, indexed in **IEEE Xplore**, **INSPEC**, **SCOPUS**.
16. T. N. T. Ibrahim, T. Marapan, S. H. Hasim, A. F. Z. Abidin, N. Omar, N. A. Nordin, H. I. Jaafar, K. Osman, Z. A. Ghani, S. F. M. Hussein, A Brief Analysis of Gravitational Search Algorithm (GSA) Publication

from 2009 to May 2013, Proceedings of International Conference Recent treads in Engineering & Technology ICRET'2014, Batam (Indonesia), 9 pp., 2014.

17. N. M. Sabri, M. Puteh, M. R. Mahmood, A Review of Gravitational Search Algorithm, International Journal of Advances in Soft Computing and Its Application, vol. 5, no. 3, pp. 1-39, 2013, indexed in **SCOPUS**.
18. N. M. Sabri, M. Puteh, M. R. Mahmood, An overview of Gravitational Search Algorithm utilization in optimization problems, Proceedings of IEEE 3rd International Conference on System Engineering and Technology ICSET 2013, Shah Alam (Malaysia), pp. 61-66, 2013, indexed in **IEEE Xplore**, **INSPEC**, **SCOPUS**.
19. S. Gao, H. Chai, B. Chen, G. Yang, Hybrid gravitational search and clonal selection algorithm for global optimization, in: Advances in Swarm Intelligence, S. Gao, H. Chai, B. Chen and G. Yang, Eds., Lecture Notes in Computer Science, vol. 7929, Springer-Verlag, Berlin, Heidelberg, pp. 1-10, 2013, indexed in **Springer Link**, **SCOPUS**.
20. A. H. Al-Mohammed, M. A. Abido, Fuzzy Controller Design Using Evolutionary Techniques for Twin Rotor MIMO System: A Comparative Study, Computational Intelligence and Neuroscience, article ID: 704301, 2015.

4. *R.-E. Precup,* ***R.-C. David****, E. M. Petriu, S. Preitl, A. S. Paul, Gravitational search algorithm-based tuning of fuzzy control systems with a reduced parametric sensitivity, in: Soft Computing in Industrial Applications, editors: A. Gaspar-Cunha, R. Takahashi, G. Schaefer, L. Costa, Advances in Intelligent and Soft Computing, vol. 96, Springer-Verlag, Berlin, Heidelberg, pp. 141-150, 2011, indexed in* ***Thomson Reuters Web of Science*** *(formerly ISI Web of Knowledge or* ***ISI Proceedings****).*

Cited in:

1. T. Venkatesh, T. Jain, Intelligent-search technique based strategic placement of synchronized measurements for power system observability, Expert Systems with Applications, impact factor (IF) = 1.975, IF according to 2013 Journal Citation Reports (JCR) released by Thomson Reuters in 2014 = **1.975**.
2. M. Davarynejad, J. van den Berg, J. Rezaei, Evaluating center-seeking and initialization bias: The case of particle swarm and gravitational search algorithms, Information Sciences, vol. 278, pp. 802-821, 2014, impact factor (IF) = 3.893, IF according to 2013 Journal Citation Reports (JCR) released by Thomson Reuters in 2014 = **3.893**.
3. Y. Kumar, G. Sahoo, A Review on Gravitational Search Algorithm and its Applications to Data Clustering & Classification, International Journal of Intelligent Systems and Applications, vol. 6, no. 6, pp. 79-93, 2014.
4. S. K. Tharun, B. J. Pandian, Tuning and Implementation of Fuzzy Logic Controller using Simulated Annealing in a Non-linear Real-time System, Proceedings of 2014 International Conference on Circuit, Power and Computing Technologies ICCPCT 2014, Nagercoil (India), pp. 916-921, 2014.

5. T. N. T. Ibrahim, T. Marapan, S. H. Hasim, A. F. Z. Abidin, N. Omar, N. A. Nordin, H. I. Jaafar, K. Osman, Z. A. Ghani, S. F. M. Hussein, A Brief Analysis of Gravitational Search Algorithm (GSA) Publication from 2009 to May 2013, Proceedings of International Conference Recent treads in Engineering & Technology ICRET'2014, Batam (Indonesia), 9 pp., 2014.
6. M. Davarynejad, Deploying Metaheuristics for Global Optimization, doctoral thesis, Delft University of Technology (The Netherlands), supervisor: Prof. Dr. J. van den Berg, 2014.
7. J.-W. Peng, Limit-cycle analysis of dynamic fuzzy control systems, Soft Computing, vol. 17, no. 9, pp. 1553-1561, 2013, impact factor (IF) = 1.304, IF according to 2013 Journal Citation Reports (JCR) released by Thomson Reuters in 2014 = **1.304**.
8. A. Biswas, K. K. Mishra, S. Tiwari and A. K. Misra, Physics-Inspired Optimization Algorithms: A Survey, Journal of Optimization, vol. 2013, Article ID 438152, 16 pp., 2013.
9. M. Davarynejad, Z. Forghany, J. van den Berg, Mass-dispersed gravitational search algorithm for gene regulatory network model parameter identification, in: Simulated Evolution and Learning, L. T. Bui, Y. S. Ong, N. X. Hoai, H. Ishibuchi and P. N. Suganthan, Eds., Lecture Notes in Computer Science, vol. 7673, Springer-Verlag, Berlin, Heidelberg, pp. 62-72, 2012, indexed in **Springer Link**, **SCOPUS**.
10. P. C. Shill, Md. F. Amin, M. A. H. Akhand and K. Murase, Optimization of interval type-2 fuzzy logic controller using quantum genetic algorithms, Proceedings of 2012 IEEE International Conference on Fuzzy Systems FUZZ-IEEE 2012, Brisbane (Australia), 8 pp., 2012, indexed in **Thomson Reuters Web of Science** (formerly ISI Web of Knowledge or **ISI Proceedings**).

***5. R.-C. David**, R.-E. Precup, E. M. Petriu, M.-B. Rădac, S. Preitl, Gravitational search algorithm-based design of fuzzy control systems with a reduced parametric sensitivity, Information Sciences (Elsevier Science), vol. 247, pp. 154-173, 2013, impact factor (IF) = 3.893, IF according to 2013 Journal Citation Reports (JCR) released by Thomson Reuters in 2014 = **3.893**.*

Cited in:

1. S. Bouallègue, F. Toumi, J. Haggège, P. Siarry, Advanced Metaheuristics-Based Approach for Fuzzy Control Systems Tuning, in: Complex System Modelling and Control Through Intelligent Soft Computations, Q. Zhu and A. T. Azar, Eds., Studies in Fuzziness and Soft Computing, vol. 319, Springer International Publishing, Cham, Heidelberg, New York, Dordrecht, London, pp. 627-653, 2015, indexed in **Springer Link**.
2. M. Davarynejad, J. van den Berg, J. Rezaei, Evaluating center-seeking and initialization bias: The case of particle swarm and gravitational search algorithms, Information Sciences, vol. 278, pp. 802-821, 2014, impact factor (IF) = 3.893, IF according to 2013 Journal Citation Reports (JCR) released by Thomson Reuters in 2014 = **3.893**.
3. X.-H. Han, X.-M. Chang, L. Quan, X.-Y. Xiong, J.-X. Li, Z.-X. Zhang, Y. Liu, Feature subset selection by gravitational search algorithm op-

timization, Information Sciences, vol. 281, pp. 128-146, 2014, impact factor (IF) = 3.893, IF according to 2013 Journal Citation Reports (JCR) released by Thomson Reuters in 2014 = **3.893**.
4. E. S. Nicoară, N. Paraschiv, F. G. Filip, A hierarchical model for multiple range production systems, Proceedings of 19th World Congress of The International Federation of Automatic Control, Cape Town (South Africa), pp. 833-838, 2014.
5. T. N. T. Ibrahim, T. Marapan, S. H. Hasim, A. F. Z. Abidin, N. Omar, N. A. Nordin, H. I. Jaafar, K. Osman, Z. A. Ghani, S. F. M. Hussein, A Brief Analysis of Gravitational Search Algorithm (GSA) Publication from 2009 to May 2013, Proceedings of International Conference Recent treads in Engineering & Technology ICRET'2014, Batam (Indonesia), 9 pp., 2014.
6. B. Xing, W.-J. Gao, Gravitational Search Algorithm, Chapter 22 in the book Innovative Computational Intelligence: A Rough Guide to 134 Clever Algorithms, authored by B. Xing and W.-J. Gao, Intelligent Systems Reference Library, vol. 62, Springer International Publishing, Cham, Heidelberg, New York, Dordrecht, London, pp. 355-364, 2014, indexed in **Springer Link**.
7. M. Davarynejad, Deploying Metaheuristics for Global Optimization, doctoral thesis, Delft University of Technology (The Netherlands), supervisor: Prof. Dr. J. van den Berg, 2014.

6. *R.-E. Precup,* ***R.-C. David****, E. M. Petriu, St. Preitl. M.-B. Radac, Novel Adaptive Charged System Search Algorithm for Optimal Tuning of Fuzzy Controllers, Expert Systems with Applications, vol. 41, no. 4, part 1, pp. 1168-1175, 2014, impact factor (IF) = 1.965, IF according to 2013 Journal Citation Reports (JCR) released by Thomson Reuters in 2014 =* ***1.965****.*

Cited in:

1. T. Nakashima-Paniagua, J. Doucette, W. Moussa, Fabrication Process Suitability Ranking for Micro-Electro-Mechanical Systems Using a Fuzzy Inference System, Expert Systems with Applications, vol. 41, no. 9, pp. 4123-4138, 2014, impact factor (IF) = 1.965, IF according to 2013 Journal Citation Reports (JCR) released by Thomson Reuters in 2014 = **1.965**.
2. J. Jesús Rubio, Adaptive least square control in discrete time of robotic arms, Soft Computing, DOI: 10.1007/s00500-014-1300-2, 2014, impact factor (IF) = 1.304, IF according to 2013 Journal Citation Reports (JCR) released by Thomson Reuters in 2014 = **1.304**.

7. *R.-E. Precup,* ***R.-C. David****, E. M. Petriu, S. Preitl, M.-B. Rădac, Fuzzy logic-based adaptive gravitational search algorithm for optimal tuning of fuzzy controlled servo systems, IET Control Theory and Applications, vol. 7, no. 1, pp. 99-107, 2013, impact factor (IF) = 1.844, IF according to 2013 Journal Citation Reports (JCR) released by Thomson Reuters in 2014 =* ***1.844****.*

Cited in:

1. C.-H. Chiu, C.-C. Chang, Wheeled human transportation vehicle implementation using output recurrent fuzzy control strategy, IET Control Theory & Applications, vol. 8, no. 17, pp.1886-1895, 2014, im-

pact factor (IF) = 1.844, IF according to 2013 Journal Citation Reports (JCR) released by Thomson Reuters in 2013 = **1.844**.

2. L. Andre, R. S. Parpinelli, Tutorial Sobre o Uso de Tecnicas para Controle Online de Parametros em Algoritmos de Inteligencia de Enxame e Computacao Evolutiva, Revista de Informatica Teorica e Aplicada, vol. 2, no. 2, pp. 90-135, 2014.
3. X. Wang, J. Long, Q. Zhu and J. Cui, "Drag-free control for cold air thrusters based on variable universe adaptive fuzzy PID", Proceedings of 2014 IEEE International Conference on Information and Automation ICIA 2014, Hailar (China), pp. 159-163, 2014.
4. T. N. T. Ibrahim, T. Marapan, S. H. Hasim, A. F. Z. Abidin, N. Omar, N. A. Nordin, H. I. Jaafar, K. Osman, Z. A. Ghani and S. F. M. Hussein, "A Brief Analysis of Gravitational Search Algorithm (GSA) Publication from 2009 to May 2013", Proceedings of International Conference Recent treads in Engineering & Technology ICRET'2014, Batam (Indonesia), 9 pp., 2014

8. *R.-E. Precup,* ***R.-C. David****, E. M. Petriu, S. Preitl, M.-B. Rădac, Experiments in fuzzy controller tuning based on an adaptive gravitational search algorithm, Proceedings of the Romanian Academy, Series A: Mathematics, Physics, Technical Sciences, Information Science (Editura Academiei Române, Bucharest), vol. 14, no. 4, pp. 360-367, 2013, impact factor (IF) = 1.115, IF according to 2013 Journal Citation Reports (JCR) released by Thomson Reuters in 2014 =* ***1.115****.*

Cited in:

1. V. Cojocaru, V. Mardari, Fuzzy controlled system for hypothermic brain therapy, Proceedings of the Romanian Academy, Series A: Mathematics, Physics, Technical Sciences, Information Science (Editura Academiei Romane, Bucharest), vol. 15, no. 4, pp. 396-402, 2014, impact factor (IF) = 1.115, IF according to 2013 Journal Citation Reports (JCR) released by Thomson Reuters in 2014 = **1.115**.

9. *R.-E. Precup,* ***R.-C. David****, E. M. Petriu, M.-B. Rădac, S. Preitl, Adaptive GSA-Based Optimal Tuning of PI Controlled Servo Systems With Reduced Process Parametric Sensitivity, Robust Stability and Controller Robustness, IEEE Transactions on Cybernetics, vol. 44, no. 11, pp. 1997-2009, 2014, impact factor (IF) = 0.000, IF according to 2013 Journal Citation Reports (JCR) released by Thomson Reuters in 2014 =* ***0.000****.*

10. *R.-E. Precup,* ***R.-C. David****, S. Preitl, E. M. Petriu, J. K. Tar, Optimal control systems with reduced parametric sensitivity based on particle swarm optimization and simulated annealing, in: Intelligent Computational Optimization in Engineering Techniques and Applications, M. Köppen, G. Schaefer and A. Abraham, Studies in Computational Intelligence, vol. 366 (Springer-Verlag), pp. 177-207, 2011, indexed in* ***Thomson Reuters Web of Science*** *(formerly ISI Web of Knowledge or* ***ISI Proceedings****).*

Cited in:

1. F. Salem, E.H.E. Bayoumi, Robust Fuzzy-PID control of three-motor drive system using Simulated Annealing Optimization, Journal of

Electrical Engineering, Vol. 13, Issue 3, 2013, pp. 284-292, indexed in **SCOPUS**.

11. ***R.-C. David****, M.-B. Rădac, S. Preitl, J. K. Tar, Particle swarm optimization-based design of control systems with reduced sensitivity, Proceedings of 5th International Symposium on Applied Computational Intelligence and Informatics (SACI 2009), Timisoara, Romania, pp. 491-496, 2009, indexed in* ***Thomson Reuters Web of Science*** *(formerly ISI Web of Knowledge or* ***ISI Proceedings****).*

12. *C.-A. Dragoş, R.-E. Precup,* ***R.-C. David****, S. Preitl, A.-I. Stînean, E. M. Petriu, Simulated annealing-based optimization of fuzzy models for magnetic levitation systems, Proceedings of 2013 Joint IFSA World Congress and NAFIPS Annual Meeting IFSA/NAFIPS 2013, Edmonton, AB, Canada, pp. 286-291, 2013, indexed in* ***Thomson Reuters Web of Science*** *(formerly ISI Web of Knowledge or* ***ISI Proceedings****).*

13. *R.-E. Precup, S. V. Spătaru, M.-B. Rădac, E. M. Petriu, S. Preitl, C.-A. Dragoş,* ***R.-C. David****, Experimental results of model-based fuzzy control solutions for a laboratory antilock braking system, in: Human-Computer Systems Interaction: Backgrounds and Applications 2, Part 2, Z. S. Hippe, J. L. Kulikowski and T. Mroczek, Eds., Advances in Intelligent and Soft Computing, vol. 99, Springer-Verlag, Berlin, Heidelberg, pp. 223-234, 2012, indexed in* ***Thomson Reuters Web of Science*** *(formerly ISI Web of Knowledge or* ***ISI Proceedings****).*

Cited in:

1. V. Cirovic, D. Aleksendric, Adaptive neuro-fuzzy wheel slip control, Expert Systems with Applications, vol. 40, no. 13, pp. 5197-5209, 2013, impact factor (IF) = 1.965, IF according to 2013 Journal Citation Reports (JCR) released by Thomson Reuters in 2014 = **1.965**.

14. *R.-E. Precup,* ***R.-C. David****, E. M. Petriu, S. Preitl, M.-B. Rădac, Gravitational search algorithms in fuzzy control systems tuning, Proceedings of 18th IFAC World Congress, Milano, Italy, pp. 13624-13629, 2011, indexed in* ***SCOPUS****.*

Cited in:

1. S. Jiang, Y. Wanga, Z. Ji, Convergence analysis and performance of an improved gravitational search algorithm, Applied Soft Computing, Applied Soft Computing, vol. 24, pp. 363-384, 2014, impact factor (IF) = 2.679, IF according to 2013 Journal Citation Reports (JCR) released by Thomson Reuters in 2014 = **2.679**.
2. Y. Kumar, G. Sahoo, A Review on Gravitational Search Algorithm and its Applications to Data Clustering & Classification, International Journal of Intelligent Systems and Applications, vol. 6, no. 6, pp. 79-93, 2014.
3. T. N. T. Ibrahim, T. Marapan, S. H. Hasim, A. F. Z. Abidin, N. Omar, N. A. Nordin, H. I. Jaafar, K. Osman, Z. A. Ghani, S. F. M. Hussein, A Brief Analysis of Gravitational Search Algorithm (GSA) Publication from 2009 to May 2013, Proceedings of International Conference Recent treads in Engineering & Technology ICRET'2014, Batam (Indonesia), 9 pp., 2014.

4. N. M. Sabri, M. Puteh, M. R. Mahmood, An overview of Gravitational Search Algorithm utilization in optimization problems, Proceedings of IEEE 3rd International Conference on System Engineering and Technology ICSET 2013, Shah Alam (Malaysia), pp. 61-66, 2013, indexed in **IEEE Xplore**, **INSPEC**, **SCOPUS**.
5. N. M. Sabri, M. Puteh, M. R. Mahmood, A Review of Search Algorithms in Fuzzy Control Systems Tuning Search Algorithm, International Journal of Advances in Soft Computing and Its Application, vol. 5, no. 3, pp. 1-39, 2013, indexed in **SCOPUS**.
6. P. B. de Moura Oliveira, E. J. Solteiro Pires, P. Novais, Gravitational Search Algorithm Design of Posicast PID Control Systems, in: Soft Computing Models in Industrial and Environmental Applications, V. Snasel, A. Abraham and E. S. Corchado, Eds., Advances in Intelligent Systems and Computing, vol. 188, pp. 191-199, Springer-Verlag, Berlin, Heidelberg, 2013, indexed in **Thomson Reuters Web of Science** (formerly ISI Web of Knowledge or **ISI Proceedings**).
7. S. Bouallègue, F. Toumi, J. Haggège, P. Siarry, Advanced Metaheuristics-Based Approach for Fuzzy Control Systems Tuning, in: Complex System Modelling and Control Through Intelligent Soft Computations, Q. Zhu and A. T. Azar, Eds., Studies in Fuzziness and Soft Computing, vol. 319, Springer International Publishing, Cham, Heidelberg, New York, Dordrecht, London, pp. 627-653, 2015, indexed in **Springer Link**.

***15. R.-C. David**, R.-E. Precup, E. M. Petriu, C. Purcaru, S. Preitl, PSO and GSA algorithms for fuzzy controller tuning with reduced process small time constant sensitivity, Proceedings of 2012 16th International Conference on System Theory, Control and Computing (ICSTCC 2012), Sinaia, Romania, 6 pp., 2012, indexed in **IEEE Xplore**, **INSPEC**, **SCOPUS**.*

Cited in:

1. S. Jayaprakasam, S. K. A. Rahim, C. Y. Leow, PSOGSA-Explore: A New Hybrid Metaheuristic Approach for Beampattern Optimization in Collaborative Beamforming, Applied Soft Computing, 2015, impact factor (IF) = 2.679, IF according to 2013 Journal Citation Reports (JCR) released by Thomson Reuters in 2014 = **2.679**.
2. F. Valdez, P. Melin, O. Castillo, A survey on nature-inspired optimization algorithms with fuzzy logic for dynamic parameter adaptation, Expert Systems with Applications, vol. 41, no. 14, pp. 6459-6466, 2014, impact factor (IF) = 1.965, IF according to 2013 Journal Citation Reports (JCR) released by Thomson Reuters in 2014 = **1.965**.
3. T. N. T. Ibrahim, T. Marapan, S. H. Hasim, A. F. Z. Abidin, N. Omar, N. A. Nordin, H. I. Jaafar, K. Osman, Z. A. Ghani, S. F. M. Hussein, A Brief Analysis of Gravitational Search Algorithm (GSA) Publication from 2009 to May 2013, Proceedings of International Conference Recent treads in Engineering & Technology ICRET'2014, Batam (Indonesia), 9 pp., 2014.
4. N. M. Sabri, M. Puteh, M. R. Mahmood, A Review of Search Algorithms in Fuzzy Control Systems Tuning Search Algorithm, International Journal of Advances in Soft Computing and Its Application, vol. 5, no. 3, pp. 1-39, 2013.

5. N. M. Sabri, M. Puteh, M. R. Mahmood, An overview of Gravitational Search Algorithm utilization in optimization problems, Proceedings of IEEE 3rd International Conference on System Engineering and Technology ICSET 2013, Shah Alam (Malaysia), pp. 61-66, 2013, indexed in **IEEE Xplore**, **INSPEC**, **SCOPUS**.

***16. R.-C. David**, R.-E. Precup, E. M. Petriu, M.-B. Rădac, C. Purcaru, C.-A. Dragoş, S. Preitl, Adaptive gravitational search algorithm for PI-fuzzy controller tuning, Proceedings of 9th International Conference on Informatics in Control, Automation and Robotics (ICINCO 2012), Rome, Italy, vol. 1, pp. 136-141, 2012, indexed in **SCOPUS**, **DBLP**.*

Cited in:

1. T. N. T. Ibrahim, T. Marapan, S. H. Hasim, A. F. Z. Abidin, N. Omar, N. A. Nordin, H. I. Jaafar, K. Osman, Z. A. Ghani, S. F. M. Hussein, A Brief Analysis of Gravitational Search Algorithm (GSA) Publication from 2009 to May 2013, Proceedings of International Conference Recent treads in Engineering & Technology ICRET'2014, Batam (Indonesia), 9 pp., 2014.
2. N. M. Sabri, M. Puteh, M. R. Mahmood, A Review of Gravitational Search Algorithm, International Journal of Advances in Soft Computing and Its Application, vol. 5, no. 3, pp. 1-39, 2013, indexed in **SCOPUS**.

***17. R.-C. David**, R.-E. Precup, S. Preitl, J. K. Tar, J. Fodor, Parametric sensitivity reduction of PI-based control systems by means of evolutionary optimization algorithms, Proceedings of 6th IEEE International Symposium on Applied Computational Intelligence and Informatics (SACI 2011), Timisoara, Romania, pp. 241-246, 2011, indexed in **IEEE Xplore**, **INSPEC**, **SCOPUS**.*

Cited in:

1. S. Md Rozali, M. F. Rahmat, A. R. Husain, Performance Comparison of Particle Swarm Optimization and Gravitational Search Algorithm to the Designed of Controller for Nonlinear System, Journal of Applied Mathematics, vol. 2014, article ID 679435, 9 pp., 2014, impact factor (IF) = 0.720, IF according to 2013 Journal Citation Reports (JCR) released by Thomson Reuters in 2014 = **0.720**.

***18. R.-C. David**, R.-E. Precup, S. Preitl, J. K. Tar, J. Fodor, Three evolutionary optimization algorithms in PI controller tuning, in: Applied Computational Intelligence in Engineering and Information Technology, editors: R.-E. Precup, S. Kovacs, S. Preitl, E. M. Petriu, Topics in Intelligent Engineering and Informatics, vol. 1, Springer-Verlag, Berlin, Heidelberg, pp. 95-106, 2012, indexed in **Springer Link**.*

***19.** R.-E. Precup, **R.-C. David**, E. M. Petriu, S. Preitl, M.-B. Rădac, Charged System Search Algorithms for Optimal Tuning of PI Controllers, Proceedings of 1st IFAC Conference on Embedded Systems, Computational Intelligence and Telematics in Control (CESCIT 2012), pp. 115-120, 2012, indexed in **SCOPUS**.*

20. ***R.-C. David****, R.-E. Precup, E. M. Petriu, St. Preitl, M.-B. Radac, L.-O. Fedorovici, Adaptive Evolutionary Optimization Algorithms for Simple Fuzzy Controller Tuning Dedicated to Servo Systems, in: Fuzzy Modeling and Control: Theory and Applications, F. Matia, G. N. Marichal and E. Jimenez, Eds., Atlantis Computational Intelligence Systems, vol. 9, Atlantis Press and Springer International Publishing, Cham, Heidelberg, New York, Dordrecht, London, pp. 159-173, 2014, indexed in* ***Springer Link****.*

21. *R.-E. Precup,* ***R.-C. David****, S. Preitl, E. M. Petriu, Design aspects of optimal PI controllers with reduced sensitivity for a class of servo systems using PSO algorithms, Facta Universitatis Series: Automatic Control and Robotics, vol. 8, no. 1, pp. 1-12, 2009.*

Cited in:

1. A. R. Gaiduk, Control systems design with disturbance rejection based on JCF of the nonlinear plant equations, Facta Universitatis, Series Automatic Control and Robotics, vol. 11, no. 2, pp. 81-90, 2012.

22. *R.-E. Precup,* ***R.-C. David****, E. M. Petriu, S. Preitl, Optimal fuzzy controllers tuned by charged system search algorithms, 2011 Online Conference on Soft Computing in Industrial Applications (WSC 16), 10 pp., 2011.*

23. *R.-E. Precup,* ***R.-C. David,*** *A.-I. Stînean, M.-B. Rădac, E. M. Petriu, Adaptive Hybrid Particle Swarm Optimization-Gravitational Search Algorithm for Fuzzy Controller Tuning, Proceedings of 2014 IEEE International Symposium on Innovations in Intelligent Systems and Applications INISTA 2014, Alberobello, Italy, pp. 14-20, 2014, indexed in* ***Thomson Reuters Web of Science*** *(formerly ISI Web of Knowledge or* ***ISI Proceedings****).*

Cited in:

1. S. Jayaprakasam, S. K. A. Rahim, C. Y. Leow, PSOGSA-Explore: A New Hybrid Metaheuristic Approach for Beampattern Optimization in Collaborative Beamforming, Applied Soft Computing, 2015, impact factor (IF) = 2.679, IF according to 2013 Journal Citation Reports (JCR) released by Thomson Reuters in 2014 = **2.679**.

24. ***R.-C. David****, R.-B. Grad, R.-E. Precup, M.-B. Rădac, C.-A. Dragoş, E. M. Petriu, An approach to fuzzy modeling of anti-lock braking systems, in: Soft Computing in Industrial Applications, V. Snasel, P. Kromer, M. Koppen and G. Schaefer, Eds., Advances in Intelligent Systems and Computing, Springer International Publishing, Berlin, Heidelberg, vol. 223, pp. 83-93, 2014, indexed in* ***Springer Link****.*

25. ***R.-C. David****, C.-A. Dragoş, R.-G. Bulzan, R.-E. Precup, E. M. Petriu, M.-B. Rădac, An approach to fuzzy modeling of magnetic levitation systems, International Journal of Artificial Intelligence, vol. 9, no. A12, pp. 1-18, 2012, indexed in* ***SCOPUS****.*

Cited in:

1. G. Betta, D. Capriglione, M. Gasparetto, E. Zappa, C. Liguori, A. Paolillo, Managing the uncertainty for face classification with 3D fea-

tures, Proceedings of 2014 IEEE International Instrumentation and Measurement Technology Conference I2MTC 2014, Montevideo (Uruguay), pp. 412-417, 2014, *indexed in **Thomson Reuters Web of Science** (formerly ISI Web of Knowledge or **ISI Proceedings**)*.

2. E. Joelianto, D. C. Anura, M. P. Priyanto, ANFIS - Hybrid Reference Control for Improving Transient Response of Controlled Systems Using PID Controller, International Journal of Artificial Intelligence, vol. 10, no. S13, pp. 88-111, 2013, indexed in **SCOPUS**.
3. D. Antić, M. Milovanović, S. Nikolić, M. Milojković, S. Perić, Simulation Model of Magnetic Levitation Based on NARX Neural Networks, International Journal of Intelligent Systems and Applications, vol. 5, no. 5, pp. 25-32, 2013.
4. D. Antić, M. Milovanović, S. Nikolić, M. Milojković and S. Perić, Primena NARX neuronske mreze za simulaciju rada sistema magnetne levitacije, Tehnika, vol. 68, no. 3, pp. 473-479, 2013.

26. *A.-S. Paul, R.-E. Precup, C. Pozna, **R.-C. David**, nDSP: A platform for audiophile software audio processing, Proceedings of IEEE International Joint Conferences on Computational Cybernetics and Technical Informatics (ICCC-CONTI 2010), Timisoara, Romania, pp. 431-436, 2010, indexed in **IEEE Xplore**, **INSPEC**, **SCOPUS**.*

27. *C.-A. Dragoş, R.-E. Precup, E. M. Petriu, M. L. Tomescu, S. Preitl, **R.-C. David,** M.-B. Rădac, 2-DOF PI-fuzzy controllers for a magnetic levitation system, Proceedings of 8th International Conference on Informatics in Control, Automation and Robotics (ICINCO 2011), Noordwijkerhout, The Netherlands, vol. 1, pp. 111-116, 2011, indexed in **SCOPUS**, **DBLP**.*

Cited in:

1. D. Antić, M. Milovanović, S. Nikolić, M. Milojković and S. Perić, Simulation Model of Magnetic Levitation Based on NARX Neural Networks, International Journal of Intelligent Systems and Applications, vol. 5, no. 5, pp. 25-32, 2013.
2. D. Antić, M. Milovanović, S. Nikolić, M. Milojković and S. Perić, Primena NARX neuronske mreze za simulaciju rada sistema magnetne levitacije, Tehnika, vol. 68, no. 3, pp. 473-479, 2013.

28. *R.-E. Precup, E. M. Petriu, C.-A. Dragoş, **R.-C. David**, Stability analysis results concerning the fuzzy control of a class of nonlinear time-varying systems, Theory and Applications of Mathematics & Computer Science, vol. 1, no. 1, pp. 2-10, 2011.*

29. *L.-O. Fedorovici, R.-E. Precup, F. Drăgan, **R.-C. David,** C. Purcaru, Embedding gravitational search algorithms in convolutional neural networks for OCR applications, Proceedings of IEEE 7th International Symposium on Applied Computational Intelligence and Informatics (SACI 2012), Timisoara, Romania, pp. 125-130, 2012, indexed in **IEEE Xplore**, **INSPEC**, **SCOPUS**, **DBLP**.*

Cited in:

1. Y. Kumar, G. Sahoo, A Review on Gravitational Search Algorithm and its Applications to Data Clustering & Classification, International

Journal of Intelligent Systems and Applications, vol. 06, pp. 79-93, 2014.

2. A.-C. Enache, V. V. Patriciu, Intrusions detection based on Support Vector Machine optimized with swarm intelligence, Proceedings of IEEE 9th International Symposium on Applied Computational Intelligence and Informatics SACI 2014, Timisoara (Romania), pp. 153-158, 2014, *indexed in* ***Thomson Reuters Web of Science*** *(formerly ISI Web of Knowledge or* ***ISI Proceedings****)*.
3. T. N. T. Ibrahim, T. Marapan, S. H. Hasim, A. F. Z. Abidin, N. Omar, N. A. Nordin, H. I. Jaafar, K. Osman, Z. A. Ghani, S. F. M. Hussein, A Brief Analysis of Gravitational Search Algorithm (GSA) Publication from 2009 to May 2013, Proceedings of International Conference Recent treads in Engineering & Technology ICRET'2014, Batam (Indonesia), 9 pp., 2014.
4. F. R. Fulginei, A. Laudani, A. Salvini, M. Parodi, Automatic and parallel optimized learning for neural networks performing MIMO applications, Advances in Electrical and Computer Engineering, vol. 13, no. 1, pp. 3-12, 2013, IF according to 2013 Journal Citation Reports (JCR) released by Thomson Reuters in 2014 = **0.552**.
5. K. RamaKrishna, Ch. V. Kameswara Rao, R. Sambasiva Rao, E-man Part 3#: Tutorial on gravitational algorithm in structure activity relationships (SXR), Journal of Applicable Chemistry, vol. 2, no. 4, pp. 698-713, 2013.
6. N. M. Sabri, M. Puteh, M. R. Mahmood, A Review of Gravitational Search Algorithm, International Journal of Advances in Soft Computing and Its Application, vol. 5, no. 3, pp. 1-39, 2013.

30. *C. Purcaru, R.-E. Precup, D. Iercan, L.-O. Fedorovici,* ***R.-C. David****, Hybrid PSO-GSA Robot Path Planning Algorithm in Static Environments with Danger Zones, Proceedings of 2013 17th International Conference on System Theory, Control and Computing (ICSTCC 2013), Sinaia, Romania, 2013, pp. 434-439, indexed in* ***Thomson Reuters Web of Science*** *(formerly ISI Web of Knowledge or* ***ISI Proceedings****).*

Cited in:

1. S. Jayaprakasam, S. K. A. Rahim, C. Y. Leow, PSOGSA-Explore: A New Hybrid Metaheuristic Approach for Beampattern Optimization in Collaborative Beamforming, Applied Soft Computing, 2015, impact factor (IF) = 2.679, IF according to 2013 Journal Citation Reports (JCR) released by Thomson Reuters in 2014 = **2.679**.
2. B. K. Oleiwi, H. Roth, B. I. Kazem, Multi objective optimization of path and trajectory planning for non-holonomic mobile robot using enhanced genetic algorithm, in: Neural Networks and Artificial Intelligence, V. Golovko and A. Imada, Eds., Communications in Computer and Information Science, vol. 440, Springer International Publishing, Cham, Heidelberg, New York, Dordrecht, London, pp. 50-62, 2014.

31. *C. Purcaru, R.-E. Precup, D. Iercan, L.-O. Fedorovici,* ***R.-C. David****, F. Dragan, Optimal robot path planning using gravitational search algorithm, International Journal of Artificial Intelligence, vol. 9, no. 13 S, pp. 1-20, 2013, indexed in* ***SCOPUS****.*

Cited in:

1. I. H. Khan, A Comparative Study of Evolutionary Algorithms, International Journal of Artificial Intelligence, vol. 12, no. 1, pp. 1-17, 2014, indexed in **SCOPUS**.
2. T. N. T. Ibrahim, T. Marapan, S. H. Hasim, A. F. Z. Abidin, N. Omar, N. A. Nordin, H. I. Jaafar, K. Osman, Z. A. Ghani and S. F. M. Hussein, A Brief Analysis of Gravitational Search Algorithm (GSA) Publication from 2009 to May 2013, Proceedings of International Conference Recent treads in Engineering & Technology ICRET'2014, Batam (Indonesia), 9 pp., 2014.
3. K. Asawarungsaengkul, T. Rattanamanee and T. Wuttipornpun, A multi-size compartment vehicle routing problem for multi-product distribution: Models and solution procedures, International Journal of Artificial Intelligence, vol. 11, no. 13 A, pp. 237-256, 2013, indexed in **SCOPUS**.

32. *L.-O. Fedorovici, R.-E. Precup,* ***R.-C. David,*** *F. Drăgan, GSA-Based Training of Convolutional Neural Networks for OCR Applications, in: Computational Intelligence Systems in Industrial Engineering, C. Kahraman, Ed., Atlantis Computational Intelligence Systems, vol. 6, Atlantis Press and Springer-Verlag, Cham, Heidelberg, New York, Dordrecht, London, pp. 481-504, 2012.*

Cited in:

1. T. N. T. Ibrahim, T. Marapan, S. H. Hasim, A. F. Z. Abidin, N. Omar, N. A. Nordin, H. I. Jaafar, K. Osman, Z. A. Ghani and S. F. M. Hussein, A Brief Analysis of Gravitational Search Algorithm (GSA) Publication from 2009 to May 2013, Proceedings of International Conference Recent treads in Engineering & Technology ICRET'2014, Batam (Indonesia), 9 pp., 2014.

These **32 publications** are organized as follows:

- **8 papers** published in **journals with impact factor indexed in Thomson Reuters Web of Science** (formerly **ISI Web of Knowledge**), with a **cumulative impact factor of 27.16** according to 2013 Journal Citation Reports (JCR) released by Thomson Reuters in 2014.
- **7 papers** published in conference proceedings and in book chapters indexed in **Thomson Reuters Web of Science** (formerly ISI Web of Knowledge or **ISI Proceedings**).
- **2 papers** published in **journals** indexed in **SCOPUS**.
- **8 papers** published in conference proceedings indexed in the international databases **IEEE Xplore**, **INSPEC**, **SCOPUS** and **DBLP**.
- **4 book chapters** published in Springer-Verlag and Atlantis Press and indexed in **Springer Link,** out of a total of **7 published book chapters**, **3 book chapters** being indexed in **Thomson Reuters Web of Science** (formerly ISI Web of Knowledge or **ISI Proceedings**).
- **2 papers** published in non-indexed international journals.
- **1 paper** published in a non-indexed international conference proceedings.

The author of this thesis is the **first author of 9** publications out of the total of 32 publications.

The paper placed in the position **22** in this list has received the **Best Paper Award** at 16th Online World Conference on Soft Computing in Industrial Applications WSC16 (Loughborough University, UK, 2011).

The publications mentioned in the above list have received a total of **124 independent citations** (the self-citations of all co-authors are excluded).

The **cumulative impact factor of these independent citations is 116.069** according to 2013 Journal Citation Reports (JCR) released by Thomson Reuters in 2014. **54** of the citations are indexed in **Thomson Reuters Web of Science** (formerly ISI Web of Knowledge, namely **42** in journal publications and **12** in conference publications, the formerly ISI Proceedings) and **28** of the citations are indexed in the **international databases** IEEE Xplore, INSPEC, SCOPUS and DBLP.

The information presented in this section was last checked on February 23rd, 2015, so possible modifications might have occurred afterwards.

REFERENCES

[Abd08] A. M. Abdel Ghany, Design of a mixed H_2/H_∞ robust PID power system stabilizer with fuzzy adaptation and simulated annealing optimization, Proceedings of 12th International Middle-East Power System Conference (MEPCON 2008), Aswan, Egypt, pp. 316–324, 2008.

[Abo13] M. S. Abou Omar, T. Y. Khedr, B. A. Abou Zalam, Particle swarm optimization of fuzzy supervisory controller for nonlinear position control system, Proceedings of 8th International Conference on Computer Engineering & Systems (ICCES 2013), Cairo, Egypt, pp. 138–145, 2013.

[Agu12] H. Aguiar e Oliveira Junior, L. Ingber, A. Petraglia, M. Rembold Petraglia, M. Augusta Soares Machado, Fuzzy modeling with fuzzy adaptive simulated annealing, in: Stochastic Global Optimization and Its Applications With Fuzzy Adaptive Simulated Annealing, H. Aguiar e Oliveira Junior, L. Ingber, A. Petraglia, M. Rembold Petraglia, M. Augusta Soares Machado, Intelligent Systems Reference Library, vol. 35, Springer-Verlag, Berlin, Heidelberg, pp. 139–148, 2012.

[Ala12] F. Alambeigi, A. Zamani, G. Vossoughi, M. R. Zakerzadeh, Robust shape control of two SMA actuators attached to a flexible beam based on DK iteration, Proceedings of 12th International Conference on Control, Automation and Systems (ICCAS 2012), Jeju Island, Korea, pp. 316–321, 2012.

[Alf11] A. Alfi, M.-M. Fateh, Intelligent identification and control using improved fuzzy particle swarm optimization, Expert Systems with Applications, vol. 38, no. 10, pp. 12312–12317, Sep. 2011.

[Alm10] M. Almaraashi, R. John, S. Coupland, A. Hopgood, Time series forecasting using a TSK fuzzy system tuned with simulated annealing, Proceedings of 2010 IEEE International Conference on Fuzzy Systems (FUZZ-IEEE 2010), Barcelona, Spain, pp. 1–6, 2010.

[Ang13] P. P. Angelov, R. R. Yager, Density-based averaging - A new operator for data fusion, Information Sciences, vol. 222, pp. 163–174, Feb. 2013.

[Anh12] H. P. H. Anh, C. T. Lam, P. H. Lam, Inverse adaptive fuzzy model identification of the 2-axes PAM robot arm, Proceedings of 2012 International Conference on Control, Automation and Information Sciences (ICCAIS 2012), Saigon, Vietnam, pp. 334–339, 2012.

[Ara03] M. Araki, H. Taguchi, Two-degree-of-freedom PID controllers, International Journal of Control, Automation, and Systems, vol. 1, no. 4, pp. 401–411, Dec. 2003.

[Ark07] J. Arkat, M. Saidi, B. Abbasi, Applying simulated annealing to cellular manufacturing system design, The International Journal of Advanced Manufacturing Technology, vol. 32, no. 5–6, pp. 531–536, March 2007.

[Asa12] T. Asada, Y. Yoshitomi, A human-machine cooperative system for generating sign language animation using thermal image processing, a fuzzy algorithm, and simulated annealing, Artificial Life and Robotics, vol. 16, no. 4, pp. 486–492, Feb. 2012.

[Ast95] K. J. Åström, T. Hägglund, PID Controllers Theory: Design and Tuning, Research Triangle Park, NC: Instrument Society of America, 1995.

[Ask12] H. Askari, S.-H. Zahiri, Decision function estimation using intelligent gravitational search algorithm, International Journal of Machine Learning and Cybernetics, vol. 3, no. 2, pp. 163–172, June 2012.

[Aza13] H. N. Azadani, R. Torkzadeh, Design of GA optimized fuzzy logic-based PID controller for the two area non-reheat thermal power system, Proceedings of 13th Iranian Conference on Fuzzy Systems (IFSC 2013), Qazvin, Iran, pp. 1–6, 2013.

[Bal06]S. Balci, J. Cakiroglus, C. Tekkayas, Engagement, exploration, explanation, extension, and evaluation (5E) learning cycle and conceptual change text as learning tools, Biochemistry and Molecular Biology Education, vol. 34, no. 3, pp. 199–203, May 2006.

[Bar95] P. Baranyi, T. D. Gedeon, L. T. Kóczy, A general method for fuzzy rule interpolation: Specialized for crisp, triangular, and trapezoidal rules, Proceedings of 3rd European Congress on Fuzzy and Intelligent Techniques (EUFIT'95), Aachen, Germany, pp. 99–103, 1995.

[Bar96] P. Baranyi, L. T. Kóczy, A general and specialised solid cutting method for fuzzy rule interpolation, Journal BUSEFAL, vol. 66, no. 1, pp. 13–22, Oct. 1996.

[Bev12] H. Bevrani, F. Habibi, P. Babahajyani, M. Watanabe, Y. Mitani, Intelligent frequency control in an AC microgrid: Online PSO-based fuzzy tuning approach, IEEE Transactions on Smart Grid, vol. 3, no. 4, pp. 1935–1944, Dec. 2012.

[Bla10] S. Blažič, D. Matko, I. Škrjanc, Adaptive law with a new leakage term, IET Control Theory & Applications, vol. 4, no. 9, pp. 1533–1542, Sep. 2010.

[Bla11] S. Blažič, A novel trajectory-tracking control law for wheeled mobile robots, Robotics and Autonomous Systems, vol. 59, no. 11, pp. 1001–1007, Dec. 2011.

[Bla13] S. Blažič, D. Matko, T. Rodič, D. Dovžan, G. Mušič, G. Klančar, The design of observers for formation-flying control, Acta Astronautica, vol. 82, no. 1, pp. 60–68, Jan. 2013.

[Bod05] M. Bodur, A. Acan, T. Akyol, Fuzzy system modeling with the genetic and differential evolutionary optimization, Proceedings of International Conference on Computational Intelligence for Modelling, Control and Automation and International Conference on Intelligent Agents, Web Technologies and Internet Commerce, Vienna, Austria, vol. 1, pp. 432–438, 2005.

[Bou12] S. Bouallègue, J. Haggège, M. Ayadi, M. Benrejeb, PID-type fuzzy logic controller tuning based on particle swarm optimization, Engineering Applications of Artificial Intelligence, vol. 25, no. 3, pp. 484–493, April 2012.

[Byb02] R. W. Bybee (Ed.), Learning Science and the Science of Learning: Science Educators' Essay Collection, NSTA Press, Arlington, VA, 2002.

[Cab06] C. Cabrita, J. Botzheim, T.D. Gedeon, A.E. Ruano, L.T. Koczy, C. Fonseca, Bacterial memetic algorithm for fuzzy rule base optimization, Proceedings of 2006 World Automation Congress (WAC '06), Budapest, Hungary, pp. 1–6, 2006.

[Car05] S. Caraman, M. Barbu, E. Ceangă, Robust multimodel control using QFT techniques of a wastewater treatment process, Control Engineering and Applied Informatics, vol. 7, no. 2, pp. 10–17, June 2005.

[Cas10] O. Castillo, R. Martínez-Marroquín, P. Melin, Bio-inspired optimization of fuzzy logic controllers for robotic autonomous systems with PSO and ACO, Fuzzy Information and Engineering, vol. 2, no. 2, pp. 119–143, June 2010.

[Cas12] O. Castillo, P. Melin, Particle swarm optimization in the design of type-2 fuzzy systems, in: Recent Advances in Interval Type-2 Fuzzy Systems, O. Castillo and P. Melin, SpringerBriefs in Applied Sciences and Technology, Berlin, Heidelberg, pp. 27–31, 2012.

[Cha12] Y.-H. Chang, C.-W. Tao, H.-W. Lin, J.-S. Taur, Fuzzy sliding-mode control for ball and beam system with fuzzy ant colony optimization, Expert Systems with Applications, vol. 39, no. 3, pp. 3624–3633, Feb. 2012.

[Cha14] W.-J. Chang, C.-P. Kuo, C.-C. Ku, Intelligent fuzzy control with imperfect premise matching concept for complex nonlinear multiplicative noised systems, Neurocomputing, DOI: 10.1016/j.neucom.2014.11.065, Dec. 2014.

[Che08] K.-H. Cheng, Hybrid learning-based neuro-fuzzy inference system: A new approach for system modeling, International Journal of Systems Science, vol. 39, no. 6, pp. 583–600, June 2008.

[Che12] D. Chen, J. Wang, F. Zou, H. Zhang, W. Hou, Linguistic fuzzy model identification based on PSO with different length of particles, Applied Soft Computing, vol. 12, no. 11, pp. 3390–3400, Nov. 2012.

[Che14] Z. Chen, X. Yuan, H. Tian, B. Ji, Improved gravitational search algorithm for parameter identification of water turbine regulation system, Energy Conversion and Management, vol. 78, pp. 306–315, Feb. 2014.

[Chu04] Z. Chu, D. Qu, L. Sun, J. Cui, Research of 2-DOF planar parallel high speed/high accuracy robot, Proceedings of Fifth World Congress on Intelligent Control and Automation (WCICA 2004), Hangzhou, China, vol. 6, pp. 4715–4719, 2004.

[Cir14] G. Ćirović, D. Pamučar, D. Božanić, Green logistic vehicle routing problem: Routing light delivery vehicles in urban areas using a neuro-fuzzy model, Expert Systems with Applications, vol. 41, no. 9, pp. 4245–4258, July 2014.

[Coe07] L. dos Santos Coelho, B. M. Herrera, Fuzzy identification based on a chaotic particle swarm optimization approach applied to a nonlinear yo-yo motion system, IEEE Transactions on Industrial Electronics, vol. 54, no. 6, pp. 3234–3245, Dec. 2007.

[Coe08] L. dos Santos Coelho, N. Nedjah, L. de Macedo Mourelle, Gaussian quantum-behaved particle swarm optimization applied to fuzzy PID controller design, in: Quantum Inspired Intelligent Systems, N. Nedjah, L. dos Santos Coelho and L. de Macedo Mourelle, Eds., Studies in Computational Intelligence, vol. 121, Springer-Verlag, Berlin, Heidelberg, pp. 1–15, 2008.

[Cor14] J. Cortés-Romero, G. A. Ramos, H. Coral-Enriquez, Generalized proportional integral control for periodic signals under active disturbance rejection approach, ISA Transactions, vol. 53, no. 6, pp. 1901–1909, Nov. 2014.

[Dan05] D. Danciu, V. Răsvan, Stability results for cellular neural networks with time delays, in: Computational Intelligence and Bioinspired Systems, J. Cabestany, A. Prieto and F. Sandoval, Eds., Lecture Notes in Computer Science, vol. 3512, Springer-Verlag, Berlin, Heidelberg, pp. 366–373, 2005.

[Dan11] D. Danciu, V. Răsvan, Systems with slope restricted nonlinearities and neural networks dynamics, in: Advances in Computational Intelligence, J. Cabestany, I. Rojas and G. Joya, Eds., Lecture Notes in Computer Science, vol. 6692, Springer-Verlag, Berlin, Heidelberg, pp. 565–572, 2011.

[Dav09] R.-C. David, M.-B. Rădac, S. Preitl, J. K. Tar, Particle swarm optimization-based design of control systems with reduced sensitivity, Proceedings of 5th

International Symposium on Applied Computational Intelligence and Informatics (SACI 2009), Timisoara, Romania, pp. 491–496, 2009.

[Dav11] R.-C. David, R.-E. Precup, S. Preitl, J. K. Tar, J. Fodor, Parametric sensitivity reduction of PI-based control systems by means of evolutionary optimization algorithms, Proceedings of 6th IEEE International Symposium on Applied Computational Intelligence and Informatics (SACI 2011), Timisoara, Romania, pp. 241–246, 2011.

[Dav12a] R.-C. David, R.-E. Precup, E. M. Petriu, M.-B. Rădac, C. Purcaru, C.-A. Dragoş, S. Preitl, Adaptive gravitational search algorithm for pi-fuzzy controller tuning, Proceedings of 9th International Conference on Informatics in Control, Automation and Robotics (ICINCO 2012), Rome, Italy, vol. 1, pp. 136–141, 2012.

[Dav12b] R.-C. David, R.-E. Precup, E. M. Petriu, C. Purcaru, S. Preitl, PSO and GSA algorithms for fuzzy controller tuning with reduced process small time constant sensitivity, Proceedings of 2012 16th International Conference on System Theory, Control and Computing (ICSTCC 2012), Sinaia, Romania, pp. 1–6, 2012.

[Dav12c] R.-C. David, C.-A. Dragoş, R.-G. Bulzan, R.-E. Precup, E. M. Petriu, M.-B. Rădac, An approach to fuzzy modeling of magnetic levitation systems, International Journal of Artificial Intelligence, vol. 9, pp. 1–18, Oct. 2012.

[Dav12d] R.-C. David, R.-E. Precup, S. Preitl, J. K. Tar, J. Fodor, Three evolutionary optimization algorithms in PI controller tuning, in: Applied Computational Intelligence in Engineering and Information Technology, R.-E. Precup, S. Kovacs, S. Preitl and E. M. Petriu, Eds., Topics in Intelligent Engineering and Informatics, vol. 1, Springer-Verlag, Berlin, Heidelberg, pp. 95–106, 2012.

[Dav13] R.-C. David, R.-E. Precup, E. M. Petriu, M.-B. Rădac, S. Preitl, Gravitational search algorithm-based design of fuzzy control systems with a reduced parametric sensitivity, Information Sciences, vol. 247, pp. 154–173, Oct. 2013.

[Dav14a] R.-C. David, R.-E. Precup, E. M. Petriu, S. Preitl, M.-B. Radac, L.-O. Fedorovici, Adaptive evolutionary optimization algorithms for simple fuzzy controller tuning dedicated to servo systems, in: Fuzzy Modeling and Control: Theory and Applications, F. Matia, G. N. Marichal and E. Jimenez, Eds., Atlantis Computational Intelligence Systems, vol. 9, Atlantis Press and Springer-Verlag, Cham, Heidelberg, New York, Dordrecht, London, pp. 159–173, 2014.

[Dav14b] R.-C. David, R.-B. Grad, R.-E. Precup, M.-B. Radac, C.-A. Dragos and E. M. Petriu, An approach to fuzzy modeling of anti-lock braking systems, in: Soft Computing in Industrial Applications, V. Snasel, P. Kromer, M. Koppen and G. Schaefer, Eds., Advances in Intelligent Systems and Computing, vol. 223, Springer International Publishing, Berlin, Heidelberg, pp. 83–93, 2014.

[Deb14] A. Deb, J. S. Roy, B. Gupta, Performance comparison of differential evolution, particle swarm optimization and genetic algorithm in the design of circularly polarized microstrip antennas, IEEE Transactions on Antennas and Propagation, vol. 62, no. 8, pp. 3920–3928, Aug. 2014.

[Der14] F. Deregeh, H. Nezamabadi-pour, A new gravitational image edge detection method using edge explorer agents, Natural Computing, vol. 13, no. 1, pp. 65–78, March 2014.

[Dra11a] C.-A. Dragoş, S. Preitl, R.-E. Precup, E. M. Petriu, A.-I. Stînean, A comparative case study of position control solutions for a mechatronics application, Proceedings of 2011 IEEE/ASME International Conference on Advanced Intelligent Mechatronics (AIM 2011), Budapest, Hungary, pp. 814–819, 2011.

[Dra11b] C.-A. Dragoş, R.-E. Precup, E. M. Petriu, M. L. Tomescu, S. Preitl, R.-C. David, M.-B. Rădac, 2-DOF PI-fuzzy controllers for a magnetic levitation sys-

tem, Proceedings of 8th International Conference on Informatics in Control, Automation and Robotics (ICINCO 2011), Noordwijkerhout, The Netherlands, vol. 1, pp. 111–116, 2011.

[Dra13] C.-A. Dragoş, R.-E. Precup, R.-C. David, S. Preitl, A.-I. Stînean, E. M. Petriu, Simulated annealing-based optimization of fuzzy models for magnetic levitation systems, Proceedings of 2013 Joint IFSA World Congress and NAFIPS Annual Meeting (IFSA/NAFIPS 2013), Edmonton, AB, Canada, pp. 286–291, 2013.

[Dub13] H. M. Dubey, M. Pandit, B. K. Panigrahi, M. Udgir, A novel swarm intelligence based gravitational search algorithm for combined economic and emission dispatch problems, in: Swarm, Evolutionary and Memetic Computing, B. K. Panigrahi, P. N. Suganthan, S. Das and S. S. Dash, Eds, Lecture Notes in Computer Science, vol. 8297, Springer-Verlag, Berlin, Heidelberg, pp. 568–579, 2013.

[Dum15] S. Duman, N. Yorukeren, I. H. Altas, A novel modified hybrid PSOGSA based on fuzzy logic for non-convex economic dispatch problem with valve-point effect, International Journal of Electrical Power & Energy Systems, vol. 64, pp. 121–135, Jan. 2015.

[Esm02] A. A. A. Esmin, A. R. Aoki, G. Lambert-Torres, Particle swarm optimization for fuzzy membership functions optimization, Proceedings of 2002 IEEE International Conference on Systems, Man and Cybernetics, Hammamet, Tunisia, vol. 3, pp. 6–9, 2002.

[Far07] E. A. Fares, M. Elbardiny, M. M. Sharaf, Adaptive fuzzy logic controller of vis-ual servoing robot system by membership optimization using genetic algorithms, Proceedings of International Conference on Computer Engineering & Systems 2007 (ICCES '07), Cairo, Egypt, pp. 15–20, 2007.

[Fed12a] L.-O. Fedorovici, R.-E. Precup, R.-C. David, F. Drăgan, GSA-based training of convolutional neural networks for OCR applications, in: Computational Intelligence Systems in Industrial Engineering, C. Kahraman, Ed., Atlantis Computational Intelligence Systems, vol. 6, Atlantis Press and Springer-Verlag, Cham, Heidelberg, New York, Dordrecht, London, pp. 481–504, 2012.

[Fed12b] L.-O. Fedorovici, R.-E. Precup, F. Drăgan, R.-C. David, C. Purcaru, Embedding gravitational search algorithms in convolutional neural networks for OCR applications, Proceedings of IEEE 7th International Symposium on Applied Computational Intelligence and Informatics (SACI 2012), Timisoara, Romania, pp. 125–130, 2012.

[Fen06] G. Feng, A survey on analysis and design of model-based fuzzy control systems, IEEE Transactions on Fuzzy Systems, vol. 14, no. 5, pp. 676–697, Oct. 2006.

[Fer13] Feriyonika, G. Dewantoro, Fuzzy sliding mode control for enhancing injection velocity performance in injection molding machine, International Journal of Artificial Intelligence, vol. 10, no. S13, pp. 75–87, March 2013.

[Fil08] F.-G. Filip, D. Popescu, M. Mateescu, Optimal decisions for complex systems - Software packages, Mathematics and Computers in Simulation, vol. 76, no. 5–6, pp. 422–429, Jan. 2008.

[Fil09] F.-G. Filip, K. Leiviskä, Large-scale complex systems, in: Springer Handbook of Automation, S. Y. Nof, Ed., Springer-Verlag, Berlin, Heidelberg, pp. 619–638, 2009.

[Fuj07] S. Fujii, S. A. Panfilov, K. Takahashi, S. V. Ulyanov, H. Watanabe, Intelligent robust control system for motorcycle using soft computing optimizer, U.S. Patent 7,251,638, issued July 31, 2007.

[Gal95] S. Galichet, L. Foulloy, Fuzzy controllers: synthesis and equivalences, IEEE Transactions on Fuzzy Systems, vol. 3, no. 2, pp. 140–148, May 1995.

[Gar13] B. Garlík, M. Křivan, Renewable energy unit commitment, with different acceptance of balanced power, solved by simulated annealing, Energy and Buildings, vol. 67, pp. 392–402, Dec. 2013.

[Gha12] R. Ghazali, Y. M. Sam, M. F. Rahmat, Zulfatman, Point-to-point trajectory tracking with two-degree-of-freedom robust control for a non-minimum phase electro-hydraulic system, Proceedings of 10th World Congress on Intelligent Control and Automation (WCICA 2012), Beijing, China, pp. 2661–2668, 2012.

[Gho04] S. P. Ghoshal, Application of GA/GA-SA based fuzzy automatic generation control of a multi-area thermal generating system, Electric Power Systems Research, vol. 70, no. 2, pp. 115–127, July 2014.

[Gol13] F. Golozari, A. Jafari, M. Amiri, Application of a hybrid simulated annealing-mutation operator to solve fuzzy capacitated location-routing problem, The International Journal of Advanced Manufacturing Technology, vol. 67, no. 5–8, pp. 1791–1807, July 2013.

[Gon15] B. González, F. Valdez, P. Melin, G. Prado-Arechiga, A gravitational search algorithm for optimization of modular neural networks in pattern recognition, in: Fuzzy Logic Augmentation of Nature-Inspired Optimization Metaheuristics, O. Castillo and P. Melin, Eds., Studies in Computational Intelligence, vol. 574, Springer-Verlag, Cham, Heidelberg, New York, Dordrecht, London, pp. 127–137, 2015.

[Guo07] Y. Guo, J. Lu, T, Zhang, K. Wu, A multi-objective optimizing control method for boiler-turbine coordinated control, Proceedings of International Conference on Mechatronics and Automation ICMA 2007), Harbin, China, pp. 3700–3705, 2007.

[Hab07] R. E. Haber, A. Alique, J. R. Alique, Optimal fuzzy control for a time-delay system using simulated annealing: An application to high-performance drilling, Proceedings of Third International Conference on Natural Computation (ICNC 2007), Haikou, Hainan, China, vol. 5, pp. 639–643, 2007.

[Hab09] R. E. Haber, R. Haber-Haber, A. Jiménez, R. Galán, An optimal fuzzy control system in a network environment based on simulated annealing. An application to a drilling process, Applied Soft Computing, vol. 9, no. 3, pp. 889–895, June 2009.

[Hab10] R. E. Haber, R. M. del Toro, A. Gajate, Optimal fuzzy control system using the cross-entropy method. A case study of a drilling process, Information Sciences, vol. 180, no. 4, pp. 2777–2792, July 2010.

[Hai10] H.-B. Mu, J. Yu, L.-Z. Liu, Traffic signals control of urban traffic intersections group based on fuzzy control, Proceedings of 2010 Seventh International Conference on Fuzzy Systems and Knowledge Discovery (FSKD 2010), Yantai, Shandong, China, vol. 2, pp. 763–767, 2010.

[Ham12] Z. A. Hamed, S. Z. M. Hashim, Hybrid PSO-black stork foraging for functional neural fuzzy network learning enhancement, Proceedings of 2012 IEEE International Conference on Systems, Man, and Cybernetics (SMC 2012), Seoul, South Korea, pp. 1339–1344, 2012.

[Hat12] A. Hatamlou, S. Abdullah, H. Nezamabadi-pour, A combined approach for clustering based on K-means and gravitational search algorithms, Swarm and Evolutionary Computation, vol. 6, pp. 47–52, Oct. 2012.

[Ho06] S.-Y. Ho, L.-S. Shu, Optimizing fuzzy neural networks for tuning PID controllers using an orthogonal simulated annealing algorithm OSA, IEEE Transactions on Fuzzy Systems, vol. 14, no. 3, pp. 421–434, June 2006.

[Hol05] D. Holliday, R. Resnick, J. Walker, Fundamentals of Physics, 7th ed., John Wiley & Sons, Hoboken, NJ, 2005.

[Hos14] A. Hosovsky, P. Michal, M. Tothova, O. Biros, Fuzzy adaptive control for pneumatic muscle actuator with simulated annealing tuning, Proceedings of IEEE 12th International Symposium on Applied Machine Intelligence and Informatics (SAMI 2014), Herl'any, Slovakia, pp. 205–209, 2014.

[Hot10] Y. V. Hote, J. R. P. Gupta, D. R. Choudhury, Kharitonov's theorem and Routh criterion for stability margin of interval systems, International Journal of Control, Automation and Systems, vol. 8, no. 3, pp. 647–654, June 2010.

[Hu12] W. Hu, G. Xiao, W.-J. Cai, PID controller design based on two-degrees-of-freedom direct synthesis, Proceedings of 2011 Chinese Control and Decision Conference (CCDC 2011), Mianyang, China, pp. 629–634, 2011.

[Hus13] P. Husek, O. Cerman, Fuzzy model reference control with adaptation of input fuzzy sets, Knowledge-Based Systems, vol. 49, pp. 116–122, Sep. 2013.

[Ibr14] A. A. Ibrahim, A. Mohamed, H. Shareef, Optimal power quality monitor placement in power systems using an adaptive quantum-inspired binary gravitational search algorithm, International Journal of Electrical Power & Energy Systems, vol. 57, pp. 404–413, May 2014.

[Int07a] The Laboratory Anti-lock Braking System Controlled from PC, User's Manual, INTECO Ltd., Krakow, Poland, 2007.

[Int07b] Modular Servo System, User's Manual, Inteco Ltd., Krakow, Poland, 2007.

[Int08] Magnetic Levitation System 2EM (MLS2EM), User's Manual, Inteco Ltd., Krakow, Poland, 2008.

[Ise89] R. Isermann, Digital Control Systems, 2nd ed., Springer-Verlag, Berlin, Heidelberg, New York, 1989.

[Iwa12] M. Iwasaki, K. Seki, Y. Maeda, High-precision motion control techniques: a promising approach to improving motion performance, IEEE Industrial Electronics Magazine, vol. 6, no. 1, pp. 32–40, Mar. 2012.

[Jad13] Z. Jadidi, V. Muthukkumarasamy, E. Sithirasenan, Metaheuristic algorithms based flow anomaly detector, Proceedings of 19th Asia-Pacific Conference on Communications (APCC 2013), Bali, Indonesia, pp. 717–722, 2013.

[Jai11] R. Jain, N. Sivakumaran, T. K. Radhakrishnan, Design of self tuning fuzzy controllers for nonlinear systems, Expert Systems with Applications, vol. 38, no. 4, pp. 4466–4476, April 2011.

[Jaj11] H. R. I. Jajarmi, A. Mohamed, H. Shareef, GSA-FL controller for three phase active power filter to improve power quality, 2011 2nd International Conference on Control, Instrumentation and Automation (ICCIA 2011), Shiraz, Iran, pp. 417–422, 2011.

[Jas14] I. F. Jasim, P. W. Plapper, Contact-state recognition of compliant motion robots using expectation maximization-based Gaussian mixtures, Proceedings of 41st International Symposium on Robotics (ISR/Robotik 2014), Munich, Germany, pp. 1–8, 2014.

[Ji14] B. Ji, X. Yuan, Z. Chen, H. Tian, Improved gravitational search algorithm for unit commitment considering uncertainty of wind power, Energy, vol. 67, pp. 52–62, April 2014.

[Jia12] H. Jiang, C. K. Kwong, Z. Chen, Y. C. Ysim, Chaos particle swarm optimization and T–S fuzzy modeling approaches to constrained predictive control, Expert Systems with Applications, vol. 39, no. 1, pp. 194–201, Jan. 2012.

[Jia14] S. Jiang, Z. Ji, Y. Shen, A novel hybrid particle swarm optimization and gravitational search algorithm for solving economic emission load dispatch prob-

lems with various practical constraints, International Journal of Electrical Power & Energy Systems, vol. 55, pp. 628–644, Feb. 2014.
[Joe13] E. Joelianto, D. C. Anura, M. Priyanto, ANFIS – hybrid reference control for improving transient response of controlled systems using PID controller, International Journal of Artificial Intelligence, vol. 10, no. S13, pp. 88–111, March 2013.
[Joh10] Z. C. Johanyák, Student evaluation based on fuzzy rule interpolation, International Journal of Artificial Intelligence, vol. 5, no. A10, pp. 37–55, Oct. 2010.
[Joh12] Z. C. Johanyák, O. Papp, A hybrid algorithm for parameter tuning in fuzzy model identification, Acta Polytechnica Hungarica, vol. 9, no. 6, pp. 153–165, Dec. 2012.
[Jos12] M. Joshani, R. Yusof, M. Khalid, A. I. Cahyadi, Swarm intelligence based fuzzy controller - a design for nonlinear water level tank, Proceedings of 2012 Third International Conference on Intelligent Systems, Modelling and Simulation (ISMS 2012), Kota Kinabalu, Malaysia, pp. 451–456, 2012.
[Jua05] C.-F. Juang, C.-H. Hsu, Temperature control by chip-implemented adaptive recurrent fuzzy controller designed by evolutionary algorithm, IEEE Transactions on Circuits and Systems I: Regular Papers, vol. 52, no. 11, pp. 2376–2384, Nov. 2005.
[Jua08] C.-F. Juang, C.-M. Lu, C. Lo, C.-Y. Wang, Ant colony optimization algorithm for fuzzy controller design and its FPGA implementation, IEEE Transactions on Industrial Electronics, vol. 55, no. 3, pp. 1453–1462, March 2008.
[Jua09] C.-F. Juang, C.-M. Lu, Ant colony optimization incorporated with fuzzy Q-learning for reinforcement fuzzy control, IEEE Transactions on Systems, Man and Cybernetics, Part A: Systems and Humans, vol. 39, no. 3, pp. 597–608, May 2009.
[Jua11] C.-F. Juang, Y.-C. Chang, Evolutionary-group-based particle-swarm-optimized fuzzy controller with application to mobile-robot navigation in unknown environments, IEEE Transactions on Fuzzy Systems, vol. 19, no. 2, pp. 379–392, April 2011.
[Kam12] S. Kamyab, A. Bahrololoum, Designing of rule base for a TSK-fuzzy system using bacterial foraging optimization algorithm (BFOA), Procedia - Social and Behavioral Sciences, vol. 32, pp. 176–183, Dec. 2012.
[Kan12] N. Kanghyun, H. Fujimoto, Y. Hori, Motion control of electric vehicles based on robust lateral tire force control using lateral tire force sensors, Proceedings of 2012 IEEE/ASME International Conference on Advanced Intelligent Mechatronics (AIM 2012), Kachsiung, Taiwan, China, pp. 526–531, 2012.
[Kar88] A. Karimi, A.V. Sebald, Computer aided design of closed-loop controllers for biomedical applications, Proceedings of the Annual International Conference of the IEEE Engineering in Medicine and Biology Society, New Orleans, LA, USAm, vol. 3, pp. 1404–1405, 1988.
[Kav10a] A. Kaveh, S. Talatahari, A novel heuristic optimization method: charged system search, Acta Mechanica, vol. 213, pp. 267–289, 2010.
[Kav10b] A. Kaveh, S. Talatahari, Optimal design of truss structures via the charged system search algorithm, Structural Multidisciplinary Optimization, vol. 37, no. 6, pp. 893–911, June 2010.
[Kav10c] A. Kaveh, S. Talatahari, A charged system search with a fly to boundary method for discrete optimum design of truss structures, Asian Journal of Civil Engineering (Building and Housing), vol. 11, no. 3, pp. 277–293, June 2010.

[Kav12a] A. Kaveh, A. F. Behnam, Cost optimization of a composite floor system, one-way waffle slab, and concrete slab formwork using a charged system search algorithm, Scientia Iranica, vol. 19, no. 3, pp. 410–416, June 2012.

[Kav12b] A. Kaveh, S. Talatahari, Charged system search for optimal design of frame structures, Applied Soft Computing, vol. 12, no. 1, pp. 382–393, Jan. 2012.

[Kav13a] A. Kaveh, A. F. Behnam, Design optimization of reinforced concrete 3D structures considering frequency constraints via a charged system search, Scientia Iranica, vol. 20, no. 3, pp. 387–396, June 2013.

[Kav13b] A. Kaveh, B. Ahmadi, Simultaneous analysis, design and optimization of structures using the force method and supervised charged system search algorithm, Scientia Iranica, vol. 20, no. 1, pp. 65–76, Feb. 2013.

[Kav14a] A. Kaveh, A. Nasrollahi, Performance-based seismic design of steel frames utilizing charged system search optimization, Applied Soft Computing, vol. 22, pp. 213–221, Sep. 2014.

[Kav14b] A. Kaveh, Simultaneous analysis, design and optimization of structures using force method and supervised charged system search, in: Computational Structural Analysis and Finite Element Methods, A. Kaveh, Springer-Verlag, Cham, Heidelberg, New York, Dordrecht, London, pp. 407–432, 2014.

[Kav14c] A. Kaveh, A multi-swarm multi-objective optimization method for structural design, in: Advances in Metaheuristic Algorithms for Optimal Design of Structures, A. Kaveh, Springer-Verlag, Cham, Heidelberg, New York, Dordrecht, London, pp. 393–426, 2014.

[Ken95a] J. Kennedy, R.C. Eberhart, Particle swarm optimization, Proceedings of IEEE International Conference on Neural Networks (ICNN ’95), Perth, Australia, pp. 1942–1948, 1995.

[Ken95b] J. Kennedy, R.C. Eberhart, A new optimizer using particle swarm theory, Proceedings of 6th International Symposium on Micro Machine and Human Science (MHS ’95), Nagoya, Japan, pp 39–43, 1995.

[Ken97] J. Kennedy, R. C. Eberhart, A discrete binary version of the particle swarm algorithm, Proceedings of 1997 IEEE International Conference on Systems, Man, and Cybernetics, Orlando, FL, USA, vol. 5, pp. 4104–4108, 1997.

[Kir83] S. Kirkpatrick, C. D. Gelatt Jr., M. P. Vecchi, Optimization by simulated annealing, Science, vol. 220, no. 4598, pp. 671–680, May 1983.

[Kha07] M. A. Khanesar, H. Tavakoli, M. Teshnehlab, M. A. Shoorehdeli, A novel binary particle swarm optimization, Proceedings of Mediterranean Conference on Control & Automation (MED ’07), Athens, Greece, pp. 1–6, 2007.

[Kha08] S. Khan, S. F. Abdulazeez, L. W. Adetunji, A. H. M. Zahirul Alam, M. Jimoh E. Salami, Design and implementation of an optimal fuzzy logic controller using genetic algorithm, Journal of Computer Science, vol. 4, no. 10, pp. 799–808, Oct. 2008.

[Kha09] S. A. Khan, A. P. Engelbrecht, Fuzzy hybrid simulated annealing algorithms for topology design of switched local area networks, Soft Computing, vol.13, no. 1, pp. 46–61, Jan. 2009.

[Kha10a] M. A. Khanesar, M. Teshnehlab, O. Kaynak, Identification of interval fuzzy models using recursive least square method, Proceedings of 2010 IEEE International Conference on Systems Man and Cybernetics (SMC 2010), Barcelona, Spain, pp. 4362–4368, Octomber 2010.

[Kha10b] M. A. Khanesar, M. Teshnehlab, E. Kayacan, O. Kaynak, A novel type-2 fuzzy membership function: Application to the prediction of noisy data, Proceedings of 2010 IEEE International Conference on Computational Intelligence

for Measurement Systems and Applications (CIMSA 2010), Taranto, Italy, pp. 128–133, 2010.

[Kha10c] N. Khaehintung, A. Kunakorn, P. Sirisuk, A novel fuzzy logic control technique tuned by particle swarm optimization for maximum power point tracking for a photovoltaic system using a current-mode boost converter with bifurcation control, International Journal of Control, Automation and Systems, vol. 8, no. 2, pp. 289–300, April 2010.

[Koc97] L. T. Kóczy, K. Hirota, Size reduction by interpolation in fuzzy rule bases, IEEE Transactions on Systems, Man, and Cybernetics, vol. 27, no. 1, pp. 14–25, Jan. 1997.

[Kum13] R. Kumar Sahu, S. Panda, U. Kumar Rout, DE optimized parallel 2-DOF PID controller for load frequency control of power system with governor deadband nonlinearity, International Journal of Electrical Power & Energy Systems, vol. 49, pp. 19–33, Jul. 2013.

[Kum14] V. Kumar, J. K. Chhabra, D. Kumar, Automatic cluster evolution using gravitational search algorithm and its application on image segmentation, Engineering Applications of Artificial Intelligence, vol. 29, pp. 93–103, March 2014.

[Kuo14] R. J. Kuo, S. Y. Hung, W. C. Cheng, Application of an optimization artificial immune network and particle swarm optimization-based fuzzy neural network to an RFID-based positioning system, Information Sciences, vol. 262, pp. 78–98, March 2014.

[Led07] S. Ledesma, M. Torres, D. Hernández, G. Aviña and G. García, Temperature cycling on simulated annealing for neural network learning, in: MICAI 2007: Advances in artificial intelligence, A. Gelbukh and A. F. Kuri Morales, Eds., Lecture Notes in Computer Science, vol. 4827, Springer-Verlag, Berlin, Heidelberg, New York, pp. 161–171, 2007.

[Li10] T.-H. S. Li, Y.-C. Huang, MIMO adaptive fuzzy terminal sliding-mode controller for robotic manipulators, Information Sciences, vol. 180, no. 23, pp. 4641–4660, Dec. 2010.

[Li12a] G. Li, W. Jin, C. Chen, Fuzzy control strategy for train lateral semi-active suspension based on particle swarm optimization, in: System Simulation and Scientific Computing, T. Xiao, L. Zhang and S. Ma, Eds., Communications in Computer and Information Science, Springer-Verlag, Berlin, Heidelberg, pp. 8–16, 2012.

[Li12b] C. Li, J. Zhou, B. Fu, P. Kou, J. Xiao, T–S fuzzy model identification with a gravitational search-based hyperplane clustering algorithm, IEEE Transactions on Fuzzy Systems, vol. 20, no. 2, pp. 305–317, April 2012.

[Li13] C. Li, J. Zhou, J. Xiao, H. Xiao, Hydraulic turbine governing system identification using T–S fuzzy model optimized by chaotic gravitational search algorithm, Engineering Applications of Artificial Intelligence, vol. 26, no. 9, pp. 2073–2082, Oct. 2013.

[Lia10] Y. Liang, L. Xu, R. Wei, H. Hu, Adaptive fuzzy control for trajectory tracking of mobile robot, Proceedings of 2010 IEEE/RSJ International Conference on Intelligent Robots and Systems (IROS 2010), Taipei, Taiwan, pp. 4755–4760, 2010.

[Lia13a] W. Liang, Y. Hu, N. Kasabov, Evolving personalized modeling system for integrated feature, neighborhood and parameter optimization utilizing gravitational search algorithm, Evolving Systems, DOI: 10.1007/s12530-013-9081-x, pp. 1–14, May 2013.

[Lia13b] C. Lian, Z. Zeng, W. Yao, H. Tang, Displacement prediction of landslide based on PSOGSA-ELM with mixed kernel, Proceedings of 2013 Sixth International Conference on Advanced Computational Intelligence (ICACI 2013), Hangzhou, China, pp. 52–57, 2013.

[Lin08] C.-J. Lin, An efficient immune-based symbiotic particle swarm optimization learning algorithm for TSK-type neuro-fuzzy networks design, Fuzzy Sets and Systems, vol. 159, no. 21, pp. 2890–2909, Nov. 2008.

[Lin09a] C.-J. Lin, Y.-C. Liu, Image backlight compensation using neuro-fuzzy networks with immune particle swarm optimization, Expert Systems with Applications, vol. 36, no. 3, part 1, pp. 5212–5220, April 2009.

[Lin09b] C.-J. Lin, C.-C. Weng, C.-L. Lee, C.-Y. Lee, Using an efficient hybrid of cooperative particle swarm optimization and cultural algorithm for neural fuzzy network design, Proceedings of 2009 International Conference on Machine Learning and Cybernetics, Baoding, China, vol. 5, pp. 3076–3082, 2009.

[Lin11] O. Linda, M. Manic, Uncertainty-robust design of interval type-2 fuzzy logic controller for delta parallel robot, IEEE Transactions on Industrial Informatics, vol. 7, no. 4, pp. 661–670, Nov. 2011.

[Lin13] C.-J. Lin, H.-T. Yau, C.-R. Lin, C.-R. Hsu, Simulation and experimental analysis for hysteresis behavior of a piezoelectric actuated micro stage using modified charge system search, Microsystem Technologies, vol. 19, no. 11, pp. 1807–1815, Nov. 2013.

[Liu00] G. Liu, W. Yang, Learning and tuning of fuzzy membership functions by simulated annealing algorithm, Proceedings of 2000 IEEE Asia-Pacific Conference on Circuits and Systems (APCCAS 2000), Tianjin, China, pp. 367–370, 2000.

[Liu10a] K. Liu, Y. Tan, X. He, An adaptive staged PSO based on particles' search capabilities, in: Advances in Swarm Intelligence, Y. Tan, Y. Shi and K. C. Tan, Eds., Lecture Notes in Computer Science, vol. 6145, Springer-Verlag, Berlin, Heidelberg, pp. 52–59, 2010.

[Liu10b] G. Liu, J.-H. Han, Y.-B. Wu, M.-J. Liu, An optimal control problem of adaptive fuzzy controllers for fuzzy control systems, Proceedings of 2010 International Conference on Intelligent Computation Technology and Automation (ICICTA 2010), Changsha, China, vol. 1, pp. 619–622, 2010.

[Liu12] Y. Liu, L. Yang, H. Duan, Adaptive fuzzy and H_∞ control of robotic manipulators with uncertainties, Proceedings of 10th World Congress on Intelligent Control and Automation (WCICA 2012), Beijing, China, pp. 74–79, 2012.

[Lu10] Z. Lu, J. Zhang, Y. Chen, T. Zhao, H. Liu, Fuzzy control model and simulation of supply air system in a test rig of low-temperature hot-water radiator system, Energy and Buildings, vol. 42, no. 3, pp. 386–392, March 2010.

[Ma10] M. Ma, L.-B. Zhang, Y. Sun, Particle Swarm optimization of T-S fuzzy model, in: Quantitative Logic and Soft Computing, B.-Y. Cao, S. Chen, G. Wang and S. Guo, Eds., Advances in Intelligent and Soft Computing, vol. 82, Springer-Verlag, Berlin, Heidelberg, pp. 447–452, 2010.

[Mal13] Y. Maldonado, O. Castillo, P. Melin, Particle swarm optimization for average approximation of interval type-2 fuzzy inference systems design in FPGAs for real applications, in: Recent Advances on Hybrid Intelligent Systems, O. Castillo, P. Melin and J. Kacprzyk, Eds., Studies in Computational Intelligence, vol. 451, Springer-Verlag, Berlin, Heidelberg, pp. 33–49, 2013.

[Man14] S. P. Mangaiyarkarasi, T. Sree Renga Raja, Optimal location and sizing of multiple static var compensators for voltage risk assessment using hybrid PSO-GSA algorithm, Arabian Journal for Science and Engineering, vol. 39, no. 11, pp. 7967–7980, Nov. 2014.

[Mar98] H. Martínez-Alfaro, S. Gómez-García, Mobile robot path planning and tracking using simulated annealing and fuzzy logic control, Expert Systems with Applications, vol. 15, no. 3–4, pp. 421–429, Oct.–Nov. 1998.

[Mar11] M. Marinaki, Y. Marinakis, G. E. Stavroulakis, Fuzzy control optimized by a multi-objective particle swarm optimization algorithm for vibration suppression of smart structures, Structural and Multidisciplinary Optimization, vol. 43, no. 1, pp. 29–42, Jan. 2011.

[Meg13] H. Megherbi, N. Megherbi, A. C. Megherbi, K. Benmahammed, Evolutionary optimization of robust and chattering-free Mamdani type fuzzy controller, Courrier du Savoir, vol. 17, pp. 77–85, Dec. 2013.

[Mer11] A. Merve Acilar, A. Arslan, Optimization of multiple input–output fuzzy membership functions using clonal selection algorithm, Expert Systems with Applications, vol. 38, no. 3, pp. 1374–1381, March 2011.

[Mil12] S. Miller, M. Gongora, J. Garibaldi, R. John, Interval type-2 fuzzy modelling and stochastic search for real-world inventory management, Soft Computing, vol. 16, no. 8, pp. 1447–1459, Aug. 2012.

[Mir10] S. Mirjalili, S. Z. M. Hashim, A new hybrid PSOGSA algorithm for function optimization, Proceedings of 2010 International Conference on Computer and Information Application (ICCIA 2010), Tianjin, China, pp. 374–377, 2010.

[Moh08] H. Mohamadi, J. Habibi, M. S. Abadeh, H. Saadi, Data mining with a simulated annealing based fuzzy classification system, Pattern Recognition, vol. 41, no. 5, pp. 1824–1833, May 2008.

[Moh13] B. Mohamed, T. Ahmed, H. Lassad, C. Abdelkader, New Allied Fuzzy C-Means algorithm for Takagi-Sugeno fuzzy model identification, Proceedings of 2013 International Conference on Electrical Engineering and Software Applications (ICEESA 2013), Hammamet, Tunisia, pp. 1–7, 2013.

[Moh14] A. Mohammadzadeh, O. Kaynak, M. Teshnehlab, Two-mode indirect adaptive control approach for the synchronization of uncertain chaotic systems by the use of a hierarchical interval type-2 fuzzy neural network, IEEE Transactions on Fuzzy Systems, vol. 22, no. 5, pp. 1301–1312, Oct. 2014.

[Nik11] T. Niknam, H. D. Mojarrad, H. Z. Meymand, A new particle swarm optimization for non-convex economic dispatch, European Transactions on Electrical Power, vol. 21, no. 1, pp. 656–679, Jan. 2011.

[Nik12] T. Niknam, R. Azizipanah-Abarghooee, M. R. Narimani, Reserve constrained dynamic optimal power flow subject to valve-point effects, prohibited zones and multi-fuel constraints, Energy, vol. 47, no. 1, pp. 451–464, Nov. 2012.

[Nik13] T. Niknam, M. R. Narimani, R. Azizipanah-Abarghooee, B. Bahmani-Firouzi, Multiobjective optimal reactive power dispatch and voltage control: A new opposition-based self-adaptive modified gravitational search algorithm, IEEE Systems Journal, vol. 7, no. 4, pp. 742–753, Dec. 2013.

[Nom07] Y. Nomura, H. Furuta, M. Hirokane, An integrated fuzzy control system for structural vibration, Computer-Aided Civil and Infrastructure Engineering, vol. 22, no. 4, pp. 306–316, May 2007.

[Obe12] O. Obe, I. Dumitrache, Adaptive neuro-fuzzy controller with genetic training for mobile robot control, International Journal of Computers, Communications & Control, vol. 6, no. 1, pp. 135–146, March 2012.

[Oh11] S. K. Oh, H. J. Jang, W. Pedrycz, A comparative experimental study of type-1/type-2 fuzzy cascade controller based on genetic algorithms and particle swarm optimization, Expert Systems with Applications, vol. 38, no. 9, pp. 11217-11229, Sep. 2011.

[Oht01] H. Ohtake, K. Tanaka, H. O. Wang, Fuzzy modeling via sector nonlinearity concept, Proceedings of Joint 9th IFSA World Congress and 20th NAFIPS International Conference, Vancouver, BC, Canada, vol. 1, pp. 127–132, 2001.

[Oli09] M. V. Oliveira, R. Schirru, Applying particle swarm optimization algorithm for tuning a neuro-fuzzy inference system for sensor monitoring, Progress in Nuclear Energy, vol. 51, no. 1, pp. 177–183, Jan. 2009.

[Oli14] H. Oliveira Jr., A. Petraglia, Establishing Nash equilibria of strategic games: a multistart fuzzy adaptive simulated annealing approach, Applied Soft Computing, vol. 19, pp. 188–197, June 2014.

[Oni12] E. Onieva, V. Milanés, J. Villagrá, J. Pérez, J. Godoy, Genetic optimization of a vehicle fuzzy decision system for intersections, Expert Systems with Applications, vol. 39, no. 18, pp. 13148–13157, Dec. 2012.

[Ozy12] S. Özyön, H. Temurtaş, B. Durmuş, G. Kuvat, Charged system search algorithm for emission constrained economic power dispatch problem, Energy, vol. 46, no. 1, pp. 420–430, Oct. 2012.

[Pan13] H. M. Dubey, M. Pandit, B. K. Panigrahi, M. Udgir, A novel swarm intelligence based gravitational search algorithm for combined economic and emission dispatch problems, in: Swarm, Evolutionary, and Memetic Computing, B. K. Panigrahi, P. N. Suganthan, S. Das and S. S. Dash, Eds., Lecture Notes in Computer Science, vol. 8297, Springer-Verlag, Cham, Heidelberg, New York, Dordrecht, London, pp. 568–579, 2013.

[Pas04] O. Păstrăvanu, M. Voicu, Necessary and sufficient conditions for componentwise stability of interval matrix systems, IEEE Transactions on Automatic Control, vol. 49, no. 6, pp. 1016–1021, June 2004.

[Pei14] J. Pei, X. Liu, P. M. Pardalos, W. Fan, S. Yang, L. Wang, Application of an effective modified gravitational search algorithm for the coordinated scheduling problem in a two-stage supply chain, The International Journal of Advanced Manufacturing Technology, vol. 70, no. 1–4, pp. 335–348, Jan. 2014.

[Pel12] E. Pellegrini, N. Pletschen, S. Spirk, M. Rainer, B. Lohmann, Application of a model-based two-DOF control structure for enhanced force tracking in a semiactive vehicle suspension, Proceedings of 2012 IEEE International Conference on Control Applications (CCA 2012), Dubrovnik, Croatia, pp. 118–123, 2012.

[Pen14] Y. Peng, X. Luo, W. Wei, A new fuzzy adaptive simulated annealing genetic algorithm and its convergence analysis and convergence rate estimation, International Journal of Control, Automation and Systems, vol. 12, no. 3, pp. 670–679, June 2014.

[Per13] L. A. M. Pereira, L. C. S. Afonso, J. P. Papa, Z. A. Vale, C. C. O. Ramos, D. S. Gastaldello, A. N. Souza, Multilayer perceptron neural networks training through charged system search and its application for non-technical losses detection, Proceedings of 2013 IEEE PES Conference on Innovative Smart Grid Technologies Latin America (ISGT LA 2013), Sao Paulo, Brazil, pp. 1–6, 2013.

[Pir13] M. M. Pirbazari, A. Khoei, K. Hadidi, Optimization of inference engine in CMOS analog fuzzy logic controllers, Proceedings of 21st Iranian Conference on Electrical Engineering (ICEE 2013), Mashhad, Iran, pp.1-6, May 2013.

[Pre97] R.-E. Precup, S. Preitl, Popov-type stability analysis method for fuzzy control systems, Proceedings of Fifth European Congress on Intelligent Technologies and Soft Computing (EUFIT'97), Aachen, Germany, vol. 2, pp. 1306–1310, 1997.

[Prei97] S. Preitl, R.-E. Precup, Introducere în conducerea fuzzy a proceselor, Editura Tehnica, Bucharest, 1997.

[Pre99] R.-E. Precup, S. Preitl, Fuzzy Controllers, Editura Orizonturi Universitare, Timisoara, 1999.
[Prei02] S. Preitl, Z. Preitl, R.-E. Precup, Low cost fuzzy controllers for classes of second-order systems, Preprints of 15th IFAC World Congress, Barcelona, Spain, paper 416, pp. 1–6, 2002.
[Pre04] R.-E. Precup, S. Preitl, M. Balas, V. Balas, Fuzzy controllers for tire slip control in anti-lock braking systems, Proceedings of IEEE International Conference on Fuzzy Systems (FUZZ-IEEE 2004), Budapest, Hungary, vol. 3, pp. 1317–1322, 2004.
[Pre06a] R.-E. Precup, S. Preitl, PI and PID controllers tuning for integral-type servo systems to ensure robust stability and controller robustness, Electrical Engineering, vol. 88, no. 2, pp. 149–156, Jan. 2006.
[Pre06b] R.-E. Precup, S. Preitl, Stability and sensitivity analysis of fuzzy control systems. Mechatronics applications, Acta Polytechnica Hungarica, vol. 3, no. 1, pp. 61–76, March 2006.
[Prei06] S. Preitl, R.-E. Precup, J. Fodor, B. Bede, Iterative feedback tuning in fuzzy control systems. Theory and applications, Acta Polytechnica Hungarica, vol. 3, no. 3, pp. 81–96, Sep. 2006.
[Pre07] R.-E. Precup, S. Preitl, PI-fuzzy controllers for integral plants to ensure robust stability, Information Sciences, vol. 177, no. 20, pp. 4410–4429, Oct. 2007.
[Pre09a] R.-E. Precup, S. Preitl, E. M. Petriu, J. K. Tar, M. L. Tomescu, C. Pozna, Generic two-degree-of-freedom linear and fuzzy controllers for integral processes, Journal of The Franklin Institute, vol. 346, no. 10, pp. 980–1003, Dec. 2009.
[Pre09b] R.-E. Precup, R.-C. David, S. Preitl, E. M. Petriu, Design aspects of optimal PI controllers with reduced sensitivity for a class of servo systems using PSO algorithms, Facta Universitatis Series: Automatic Control and Robotics, vol. 8, no. 1, pp. 1–12, Dec. 2009.
[Pre09c] R.-E. Precup, M. L. Tomescu, S. Preitl, Fuzzy logic control system stability analysis based on Lyapunov's direct method, International Journal of Computers, Communication & Control, vol. 4, no. 4, pp. 415–426, Dec. 2009.
[Pre11a] R.-E. Precup, H. Hellendoorn, A survey on industrial applications of fuzzy control, Computers in Industry, vol. 62, no. 3, pp. 213–226, Apr. 2011.
[Pre11b] R.-E. Precup, R.-C. David, E. M. Petriu, S. Preitl, Optimal fuzzy controllers tuned by charged system search algorithms, 2011 Online Conference on Soft Computing in Industrial Applications (WSC 16), pp. 1–10, 2011.
[Pre11c] R.-E. Precup, R.-C. David, S. Preitl, E. M. Petriu, J. K. Tar, Optimal control systems with reduced parametric sensitivity based on particle swarm optimization and simulated annealing, in: Intelligent Computational Optimization in Engineering Techniques and Applications, M. Köppen, G. Schaefer and A. Abraham, Eds., Springer-Verlag, Berlin, Heidelberg, pp. 177–207, 2011.
[Pre11d] R.-E. Precup, R.-C. David, E. M. Petriu, S. Preitl, M.-B. Rădac, Gravitational search algorithms in fuzzy control systems tuning, Proceedings of 18th World Congress of the International Federation of Automatic Control (IFAC 2011), Milano, Italy, pp. 13624–13629, 2011.
[Pre11e] R.-E. Precup, R.-C. David, E. M. Petriu, S. Preitl, A. S. Paul, Gravitational search algorithm-based tuning of fuzzy control systems with a reduced parametric sensitivity, in: Advances in Intelligent and Soft Computing, A. Gaspar-Cunha, R. Takahashi, G. Schaefer, and L. Costa, Eds., Advances in Intelligent

and Soft Computing, vol. 96, Springer-Verlag, Berlin, Heidelberg, pp. 141−150, 2011.

[Pre11f] R.-E. Precup, E. M. Petriu, C.-A. Dragoş, R.-C. David, Stability analysis results concerning the fuzzy control of a class of nonlinear time-varying systems, Theory and Applications of Mathematics & Computer Science, vol. 1, no. 1, pp. 2–10, April 2011.

[Pre12a] R.-E. Precup, R.-C. David, E. M. Petriu, S. Preitl, M.-B. Rădac, Novel adaptive gravitational search algorithm for fuzzy controlled servo systems, IEEE Transactions on Industrial Informatics, vol. 8, no. 4, pp. 791–800, Nov. 2012.

[Pre12b] R.-E. Precup, R.-C. David, E. M. Petriu, S. Preitl, M.-B. Rădac, Fuzzy control systems with reduced parametric sensitivity based on simulated annealing, IEEE Transactions on Industrial Electronics, vol. 59, no. 8, pp. 3049–3061, Aug. 2012.

[Pre12c] R.-E. Precup, S. V. Spătaru, M.-B. Rădac, E. M. Petriu, S. Preitl, C.-A. Dragoş, R.-C. David, Experimental results of model-based fuzzy control solutions for a laboratory antilock braking system, in: Human-Computer Systems Interaction: Backgrounds and Applications 2, Part 2, Z. S. Hippe, J. L. Kulikowski and T. Mroczek, Eds., Advances in Intelligent and Soft Computing, vol. 99, Springer-Verlag, Berlin, Heidelberg, pp. 223–234, 2012.

[Pre12d] R.-E. Precup, R.-C. David, E. M. Petriu, S. Preitl, M.-B. Rădac, Charged system search algorithms for optimal tuning of PI controllers, Proceedings of 1st IFAC Conference on Embedded Systems, Computational Intelligence and Telematics in Control (CESCIT 2012), Würzburg, Germany, pp. 115–120, 2012.

[Pre13a] R.-E. Precup, R.-C. David, E. M. Petriu, M.-B. Rădac, S. Preitl, J. Fodor, Evolutionary optimization-based tuning of low-cost fuzzy controllers for servo systems, Knowledge-Based Systems, vol. 38, pp. 74–84, Jan. 2013.

[Pre13b] R.-E. Precup, R.-C. David, E. M. Petriu, S. Preitl, M.-B. Rădac, Fuzzy logic-based adaptive gravitational search algorithm for optimal tuning of fuzzy-controlled servo systems, IET Control Theory and Applications, vol. 7, no. 1, pp. 99–107, Jan. 2013.

[Pre13c] R.-E. Precup, R.-C. David, E. M. Petriu, S. Preitl, M.-B. Rădac, Experiments in fuzzy controller tuning based on an adaptive gravitational search algorithm, Proceedings of the Romanian Academy, Series A: Mathematics, Physics, Technical Sciences, Information Science, vol. 14, no. 4, pp. 360–367, Dec. 2013.

[Pre13d] R.-E. Precup, R.-C. David, E. M. Petriu, S. Preitl, M.-B. Rădac, Fuzzy logic-based adaptive gravitational search algorithm for optimal tuning of fuzzy controlled servo systems, IET Control Theory and Applications, vol. 7, no. 1, pp. 99–107, Jan. 2013.

[Pre13e] R.-E. Precup, M.-B. Rădac, M. L. Tomescu, E. M. Petriu, S. Preitl, Stable and convergent iterative feedback tuning of fuzzy controllers for discrete-time SISO systems, Expert Systems with Applications, vol. 40, no. 1, pp. 188–199, Jan. 2013.

[Pre14a] R.-E. Precup, R.-C. David, E. M. Petriu, M.-B. Rădac, S. Preitl, Adaptive GSA-based optimal tuning of PI controlled servo systems with reduced process parametric sensitivity, robust stability and controller robustness, IEEE Transactions on Cybernetics, vol. 44, no. 11, pp. 1997–2009, Nov. 2014.

[Pre14b] R.-E. Precup, R.-C. David, A.-I. Stînean, M.-B. Rădac, E. M. Petriu, Adaptive hybrid particle swarm optimization-gravitational search algorithm for fuzzy controller tuning, Proceedings of 2014 IEEE International Symposium on

Innovations in Intelligent Systems and Applications (INISTA 2014), Alberobello, Italy, pp. 14–20, 2014.

[Pre14c] R.-E. Precup, R.-C. David, E. M. Petriu, S. Preitl, M.-B. Rădac, Novel adaptive charged system search algorithm for optimal tuning of fuzzy controllers, Expert Systems with Applications, vol. 41, no. 4, part 1, pp. 1168–1175, March 2014.

[Prei99] S. Preitl, R.-E. Precup, An extension of tuning relations after symmetrical optimum method for PI and PID controllers, Automatica, vol. 35, no. 10, pp. 1731–1736, Oct. 1999.

[Prei10] S. Preitl, R.-E. Precup, C.-A. Dragoş, M.-B. Rădac, Tuning of 2-DOF fuzzy PI(D) controllers. Laboratory applications, Proceedings of 11th IEEE International Symposium on Computational Intelligence and Informatics (CINTI 2010), Budapest, Hungary, pp. 237–242, 2010.

[Pur13a] C. Purcaru, R.-E. Precup, D. Iercan, L.-O. Fedorovici, R.-C. David, F. Drăgan, Optimal robot path planning using gravitational search algorithm, International Journal of Artificial Intelligence, vol. 9, no. S13, pp. 1–20, March 2013.

[Pur13b] C. Purcaru, R.-E. Precup, D. Iercan, L.-O. Fedorovici, R.-C. David, Hybrid PSO-GSA robot path planning algorithm in static environments with danger zones, Proceedings of 2013 17th International Conference on System Theory, Control and Computing (ICSTCC 2013), Sinaia, Romania, pp. 434–439, 2013.

[Ras07] E. Rashedi, Gravitational search algorithm, M.Sc. thesis, Shahid Bahonar University of Kerman, Kerman, Iran, 2007.

[Ras09] E. Rashedi, H. Nezamabadi-pour, S. Saryazdi, GSA: A gravitational search algorithm, Information Sciences, vol. 179, no. 13, pp 2232–2248, 2009.

[Ras10] E. Rashedi, H. Nezamabadi-pour, S. Saryazdi, BGSA: binary gravitational search algorithm, Natural Computing, vol. 9, no.3, pp. 727–745, 2010.

[Ros00] E. Rosenwasser, R. Yusupov, Sensitivity of Automatic Control Systems, CRC Press, Boca Raton, FL, 2000.

[Roy13] A. Roy, K. D. Sharma, Gravitational search algorithm and Lyapunov theory based stable adaptive fuzzy logic controller, Procedia Technology, vol. 10, 2013, pp. 581–586, Dec. 2013.

[Sad14] J. Sadeghi, S. Sadeghi, S. T. A. Niaki, Optimizing a hybrid vendor-managed inventory and transportation problem with fuzzy demand: An improved particle swarm optimization algorithm, Information Sciences, vol. 272, pp. 126–144, July 2014.

[Sah15] R. K. Sahu, S. Panda, G. T. Chandra Sekhar, A novel hybrid PSO-PS optimized fuzzy PI controller for AGC in multi area interconnected power systems, International Journal of Electrical Power & Energy Systems, vol. 64, pp. 880–893, Jan. 2015.

[Sak13] B. Sakeen, N. K. Bachache, W. Shaorong, Frequency control of PV-Diesel hybrid power system using optimal fuzzy logic controller, Proceedings of IEEE 11th International Conference on Dependable, Autonomic and Secure Computing (DASC 2013), Chengdu, China, pp. 174–178, 2013.

[San12] D.-T. Sang, D.-M. Woo, D.-C. Park, Centroid neural network with simulated annealing and its application to color image segmentation, in: Neural Information Processing, T. Huang, Z. Zeng, C. Li and C. S. Leung, Eds., Lecture Notes in Computer Science, vol. 7665, Springer-Verlag, Berlin, Heidelberg, pp. 1–8, 2012.

[Sil12] A. S. Silveira, J. E. N. Rodríguez, A. A. R. Coelho, Robust design of a 2-DOF GMV controller: A direct self-tuning and fuzzy scheduling approach, ISA Transactions, vol. 51, no. 1, pp. 13–21, Jan. 2012.

[Sch03] B. Schutz, Gravity from the Ground Up, Cambridge University Press, Cambridge, 2003.

[Sha14] B. Shaw, V. Mukherjee, S.P. Ghoshal, Solution of reactive power dispatch of power systems by an opposition-based gravitational search algorithm, International Journal of Electrical Power & Energy Systems, vol. 55, pp. 29–40, Feb. 2014.

[She13] M. Sheikhan, M. Sharifi Rad, Gravitational search algorithm–optimized neural misuse detector with selected features by fuzzy grids–based association rules mining, Neural Computing and Applications, vol. 23, no. 7–8, pp. 2451–2463, Dec. 2013.

[She14] M. Sheikhan, Z. Jadidi, Flow-based anomaly detection in high-speed links using modified GSA-optimized neural network, Neural Computing and Applications, vol. 24, no. 3–4, pp. 599–611, March 2014.

[Shu08] S. K. Shukla, Y. J. Son, M. K. Tiwari, Fuzzy-based adaptive sample-sort simulated annealing for resource-constrained project scheduling, The International Journal of Advanced Manufacturing Technology, vol. 36, no. 9–10, pp. 982–995, April 2008.

[Sin14] P. Singh, B. Borah, Forecasting stock index price based on M-factors fuzzy time series and particle swarm optimization, International Journal of Approximate Reasoning, vol. 55, no. 3, pp. 812–833, March 2014.

[Skr05] I. Škrjanc, S. Blažič, Predictive functional control based on fuzzy model: design and stability study, Journal of Intelligent and Robotic Systems, vol. 43, no. 2–4, pp. 283–299, Aug. 2005.

[Sol13] M. R. Soltanpour, M. H. Khooban, A particle swarm optimization approach for fuzzy sliding mode control for tracking the robot manipulator, Nonlinear Dynamics, vol. 74, no. 1–2, pp. 467–478, Oct. 2013.

[Sti12a] A.-I. Stînean, S. Preitl, R.-E. Precup, E. M. Petriu, C.-A. Dragoş, M.-B. Rădac, 2-DOF PI(D) Takagi-Sugeno and sliding mode controllers for BLDC drives, Proceedings of 15th International Power Electronics and Motion Control Conference (EPE-PEMC 2012 ECCE Europe), Novi Sad, Serbia, pp. DS2a.7-1–DS2a.7-6, 2012.

[Sti12b] A.-I. Stînean, S. Preitl, R.-E. Precup, E. M. Petriu, C.-A. Dragoş, M.-B. Rădac, Takagi-Sugeno fuzzy control solutions for BLDC drives, Proceedings of 2012 International Symposium on Power Electronics, Electrical Drives, Automation and Motion (SPEEDAM 2012), Sorrento, Italy, pp. 724–729, 2012.

[Su13] X. Su, P. Shi, L. Wu, Y.-D. Song, A novel control design on discrete-time Takagi-Sugeno fuzzy systems with time-varying delays, IEEE Transactions on Fuzzy Systems, vol. 21, no. 4, pp. 655–671, Aug. 2013.

[Sug99] M. Sugeno, On stability of fuzzy systems expressed by fuzzy rules with singleton consequents, IEEE Transactions on Fuzzy Systems, vol. 7, no. 2, pp. 201–224, April 1999.

[Sy08] M. V. Sy, P.X. Minh, Fuzzy model predictive control using Takagi-Sugeno model, Proceedings of 2008 International Conference on Control, Automation and Systems (ICCAS 2008), Seoul, Korea, pp.632-637, Oct. 2008.

[Sza12] T. Szabo, M. Buchholz, K. Dietmayer, Model-predictive control of powershifts of heavy-duty trucks with dual-clutch transmissions, Proceedings of IEEE 51st Annual Conference on Decision and Control (CDC 2012), Maui, HI, USA, pp. 4555–4561, 2012.

[Tal11a] N. Talbi, K. Belarbi, Optimization of fuzzy controller using hybrid tabu search and particle swarm optimization, Proceedings of 2011 11th International Conference on Hybrid Intelligent Systems (HIS 2011), Melacca, Malaysia, pp. 561–565, 2011.

[Tal11b] N. Talbi, K. Belarbi, Fuzzy rule base optimization of fuzzy controller using Hybrid Tabu Search and Particle Swarm Optimization learning algorithm, Proceedings of 2011 World Congress on Information and Communication Technologies (WICT 2011), Mumbai, India, pp. 1139–1143, 2011.

[Tan08] X.-D. Tang, J. P. Yong, H. Zhang, G.-C. Lu, Improved PSO-based S plane controller for motion control of underwater vehicle, Proceedings of Chinese Control and Decision Conference (CCDC 2008), Yantai, Shandong, China, pp. 2843–2848, 2008.

[Tay11] K. M. Tay, C. P. Lim, Optimization of Gaussian fuzzy membership functions and evaluation of the monotonicity property of fuzzy inference systems, Proceedings of 2011 IEEE International Conference on Fuzzy Systems (FUZZ-IEEE 2011), Taipei, China, pp. 1219–1224, 2011.

[Teo12] H.-N. Teodorescu, Taylor and bi-local piecewise approximations with neuro-fuzzy systems, Studies in Informatics and Control, vol. 21, no. 4, pp. 367–376, Dec. 2012.

[Tik11] D. Tikk, Z. C. Johanyák, S. Kovács, K.W. Wong, Fuzzy rule interpolation and extrapolation techniques: Criteria and evaluation guidelines, Journal of Advanced Computational Intelligence and Intelligent Informatics, vol. 15, no. 3, pp. 254–263, May 2011.

[Tor11] Y. Torun, G. Tohumoğlu, Designing simulated annealing and subtractive clustering based fuzzy classifier, Applied Soft Computing, vol. 11, no. 2, pp. 2193–2201, March 2011.

[Tur12] M. Turki, S. Bouzaida, A. Sakly, F. M'Sahli, Adaptive control of nonlinear system using neuro-fuzzy learning by PSO algorithm, Proceedings of 16th IEEE Mediterranean Electrotechnical Conference (MELECON 2012), Yasmine Hammamet, Tunisia, pp. 519–523, 2012.

[Val08] Y. del Valle, G. K. Venayagamoorthy, S. Mohagheghi, J. C. Hernandez, R. G. Harley, Particle swarm optimization: Basic concepts, variants and applications in power systems, IEEE Transactions on Evolutionary Computation, vol. 12, no. 2, pp. 171–195, April 2008.

[Vas10] J. Vaščák, L. Madarász, Adaptation of fuzzy cognitive maps - a comparison study, Acta Polytechnica Hungarica, vol. 7, no. 3, pp. 109–122, Sep. 2010.

[Vij13] J. Vijaya Kumar, D. M. Vinod Kumar, K. Edukondalu, Strategic bidding using fuzzy adaptive gravitational search algorithm in a pool based electricity market, Applied Soft Computing, vol. 13, no. 5, pp. 2445–2455, May 2013.

[Vil12] R. Vilanova, V. M. Alfaro, O. Arrieta, Simple robust autotuning rules for 2-DoF PI controllers, ISA Transactions, vol. 51, no. 1, pp. 30–41, Jan. 2012.

[Vil13] R. Villafuerte, S. Mondie, R. Garrido, Tuning of proportional retarded controllers: Theory and experiments, IEEE Transactions on Control Systems Technology, vol. 21, no. 3, pp. 983–990, March 2013.

[Vis04] A. Visioli, A new design for a PID plus feedforward controller, Journal of Process Control, vol. 14, no. 4, pp. 457–463, June 2004.

[Vra11] D. Vrancic, S. Strmcnik, Design of 2-DOF PI controller for integrating processes, Proceedings of 8th Asian Control Conference (ASCC 2011), Kaohsiung, Taiwan, China, pp. 1135–1140, 2011.

[Wai07] R.-J. Wai, K.-L. Chuang, J.-D. Lee, Total sliding-model-based particle swarm optimization control design for linear induction motor, Proceedings of

IEEE Congress on Evolutionary Computation (CEC 2007), Singapore, pp. 4729–4734, 2007.

[Wan10] D. Wang, F. Wang, Design of PDC controller based on T-S fuzzy model for magnetic bearing of high-speed motors, Proceedings of 3rd IEEE International Conference on Computer Science and Information Technology (ICCSIT 2010), Chengdu, China, vol. 1, pp. 602–606, 2010.

[Wan12a] J. Wang, S. Lai, Y. He, Applying soft computing in material molding, in: Advances in Future Computer and Control Systems, D. Jin and S. Lin, Eds., Advances in Intelligent and Soft Computing, vol. 159, Springer-Verlag, Berlin, Heidelberg, pp. 163–168, 2012.

[Wan12b] H. P. Wang, A. Pintea, N. Christov, P. Borne, D. Popescu, Recursive model free control of variable speed wind turbine systems, Proceedings of 2012 IEEE International Conference on Control Applications (CCA 2012), Dubrovnik, Croatia, pp. 1541–1546, 2012.

[Wat10] S. K. Wattamwar, S. Weiland, T. Backx, Identification of low-order parameter-varying models for large-scale systems, Journal of Process Control, vol. 20, no. 2, pp. 158–172, Feb. 2010.

[Wu11] H. Wu, H.-Z. Li, G.W. Wang, H.-L. Chen, X.-K. Li, A novel spam filtering framework based on fuzzy adaptive particle swarm optimization, Proceedings of 2011 International Conference on Intelligent Computation Technology and Automation (ICICTA 2011), Shenzhen, China, vol. 1, pp. 38–41, 2011.

[Wu14] W. Yu, W. Chen, Trajectory-shaping guidance with final speed and load factor constraints, ISA Transactions, DOI: 10.1016/j.isatra.2014.11.017, Dec. 2014.

[Xia10] P. Xiaohong, M. Zhi, X. Laisheng, Research and application on GA-based two-stage fuzzy temperature control system for a type of industrial furnace, Proceedings of 2010 International Conference on Electrical and Control Engineering (ICECE 2010), Wuhan, China, pp. 1558–1561, 2010.

[Xue14] X. Ding, Z. Xu, M. Liu, J. Wu, T-S model identification based on silhouette index and improved gravitational search algorithm, Proceedings of 33rd Chinese Control Conference (CCC 2014), Nanjing, China, pp. 4423–4428, 2014.

[Yam06] Y. Yam, M. L. Wong, P. Baranyi, Interpolation with function space representation of membership functions, IEEE Transactions on Fuzzy Systems, vol. 14, no. 3, pp. 398–411, June 2006.

[Yan10] M. Yang, X. Wang, Design for fuzzy backstepping controller of permanent magnet synchronous motor, Proceedings of 2010 IEEE Conference on Cybernetics and Intelligent Systems (CIS 2010), Singapore, pp. 201–205, 2010.

[Yon11] Yongzhi, J., Kunlun, Z., Jian, X., Modeling of gap sensor for high-speed Maglev train based on fuzzy neural network, Proceedings of Eighth International Conference on Fuzzy Systems and Knowledge Discovery (FSKD 2011), Shanghai, China, vol. 1, pp. 650–654, 2011.

[Yu03] S.-S. Yu, S.-J. Wu, T.-T. Lee, Application of neural-fuzzy modeling and optimal fuzzy controller for nonlinear magnetic bearing systems, Proceedings of IEEE/ASME International Conference on Advanced Intelligent Mechatronics (AIM 2003), Kobe, Japan, vol. 1, pp. 7–11, 2003.

[Yua14] X. Yuan, B. Ji, Z. Chen, Z. Chen, A novel approach for economic dispatch of hydrothermal system via gravitational search algorithm, Applied Mathematics and Computation, vol. 247, pp. 535–546, Nov. 2014.

[Zar14] A. Zarrabi, K. Samsudin, Task scheduling on computational grids using gravitational search algorithm, Cluster Computing, vol. 17, no. 3, pp. 1001–1011, Sep. 2014.

[Zha12] G.-F. Zhang, L.-H. He, R.-H. Yu, J.-C. He, Fuzzy measure-based fuzzy rule interpolation based on PSO-based fuzzy integral-learning techniques, Proceedings of 2012 International Conference on Machine Learning and Cybernetics (ICMLC 2012), Shaanxi, China, vol. 1, pp. 219–225, 2012.

[Zhe11] T. Zheng, F. Ma, K. Zhang, Estimation of reference vehicle speed based on T-S fuzzy model, Proceedings of International Conference on Advanced in Control Engineering and Information Science, Dali, China, vol. 15, pp. 188–193, 2011.

[Zir13] M. M. Zirkohi, M. M. Fateh, M. A. Shoorehdeli, Type-2 fuzzy control for a flexible-joint robot using voltage control strategy, International Journal of Automation and Computing, vol. 10, no. 3, pp. 242–255, June 2013.